



School of Engineering & School of Dentistry

MICROFLUIDIC PRODUCTION OF STEM-CELL MICROCAPSULES FOR SPINAL CORD INJURY REPAIR

Lorena Hidalgo San José BSc, MSc

This thesis is being submitted to Cardiff University in partial fulfilment
of the requirements for the degree of Doctor of Philosophy

February 2017



Cardiff Institute of
Tissue Engineering and Repair
(CITER)

EPSRC

Engineering and Physical Sciences
Research Council

Declaration

This work has not been submitted in substance for any other degree or award at this or any other university or place of learning, nor is being submitted concurrently in candidature for any degree or other award.

Signed (candidate) Date

STATEMENT 1

This thesis is being submitted in partial fulfilment of the requirements for the degree of PhD

Signed(candidate) Date

STATEMENT 2

This thesis is the result of my own independent work/investigation, except where otherwise stated. Other sources are acknowledged by explicit references. The views expressed are my own.

Signed (candidate) Date

STATEMENT 3

I hereby give consent for my thesis, if accepted, to be available for photocopying and for inter-library loan, and for the title and summary to be made available to outside organisations.

Signed(candidate) Date

STATEMENT 4: PREVIOUSLY APPROVED BAR ON ACCESS

I hereby give consent for my thesis, if accepted, to be available for photocopying and for inter-library loans after expiry of a bar on access previously approved by the Academic Standards & Quality Committee.

Signed(candidate) Date

Table of Contents

| | |
|---|-------------|
| Acknowledgements..... | XI |
| Abstract | XIII |
| Aims of the Project..... | XV |
| List of Abbreviations | XVII |
| Table of Figures..... | XIX |
| Chapter 1. Introduction..... | 21 |
| 1.1 SPINAL CORD INJURY | 25 |
| 1.1.1 Anatomy and Physiology of the Spinal Cord | 25 |
| 1.1.2 Pathophysiology | 32 |
| 1.1.3 Tissue engineering approaches for SCI | 34 |
| 1.2 STEM CELLS | 37 |
| 1.2.1 Embryonic Stem Cells | 37 |
| 1.2.1.1 Neural Stem Cells | 39 |
| 1.2.2 Adult Stem Cells | 40 |
| 1.2.2.1 Dental Pulp Stem Cells | 41 |
| 1.2.2.1.1 Neuronal Regenerative potential of DPSCs..... | 44 |
| 1.3 CELL ENCAPSULATION..... | 48 |
| 1.3.1 Requirements of cell encapsulation systems | 49 |
| 1.3.1.1 Stability | 49 |
| 1.3.1.2 Permeability | 50 |
| 1.3.1.3 Diffusion..... | 52 |
| 1.3.2 Applications of cell encapsulation | 53 |
| 1.3.2.1 Immunoisolation in transplantation therapy | 53 |
| 1.3.2.2 Local and systemic controlled release of drugs and growth factors | 54 |
| 1.3.2.3 3D culture systems..... | 55 |
| 1.3.3 Cell encapsulation techniques..... | 56 |

| | |
|--|-----------|
| 1.4 BIOMATERIALS..... | 59 |
| 1.4.1 Alginate | 59 |
| 1.4.1.1 General properties..... | 60 |
| 1.4.1.2 Hydrogel formation and biodegradation | 61 |
| 1.4.1.2.1 Ionic cross-linking | 62 |
| 1.4.1.2.2 Covalent cross-linking..... | 64 |
| 1.4.1.2.3 Alginate biodegradation | 65 |
| 1.4.1.3 Alginate applications in biomedical science | 66 |
| 1.4.2 Collagen..... | 67 |
| 1.4.2.1 General properties..... | 67 |
| 1.4.2.2 Isolation, cross-linking and degradation | 68 |
| 1.4.2.2.1 Natural sources of collagen | 68 |
| 1.4.2.2.2 Collagen cross-linking | 69 |
| 1.4.2.2.3 Collagen biodegradation | 70 |
| 1.4.2.3 Collagen applications in biomedical science..... | 71 |
| 1.5 MICROFLUIDICS | 73 |
| 1.5.1 Physics in Microfluidics | 73 |
| 1.5.2 Droplet-based microfluidics | 76 |
| 1.5.2.1 Physics involved in droplet formation | 77 |
| 1.5.2.2 Microfluidic formats for droplet generation..... | 79 |
| 1.5.2.2.1 Co-flowing | 79 |
| 1.5.2.2.2 T-junction | 80 |
| 1.5.2.2.3 Flow focusing..... | 82 |
| 1.5.3 Microfluidics and Biomedical Research | 84 |
| 1.5.3.1 Cell manipulation..... | 85 |
| Chapter 2. Development of a Microfluidic Chip to Produce Alginate Microspheres..... | 87 |
| 2.1 INTRODUCTION..... | 89 |
| 2.2 AIMS AND OBJECTIVES | 90 |
| 2.3 MATERIALS AND METHODS..... | 91 |
| 2.3.1 Microfluidic reagents | 91 |

| | |
|---|------------|
| 2.3.2 Preparation of microfluidic reagents | 92 |
| 2.3.3 Chip design and manufacturing | 92 |
| 2.3.4 Microfluidic device setup | 93 |
| 2.3.5 Imaging..... | 94 |
| 2.3.6 Statistics | 94 |
| 2.4 RESULTS..... | 96 |
| 2.4.1 Development of a customized microfluidic chip to produce alginate microcapsules..... | 96 |
| 2.4.2 Optimization of the reagents concentration..... | 102 |
| 2.4.3 Optimization of flow rates | 104 |
| 2.5 DISCUSSION | 109 |
| Chapter 3. Optimization of Stem Cell Encapsulation in ECM-based Microcapsules..... | 117 |
| 3.1 INTRODUCTION..... | 119 |
| 3.2 AIMS & OBJECTIVES | 121 |
| 3.3 MATERIALS & METHODS..... | 122 |
| 3.3.1 Cell culture | 122 |
| 3.3.1.1 Dental pulp stem cell culture | 122 |
| 3.3.1.2 Passaging DPSC Cultures | 122 |
| 3.3.1.3 Cryopreservation and re-establishment of DPSCs | 123 |
| 3.3.1.4 Embryonic neural stem cell culture | 124 |
| 3.3.1.5 Subculturing NSC cultures..... | 124 |
| 3.3.2 Viability and proliferation assays | 125 |
| 3.3.2.1 Trypan Blue Exclusion Assay | 125 |
| 3.3.2.2 MTT Assay | 126 |
| 3.3.2.3 Live/Dead [®] Viability/Cytotoxicity Assay..... | 127 |
| 3.3.2.4 CellTrace™ Far Red staining for proliferation analysis by Flow Cytometry | 128 |
| 3.3.2.5 Inhibition of cell proliferation with Mitomycin C..... | 130 |
| 3.3.3 Encapsulation of stem cells | 131 |
| 3.3.3.1 Preparation of encapsulation matrix solutions | 131 |

| | |
|--|-----|
| 3.3.3.1.1 Alginate matrix | 131 |
| 3.3.3.1.2 Alginate-collagen matrix..... | 131 |
| 3.3.3.2 Production of cell-laden microspheres | 131 |
| 3.3.4 Cell release from microspheres | 132 |
| 3.3.5 Estimation of number of cells per bead | 133 |
| 3.3.6 Neuronal differentiation | 133 |
| 3.3.6.1 NSCs neuronal differentiation | 134 |
| 3.3.6.2 DPSCs neuronal differentiation | 134 |
| 3.3.7 Immunocytochemistry staining..... | 135 |
| 3.3.8 Cellular Imaging..... | 136 |
| 3.3.8.1 Phase contrast imaging..... | 136 |
| 3.3.8.2 Fluorescent imaging..... | 136 |
| 3.3.8.3 Confocal laser scanning microscopy | 136 |
| 3.3.8.4 Image processing | 137 |
| 3.3.9 Statistics | 137 |
| 3.4 RESULTS..... | 138 |
| 3.4.1 Study of the cytotoxicity of the reagents used on stem cells | 138 |
| 3.4.2 Optimization of microcapsule initial cell seeding density | 143 |
| 3.4.2.1 Study of cell survival within alginate microcapsules using the Trypan Blue Exclusion Assay..... | 146 |
| 3.4.2.2 Live/Dead® Viability Assay and confocal imaging of encapsulated cells..... | 149 |
| 3.4.2.3 Cell proliferation studies within alginate microcapsules | 151 |
| 3.4.3 Modification of the encapsulation matrix..... | 153 |
| 3.4.3.1 Cell viability and proliferation: comparison between alginate and alginate-collagen microcapsules | 154 |
| 3.4.3.1.1 Trypan Blue exclusion assay | 154 |
| 3.4.3.1.2 Live/Dead® Viability Assay and confocal imaging..... | 156 |
| 3.4.3.1.3 MTT proliferation assay..... | 158 |
| 3.4.4 Study of cell turnover within alginate-collagen microcapsules using CellTrace™ staining and flow cytometry | 161 |

| | |
|--|------------|
| 3.4.5 Cell functionality studies upon release from alginate-collagen microspheres .. | 163 |
| 3.4.5.1 Cell proliferation potential | 163 |
| 3.4.5.2 Stemness and neuronal differentiation potential | 165 |
| 3.5 DISCUSSION | 170 |
| 3.5.1 Cytotoxicity of reagents used on stem cells | 170 |
| 3.5.2 Viability and proliferation of encapsulated cells | 172 |
| 3.5.3 Cell functionality upon release from microcapsules | 179 |
| | |
| Chapter 4. Transplantation of Encapsulated Stem Cells into an Organotypic Model of Spinal Cord Injury | 185 |
| 4.1 INTRODUCTION | 187 |
| 4.2 AIMS & OBJECTIVES | 189 |
| 4.3 MATERIALS & METHODS | 189 |
| 4.3.1 Animals | 189 |
| 4.3.2 Dissection and preparation of murine spinal cord explants | 189 |
| 4.3.3 Transplantation of encapsulated cells | 190 |
| 4.3.4 Cryosectioning of spinal cord tissue samples | 191 |
| 4.3.5 Apoptosis Tunel Assay | 191 |
| 4.3.6 Immunohistochemical staining of spinal slice cultures | 192 |
| 4.4 RESULTS | 194 |
| 4.4.1 Development of a method for the transplantation of encapsulated stem cells into an organotypic model of spinal cord injury | 194 |
| 4.4.2 Analysis of cell survival after transplantation | 201 |
| 4.4.3 Study of the neuronal marker levels within encapsulated stem cells transplanted into ex vivo spinal cord cultures | 203 |
| 4.5 DISCUSSION | 207 |
| | |
| Chapter 5. General Discussion | 216 |
| | |
| REFERENCES | 232 |
| | |
| APPENDIX I: Tables of antibodies | 266 |

| | |
|--|------------|
| APPENDIX II: ISOTYPE CONTROL IN MONOLAYER CULTURES..... | 267 |
| APPENDIX III: APOPTOSIS TUNEL ASSAY POSITIVE CONTROL | 268 |
| APPENDIX IV: EX VIVO ISOTYPE CONTROL..... | 269 |
| APPENDIX V: ENDOGENOUS PRODUCTION OF NEURONAL MARKERS | 271 |

Acknowledgements

Firstly, I would like to thank my supervisors Prof David Barrow, Prof Phil Stephens and Prof Bing Song for their continuous guidance, encouragement and support throughout the last three years. Not only have they contributed to my development as an independent researcher, but also helped me to build self-confidence.

Many thanks to my colleagues in the School of Engineering Dr Alex Morgan and Dr Jin Li for having helped me with the microfluidic device design, manufacture and set up, and a special thank you to my colleague and friend Divesh, for providing the fun inside and outside the office.

I would also like to mention some of my colleagues in the School of Dentistry: Ahmed, Nadia, Clotilde and Matt, I really enjoyed our conversations between experiments, you guys made my days in the lab. Special mention to Joana, I would have liked you to arrive earlier, but at least I am lucky to have had the opportunity to meet you.

I also want to thank all the amazing friends that I have had the pleasure to meet in Cardiff. Lourdes and Jorge, you have helped me tremendously and I will always be indebted with you. Borja, you have contributed to most of the funniest moments I have lived in Cardiff, and things weren't the same after you left. Alessandra, you have been my greatest support in Cardiff and I will hugely miss you.

Carlos, your unconditional love and infinite patience have allowed me to achieve more than I ever thought I could. Your encouragement and confidence have been essential for the completion of this thesis.

Soraya, muchas gracias por tu amistad y cariño incluso a miles de kilómetros de distancia. Los pequeños momentos que hemos pasado juntas estos últimos años valen por mil.

Por último, me gustaría dar las gracias por tener a los padres más maravillosos del mundo: Jose y Beli. Gracias a vuestro grandísimo esfuerzo y trabajo duro he llegado a donde estoy. Sin vuestro apoyo, cariño y paciencia, nada de esto hubiera pasado.

Abstract

Stem cell therapy demonstrates much promise for the replacement of damaged tissue in several diseases, including spinal cord injury. However, challenges around the control of stem cell fate *in situ* still hinders effective recovery of the normal tissue function. Stem cell encapsulation permits their immobilization within biocompatible scaffolds, allowing for a better control of parameters such as proliferation, integration, migration and differentiation within the host tissue. A customized microfluidic device was developed for the production of alginate microcapsules. The diameter of such microcapsules could be easily controlled by the modification of the fluids flow rates, allowing for the reproducible production of highly monodisperse microcapsules. This microfluidic method was then successfully applied for the encapsulation of two different types of stem cells: (i) Neural Stem Cells and (ii) Dental Pulp Stem Cells. Both cell types demonstrated survival within the alginate microcapsules for up to three weeks in culture. However, an early egress of cells from inside to outside of the microcapsules was observed 3 days post-encapsulation. In order to delay such cell escape, alginate microcapsules were modified through the addition of type I collagen. The alginate-collagen microcapsules permitted similar rates of cell survival and permitted the delay of cell egress until 10 days after encapsulation. Stem cells demonstrated a retention of their stem cell and neuronal differentiation properties upon selective release from alginate-collagen microcapsules, as demonstrated by high proliferation rates and the production of stem cell and neuronal markers. When cell-laden microcapsules were transplanted into an *ex vivo* SCI model the microcapsules were able to effectively retain the transplanted stem cells at the site of implantation. Transplanted cells survived up to 10 days in culture after transplantation and demonstrated the production of neuronal markers within the cord cultures. The results presented in this thesis demonstrate the ability of stem cells to retain their viability and neuronal differentiation capacity within alginate-collagen microcapsules, thereby providing a promising future therapy for the treatment of spinal cord injury.

Aims of the Project

The main objective of this thesis was to attempt to encapsulate stem cells within biocompatible scaffolds for further application in regenerative medicine, specifically, in spinal cord injury (SCI) repair. It was hypothesized that the encapsulation of stem cells within biocompatible scaffolds would permit a better control of stem cell parameters, such as proliferation, migration, integration and differentiation. Hence, the aims of this thesis can be described as follows:

- 1) The development of a customized microfluidic device for the production of alginate and alginate-collagen microcapsules and the optimisation of microfluidic parameters to reproducibly produce polymer microcapsules with diameters $< 500\mu\text{m}$
- 2) The application of the microfluidic device for the viable, long-term encapsulation of stem cells
- 3) To compare the behaviour of encapsulated stem cell types, including cell viability and proliferation and the maintenance of stem cell and neuronal differentiation potential upon release from microcapsules
- 4) To study the behaviour of encapsulated cells within an *ex vivo* SCI model as a precursor to future (outside of this thesis), pre-clinical studies

List of Abbreviations

| | |
|--------|---|
| ASCs | Adult stem cells |
| ATP | Adenosine triphosphate |
| BDNF | Brain-derived neurotrophic factor |
| bFGF | Basic fibroblast growth factor |
| BMSCs | Bone marrow stromal cells |
| BrdU | Bromodeoxyuridine |
| BSA | Bovine serum albumin |
| Ca | Capillary number |
| cAMP | Cyclic adenosine monophosphate |
| CNS | Central nervous system |
| CNTF | Ciliary neurotrophic factor |
| DMSO | Dimethyl sulfoxide |
| DNA | Deoxyribonucleic acid |
| DPSCs | Dental pulp stem cells |
| dUTP | Deoxyuridine triphosphate |
| ECM | Extracellular matrix |
| EGF | Epidermal growth factor |
| ELISA | Enzyme-linked immunosorbent assay |
| ESCs | Embryonic stem cells |
| EthD-1 | Ethidium homodimer-1 |
| FGF | Fibroblast growth factor |
| GDNF | Glial cell line-derived neurotrophic factor |
| GFP | Green fluorescence protein |
| HA | Hyaluronic acid |
| HEPES | N-2-hydroxyethylpiperazine-N'-2-ethanesulfonic acid |
| HPLC | High performance liquid chromatography |
| HSCs | Hematopoietic stem cells |
| iPSCs | Induced pluripotent stem cells |
| ITSS | Insulin-transferrin-sodium selenite supplement |
| IVF | In vitro fertilization |

| | |
|------|--|
| LIF | Leukaemia inhibitory factor |
| MSCs | Mesenchymal stem cells |
| MTT | 3-(4,5-dimethylthiazol-2-yl)-2,5-diphenyltetrazolium bromide |
| NEAA | Non-essential amino acids |
| NGF | Nerve growth factor |
| NSCs | Neural stem cells |
| NT | Neurotrophin |
| NT-3 | Neurotrophin-3 |
| PBS | Phosphate buffered saline |
| PDL | Poly-D-lysine |
| PDMS | Polydimethylsiloxane |
| PFA | Paraformaldehyde |
| PLL | Poly-L-lysine |
| PLO | Poly-L-ornithine |
| PNS | Peripheral Nervous System |
| PTFE | Polytetrafluoroethylene |
| Re | Reynolds number |
| RGD | Arginine-glycine-aspartic acid |
| SAV | Surface area to volume |
| SCI | Spinal cord injury |
| SVZ | Subventricular zone |
| TdT | Terminal deoxynucleotidyl transferase |

Table of Figures

| | |
|--|-----|
| FIGURE 1.1. SCHEMATIC REPRESENTATION OF THE SPINAL CORD ANATOMY AND FUNCTION..... | 27 |
| FIGURE 1.2. ACTION POTENTIAL TRANSMISSION ALONG THE AXON..... | 30 |
| FIGURE 1.3. SCHEMATIC REPRESENTATION OF THE ACTION POTENTIAL PROPAGATION THROUGH SALTATORY CONDUCTION | 30 |
| FIGURE 1.4. CHEMICAL STRUCTURE OF ALGINATE..... | 60 |
| FIGURE 1.5. REPRESENTATION OF ALGINATE ION CROSS-LINKING INTO AN “EGG-BOX” STRUCTURE..... | 62 |
| FIGURE 1.6. GRAPHICAL REPRESENTATION OF TURBULENT AND LAMINAR FLOW REGIMES..... | 74 |
| FIGURE 1.7. CONTACT ANGLE..... | 79 |
| FIGURE 1.8. DROPLET FORMATION IN A CO-FLOWING SYSTEM..... | 80 |
| FIGURE 1.9. DROPLET FORMATION IN A T-JUNCTION..... | 81 |
| FIGURE 1.10. DROPLET GENERATION IN A FLOW FOCUSING DEVICE..... | 83 |
| FIGURE 2.1. MICROFLUIDIC DEVICE..... | 95 |
| FIGURE 2.2. CHIP DESIGN FOR THE PRODUCTION OF ALGINATE MICROCAPSULES..... | 97 |
| FIGURE 2.3. SHIELDING FLOW..... | 98 |
| FIGURE 2.4. LAMINAR FLOW..... | 100 |
| FIGURE 2.5. GEOMETRY OF MICROFLUIDIC CHIPS..... | 100 |
| FIGURE 2.6. COLLECTION OF ALGINATE MICROCAPSULES..... | 101 |
| FIGURE 2.7. OPTIMIZATION OF CaCO_3 CONCENTRATION..... | 103 |
| FIGURE 2.8. VARIATION OF BEAD DIAMETERS WITH FLOW RATES..... | 107 |
| FIGURE 2.9. ALGINATE MICROCAPSULES OF DIFFERENT SIZES PRODUCED BY A COMBINATION OF DIFFERENT FLOW RATES | 108 |
| FIGURE 3.1. ABSORPTION AND FLUORESCENCE EMISSION SPECTRA OF GFP AND ETHD-1..... | 128 |
| FIGURE 3.2. VIABILITY OF DPSCS AND NSCS RESUSPENDED IN MINERAL OIL OR IN 0.3 % ACETIC ACID IN MINERAL OIL..... | 141 |
| FIGURE 3.3. VIABILITY OF DPSCS AND NSCS RESUSPENDED IN 0.3% (v/v) ACETIC ACID IN CULTURE MEDIUM..... | 141 |
| FIGURE 3.4. VIABILITY OF DPSCS RESUSPENDED IN 2% (w/v) ALGINATE SOLUTION CONTAINING 5 MG/ML CaCO_3 | 142 |
| FIGURE 3.5. ENCAPSULATED NSCS AND DPSCS WITHIN ALGINATE MICROCAPSULES..... | 144 |
| FIGURE 3.6. ENCAPSULATED CELLS IN ALGINATE MICROCAPSULES..... | 145 |
| FIGURE 3.7. GRAPH SHOWING THE INFLUENCE OF INITIAL CELL DENSITY ON CELLS VIABILITY..... | 148 |
| FIGURE 3.8. CONFOCAL IMAGES OF ENCAPSULATED STEM CELLS WITHIN ALGINATE MICROSPHERES STAINED WITH ETHD-1 | 150 |
| FIGURE 3.9. GRAPH OF MTT ASSAY ON DAYS 1, 3, 7 AND 10 AFTER ENCAPSULATION..... | 151 |
| FIGURE 3.10. BRIGHT FIELD IMAGES OF ENCAPSULATED CELLS AFTER FORMAZAN FORMATION IN MTT ASSAY..... | 152 |
| FIGURE 3.11. GRAPH SHOWING THE INFLUENCE OF THE ENCAPSULATION MATRIX ON CELL VIABILITY..... | 155 |
| FIGURE 3.12. CONFOCAL IMAGES OF ENCAPSULATED STEM CELLS WITHIN ALGINATE-COLLAGEN MICROSPHERES STAINED WITH ETHD-1..... | 157 |

| | |
|---|-----|
| FIGURE 3.13. <i>GRAPH OF MTT ASSAY ON DAYS 1, 3, 7 AND 10 AFTER ENCAPSULATION WITHIN ALGINATE AND ALGINATE-COLLAGEN MICROCAPSULES.</i> | 159 |
| FIGURE 3.14. <i>BRIGHT FIELD IMAGES OF ENCAPSULATED CELLS AFTER FORMAZAN FORMATION.</i> | 160 |
| FIGURE 3.15. <i>STUDY OF DPSC PROLIFERATION WITHIN ALGINATE-COLLAGEN MICROCAPSULES</i> | 162 |
| FIGURE 3.16. <i>NSCs AND DPSCs PROLIFERATION UPON RELEASE FROM ALGINATE-COLLAGEN MICROCAPSULES.</i> | 164 |
| FIGURE 3.17. <i>MORPHOLOGY CHANGES DURING NEURONAL DIFFERENTIATION OF NSCs AND DPSCs.</i> | 167 |
| FIGURE 3.18. <i>IMMUNOCYTOCHEMICAL STAINING OF NSCs BEFORE AND AFTER NEURONAL DIFFERENTIATION.</i> | 168 |
| FIGURE 3.19. <i>IMMUNOCYTOCHEMICAL STAINING OF DPSCs BEFORE AND AFTER NEURONAL DIFFERENTIATION.</i> | 169 |
| FIGURE 4.1. <i>APPROACHES FOR INJURY INDUCTION INTO AN EX VIVO MODEL OF SCI.</i> | 195 |
| FIGURE 4.2. <i>SCI INDUCTION AND TRANSPLANTATION OF ENCAPSULATED CELLS</i> | 197 |
| FIGURE 4.3. <i>SPINAL CORD LONGITUDINAL SECTION AFTER TRANSPLANTATION OF ENCAPSULATED CELLS.</i> | 198 |
| FIGURE 4.4. <i>BEHAVIOUR COMPARISON OF NON-ENCAPSULATED AND ENCAPSULATED CELLS TRANSPLANTED IN SPINAL CORD SLICE CULTURES</i> | 199 |
| FIGURE 4.5. <i>BRIGHT FIELD IMAGES OF CELLS AT THREE DIFFERENT CONDITIONS BEFORE ENCAPSULATION AND TRANSPLANTATION.</i> | 200 |
| FIGURE 4.6. <i>APOPTOSIS TUNEL ASSAY OF ENCAPSULATED CELLS TRANSPLANTED INTO AN EX VIVO MODEL OF SCI</i> | 202 |
| FIGURE 4.7. <i>EXPRESSION OF NEURONAL MARKERS BY UNDIFFERENTIATED DPSCs (CELL TYPE 1)</i> | 204 |
| FIGURE 4.8. <i>EXPRESSION OF NEURONAL MARKERS BY NEURALISED DPSCs (CELL TYPE 2)</i> | 205 |
| FIGURE 4.9. <i>EXPRESSION OF NEURONAL MARKERS BY UNDIFFERENTIATED NSCs (CELL TYPE 3)</i> | 206 |

Chapter 1. Introduction

The field of regenerative medicine offers the potential to treat a multitude of debilitating and deadly conditions such as myocardial infarction (Bai *et al.* 2011), diabetes (Acarregui *et al.* 2014) and spinal cord injury (Fan *et al.* 2017), by replacing and regenerating lost or damaged tissue. Stem cells are ideal candidates to regenerate injured tissues, due to their potential to become into different cell lineages. However, the poor control of stem cell fate *in situ* and the loss of transplanted cells due to immune responses limit their clinical application (Li *et al.* 2016). Hence, the immobilization of stem cells within biocompatible scaffolds has gained great attention over the last decades in the field of regenerative medicine (Asghari *et al.* 2017). Immobilized cells within biomaterials permits their protection from potential harmful agents at the site of implantation, while allowing for a better control of cell parameters, including integration, migration, proliferation and differentiation (Banerjee *et al.* 2009; Jun *et al.* 2013).

It has been demonstrated that the physico-chemical properties of biomaterials have a profound influence in the stem cell behaviour mechanisms. Hence, the selection of the biomaterial is of a key importance to guarantee the correct performance of the grafted cells. Alginate is one of the most used scaffolds in regenerative medicine due to its biocompatibility, low toxicity, relatively low cost and mild gelation conditions (Lee & Mooney 2012). Its versatility permits the modification of its mechanical properties depending on the desired application. However, despite these advantageous features, alginate itself may not be an ideal material, since it is unable to specifically interact with mammalian cells (Rowley *et al.* 1999). Cell anchorage is critical in many cellular functions including migration, proliferation and differentiation. Hence, alginate has been usually combined with

other biomaterials, such as collagen. Because collagen is the main component of the extracellular matrix, it is also one of the most used biomaterials for cell immobilization. The high content of amino acids, makes collagen a biologically active material which promotes excellent cell adhesion and growth. Furthermore, collagen is biodegradable and so allow immobilized cells, over time, to produce their own extracellular matrix and replace the degraded scaffold.

Among the biomaterials geometry, microcapsules are often the preferred format for cell immobilization due to their high surface area to volume ratio, which enhances mass transfer through the polymer membrane (Liu *et al.* 2014). Because the reproducibility of the size of microcapsules is critical in clinical application, microfluidics has gained the attention of researches to produce cell-laden microcapsules (Jang *et al.* 2016). This technology offers a tight control of the parameters governing the formation of microcapsules and allows to work in a sealed environment, thereby avoiding potential cross-contamination.

Thus, previous research has reported that the therapeutic delivery of encapsulated stem cells is a promising approach for increasing cell survival in tissue regeneration. Therefore, the overall aims of this thesis were to develop a customized microfluidic device for stem cell encapsulation within alginate or alginate-collagen microcapsules, and further application into an *ex vivo* SCI model.

1.1 Spinal Cord Injury

Spinal cord injury (SCI) involves devastating neurological deficits resulting in permanent functional motor and sensory loss. The lack of effective treatments to overcome this condition explains the increasing interest among the scientific community to investigate and develop novel therapies (Zeb *et al.* 2016; Karsy & Hawryluk 2017).

There are different causes of SCI, generally grouped into (i) non-traumatic and (ii) traumatic causes. Non-traumatic causes include arthritis, cancer, inflammation, infections or disk degeneration (Prasad & Schiff 2005; Ward *et al.* 2015). These conditions provoke a compression on the spinal cord leading to the loss of its normal function. Traumatic causes involve the physical disruption of the spine due to traffic accidents, acts of violence, falls and sports injuries, amongst others (Chen *et al.* 2013).

1.1.1 Anatomy and Physiology of the Spinal Cord

The spinal cord (SC) is a bundle of nerves that extends from the brain down to the lumbar region of the vertebral column. The interior of the cord is made of grey matter, forming a butterfly-shaped cross-sectional area that is mainly composed of cell bodies. It is surrounded by white matter, which is formed by myelinated axons, named tracts. The spinal cord is covered by the meninges, a group of fibrous membranes including the dura mater, arachnoid and the innermost pia mater, that give support and protection to the spinal cord (O’Rahilly *et al.* 2004) (**Figure 1.1A**). Along with the brain, the spinal cord forms the Central Nervous System (CNS), and it

enables the transmission of information between the brain and the peripheral nervous system (PNS), controlling both somatic and autonomic reflexes (**Figure 1.1B**).

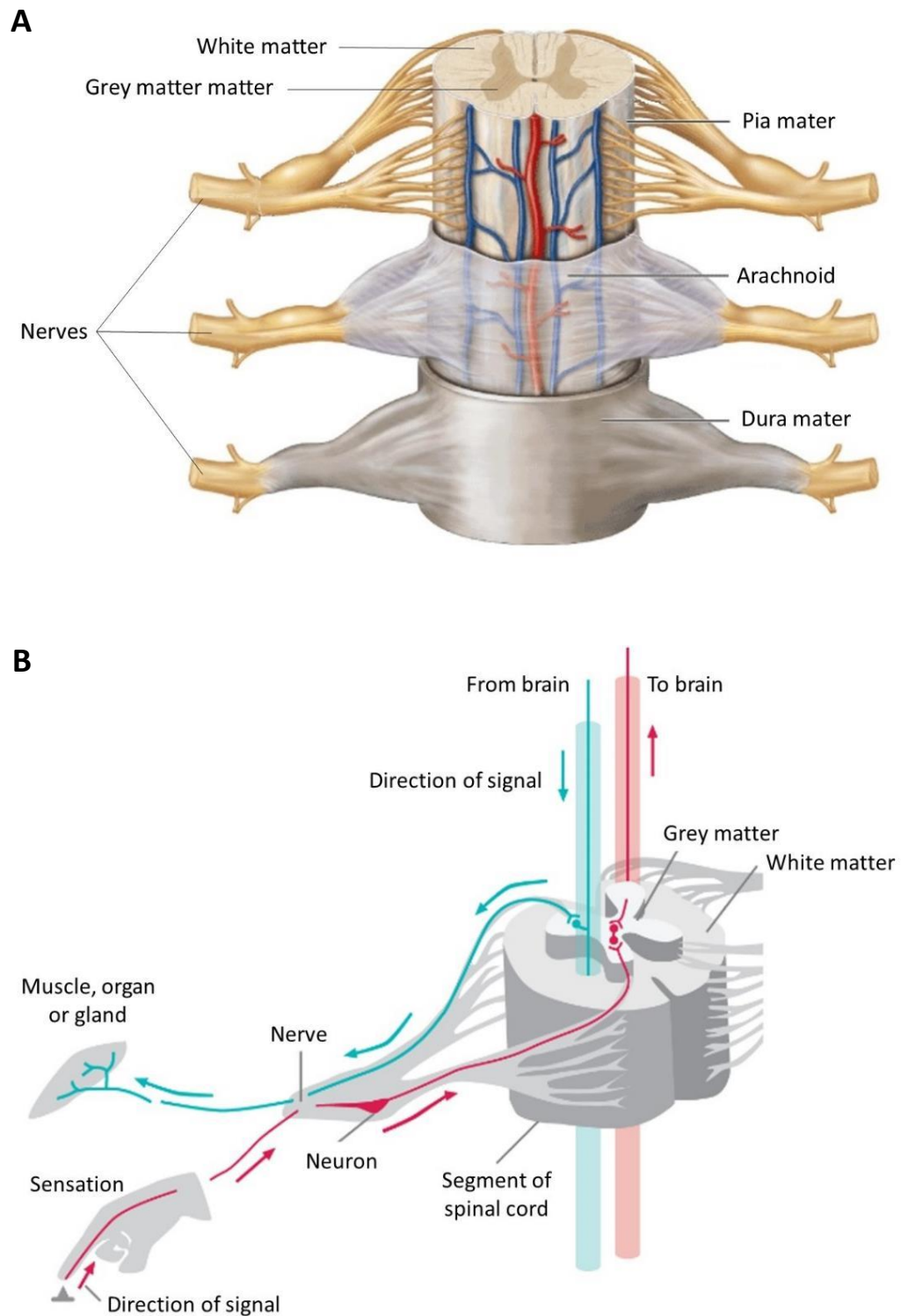


Figure 1.1. Schematic representation of the spinal cord anatomy and function. A) The SC is made of grey matter, mainly composed of cell bodies. This is surrounded by white matter, which is formed by myelinated axons (tracts). SC is protected by the meninges (dura mater, arachnoid and pia mater). B) SC enables the transmission of information between the brain and the PNS, controlling both somatic and autonomic reflexes. Adapted from Mescher (2016)

Among the different types of neuronal cells in the spinal cord, neurons are responsible for the transmission of electrical signals between the CNS and the PNS through a highly connected neuronal network. Neurons are identified by the expression of β -III tubulin, microtubule associated protein 2 (Map2) (Caceres *et al.* 1986) and diverse types of neurofilaments (NF) (Lee & Cleveland 1996). Their multipolar morphology allows neurons to receive chemical signals from other neurons and transmit them via axonal projections (synapses) over long distances. There are several types of neurons and each of them plays a different role in the transmission of an electrical signal. Sensory neurons bring information from the receptor to the spinal cord and link, through the interneurons, with the motor neurons that carry impulses out to the effector, such as muscles or glands (Sheerin 2004).

Neurons have a characteristic electrically excitable membrane that allows the generation of action potentials and therefore, the transmission of information along the spinal cord. At resting state, neurons contain high intracellular concentration of K^+ and low concentration of Na^+ and their neuronal membranes are held at a low potential. Chemical stimulation provokes the membrane depolarization to its threshold potential, which in turn leads to the opening of voltage-activated ion channels and the entrance of Na^+ ions into the cell, starting an action potential. The action potential travels along the neuron as Na^+ channels open. As soon as depolarization is complete (peak action potential), Na^+ channels inactivate and K^+ channels open, allowing K^+ to leave the cell, bringing the membrane potential to more negative values than the cell's normal resting potential (hyperpolarization).

Passive diffusion of the extra K^+ ions out of the cell through the potassium leakage channels, allows the cell to return to its resting membrane potential (**Figure 1.2**).

In order to achieve an efficient action potential transmission over long distances, axons are covered by myelin sheaths. Myelin acts as an insulator preventing current loss from the axons and increasing the speed of the axon potential conduction. There are specific areas in the axon uncovered by myelin, called nodes of Ranvier (Tasaki & Mizuguchi 1948). These myelin sheath gaps are highly rich in Na^+ and K^+ channels, allowing the regeneration of the action potential repeatedly along the axon, accelerating the action potential transmission. Since action potentials "jump" from one node to the next, this process is known as saltatory conduction (Purger *et al.* 2016) (**Figure 1.3**).

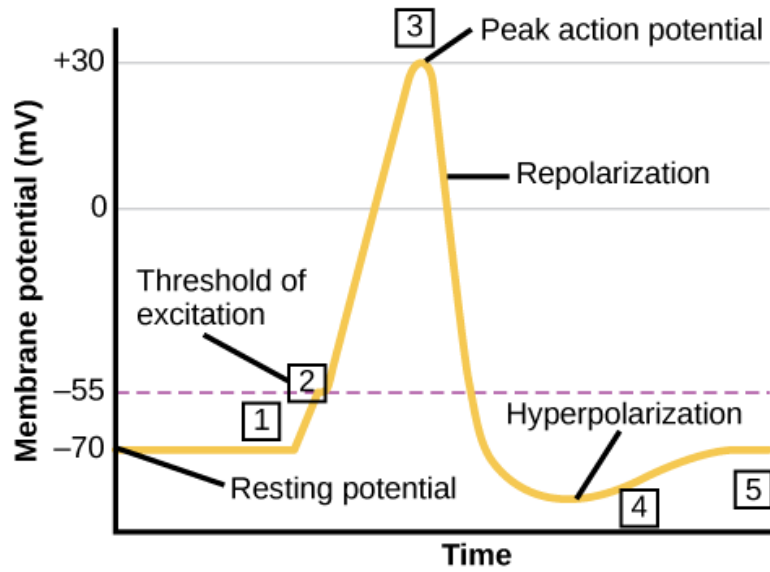


Figure 1.2. Action potential transmission along the axon. (1) A chemical stimulus causes the neuronal membrane depolarization toward the threshold potential. (2) When the threshold of excitation is reached, Na^+ channels open and the membrane depolarizes. (3) At the peak action potential, K^+ channels open and there is an efflux of K^+ out of the cell. Simultaneously, Na^+ channels close. (4) The membrane becomes hyperpolarized as K^+ ions continue to leave the cell. (5) The K^+ channels close and K^+ leaves the cell by passive diffusion through potassium leakage channels.

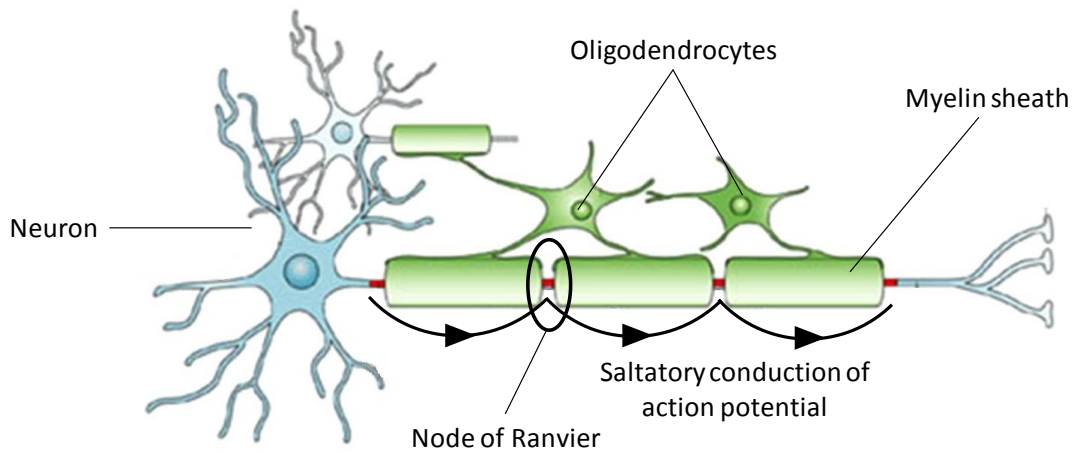


Figure 1.3. Schematic representation of the action potential propagation through saltatory conduction. The transmission of action potentials over long distances is enabled by axons myelination. Nodes of Ranvier allow the regeneration of action potentials repeatedly, “jumping” from one node to the next (saltatory conduction). Adapted from Siddique & Thakor 2013.

Oligodendrocytes synthesize myelin providing insulation to axons, but also, they provide trophic support to neurons by the production of glial cell line-derived neurotrophic factor (GDNF), brain-derived neurotrophic factor (BDNF) and insulin-like growth factor-1 (IGF-1) (Bradl & Lassmann 2010). Numerous processes extend from the body of oligodendrocytes, allowing one single cell to myelinate multiple axons (Watkins *et al.* 2008). Oligodendrocytes are identified by the expression of myelin-associated proteins such as myelin basic protein (MBP), myelin/oligodendrocyte specific protein (MOSP) or galactocerebroside (GalC) (Bucht & Baron-Van Evercooren 2009).

The CNS possesses its own set of immune cells, called the microglia. These cells are identified by the expression of cell surface markers such as CD11b, CD45 and ionized calcium binding adaptor molecule 1 (IBA-1) (Sedgwick *et al.* 1991). Microglia form a network of cells distributed throughout the central nervous system. They act as macrophages, phagocytosing and scavenging the CNS for damaged or unnecessary neurons and infectious agents (Gehrmann *et al.* 1995). Furthermore, microglia play a key role in inflammation, releasing active molecules that activate a cascade of inflammation events as a response after damage or infection (Aloisi 2001).

Homeostatic support to neuronal cells is provided by astrocytes. These star-shaped cells are identified by the expression of glial fibrillary acidic protein (GFAP) and S100b calcium-binding protein (Nolte *et al.* 2001; Ogata & Kosaka 2002). As part of their supporting role in the CNS, they provide biochemical support to endothelial cells that form the blood–brain barrier, supply nutrients to the nervous tissue and maintain the extracellular ion balance. They are also responsible for the scarring

process following SCI (Kimelberg & Nedergaard 2010). Hence, a highly controlled coordination of all the neuronal cell types is of a key importance in the maintenance of the proper function of the spinal cord.

1.1.2 Pathophysiology

Spinal cord injuries can cause the permanent loss of motor and sensory function. Depending on the location and severity of the damage, injury can be *complete*, leading to a total loss of function, or *incomplete*, where some motor and sensory function remains in the organism. SCI creates a highly complex inhibitory environment with a multitude of obstacles that limit the recovery. When the spinal cord is injured, there is a physical disruption of axons, cell membranes and blood vessels, which occurs as the direct result of the mechanical trauma. This primary injury provokes a cascade of cellular and biochemical reactions that leads to further damage and the significant expansion of the injury site, known as secondary injury (Fleming *et al.* 2006).

Primary injury occurs as a result of blunt impact, compression or penetrating trauma. Blunt impact leads to concussion, contusion, laceration, transection or intraparenchymal haemorrhage, whereas hyperflexion, hyperextension, axial loading, and severe rotation might be caused by cord compression. Penetrating trauma can occur as a result of gunshots and stab wounds. Immediately after mechanical trauma, cell membranes become disrupted leading to cell necrosis at the point of impact (Hulsebosch 2002). The physical insult of the cord also leads to the

disruption of the blood-spinal cord barrier, allowing immediate neutrophil invasion into the neural tissue and activation of resident microglia (Fleming *et al.* 2006).

In a secondary injury, activated microglia release pro-inflammatory molecules attracting blood monocytes to the lesion site and hence, increasing the inflammation (Donnelly & Popovich 2008). The release of proteolytic and oxidative enzymes by activated microglia leads to DNA and protein damage, which subsequently drives cell death and disruption of neuronal signalling (Fleming *et al.* 2006). Activated microglia also release neurotransmitters, such as glutamate, causing their accumulation and the loss of homeostasis, thereby provoking cell death via excitotoxic mechanisms (Yanase *et al.* 1995). Oligodendrocytes are damaged by macrophages at the lesion site after the injury and continue to undergo apoptosis in the neural tissue for many weeks after SCI (Comalada *et al.* 2012). The result of the loss of oligodendrocytes is the demyelination of axons (Hains *et al.* 2003). During the process of demyelination, axons are directly exposed to damaging effects such as inflammatory cytokines and free radicals, leading to neuronal loss. As a result, demyelination leads to delays in conduction or even its total disruption (McTigue 2008).

Activation of an inflammatory response contributes to the formation of axonal growth-inhibitory glial scar and the production of pro-inflammatory radicals, leading to a harsh environment at site of injury which is responsible for the limited regeneration capacity of the injured spinal cord (Rolls *et al.* 2008). Several days after the primary injury, astrocytes migrate towards the injury site and proliferate forming a tight interwoven called the glial scar (Kawano *et al.* 2012). The glial scar is regarded as a mechanically obstructive barrier, preventing the infiltration of immune cells and

inflammatory molecules to restrict the damage area (Cregg *et al.* 2014). The expression of inhibitory molecules, such as chondroitin sulphate proteoglycans, contributes to the glial scar inhibiting axonal regrowth (McKeon *et al.* 1991). However, recent studies have demonstrated that astrocytes express multiple axon-growth-supporting molecules suggesting that, contrary to the widely established consideration, astrocyte scar formation might aid rather than prevent axon regeneration in the central nervous system (Anderson *et al.* 2016).

1.1.3 Tissue engineering approaches for SCI

Microglia activation following SCI is maximal between 3 and 7 days post-injury, causing widespread cell damage and deterioration of the extracellular matrix (Sinescu *et al.* 2010). These inflammatory events in the first week after SCI create a hostile environment, which is lethal to transplanted cells. This explains the low effectivity of cell replacement therapies during this period of time (Okano *et al.* 2003; Coyne *et al.* 2006). Hence, researches have attempted different strategies for the successful grafting of transplanted cells. Most of these therapies centre on cell injection following the acute *phase* of SCI, when the release of inhibitory and lethal molecules has ceased. However, the already formed glial scar hinders the integration of the transplanted cells within the host tissue, preventing regeneration of damaged tissue (Coyne *et al.* 2006; Cregg *et al.* 2014).

The variety of processes inhibitory to axonal regeneration caused by SCI creates a multitude of obstacles limiting recovery, which together hinder the effectiveness of single therapeutic interventions. This challenge has encouraged the

development of combination strategies that work together synergistically to improve recovery. Seemingly, the most effective approach should incorporate the integration of scaffolds along with therapeutic molecules and/or cells into the site of injury. Scaffolds help direct and organize the grafted cells providing a bridge through which the regenerating axons can be properly guided through the injury gap, at the same time that grafted cells and therapeutic molecules provide trophic support to regenerating axons. This increases the healing effects of the scaffold. Several scaffolds have been successfully utilized as support for transplanted cells, including matrigel (Pinzon *et al.* 2001), fibrin (Meijs *et al.* 2004) and poly(α -hydroxy acids) (Teng *et al.* 2002). However, only collagen and alginate constructs will be introduced in detail in this section, since these are the hydrogels utilized in this thesis.

Due to the versatility of alginate, this hydrogel has been utilized for the immobilization of numerous cell types in different construct shapes. Alginate sponges supported the migration, differentiation and integration of foetal rat hippocampus neurospheres into the injured spinal cord (Wu *et al.* 2001). In another study, alginate microcapsules containing BDNF promoted the growth of regenerating axons through the implanted microcapsules, leading to functional improvement of the affected limbs in a rat *in vivo* SCI model (Tobias *et al.* 2005). In a different approach, NSCs immobilized within alginate fibres migrated into injured spinal cord of mice and they differentiated towards the three neural cell types, neurons, oligodendrocytes, and astrocytes (Sugai *et al.* 2015).

Like alginate, the ease of manipulation of collagen into various shapes/structures has permitted its application to fill the gap invoked after SCI,

thereby providing support to wound healing cells. Application of cross-linked collagen and collagen filaments has been studied in animal models of SCI and demonstrated to increase regenerative activity in the spinal cord with a subsequent improvement in the functional disability (Yoshii *et al.* 2004). The use of collagen gels as vehicles to transplant neonatal astroglial cells into the injured spinal cord of the adult rat allowed the precise application of these cells into the lesion gap (Joosten *et al.* 2004). The presence of transplanted neonatal astroglial cells demonstrated a significant increase in the number of ingrowing neurofilament-positive fibres, resulting in a modest but temporary improvement of locomotor recovery. More recently, a collagen construct bound to epidermal growth factor receptor (EGF) antibody Fab fragment was transplanted into an acute rat SCI model (Fan *et al.* 2017). By neutralization of the myelin inhibitory molecules, the construct promoted neurogenesis of endogenous injury-activated neural stem cells (NSCs). NSCs differentiated into mature functional neurons that were able to reconnect the injured gap.

1.2 Stem Cells

Stem cells are unspecialized cells with an enhanced renewal capacity and the potential to differentiate towards multiple lineages, depending on external stimuli controlled by the stem cell niche (Moore & Lemischka 2006). These unique features make stem cells ideal candidates for use as a renewable source for cell therapy in regenerative medicine, repairing or replacing damaged tissues. Depending on the tissue of origin, stem cells are classified as embryonic or adult stem cells.

1.2.1 Embryonic Stem Cells

Embryonic stem cells (ESCs) are isolated from the inner cell mass of the blastocyst, an early stage embryo produced about 5 days after fertilization (Evans & Kaufman 1981; Martin 1981). These cells have the potential to differentiate into any cell type within the three germ layers: ectoderm, mesoderm and endoderm, and thus, they are pluripotent stem cells. This pluripotent state is conserved through regulatory networks composed of transcription factors and signalling cascades, where Oct4, Nanog and Sox2 have essential roles in maintaining ESCs self-renewal capacity. Alterations in these signals promote differentiation towards specific cell types (Boyer *et al.* 2005).

Oct4 expression is restricted to pluripotent cells and thus, a loss of pluripotency in ESCs is often accompanied by Oct4 downregulation (Thomson *et al.* 2011). Oct4 must be present at appropriate levels to maintain pluripotency, since an increase causes differentiation towards endoderm and mesoderm lineages, and a

decrease leads to the formation of the outer cell mass of the blastocyst, the trophectoderm (Niwa *et al.* 2000). Nanog is another key regulator of pluripotency. Like Oct4, its expression is restricted to pluripotent cells and is downregulated upon differentiation. It plays a critical role in regulating the cell fate of pluripotent ESCs, preventing differentiation (Chambers *et al.* 2003). High levels of Nanog can maintain mouse ESCs self-renewal capacity independent of extrinsic signals (Chambers *et al.* 2003) and enables human ESCs grow in feeder-free conditions (Darr *et al.* 2006). Together with Oct4 and Nanog, regulation of Sox2 expression levels is essential in the maintenance of ESCs pluripotency. Adachi and co-workers reported that both upregulation and downregulation of Sox2 led to a decrease in Nanog and Oct4 expression, causing trophectoderm differentiation (Adachi *et al.* 2010).

During embryonic development, the blastocyst is reorganized into a laminar structure called gastrula in a process known as gastrulation. The gastrula contains the three primary germ layers: ectoderm, mesoderm, and endoderm that further differentiate into different tissues. Endoderm, the most internal germ layer, forms the lining of digestive system and respiratory system. Ectoderm, the most exterior germ layer forms the epidermis, and the neural crest, which later forms the nervous system. Mesoderm, the middle germ layer, forms muscle, the skeletal system, and the circulatory system. As the embryo develops, stem cells capacity to differentiate into more specialized cells becomes more restricted towards the tissue of origin (Nichols & Smith 2012).

Mouse embryonic stem cells can be isolated and propagated indefinitely without undergoing cell senescence *in vitro* when cultured in the presence of

leukaemia inhibitory factor (LIF) (Smith *et al.* 1992). Upon removal of LIF, mouse ESCs spontaneously differentiate towards progenitor cells of the three embryonic germ layers: mesoderm, endoderm, and ectoderm (Keller 2005). These findings highlight the enormous potential of ESCs for the treatment of a variety of diseases due to their ability to differentiate into any cell type within the three germ layers. However, the therapeutic application of human ESCs is still debated due to ethical concerns derived from the fact that their isolation involves the destruction of the embryo. Also, their application in human therapy is controversial due to problems of allogeneic rejection and concerns about uncontrolled development of malignancies (Hentze *et al.* 2007).

1.2.1.1 Neural Stem Cells

NSCs are present in both embryonic and adult tissues. Isolation of NSCs from the adult mammalian central nervous system was first described by Reynolds & Weiss in 1992 using a novel serum-free culture system, the neurosphere assay (NSA). The same procedure can be applied for the isolation of embryonic NSCs (Azari *et al.* 2011). After isolation, NSCs can be cultured *in vitro* in the presence of EGF and/or basic fibroblast growth factor (bFGF). Cells proliferate giving rise to neurospheres which can be passaged over extended periods of time, demonstrating long-term self-renewal and multipotency capacities (Zhao *et al.* 2005). However, upon removal of growth factors, neurosphere-derived cells are induced to differentiate towards the three neuronal phenotypes: neurons, astrocytes and oligodendrocytes (Pagano *et al.* 2000; Guo *et al.* 2012).

NSCs are typically characterised by the expression of nestin and musashi. Nestin is an intermediate filament protein expressed by NSCs (Morshead *et al.* 1994). Upon differentiation, nestin becomes downregulated and is replaced by tissue-specific intermediate filament proteins (Michalczyk & Ziman 2005). Musashi is an RNA-binding protein that regulates the translation of target mRNAs during neural development. This marker contributes to the maintenance of mammalian adult neural stem cell populations (Sakakibara *et al.* 2002).

1.2.2 Adult Stem Cells

Most of the differentiated cells in adult tissues have a relatively short life span and are continuously replaced by new cells generated from stem/progenitor cells. In the adult mammalian organism, stem cells are found in almost all tissues and play a key role in maintaining cell genesis and renewal in different tissues and organs during the life span of the animal as part of the natural aging process, or after cell loss due to injury or disease (Pessina & Gribaldo 2006).

One of the main differences between embryonic and adult stem cells (ASCs) is their ability to differentiate into different cell types; that is, their potency. Whilst ESCs are pluripotent, ASCs are multipotent or unipotent, in that their differentiation potential is more restricted and depends on their tissue of origin (Wagers & Weissman 2004). However, several observations proved that these tissue-specific stem cells are able, under suitable conditions, to “transdifferentiate” towards a wider range of cell types, regardless whether these tissues are derived from the same germ layer or not (Anderson *et al.* 2001). This observation opens a new spectrum of

possibilities for adult stem cells to be used in regenerative medicine. In fact, a relatively new source of ASCs with pluripotency capacity was discovered in 2006, referred to as Induced Pluripotent Stem Cells (iPSCs) (Takahashi & Yamanaka 2006). These cells were reprogrammed from adult fibroblasts through the addition of defined factors and demonstrated to have the primary properties of ESCs. Thus, iPSCs can be developed from autologous somatic cells, avoiding ethical and immune problems.

As outlined at the beginning of this section, ASCs can be found in the majority of tissues within the organism. Amongst these tissues, the bone marrow is the most widely used source for the isolation of stem cells (Soleimani & Nadri 2009; Huang *et al.* 2015). There are two stem cell types derived from the bone marrow: Hematopoietic Stem Cells (HSCs), that give rise to all blood cell types (Eaves 2015) and Mesenchymal Stem Cells (MSCs; also known as Mesenchymal Stromal Cells), which are the source of osteocytes, chondrocytes, and adipocytes (Gimble *et al.* 2008). However, the painful and invasive procedures involved in the isolation of BMSCs from bone marrow have encouraged researches to seek alternative sources of stem cells (Pendleton *et al.* 2013).

1.2.2.1 Dental Pulp Stem Cells

The dental pulp is the soft tissue found in the inner part of the tooth, which is mainly formed of connective tissue, blood capillaries, nerves and several cell types, including fibroblasts, odontoblasts and immune cells (Liu *et al.* 2006). The dental pulp acts as a sensory organ through nerves that perceive changes in temperature and

pressure. It constitutes a protectant part of the tooth, triggering immune responses against oral pathogens (Jontell *et al.* 1998). During tooth development, dental pulp is the responsible for the formation of primary dentin through the production of odontoblasts. After completion of root development, secondary dentin is produced through life at a slower rate. In cases of mild injury, odontoblasts produce reactionary dentin (Smith *et al.* 1995). However, after severe trauma, such as caries or fracture, odontoblasts are damaged and subsequently die. Hence, newly produced odontoblast-like cells migrate towards the injured dentine surface and secrete reparative dentin, providing a protective barrier to the dental pulp (Liu *et al.* 2006).

The ability to create new odontoblasts throughout life in response to damage suggested the existence of a source of stem cells within the dental pulp. Gronthos *et al.* in 2000 isolated a clonogenic, rapidly proliferative population of cells from adult human dental pulp, which were termed Dental Pulp Stem Cells (DPSCs). After comparison with BMSCs, both cell types shared a similar immunophenotype *in vitro* but they showed different cell fate *in vivo*. When DPSCs were first described, it was suggested that their differentiation potential was restricted towards odontoblast-like cells, as demonstrated by the ability to form a dentin-like structure *in vivo* (Gronthos *et al.* 2000). However, further studies showed their potential to differentiate into adipocytes and neuronal-like cells, suggesting that DPSCs are an easily accessible source of multipotent stem cells (Gronthos *et al.* 2002).

More recently, a set of markers has been described which characterise DPSCs (Kawashima 2012). These markers include STRO-1, CD29, CD44, CD73, CD90, CD105,

CD146, CD166 and CD271, which are typically expressed by MSCs. Hence, DPSCs are generally classified under this cell type. However, DPSCs represent a heterogeneous population of cells, and their marker expression profile vary depending on their isolation source (Graziano *et al.* 2008; Karaöz *et al.* 2010). This can be explained due to the existence of two different origins for these stem cells, the neural crest and the mesoderm (Komada *et al.* 2012). In fact, DPSCs can be isolated from different stem cell niches within the pulp, giving rise to stem cell populations with different proliferative and differentiation potentials (Shi & Gronthos 2003; Løvschall *et al.* 2005; Lizier *et al.* 2012). This heterogeneity has been investigated in our lab in respect of their potential for neuronal differentiation (Young *et al.* 2016). These results led to the conclusion that the expression of nestin by some clonogenic populations of DPSCs could be used as a marker to identity cell populations with neuronal differentiation potential.

Due to the expression of mesenchymal (Ponnaiyan & Jegadeesan 2014) and ESC markers (Kerkis *et al.* 2007), various studies have been performed to evaluate the differentiation potential of DPSCs, revealing that they have the ability to produce many kinds of cell populations and tissues (Tatullo *et al.* 2015). However, due to the wide repertoire of possibilities of DPSCs in regenerative medicine, only the potential for neuronal differentiation and repair will be considered in this thesis.

1.2.2.1.1 Neuronal Regenerative potential of DPSCs

Several protocols have been developed for *in vitro* differentiation of DPSCs into neuronal cells, based on the differentiation mechanisms of NSCs *in vitro*. NSCs are maintained as multipotent cells in culture in the presence of mitogens such as bFGF and EGF. However, removal of these growth factors from the culture medium leads to the differentiation of NSCs towards neuronal cells (Pagano *et al.* 2000; Guo *et al.* 2012). Based on this method, DPSCs have been differentiated into neuronal-like cells (Hisham *et al.* 2013). When cultured in serum and growth factor free medium, DPSCs ceased proliferation and differentiated into neuronal-like cells as demonstrated by the development of multiple neurites and the expression of neuronal markers such as nestin, map2 and β -III tubulin.

Nonetheless, expression of neuronal markers is only a pre-requisite for neuronal differentiation. In order to successfully apply DPSCs for the treatment of CNS diseases, differentiated cells must be proven functionally active. Patch-clamp electrophysiology recording techniques have been applied to assess the functionality of neuronal-like cells differentiated from DPSCs (Arthur *et al.* 2008; Király *et al.* 2009; Gervois *et al.* 2015). Among the protocols developed for neuronal differentiation of DPSCs, only a few have demonstrated the production of functionally active neurons. Kanafi *et al.* (2014) demonstrated for the first time that it was possible to produce functional dopaminergic neurons from DPSCs when the cells were cultured under the presence of midbrain cues, including sonic hedgehog (SHH), fibroblast growth factor 8 (FGF8) and bFGF. Functional activity of differentiated DPSCs was demonstrated by the secretion of dopamine upon stimulation with KCl and ATP, and the intracellular Ca^{2+} influx in the presence of KCl.

The differentiation of DPSCs towards functionally active neuronal cells has been also achieved following a two-step protocol (Gervois *et al.* 2015). Neuronal induction was acquired through the formation of neurospheres when DPSCs were cultured with mitogenic growth factors in low-adherence plates. In a second step, cells underwent neuronal maturation based on cAMP and neurotrophin-3 (NT-3) signalling after seeding on poly-l-ornithine (PLO)/laminin coated plates. Patch-clamp assessment showed that differentiated cells were able to set a single action potential, demonstrating functional activity.

In addition to the ability of neuronal lineage differentiation, DPSCs have the potential for secretion of trophic factors, affecting the behaviour of neighbouring cells. Nosrat *et al.* (2004) compared the behaviour of dopaminergic neurons cultured *in vitro* with and without DPSCs in the absence of exogenous neurotrophic factors. Results revealed that neurons developed elaborate neurites only when they were co-cultured with DPSCs, suggesting the key role of DPSCs in the growth and maintenance of neurons *in vitro* by the release of growth factors. Also, the release of neurotrophins by DPSCs promoted the neuronal differentiation of stem cells in a 3D culture system (Soria *et al.* 2011). These findings suggest new criteria for the design of cell therapy experiments in animal models to assist the repair of lesions in the CNS, based not only on the direct cellular replacement, but also on the application of DPSCs as trophic support for regenerating cells.

The promising results obtained *in vitro* have encouraged researches to assess the regeneration potential of DPSCs within the CNS *in vivo*. The capacity of DPSCs to promote growth and differentiation of stem cells through the release of growth

factors has been observed after injection in the mouse hippocampus (Huang *et al.* 2008). The grafted DPSCs promoted proliferation, cell recruitment and maturation of endogenous stem cells through modulation of the local microenvironment by promoting growth factor signalling. A similar behaviour was observed in a rodent stroke model (Leong *et al.* 2012). The intracerebral transplantation of human DPSCs resulted in significant improvement in forelimb sensorimotor function several weeks after treatment. However, a low percentage of the grafted cells survived, suggesting that functional improvement was more likely to be mediated through DPSC-dependent paracrine effects than direct cellular replacement. However, when DPSCs were transplanted into rats' spinal cords after complete transection, they promoted the regeneration of transected axons through three major neuroregenerative mechanisms, including cellular replacement (Sakai *et al.* 2012). It was observed that transplanted DPSCs differentiated into mature oligodendrocytes, replacing lost cells after SCI. But also, the grafted cells prevented apoptosis of endogenous neural cells and inhibited multiple axon growth inhibitors, improving the preservation of neuronal filaments and myelin sheaths.

DPSCs provide an easily available source of stem cells with promising potential for the treatment of neurodegenerative diseases. Their isolation through a minimally invasive procedure, offers some benefits when compared with BMSCs. Unlike the use of ESCs, DPSCs also provides benefits in that their use does not raise ethical concerns. Finally, these ASCs can be isolated from patients for autologous transplantation without risk of immunological rejection, avoiding the use of immunosuppressants and hence, preventing damage to vital organs due to the use

of these drugs (Halloran 2004). Hence, all the benefits mentioned above justify the increasing interest for clinical use of DPSCs in the treatment of a number of diseases.

1.3 Cell encapsulation

As outlined in the previous section, stem cells are potent therapeutic tools to treat several diseases based on their ability to differentiate towards a desired lineage, or, by providing trophic support to regenerating tissues. However, it is difficult to control the behaviour and cell fate within an organism. It is also necessary to find a suitable stem cell delivery system in order to control cell parameters *in situ*, such as proliferation, migration, integration and differentiation. To this end, cell encapsulation technology has arisen as a method for cell immobilization within a biocompatible and semipermeable scaffold, protecting the encapsulated cells from an adverse environment post-grafting.

The first reported attempt of cell immunoisolation was made in the early 1930s (Bisceglie 1933). Bisceglie filled a gelatine membrane with tumour cells harvested from a mouse carcinoma, which was then inserted into the peritoneal cavity of a guinea pig. Upon removal of the graft 12 days after implantation, it was observed that the cells within the membrane were still alive. Although the focus of the experiment was to investigate tumour immunology, this observation led to the discovery of a new methodology for cell implantation.

Cell encapsulation has been the focus of many researchers in order to protect the enclosed biological material from potential hazardous processes (Freimark *et al.* 2010). Specifically, cell microencapsulation represents a strategy that aims to overcome the present difficulties related to whole organ graft rejection, and consequently, the requirements for use of immunosuppressive drugs. In the case of autologous transplantation, where the patient receives cells from themselves,

cellular rejection is not an issue. However, grafted cells might still need protection from the adverse environment created at the damaged site, as in SCI (Fleming *et al.* 2006). Also, cell encapsulation has been demonstrated to be useful in directing the cell fate of immobilized cells, suggesting that cell fate can be controlled by the composition/structure of the encapsulation matrix (Ghasemi-Mobarakeh 2015).

1.3.1 Requirements of cell encapsulation systems

The microcapsule system must meet some distinct requirements in order to guarantee both the survival of the encapsulated cells and a successful clinical outcome. These requisites include capsule stability, permeability and diffusion.

1.3.1.1 Stability

The mechanical stability of the microcapsules needs to be such that it can withstand the shear stress induced during production, handling and application during a surgical procedure. The desired mechanical properties of microcapsules depend on their application. For example, applications such as bone and cartilage grafts, or, sustained release of therapeutic molecules over extended periods of time, requires a long-term stability of the polymer microcapsules (Zhu & Marchant 2011; Tiwari *et al.* 2012). In these cases, degradation of capsules due to chemical changes is undesirable, since capsules will quickly lose integrity, the graft will be lost and hence, the therapeutic effect will be interrupted. In other applications, microcapsules are utilized as vehicles for cell and/or drug delivery (Santoro *et al.*

2014). Under these conditions capsules should provide protection from the immune response but they should progressively degrade as inflammation decreases to allow for the delivery of the encapsulated material. The mechanical strength can be controlled by changing the polymer concentration, polymerization conditions, or by introducing various functional groups (Coutinho *et al.* 2010).

1.3.1.2 Permeability

In the situation whereby the application involves the transplantation of encapsulated cells, the capsule membrane should be impermeable to antibodies and immune cells, thereby providing protection for the encapsulated cells from the immune response after grafting. However, this will depend upon the type of transplantation. Autografts should not trigger any immune response since the transplanted biological material derives from the same patient. In the case of allografts, where cells from an individual are transplanted to a different individual, it is potentially enough to prevent contact between immune cells of the host and the donor cells through a physical barrier, such as that provided by the capsule membrane (Duvivier-Kali *et al.* 2001). However, simple systems are not effective in the case of xenografts (cross species transplantation), where biological material from one specie is transplanted into a patient of a different specie, i.e. from animals to humans. Transplants across different species barriers are subject to strong immunologic rejection, hindering the success of xenogeneic transplantation (Yang & Sykes 2007). Xenogeneic cells contain pathogen-associated molecular patterns (PAMPs) that are recognized by the host and activate the innate immune cell system

that, in turn, activates the classical complement pathway. This activation leads to the production of antibodies that accumulate on the surface of the implanted capsules, triggering the mobilization of cells and producing inflammatory mediators towards the implantation site (Wang & Yang 2012). During these responses, many cytokines that are small enough to pass through the capsule membrane are produced, further contributing to the failure of the encapsulated cells (Juste *et al.* 2005). The final result of this cascade is the envelopment of the capsules by inflammatory cells and fibroblasts that scavenge almost all oxygen and nutrients and lead to ischemic compromise of the surviving cells in the capsules. Under ischemia conditions, cells produce specific factors that lead to a progressive fibrosis, and gives rise to a further loss of cell functionality (Sun *et al.* 2009).

As a consequence of the vigorous immunological responses triggered in xenogeneic transplantation, stricter encapsulation requirements should be considered. In these cases, additional coating of the capsule membrane is then required to block the entrance of cytokines. The xenotransplantation of rat islets in diabetic minipigs without immunosuppressive therapy was successfully achieved by means of cell encapsulation in a membrane system that included an additional barrier between the capsule membrane and the interface with the recipients (Neufeld *et al.* 2013). In a different approach, a multifunctional hydrogel-based scaffold consisting of murine cell-loaded alginate-poly-l-lysine-alginate (APA) microcapsules and dexamethasone (DXM)-loaded poly(lactic-co-glycolic) acid (PLGA) microspheres embedded in alginate hydrogel was injected in an *in vivo* rat model (Acarregui *et al.* 2014). The system did not trigger inflammation responses and it allowed for the continuous and localized release of DXM.

1.3.1.3 Diffusion

Another parameter that should be controlled in order to increase the survival chance of the encapsulated cells is the diffusion of molecules in and out of the capsule. The encapsulation material should permit the bidirectional diffusion of oxygen and nutrients inside the capsule and the efflux of waste products and therapeutic molecules, such as growth factors. In this sense, membrane permeability can be tailored depending on the polymer composition. Thus, by controlling the molecular weight and degree of cross-linking of the polymer, the pore size can be modified in order to allow the bidirectional diffusion of molecules (Vaithilingam & Tuch 2011). The diffusion rate of a molecule through a membrane is determined by its size and charge, and the charge of the polymer membrane (Danysh *et al.* 2010). Hence, these are factors to consider when selecting the appropriate encapsulation material. In order to ensure the survival of encapsulated cells, oxygen and nutrients not only have to pass through the polymer membrane, but also need to reach the centre of the capsule to provide nutrition to every cell. Hence, capsules of appropriate diameter must be produced in order to guarantee an effective oxygenation and nutritional regime for the encapsulated cells (Ogbonna *et al.* 1991). Also, it has been demonstrated that the diameter of the capsule could influence the immune response against the grafting. Sakai *et al.* (2006) observed that inflammatory reaction was much lower when employing smaller microcapsules (100 μm), in comparison to larger sized microcapsules (300 – 1000 μm). In this respect, the selection of the encapsulation technology is crucial to achieve monodisperse microcapsules with a controllable diameter.

1.3.2 Applications of cell encapsulation

Advances in the fields of cell therapy and biomaterials have triggered the increased interest and progress of cell encapsulation technology (Burdick *et al.* 2016). This technique was first utilised to overcome the problems related to organ graft rejection and the need to use immunosuppressive drugs. However, the versatility of this technique, born from the great number of biomaterials and cell types that can be combined, has allowed its application in other fields, such as *in vitro* culture (Mei *et al.* 2014; Chen *et al.* 2015) or controlled release of drugs and growth factors (Qutachi *et al.* 2013; Nam *et al.* 2016).

1.3.2.1 Immunoisolation in transplantation therapy

Cell encapsulation has been widely applied for the immobilization of allogeneic or xenogeneic cells in a semipermeable but immunoprotective membrane to suppress immune rejection after grafting (Lee & Bae 2000; Emerich & Winn 2001; Hao *et al.* 2005). Pancreatic islet transplantation has shown improved graft function in the treatment of type I diabetes. However, adequate long-term therapeutic effect has not yet been demonstrated, and patients still require immunosuppression to prevent rejection (Van Belle & Von Herrath 2008). Cell encapsulation offers a transplantation means to avoid the need for toxic immunosuppressives, while increasing the chances of graft function and survival. Thus, islet encapsulation has proven to be effective in many studies, including allogeneic and xenogeneic transplantation (Duvivier-Kali *et al.* 2001; Neufeld *et al.* 2013). Microencapsulation

of therapeutic cells also represents a promising therapy for the treatment of other diseases, such as haemophilia B. Immunoisolation of myoblasts secreting factor IX (FIX) and further transplantation into mice permitted the improvement of FIX plasma levels without the activation of the immune response (Wen *et al.* 2007).

1.3.2.2 Local and systemic controlled release of drugs and growth factors

Living cellular systems can provide unlimited release of active compounds. Hence, encapsulation of therapeutic cells offers a tuneable method for an effective and controlled drug delivery. Encapsulated delivery systems present numerous advantages compared to conventional dosage forms, including improved efficacy, reduced toxicity and improved patient convenience (Singh *et al.* 2010). Microcapsules offer an effective protection of the encapsulated active agent against degradation. Also, by controlling the degradation rate of the polymer membrane it is possible to accurately control the release rate of the active compound (Kamaly *et al.* 2016). Furthermore, the small size of microcapsules offers an easy and minimally invasive administration methodology. For example, the systemic delivery of therapeutic factors represents an issue in the treatment of CNS conditions, where the blood/brain barrier hinders their administration (Pardridge 2005). In this case, immunoisolated cellular implants that produce therapeutic drugs could be directly implanted into the region of interest, providing continuous drug delivery (Emerich & Thanos 2006). The application of this technology has led to the establishment of some patented works. For example, the implantation of encapsulated PC12 cells into individuals suffering from Parkinson's disease slowed or prevented the degenerative

processes of the disease by releasing dopamine and other factors (Emerich *et al.* 1998).

1.3.2.3 3D culture systems

The viability, renewal and differentiation of stem cells towards a particular lineage are dependent on the properties of the cellular microenvironment or niche (Discher *et al.* 2009). Cell microencapsulation provides the cells with a three dimensional structure similar to that found *in vivo*, which allows for *in vitro* investigation of the influence of microenvironments on cell behaviour and fate.

Cell proliferation within microcapsules can be controlled by modification of the polymer concentration. This is dependent upon the cell type and the encapsulation material. For example, it was determined that the viability and proliferation of ESCs were optimum within 1% (w/v) alginate hydrogels, whereas higher or lower concentrations gave rise to a decrease in cell viability and proliferation rate (Wang *et al.* 2009). The degree of cell attachment can be also controlled depending on the polymer composition. Modification of alginate hydrogels with arginine-glycine-aspartic acid (RGD) residues increased cellular attachment and elongation, forming a dense network of cells (Markusen *et al.* 2006). A similar effect was observed in encapsulated cardiomyocytes within alginate-collagen microcapsules, where the cells spread and proliferated giving rise to functional multilayer heart-like tissues (Bai *et al.* 2011).

Stem cell differentiation can be guided through the interaction of encapsulated cells with the encapsulation polymer. The influence of alginate

encapsulation parameters on ESC phenotype has been investigated (Wilson *et al.* 2014a). Results revealed that cell encapsulation delayed the differentiation process, regardless of alginate composition. However, encapsulation within alginates with a high content of mannuronic residues promoted differentiation towards a primitive endoderm phenotype. In a different approach, alginate microcapsules were loaded with retinoic acid, leading to neural lineage differentiation of the encapsulated ESCs (Li *et al.* 2011). The differentiation within microcapsules can be also mediated through cell-cell interactions. For instance, ESCs were induced to hepatic differentiation through the formation of cell aggregates within alginate/poly-L-lysine (PLL) microcapsules, which was controlled by the initial seeding density (Maguire *et al.* 2007).

1.3.3 Cell encapsulation techniques

Microencapsulation within spherical microparticles offers many benefits over other encapsulation geometries, including a high surface area to volume ratio, a high resistance to mechanical stress, a relatively short diffusion path length and access to a number of implantation sites by injection (De Vos *et al.* 2006). However, in order to apply cell encapsulation technology in clinical therapies, the production of uniform capsules with excellent repeatability and reproducibility is required. Formation of monodisperse droplets is of a great importance in order to accurately estimate the cell/drug dosage. Hence, the development of new technologies aims for the continuous production of polymer microcapsules similar in size and morphology.

The simplest technique to produce polymer droplets is by conventional emulsification. In this method, an aqueous polymer solution containing cells is rapidly stirred with an immiscible phase containing cross-linking agents to form small, spherical droplets of one phase within the other (Poncelet *et al.* 1992). The method does not require the use of sophisticated equipment. However, one of the main problems of this technique is the production of microcapsules with very different size and shape, which hinders its application in clinical therapies (Hoesli *et al.* 2011).

Interfacial polymerization represents an alternative to conventional emulsification methods in which the size of the capsule can be easily controlled. In this method, one phase containing the cell suspension and a reactive monomer is dispersed into a second immiscible phase to which is added a second monomer. Both monomers react at the droplet surface (interface) forming a polymeric membrane (Neufeld *et al.* 2014). However, this technique requires the use of organic solvents that are harmful to cells, compromising their viability (Khademhosseini *et al.* 2005).

A different approach to obtain high monodispersity droplets is electrostatic extrusion. In this method, a narrow stream of polymer containing cell suspension is extruded through a small needle or nozzle, whereupon it breaks up into droplets which are collected in a gelling bath. In order to enhance droplet formation, an electrostatic potential is established between the needle and the gelling bath, thus attracting the droplets towards the bath. This method permits the production of microcapsules down to 50 μm in diameter (Bugarski *et al.* 1994). In contrast to emulsion techniques, this technology is reproducible, controllable, and produces beads that are uniform in size. Further, the production process is performed under

mild stress conditions without the use of any organic solvents that can inhibit cell activity and cause serious damaging effects. However, the use of a high electric field might affect cell survival (Vaithilingam & Tuch 2011).

Amongst the techniques described above, droplet extrusion represents one of the most widely used methods for cell encapsulation due to the benefits over other conventional techniques. However, polymer cross-linking takes place in a second step upon collection in a gelling bath. Under these conditions, gelation occurs in an uncontrolled manner and only the outer layer of the capsule is cross-linked, leading to a capsule with a solid shell and a liquid core, which affects the mechanical stability. Hence, although the droplets size can be accurately selected, cross-linking in the gelling bath is not precisely controlled, leading to capsules with random uncontrolled shapes where the gelation of different capsules from the same batch may vary (Capretto *et al.* 2008).

Microfluidic technology overcomes the limitations mentioned above. This technique generates cell-laden microcapsules offering the capability for high-throughput variation in their diameter and mechanical properties by supplying multiple flows of precursor fluids at varying relative flow rates and concentrations (Velasco *et al.* 2012). Microfluidic platforms allow work in a sealed environment protected from the atmosphere, thereby eliminating the risk of cross-contamination from bacteria or small molecules. In addition, microfluidic cell encapsulation can be easily carried out in inexpensive, sterile, dust-free, and disposable devices (Morgan *et al.* 2016). The principles and biomedical applications of microfluidic technology will be further explained in **Section 1.5**.

1.4 Biomaterials

A biomaterial is defined as a material intended to interface with biological systems to evaluate, treat, augment or replace any tissue, organ or function within the body (Williams 1999). In order for it to be used as scaffold for tissue engineering, a biomaterial should be biocompatible, that is, the biomaterial should not interact with biological systems in the host leading to inflammation or any adverse response (Williams 2015). Depending on the application, the material should have specific mechanical properties and a controllable degradation rate, as well as an appropriate microstructure to allow for the performance of the biological function of the encapsulated system, for example cells or macromolecules (Lee & Mooney 2001).

Several categories of biomaterials have been developed and tested for tissue engineering purposes over the last few decades (O'Brien 2011). However, only alginate and collagen will be discussed in relation to this thesis.

1.4.1 Alginate

Alginate is one of the most used biomaterials in biomedical applications such as drug delivery, wound healing and tissue engineering (Lee & Mooney 2012). This is due to its favourable properties, which include biocompatibility, mild gelling conditions, easy manipulation, low toxicity, relatively low cost and a three-dimensional structure *in vitro* which is similar to that found *in vivo*. The wide variety of patterns in which alginate can be prepared, such as microcapsules

(Zhang & He 2009), sponges (Shapiro & Cohen 1997), foams (Andersen *et al.* 2012) and fibres (Xu *et al.* 2017) explains its numerous applications.

1.4.1.1 General properties

Alginate is a naturally occurring anionic and hydrophilic polysaccharide typically extracted from brown algae (Hirst 1965). It is a linear block copolymer formed by (1, 4) linked β -d-mannuronate (M) and α -l-guluronate (G) residues (**Figure 1.4**). The G/M ratio, the length of each block, and the molecular weight are dependent on the initial source of the material .

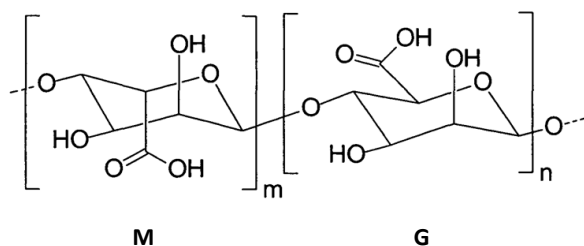


Figure 1.4. Chemical structure of alginate. Alginate is a linear block copolymer formed by (1, 4) linked β -d-mannuronate (M) and α -l-guluronate (G) residues. Adapted from Wallace *et al.* 2010.

Only the G-blocks are believed to participate in ion cross-linking with divalent cations. Therefore, the G/M ratio and sequence are key factors affecting the physical properties of alginate and its hydrogels. Alginates with high ratios of G blocks provide stiffer hydrogels with high viscosities. On the other hand, alginates with a high content in M blocks have a better long-term stability, since M blocks decrease the

number of reactive positions available for hydrolysis degradation (Sun & Tan 2013). Molecular weight also plays a key role in the physical properties of alginate hydrogels. High molecular weight alginates provide gels with greater mechanical properties (Kong *et al.* 2004).

The factors affecting alginate biocompatibility are still unclear. It has been reported that biocompatibility depends on the G/M ratio, suggesting that high M content alginates are immunogenic (Otterlei *et al.* 1991). However, more recent studies demonstrated no host cell adhesion on high M content alginates after implantation in the peritoneal cavity of mice (Tam *et al.* 2011). Since alginate is isolated from natural sources, its toxicity might be due to the impurities that may remain after alginate purification, such as heavy metals, endotoxins, proteins and polyphenolic compounds (Dusseault *et al.* 2006). The reduction of protein content in alginate hydrogels induced significantly less pericapsular cell adhesion when implanted into mouse peritoneum (Ménard *et al.* 2010), suggesting that purification methods are crucial in order to eliminate any potential cytotoxic agent

1.4.1.2 Hydrogel formation and biodegradation

A hydrogel is a three-dimensional network of cross-linked hydrophilic polymer chains with a high water content. The physicochemical properties of hydrogels depends upon the precise cross-linking method employed, the degree of cross-linking, the molecular weight, and chemical composition of the polymers (Lee & Mooney 2012). Whilst alginate hydrogels can be prepared by using different cross-linking methods, covalent cross-linking involves permanently bonded alginate chains.

Ionic cross-linking allows the reversion of the process, which is desirable in numerous biomedical applications.

1.4.1.2.1 Ionic cross-linking

Ionic cross-linking is the most commonly used strategy to produce alginate hydrogels. The method involves the combination of an alginate solution with divalent cations (Sun & Tan 2013). These ions are believed to specifically bind G blocks of the alginate chains, since their spatial disposition allows a greater degree of coordination (Draget *et al.* 1997). Coordinated alginate chains overlay on adjacent chains, forming an “egg-box” structure (Grant *et al.* 1973) (**Figure 1.5**).

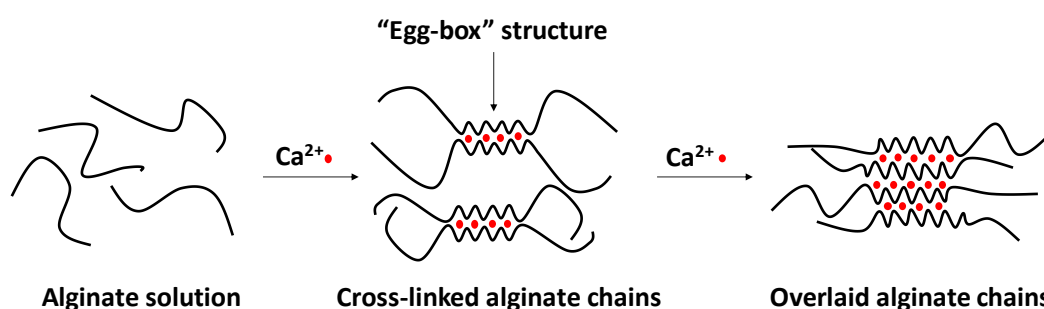


Figure 1.5. Representation of alginate ion cross-linking into an “egg-box” structure. Divalent cations specifically bind G blocks. Coordinated alginate chains overlay on adjacent chains forming an “egg-box” structure.

The most common cation used to form alginate hydrogels is Ca^{2+} . This cation, in the form of CaCl_2 , has been extensively used for alginate external gelation (Yang *et al.* 2000; Knezevic *et al.* 2002; Shintaku *et al.* 2007). In this approach, calcium salt is dissolved in an aqueous phase and brought into contact with alginate solution.

Calcium chloride is highly soluble in water, giving rise to very quick, but poorly controlled gelation (Liu *et al.* 2006; Shintaku *et al.* 2007). In order to delay gelation, and therefore have a better control over the gelation rate, researchers have utilised an internal gelation strategy. Low soluble calcium salts, such as CaSO_4 and CaCO_3 , are dispersed in the alginate solution and, upon reduction of the pH, calcium ions are released, provoking alginate cross-linking and formation of the gel structure in a more controlled manner (Branco da Cunha *et al.* 2014; Schmitt *et al.* 2015). Slower gelation times, involving a more controlled cross-linking, leads to hydrogels with a greater degree of uniformity with enhanced mechanical properties (Kuo & Ma 2001).

The main feature of ionically cross-linked alginate hydrogels is their limited long-term stability. However, whilst this could be considered as a drawback for some applications, it might actually be beneficial for others. Alginate hydrogels have been utilised as vehicles to protect transplanted cells from an adverse immune response, and to control cell parameters such as cell migration, proliferation and differentiation at the site of implantation (Banerjee *et al.* 2009; Jun *et al.* 2013). Therefore, alginate hydrogels can provide therapeutic effects while degrading as the cellular system replaces the artificial matrix. Ionically cross-linked alginate gels can be easily dissolved by ionic interchange reactions with monovalent ions. This situation naturally occurs *in vivo*, where calcium ions are interchanged with sodium ions (Guarino *et al.* 2015). However, a tight control of alginate degradation is required for this type of application, to control cell viability and therapeutic effect after implantation.

1.4.1.2.2 Covalent cross-linking

The need for improving the long-term stability of alginate hydrogels for some applications in tissue engineering gave rise to the development of new methods for cross-linking. Covalent cross-linking with poly(ethylene glycol)-diamines provides alginate hydrogels with improved mechanical properties due to permanent bonds in carboxylic groups from the G blocks.

The stress applied on alginate hydrogels has different effects depending on the cross-linking method. The bonds in an ionic cross-linked alginate are dissociated, which can provoke a plastic deformation, leading to the loss of its water content and the re-formation of random bonds. By contrast, covalently cross-linked hydrogels do not experience any bond dissociation, and the stress relaxes mainly through migration of water, giving rise to elastic deformation (Zhao *et al.* 2010). The mechanical properties of covalently cross-linked alginate hydrogels depend on the number of cross-linking molecules. It has been reported that the use of bifunctional molecules, such as poly(acrylamide-co-hydrazide) or adipic acid dihydrazide, provides multiple attachment points in the gel, thereby enhancing its mechanical properties and delaying the degradation rates (Lee *et al.* 2004). However, the main drawback of covalent cross-linking is the potential toxic effect of unreacted molecules, involving a necessary washing step after gel formation (Chan *et al.* 2015).

As an alternative to chemical cross-linking, photo cross-linking has been also applied as a covalent method for alginate gelation (Bruchet & Melman 2015). However, the technique has some limitations when applied to the production of scaffolds for tissue engineering. Cells are exposed to ultraviolet light, the

photoinitiators used may be cytotoxic and the use of organic solvents is often required to dissolve these photo initiators (Bruchet & Melman 2015). Nonetheless, alternative methods that minimize the exposure to UV light and the use of organic solvent have been investigated, allowing the application of photo cross-linking hydrogels for cell immobilization (Rouillard *et al.* 2011).

1.4.1.2.3 Alginate biodegradation

Alginate is non-degradable in mammals since they lack the enzymes responsible for cleavage of the polymer chains (alginate lyases). But, as mentioned above, ionically cross-linked alginate hydrogels can be dissolved by diffusion of calcium ions to the surrounding medium and interchange with other monovalent cations. However, although hydrogels can dissolve, the average molecular weight of released alginate strands is typically above the renal clearance threshold, and therefore, they are not completely removed from the organism (Al-Shamkhani & Duncan 1995). *In vivo* degradation of alginate hydrogels is desirable in some applications including drug delivery and cell transplantation. This has contributed to the modification of alginate chemistry in order to render it as a biodegradable material (Yang *et al.* 2011). One such approach consists of the partial oxidation of alginate chains with sodium periodate, leading to a water degradable polymer (Boontheekul *et al.* 2005).

1.4.1.3 Alginate applications in biomedical science

The favourable properties of alginate hydrogels have allowed for their numerous applications in different areas within the biomedical field, such as wound healing, drug delivery, tissue engineering, and cell culture. Unlike traditional dressings, alginate hydrogels maintain a moist microenvironment and minimize bacterial infection at the wound site, promoting wound healing by rapid epithelialization (Suzuki *et al.* 1998; Wang *et al.* 2015; Babavalian *et al.* 2015). Alginate hydrogels have the ability to adjust to the shape of the wound, which permits their implantation into the body in a minimally invasive manner, and filling irregularly shaped cavities (Thornton *et al.* 2004). The incorporation of cells and bioactive molecules within the hydrogels permits their application in tissue engineering therapies, providing restoration of damaged tissues (Fragonas *et al.* 2000; Di *et al.* 2016).

Alginate hydrogels have been also used in 3D cell culture systems (Andersen *et al.* 2015). Since alginate does not promote cell adhesion by itself, due to the lack of mammalian cell receptors and its low protein adsorption, alginate hydrogels have been modified to include molecules to promote cell attachment (i.e., cell-interactive alginates), for example, RGD sequences (Alsberg *et al.* 2001). Sequences can be introduced in alginate chains by water-soluble carbodiimide chemistry (Rowley *et al.* 1999). Such modifications have been demonstrated to promote cell proliferation and differentiation (Alsberg *et al.* 2001; Rowley & Mooney 2002; Markusen *et al.* 2006;).

1.4.2 Collagen

Along with alginate, collagen is one of the most widely reported biomaterials (Parenteau-Bareil *et al.* 2010). The main advantage of collagen over other synthetic biomaterials is its tolerance within the organism. Its application in the biomedical field is due to its characteristics such as weak antigenicity, cell attachment ability, biodegradability and biocompatibility (Silvipriya *et al.* 2015).

1.4.2.1 General properties

Collagen is the most abundant protein in animals constituting 30% of all protein found in the body and the main component of the extracellular matrix. Collagen plays important cohesion roles in tissues and organs, providing hydration, resistance, elasticity and flexibility (Muiznieks & Keeley 2013). Collagen also affects the biological functions of cells such as cell survival, proliferation and differentiation (Pickering 2001).

A collagen molecule is made up of three polypeptide chains arranged in the form of a triple helix wrapped around one another in a right-handed helical structure (Pauling & Corey 1951; Ramachandran & Kartha 1954). The high content of the three amino acids, glycine, proline, and hydroxyproline, is responsible for the helix formation, that maintains the strands by the formation of hydrogen bonds between adjacent -CO and -NH groups, and also by covalent bonds (Lodish *et al.* 2000) . Collagen is packed into hexagonal and quasi-hexagonal shapes forming fibrillar collagen types.

To date more than twenty types of collagen within the organism have been discovered (Silvipriya *et al.* 2015). Whilst all types of collagen have a characteristic triple helix, the length of the helix and the size and nature of non-helical portion varies dependant on the type (Miller 1984). Type I collagen is the most abundant and the most utilised collagen type in biomedical applications (Zhang *et al.* 2011).

1.4.2.2 Isolation, cross-linking and degradation

1.4.2.2.1 Natural sources of collagen

Collagen can be found within the tissues of numerous animals. Bovine skin and bone have represented the main industrial source of collagen (Silvipriya *et al.* 2015). However, due to the outbreak of diseases, such as transmissible spongiform encephalopathies, and the high costs related to collagen extraction and purification, alternative sources of collagen have been considered. Collagen isolation from rat tail is a cost-effective technique and guarantees the isolation of a high reproducible concentration of collagen (Rajan *et al.* 2006). As such, rat tail collagen (type I) is extensively utilized in biomedical engineering research (Chan *et al.* 2010; Guo & Kong 2002; Meghezi *et al.* 2015). Also, researchers have considered a relatively new source of collagen. It has been demonstrated that marine collagen from fish scales, skin, and bone has excellent bioactive properties such as biocompatibility, low antigenicity, high biodegradability, and cell growth potential (Phanat *et al.* 2010; Addad *et al.* 2011; Cho *et al.* 2014).

1.4.2.2.2 Collagen cross-linking

Like alginate, there are two types of cross-linking methods frequently employed for improving the mechanical stability of collagen scaffolds: physical methods and chemical methods. Physical methods include the use of photooxidation (Choi *et al.* 2013), dehydrothermal treatments (Haugh *et al.* 2009) and ultraviolet irradiation (Davidenko *et al.* 2016). However, the mechanical stability provided by physically cross-linked collagens is poor (Ma *et al.* 2004). Hence, when higher cross-linking degrees are required, chemical cross-linking becomes the favoured option.

Traditionally, glutaraldehyde has been the most used agent for covalent cross-linking of collagen (Cheung, *et al.* 1985; Roe *et al.* 1990; Ruijgrok *et al.* 1994; Xuemei *et al.* 2007). At neutral pH, glutaraldehyde reacts with amino groups bridging two adjacent polypeptide chains and enhancing the biological stability of collagen. However, it has been reported that glutaraldehyde induces cytotoxicity due to unreacted residues or the release of monomers and small polymers during enzymatic degradation (Gough *et al.* 2002; Ju *et al.* 2010). Therefore, several alternative cross-linking agents have been used, such as carbodiimides and polyepoxy compounds (Tang & Yue 1995; Li *et al.* 2013). Alternatively, a naturally occurring cross-linking reagent, genipin, has received an increasing interest in biomedical applications due to its low cytotoxicity (Mi *et al.* 2002; Liang *et al.* 2003; Li *et al.* 2014).

1.4.2.2.3 Collagen biodegradation

Degradation of collagen in mammals is due to the existence of specific enzymes, namely, matrix metalloproteinases (MMPs) (Harrington 1996). These enzymes are produced by fibroblasts, which can be stimulated to synthesize new enzyme for release outside of the cell (Wilhelm *et al.* 1986). Under several inflammatory conditions, such as rheumatoid synovitis or inflammatory arthritis, modulation of MMP production is mediated by interactions with surrounding inflammatory cells, which trigger an increase in collagenase synthesis, and therefore, progressive cartilage degradation can occur (Moore *et al.* 2000; Vincenti & Brinckerhoff 2002). MMPs have a differential rates of collagen hydrolysis, with different MMPs hydrolysing specific types of collagen (Fields 2013).

These enzymes are also synthesized by some bacteria, such as *Clostridium histolyticum* (MacLennan *et al.* 1953). Bacterial collagenase (an example of an MMP) has several applications in biotechnology and medicine and it has been widely used in laboratories to dissociate tissues and isolate cells (Suggs *et al.* 1992; Kurup & Bhonde 2002; Szot *et al.* 2009; Numpaisal *et al.* 2016). Also, *C. histolyticum* collagenase is used for *in vitro* degradation of collagen-based scaffolds (Sang *et al.* 2011; Perez *et al.* 2014).

1.4.2.3 Collagen applications in biomedical science

Collagen's ability to form fibres with enhanced strength and stability through its self-aggregation and cross-linking makes it a good candidate to be utilised as scaffold in biomedical applications. Type I collagen has been extensively used as a hydrogel in tissue engineering, due to its abundance and tendency to self-assembly (Cen *et al.* 2008).

Collagen can be loaded with drugs by hydrogen or covalent bonding, or simple entrapment in controlled drug release and wound healing applications (Marks *et al.* 1991; Lazovic *et al.* 2005). Drug-laden collagen films have been used as drug delivery systems in the treatment of a range of illnesses and infections, such as corneal infection (Bloomfield *et al.* 1978) and cancer (Sato *et al.* 1996). Collagen inserts allowed for the delivery of high doses of active molecules at the site of implantation in a non-traumatic manner and demonstrated a long-term maintenance of the drug at the target site.

Collagen's ability to promote cell proliferation and differentiation has also been exploited for the construction of 3D scaffolds in tissue engineering (Glowacki and Mizuno 2008). However, collagen has poor mechanical properties and it is usually combined with other biomaterials for long-term biomedical applications. Calcium phosphate is a common substrate used along with collagen for bone regeneration, because it provides the scaffold with the sufficient mechanical strength (Al-Munajjed *et al.* 2008). Collagen's porous structure also allows for the encapsulation of therapeutic cells and their use as controlled delivery systems to induce histogenesis *in vivo* (Nillesen *et al.* 2007; Lee *et al.* 2009).

Collagen is also an excellent substrate for cell immobilization and culture due to its ability to promote cell attachment. Hence, collagen has been used for the production of scaffolds for 3D cell culture, allowing for more realistic *in vitro* studies, since such 3D scaffolds provide the cells with a similar structure to that found *in vivo*. Unlike standard 2D culture, cells seeded within collagen scaffolds can maintain their *in vivo* morphology and three-dimensional structure, thereby improving their function, as shown by *in vitro* studies (Mei *et al.* 2014).

1.5 Microfluidics

Microfluidics can be defined as the science or technology that manipulates very small volumes of fluids, in the range of micro- to picolitres, flowing in networks of channels with micrometric dimensions (Stone *et al.* 2004). The drastic reduction in length scale involves changes in the physical properties of fluids, giving rise to new phenomena that are not observed in the macroscale (Brody *et al.* 1996). Microfluidics aims to understand this behaviour for further application in science and technology.

1.5.1 Physics in Microfluidics

The behaviour of fluids can be described through a dimensionless magnitude known as the Reynolds number (Reynolds 1883). This magnitude defines the flow pattern of a fluid under specific conditions by the correlation of inertial forces to viscous forces. The Reynolds number (Re) is defined as follows:

$$\text{Re} = \frac{\text{Inertial forces}}{\text{Viscous forces}} = \frac{\rho v L}{\mu} \quad \text{(Equation 1.1)}$$

Where ρ is the density of the fluid, v is the velocity of the fluid with respect to the object through which is flowing, L is the cross section area of the object, and μ is the dynamic viscosity of the fluid. Depending on the Re value, the flow pattern of a fluid can be defined as turbulent or laminar (**Figure 1.6**). In the macroscale, where interfacial forces are dominant, Re are high and the fluid flows in a turbulent regime. Turbulent regimes are characterized by irregular fluctuations or mixing, and the

speed of the fluid at a point is continuously undergoing changes in both magnitude and direction. In contrast, low Re are typical for microsystems, where channel dimensions are reduced and viscous forces are predominant. This leads to fluids flowing in a laminar regime, in which the fluid moves in smooth paths or layers, with minimal disruption between them. The transition between the two regimes depends on the channel geometry. In a straight channel it typically occurs at $Re = 2300$ (Ong *et al.* 2008). In laminar flow regimes, two or more miscible fluid streams in contact with each other, flow side by-side, with mixing occurring via interfacial diffusion (Ismagilov *et al.* 2000). The velocity of flow varies from zero at the walls to a maximum along the cross-sectional centre of the channel, which can permit the separation of particles depending on their size and velocities (Weigl & Yager 1999).

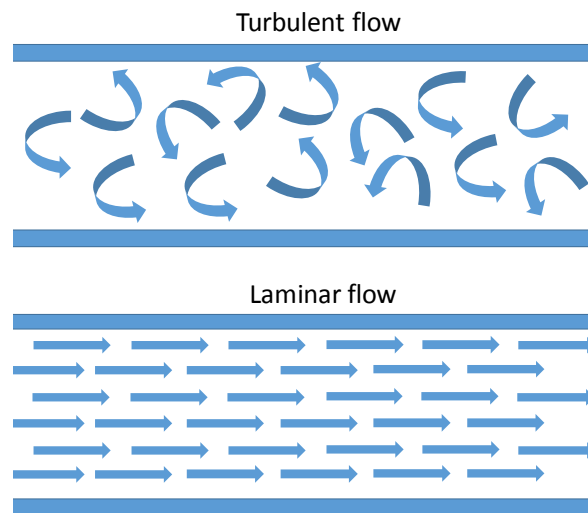


Figure 1.6. Graphical representation of turbulent and laminar flow regimes. Flow regime can be predicted through the Re . The transition between the two regimes depends on the channel geometry. In a straight channel it typically occurs at $Re = 2000$. Turbulent flow is characterized by irregular fluctuations or mixing. In laminar flow, fluid flows in parallel layers, with no disruption between layers.

The reduction in length scales also affects the diffusion rate of the molecules. Diffusion is the process by which molecules move from a region of high concentration to a region of low concentration. The diffusion coefficient of a particle is defined by the following equation:

$$D = \frac{d^2}{2t} \quad \text{(Equation 1.2)}$$

Where D is the diffusion rate and d is the distance a particle moves in a time t . Since distance varies to the square power, diffusion rates are very high on the microscale. This reduction in diffusion times can be utilized in order to accelerate experimentation times of chemical reactions in microchannels (DeMello 2006). Another characteristic of microscale systems is the high surface area to volume ratio (SAV), which can lead to unconventional dominant forces. Thus, large SAVs typically make surface forces dominant, while greatly reducing the influence of inertial forces.

Because interfacial phenomena become dominant in microfluidic systems, surface tension forces are also significant when compared to the macroscale. Surface tension is the result of cohesion forces between liquid molecules at the liquid/gas interface. When surface tension forces are dominant, the fluid acquires the minimum surface area possible, that is, the total area that the surface of the object occupies. Surface tension forces play an important role in droplet-based microfluidics, which will be discussed in the next section.

1.5.2 Droplet-based microfluidics

Microfluidic systems can operate within a continuous-flow regime or droplet/segmented-flow regime. In continuous systems, liquid streams flow through microchannels with no interruption. This method is usually acquired for large-scale applications, such as chemicals separation (Pamme 2007). However, issues related with fluid interaction with channel walls, cross-contamination and long channel lengths, hinders its application in those situations where a high precision of fluid manipulation is required (Lignos *et al.* 2012). Droplet-based microfluidics overcomes the problems mention above. In this approach, the manipulation of droplets, instead of microflows, reduces the volume of sample liquid, providing an additional miniaturization step. In biomedical research, droplets have the potential to become important tools for drug delivery and biosensing. In order for them to function properly, correct dosing and manufacturing must be ensured. Droplet microfluidics has been shown to generate highly monodisperse droplets with size variations smaller than 1% (Nisisako *et al.* 2006). Hence, the precise generation and repeatability of droplets, makes droplet-based microfluidics a potent high-throughput platform for biomedical research.

1.5.2.1 Physics involved in droplet formation

Droplet-based microfluidics consists on the formation and manipulation of discrete droplets within an immiscible continuous phase. Typically, the two phases involved are liquid, although the formation of droplets in a liquid/gas system is also possible (Jiang *et al.* 2015). In liquid-liquid systems, droplets of one phase (dispersed phase) are produced as a result of the shear force generated by the continuous phase and the surface tension at the fluid-fluid interface (Teh *et al.* 2008). Hence, the surface tension is a critical parameter that affects the evolution of the interface between two phases during the droplet formation. Surface tension can be defined as an energy per unit area, which acts to minimise the total surface area, so as to reduce the free energy of the interface. The minimum area for a given volume is a sphere, which is the shape taken by a droplet. But also, viscous forces are important in the droplet formation. As outlined in the previous section, fluids flowing in micrometric dimensions typically have low Re , which means that viscous forces become dominant over inertial forces. In the mechanisms underlying droplet formation, surface tension and viscosity compete with each other, since both tend to become important at small scales (Baroud *et al.* 2010). The relative strength of these two forces is expressed by the following equation:

$$Ca = \frac{\mu V}{\sigma} \quad (\text{Equation 1. 3})$$

where Ca is the Capillary number, μ is the viscosity of the continuous phase, V is the velocity of the continuous phase, and σ is the surface tension at the interface between the two phases. Above a certain critical capillary number, droplet break off

occurs. However, this number depends on the system (Nisisako *et al.* 2005; Song *et al.* 2006; Anna & Mayer 2006).

Droplet formation is also significantly affected by the wetting properties of the channel walls. Wetting can be defined as the ability of a liquid to cover a solid surface, and depends on the physico-chemical properties of the surface. It can be quantified through the contact angle (θ), which is the angle, conventionally measured through the liquid, where a liquid–vapour interface meets a solid surface (**Figure 1.7**). Controlling the wetting of the channel walls by the dispersed phase is important in order to prevent its adhesion to the walls and produce highly spherical droplets. In the case where hydrophilic droplets are generated within a continuous hydrophobic phase, namely water in oil (W/O) emulsions, channel walls should be hydrophobic, in order to maximize the contact angle between the droplet and the wall surface. For such applications, polydimethylsiloxane (PDMS) devices are frequently used to fabricate the microfluidic channels (Friend & Yeo 2010). However, PDMS undergoes swelling and deformation in the presence of strong organic solvents and uncontrolled adsorption of substances is a major problem (Uchida *et al.* 2003). Hence, other materials such as glass (Utada *et al.* 2005) silicon (Pollack *et al.* 2002) and polytetrafluoroethylene (PTFE), commonly known as Teflon (Walsh *et al.* 2016), are used instead.

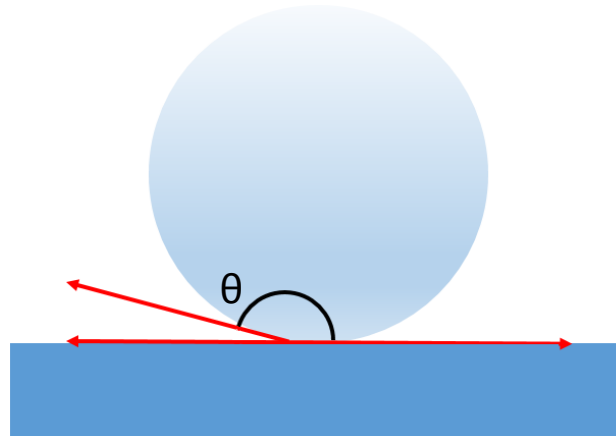


Figure 1.7. *Contact angle.* High contact angles occur when a hydrophilic droplet gets in contact with a hydrophobic surface. The repulsion forces between the two substrates provokes high surface tension at the interface, thereby producing highly spherical droplets.

1.5.2.2 Microfluidic formats for droplet generation

1.5.2.2.1 Co-flowing

In co-flowing devices, one fluid flows inside the inner capillary while the other fluid flows through the outer capillary in the same direction, resulting in a coaxial flow of the two fluids (Cramer *et al.* 2004) (**Figure 1.8**). The breakup of the liquid stream into droplets occurs under two different regimes: dripping and jetting. When the fluids flow at low flow rates, monodisperse droplets are formed at the tip of the capillary orifice, in a dripping mode. If the flow rate of either fluid is increased beyond a certain critical limit, the result is a jet, a long stream of the inner fluid with drops forming downstream. The transition from dripping to jetting occurs when the continuous phase velocity increases above a critical value (Utada *et al.* 2007). This value decreases as the flow rate of the dispersed phase increases. It also depends on the viscosities of the inner and outer phases, as well as on the interfacial tension.



Figure 1.8. *Droplet formation in a co-flowing system.* a) Dispersed phase flows through the inner capillary while the continuous phase flows through the outer capillary in the same direction, resulting in a coaxial flow of the two fluids. b) Dripping mode: when the fluids flow at low rates, monodisperse droplets are formed at the tip of the capillary orifice c) Jetting mode: if the flow rate of either fluid is increased beyond a certain critical limit, the result is a jet, a long stream of the inner fluid with drops forming downstream. Scale bar = 50 μ m. Adapted from Utada *et al.* 2007.

1.5.2.2.2 T-junction

In the T-junction format, the two phases flow through two perpendicular channels until they meet at the junction (Sivasamy *et al.* 2011) (**Figure 1.9**). There are three regimes in this format, which are dripping, squeezing and parallel flowing (Garstecki *et al.* 2006). At high Ca, droplet formation occurs through dripping mode. The dispersed phase stream does not enter the continuous phase, and droplet formation occurs before the junction due to the action of the shear stress. Alternatively, if the capillary number is low, surface tension is dominant and the formed droplets obstruct the channel, constricting the continuous phase. As a consequence, there is a dramatic increase in the hydrodynamic pressure upstream of

the droplet, which in turn induces the droplet pinch-off. When the dispersed phase flow rate is higher than the continuous flow rate, the squeezing regime develops into the formation of parallel flowing streams (Guillot & Colin 2005). The transition from dripping to squeezing modes depends on the balance of the forces involved, including dynamic pressure, surface tension, viscous and inertial forces (De menech *et al.* 2008).

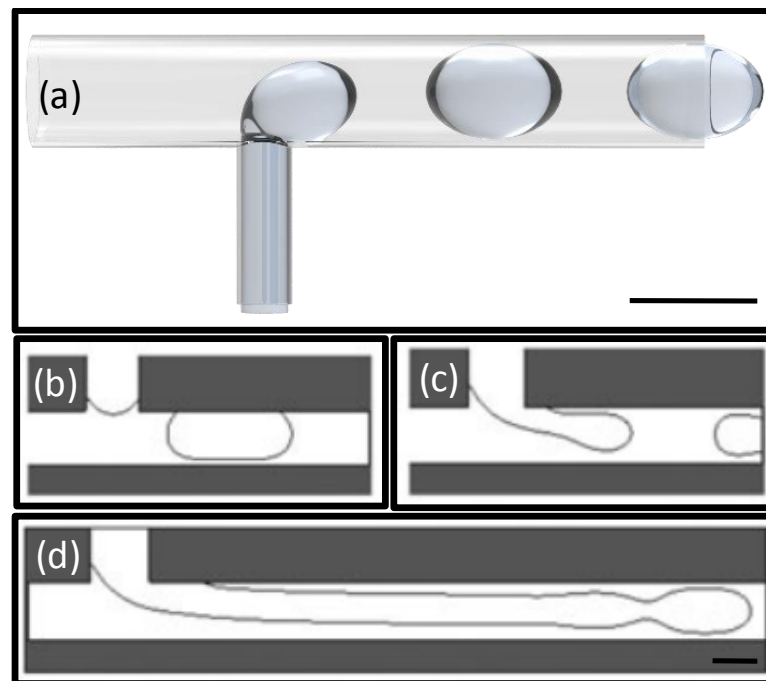


Figure 1.9. *Droplet formation in a T-junction.* a) The two phases flow through two perpendicular channels until they meet at the junction. b) Dripping: the dispersed phase stream does not enter the continuous phase, and droplet formation occurs before the junction due to the action of the shear stress. c) Squeezing: the formed droplets obstruct the channel constricting the continuous phase. As a consequence, there is a dramatic increase in the hydrodynamic pressure upstream of the droplet, which in turn induces the droplet pinch-off. d) Parallel flowing: when the dispersed phase flow rate is higher than the continuous flow rate, the squeezing regime develops into the formation of parallel flowing streams. Scale bar = 100 μ m. Adapted from De menech *et al.* 2008.

1.5.2.2.3 Flow focusing

In the flow-focusing format, the dispersed and continuous phases are forced through a narrow nozzle in the microfluidic device (Dreyfus *et al.* 2003; Anna *et al.* 2003) (**Figure 1.10**). This system integrates a symmetric design that provides a shearing stress on the dispersed phase by two counter-flowing streams of the continuous phase, which enables more controlled and stable generation of droplets. Like the previous formats, the droplet formation process depends on the balance of the forces involved. Four different droplet breakup regimes have been identified in flow focusing devices: squeezing, dripping, jetting and thread formation. In squeezing mode, the dispersed phase flows through the nozzle and grows until the droplet breaks off, which is entirely provoked by the shear force of the continuous phase. Droplets formed in this mode are similar in size to the channel dimensions and are highly monodisperse. In the dripping mode the droplet formation is controlled by both the shear force generated by the continuous phase and the surface tension at the interface, leading to smaller droplets (Eggers 1993). In the jetting mode, the dispersed stream extends considerably further downstream on the channel and droplet generation takes place due to Rayleigh-Plateau instabilities (Plateau 1849; Rayleigh 1879). When the flow rate of the dispersed phase is higher than the continuous phase, the shear force is not high enough to produce the stream pinch-off and the dispersed phase flows downstream the channel within the continuous phase forming a long thread.

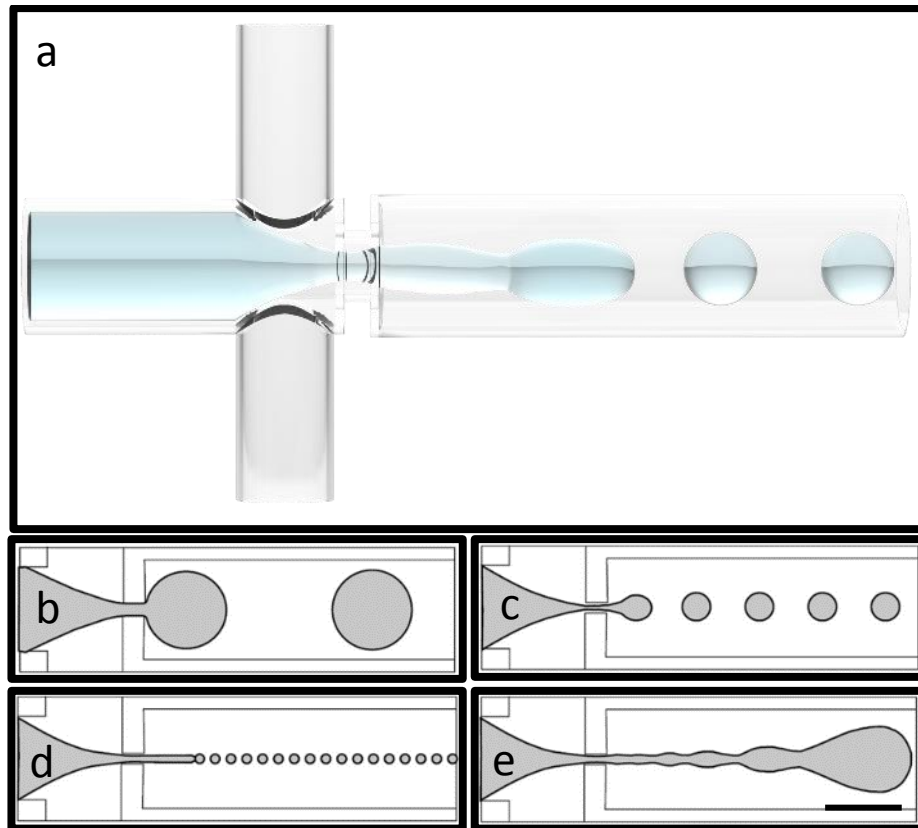


Figure 1.10. *Droplet generation in a flow focusing device.* a) The dispersed and continuous phases are forced through a narrow nozzle. This system integrates a symmetric design that provides a shearing stress on the dispersed phase by two counter-flowing streams of the continuous phase. b) Squeezing: the dispersed phase flows through the nozzle and grows until the droplet breaks off due to the shear force of the continuous phase. c) Dripping: droplet formation is controlled by the shear force generated by the continuous phase and the surface tension at the interface. d) Jetting: the dispersed stream extends considerably further downstream on the channel and droplet generation takes place due to Rayleigh-Plateau instability. e) Threading: when the flow rate of the dispersed phase is higher than the continuous phase, the shear force is not high enough to produce the stream pinch-off and the dispersed phase flows downstream the channel within the continuous phase forming a long thread. Scale bar = 100 μ m. Adapted from Sullivan & Stone 2008.

1.5.3 Microfluidics and Biomedical Research

The miniaturization process leads to the observation of new phenomena, thereby allowing the performance of techniques and experiments not possible on the macroscale. This enables new functionality and experimental paradigms to emerge (Beebe *et al.* 2002). Microfluidic devices offer the possibility of working with smaller reagent volumes and shorter reaction times, thereby reducing experimentation costs. Micrometric dimensions permit a better control of physical and chemical properties, which in turn allows the creation of more uniform reaction conditions to obtain products with higher grade (Streets & Huang 2013). The reduction in dimensions' scale permits the integration of an entire laboratory onto a single chip, or multichip module (i.e., lab-on-a-chip devices) (Guber *et al.* 2004) allowing the automatization of complex multistep processes.

Microfluidics based approach allows the high-throughput of small sample volumes and ease of automation, thereby reducing experimental costs and times. This permits the expansion of point-of-care testing, which is defined as diagnostic testing at, or near, the site of patient care, to make the test convenient and immediate. Patients can receive testing results within minutes, by utilizing miniaturized and portable devices (e.g., blood glucose meter). Such devices can be used in hospitals, or simply by patients by themselves at home, without any professional knowledge or particular skill (Sia & Kricka 2008). The low volumes of sample required by these devices permits sample collection in a minimally invasive manner.

1.5.3.1 Cell manipulation

Cell differentiation *in vitro* is typically achieved by the exposure of cells to suitable differentiation cocktails, containing biochemical factors that lead to signalling cascades within the cell and determine their phenotype (Ntambi & Kim 2000; Gao *et al.* 2014). However, cell differentiation in living organisms is also affected by other external factors, such as mechanical stress induced by surrounding extracellular matrix (ECM) (Janmey & Miller 2011). Microfluidic devices are capable of generating highly controlled shear stress gradients in physiological conditions, providing a tool for the *in vitro* differentiation of cells in a more realistic manner (Kim *et al.* 2017).

Microfluidics has also been used to develop micromolds for cell patterning (Tan & Desai 2003; Kuribayashi-Shigetomi *et al.* 2010). Such micromolds allows the patterning of several hundreds of different cell types and biomaterials, providing a simple and fast technique to produce complex tissue constructs or even whole organs (organ-on-a-chip) (Bhatia & Ingber 2014). Cell patterning provides a method for studying the functional significance of tissue architecture at the resolution of individual cells, and the molecular interactions between cell types underlying processes such as embryonic morphogenesis (Suri *et al.* 2013), the formation of the blood–brain barrier (Van der Helm *et al.* 2016), and tumour angiogenesis (Stroock & Fischbach 2010).

In vitro fertilization (IVF) is another field that takes advantage of microfluidic technology. Conventional IVF technique involves manual manipulation and pipetting, therefore requiring the need for highly experienced professionals to achieve

satisfactory results. The use of microfluidic systems for IVF, permits the integration of oocyte trapping, fertilization and subsequent embryo culture in a single device, thereby simplifying the whole process (Suh *et al.* 2006; Han *et al.* 2010).

Chapter 2. Development of a
Microfluidic Chip to Produce Alginate
Microspheres

2.1 Introduction

Microfluidics has been broadly applied over recent years to the production of monodispersed, microscopic droplets, specifically for the production of polymer microspheres (Choi *et al.* 2007; Liu *et al.* 2013). However, few authors have employed the use of microfluidic devices along with internal gelation for the on-site production of such microdroplets (Liu *et al.* 2013). Whereas external gelation involves two steps for the production and gelation of droplets, internal gelation permits the formation and *on chip* cross-linking of polymer beads, thereby potentially enabling the automatization of the entire process (Maeda *et al.* 2012). Furthermore, the monodispersity of beads is greater, due to the more consistent gelation process conditions (Chan *et al.* 2002).

Several strategies exist for polymer emulsification in microfluidic devices based on the network layout of microfluidic channels (**Section 1.5.2.2**). The simplest method involves two immiscible fluids co-flowing in the same capillary, giving rise to droplet formation due to the shear force generated by the outer phase (Cramer *et al.* 2004). In a different approach, droplets can also be generated within T-junction devices, where dispersed and continuous phases meet at an angle of 90 degrees (Sivasamy *et al.* 2011). Finally, flow focusing devices provide a method in which both phases flow in perpendicular directions and are then forced through the same channel (Dreyfus *et al.* 2003). The large number of geometrical aspect ratios characterizing flow-focusing devices permits a better and more accurate control of droplet formation. Hence, this strategy was used to produce alginate microcapsules in this thesis.

Alginate microcapsules should maintain their integrity for extended periods of time, allowing for a long-term protection of the encapsulated cells. At the same time, the porosity of the microcapsules should be high, to guarantee an effective mass transfer, thereby providing higher cell survival rates (Smidsrød & Skjåk-Braek 1990). Alginates possessing a high guluronic acid content (medium viscosity alginates) develop stiffer, more porous gels. Conversely, alginates rich in mannuronic acid residues (low viscosity alginates) produce softer, less porous microcapsules, which tend to disintegrate easier after long culture periods (Lee & Mooney 2012). The viscosity of the matrix affects cell survival in that pre-polymer solutions with high viscosities need great shear forces to produce droplets, which can damage cell membrane (Gray 1997).

2.2 Aims and Objectives

The aims of this chapter were for the microfluidic production of alginate droplets and *on chip* gelation with a target, average diameter of $\sim 500\mu\text{m}$. To this end, a PTFE microfluidic device was fabricated using milling machinery. Optimization of the microfluidic parameters was investigated: namely with respect to droplet generation strategy, channel geometry and fluid flow rates.

2.3 Materials and Methods

2.3.1 Microfluidic reagents

- Medium viscosity alginic acid sodium salt from brown algae, mineral oil and glacial acetic acid were purchased from Sigma-Aldrich, UK.
- Oil Blue N and Oil Red O were used to stain the mineral oil and purchased from Sigma-Aldrich, UK.
- Nanocrystalline precipitated calcium carbonate (average particle size 70nm) was purchased from Specialty Minerals, Birmingham, UK.
- Red food dye (Silver Spoon) was used to stain the alginate solution.

2.3.2 Preparation of microfluidic reagents

Nanocrystalline precipitated CaCO_3 was dispersed in distilled water. Sigma *Medium Viscosity* sodium alginate was added to the CaCO_3 suspension. The blend was stirred for 2 hours at 37°C . Concentrations of CaCO_3 and alginate are specified in **Section 2.4.2**. Glacial acetic acid was dissolved in mineral oil at a final concentration of 0.3% (v/v).

2.3.3 Chip design and manufacturing

Microchannels were machined into PTFE discs using a Computer Numerical Controlled milling machine (LPKF C30) after being designed using SolidWorks software and then exported to CircuitCAM 5.0 (LPKF, Germany) as .DXF files. The software allowed milling procedures to be assigned to cut the appropriate regions of the chip. The file was then exported to BoardMaster (LPKF, Germany) where tools were assigned to the milling procedures. The BoardMaster software controlled the micromachining tool. BoardMaster software controls the tool movement in the X and Y planes, whereas the Z plane is controlled by manual adjustment to the desired depth. To ensure a good surface finish within the channels, and to minimise the stress placed on the tool, multiple machine passes were used; typically, only increasing the depth by a quarter of the tool diameter for each pass. Milling was carried out with a milling drill spin speed of 30,000 rpm. Inlet and outlet holes were drilled at 3.25mm from the edge of the PTFE chip. These positions lined up with holes in a prefabricated metallic manifold. The chips were polished before and after milling

to obtain a smooth and flat surface. Polishing was performed by hand by rubbing the PTFE chip over a series of sandpapers of increasing fineness with a cotton polish as the final stage (240-2500 grade SiC grinding paper for metallography, BUEHLER).

2.3.4 Microfluidic device setup

The microfluidic device used in all experiments consisted of a metallic manifold into which HPLC fluid connectors (Sigma-Aldrich, UK) were introduced perpendicularly through holes sealed with nitrile rubber O-rings (Sealmasters, Cardiff, UK), allowing fluid to flow in the channels of previously machined PTFE disc (50mm diameter x 6mm thickness, Good Fellow, Huntingdon, UK) located within the manifold. A fluorinated ethylene propylene (FEP) film (5cm diameter, 0.1mm thickness; Good Fellow, Huntingdon, UK) was placed in between the PTFE chip and a borosilicate glass disc cover (5cm diameter x 10mm thickness; PI-KEM Ltd, Staffordshire, UK). A metallic clamping piece was screwed to the manifold, allowing the entire assembly to be compression sealed. Fluids were introduced into the microfluidic channels through sterile 1/16-inch outer diameter PTFE tubing (Sigma-Aldrich, UK) using syringe pumps (KD Scientific – Linton Instrumentation, Norfolk, UK).

2.3.5 Imaging

Droplet formation movies were recorded with a high-speed camera (Megaspeed MS40K) attached to an optical microscope (Nikon MM-800). Megaspeed AVI player software permitted the images acquisition of microfluidic channels. Images of alginate microcapsules were acquired with an Eclipse TS100 inverted phase contrast light microscope (Nikon, Japan) with a camera attachment (Canon, Japan).

2.3.6 Statistics

Data are represented as mean \pm SEM. Statistical significance was determined by Student's t test. $P < 0.05$ was considered statistically significant.

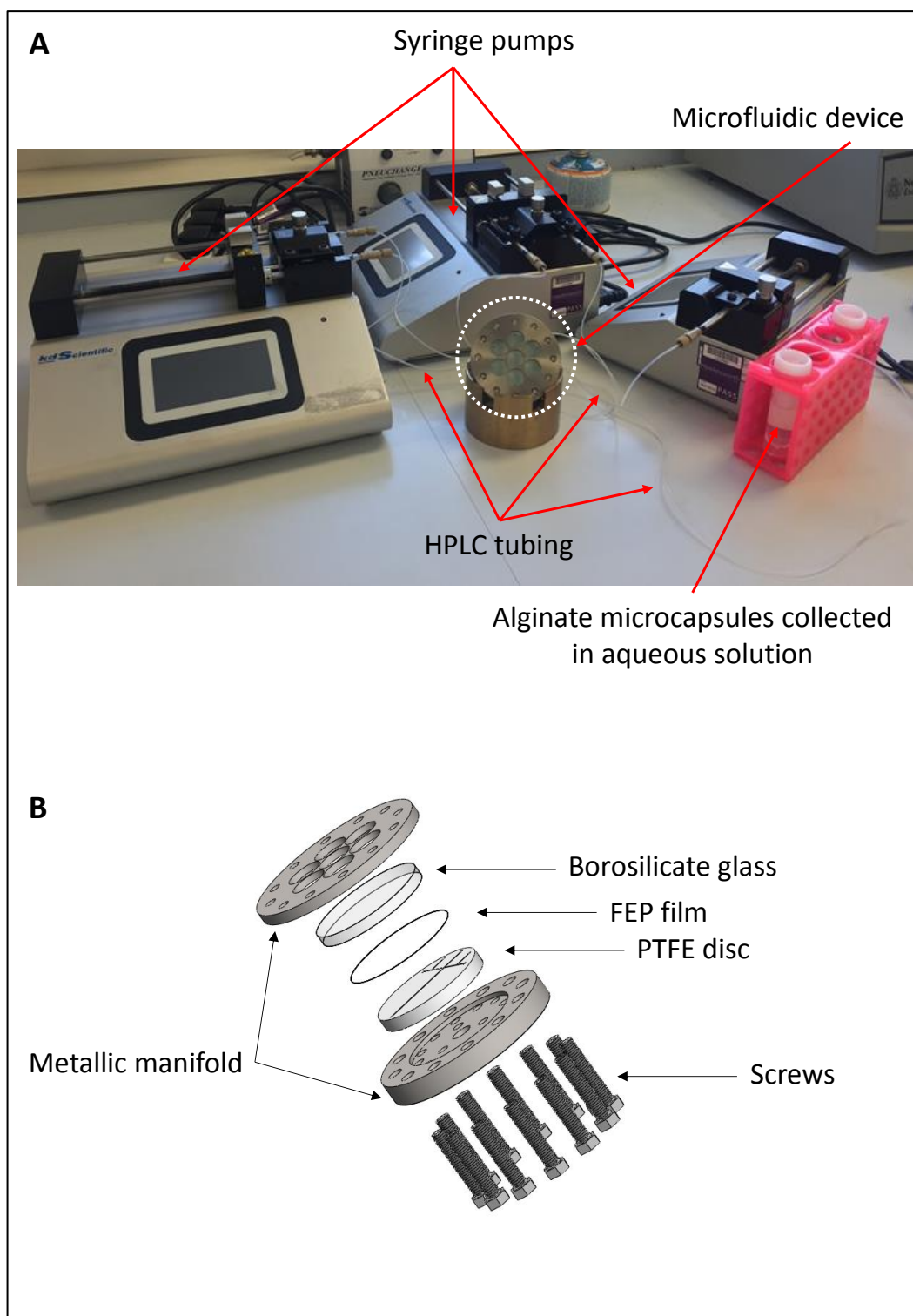


Figure 2.1. *Microfluidic device.* A) Picture of the whole set up used for the microfluidic experiments. The microfluidic device was connected through HPLC tubing to syringes containing the fluids. Flow rates were controlled by syringe pumps. B) Detailed diagram showing each component of the microfluidic device.

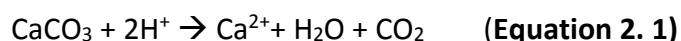
2.4 Results

2.4.1 Development of a customized microfluidic chip to produce alginate microcapsules

PTFE was chosen as the material to fabricate the microfluidic device. Due to its physical properties, PTFE is a hydrophobic material with excellent wetting features (Walsh *et al.* 2016). Its high contact angle is stable along the surface as a consequence of its non-reactivity. Therefore, it is possible to produce highly stable water in oil emulsions without the use of surfactants, hence minimizing cell damage and the number of washing steps. The high melting point of PTFE allowed for its heated sterilization prior to any experiment carried out with live mammalian cells.

Since the ultimate goal of this thesis was the encapsulation of stem cells, flow focusing was selected as the strategy to produce polymer micro beads. In this method the dispersed phase is barely stressed and therefore is suitable for the encapsulation of cells, with no decrease in their viability (Martín-Banderas *et al.* 2005). In flow focusing devices, the dispersed and continuous phases are forced through a narrow nozzle in the microfluidic device. The shear force generated by the continuous flow provokes the dispersed phase to break off into droplets. This method enabled the production of alginate droplets and gelation in one unique step. Flow focusing allows for the production of droplets with greater dynamic size range from a given device compared with other strategies, e.g. T-junction (Baroud *et al.* 2010).

To prevent prompt alginate cross-linking (the initial ECM molecule under investigation) CaCO_3 was utilised as calcium ions source. This salt has a low solubility at neutral pH in aqueous solutions, which allowed for its dispersion into the alginate solution (dispersed phase). A solution of acetic acid in mineral oil (continuous phase) was used in order to trigger the release of Ca^{2+} according to the following chemical equation:



Preliminary experiments using the chip layout in **Figure 2.2** demonstrated that almost instantaneous ($\sim < 1\text{s}$) alginate gelation occurred, at location 'A', causing the formation of a solidified alginate membrane, which eventually (in a matter of seconds) blocked the alginate inlet port, leading to a stalling of the syringe pump.

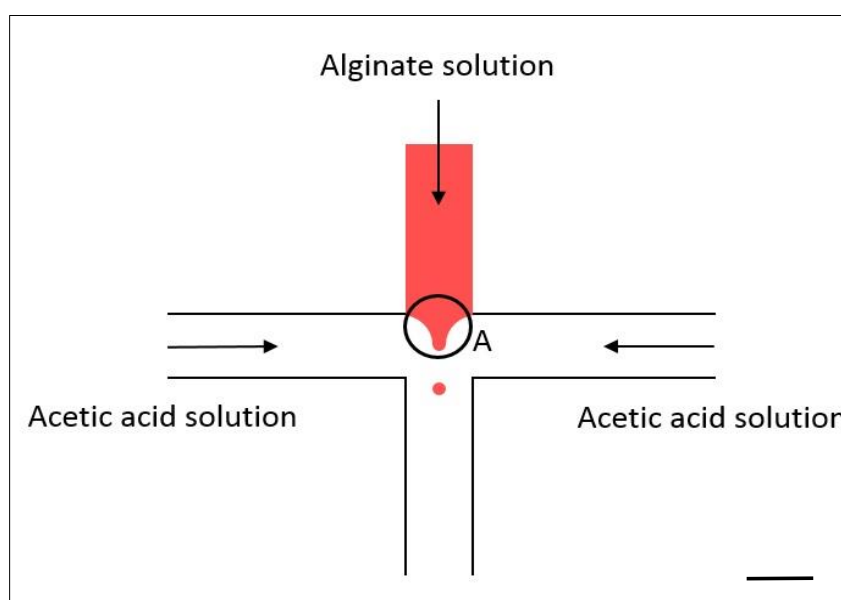


Figure 2.2. Chip design for the production of alginate microcapsules. Alginate gelation occurred at the junction, provoking the blockage of the channels and therefore the disruption of alginate emulsification. Scale bar = $500\mu\text{m}$.

In order to prevent an immediate gelation at the site of droplet formation, an additional phase containing mineral oil was incorporated in the design (**Figure 2.3**). This new phase worked as a “shielding flow” preventing alginate solidification at the junction (Workman *et al.* 2007). As mentioned in **Section 1.5.1**, fluid properties dramatically change when they are infused through networks of channels of micrometric dimensions. Under these conditions, fluids flow in a laminar regime, where parallel layers of liquid flow with minimal disruption between them and run parallel to the channel walls. However, particles move through different layers by diffusion. This phenomenon allowed the acetic acid present in the continuous phase to diffuse through the shielding flow and reach the alginate droplets, provoking their controlled gelation.

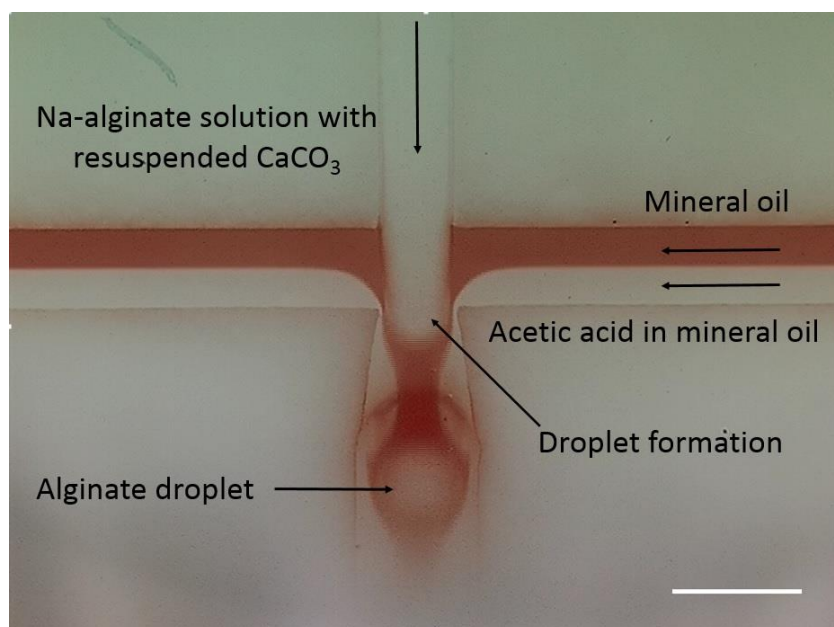


Figure 2.3. *Shielding flow.* Alginate gelation *on chip* can be delayed by adding a “shielding phase”. Due to the laminar flow, the two miscible phases (shielding and proton source) flow in parallel layers through the same channel with no disruption between layers. Protons diffuse through the different layers to finally reach the alginate, provoking its gelation. Scale bar = 800 μ m.

The thickness of each phase could be easily controlled by the modification of their flow rates, thereby modifying alginate gelation kinetics. At low shielding phase flow rates (red) and high acetic acid flow rates (white), the shielding stream was narrow and the diffusion of protons towards alginate droplets was faster, allowing for quicker gelation times (**Figure 2.4 A**). In contrast, when the flow rate of the shielding phase was increased, the flow stream was wider and the diffusion of protons through the channel was delayed, allowing for slower gelation times (**Figure 2.4 B**). A flow rates ratio of 1:1 was selected for subsequent experiments, in order to produce alginate droplets with slow cross-linking rates. This avoided the blockage of microfluidic channels and ensured a uniform gelation through the entire droplet.

Through the addition of the shielding flow, the premature gelation of alginate was prevented and continuous droplet formation was then achieved. Since alginate cross-linking was delayed, chip channels were designed in order to increase the path length so that alginate gelation took place before leaving the microfluidic device. Towards this end, the main channel was fabricated in a meander-like format (**Figure 2.5 A**). However, an inconsistent droplet flow was observed due to the adhesion of alginate on the walls as a consequence of changes in directions. Therefore, a modification on this initial design was required. To this end, it was considered that a straight channel would overcome the issues previously mentioned (**Figure 2.5 B**). A longer outlet HPLC tubing was used in order to compensate the channel shortening. Alginate beads were collected in distilled water, with no further processes needed (**Figure 2.6**).

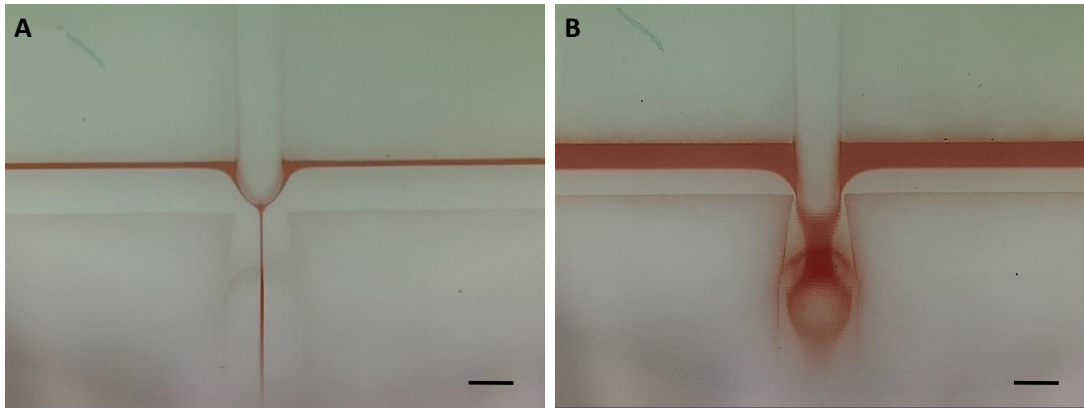


Figure 2.4. *Laminar flow.* Two miscible phases (red corresponding to mineral oil, and horizontal white to acetic acid in mineral oil) flowing in parallel layers through the same channel. The thickness of each phase could be modified by the alteration of their flow rates. A) Flow ratio 1:10. B) Flow ratio 1:1. Scale bar = 500 μ m.

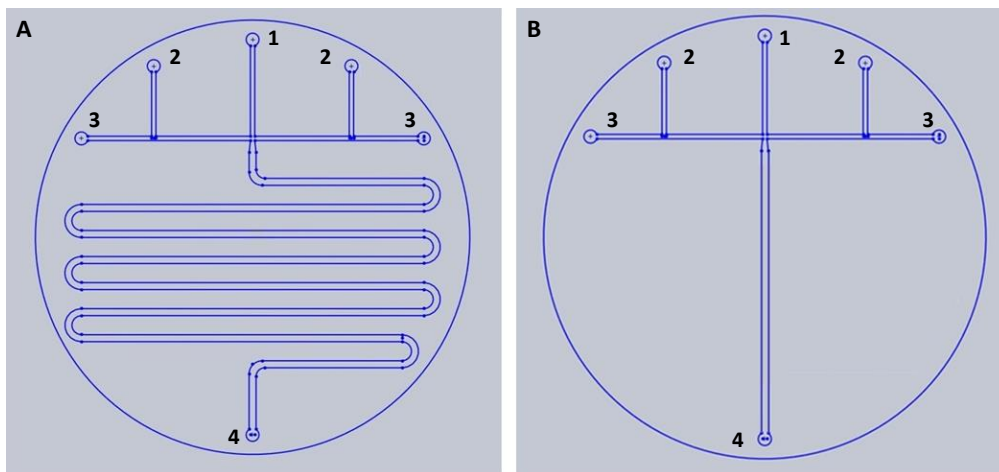


Figure 2.5. *Geometry of microfluidic chips.* Both chips were formed by 5 inlets: alginate was introduced into the chip through inlet 1; the shielding phase (mineral oil) flowed through inlets 2 protecting a prompt alginate gelation. Acetic acid in mineral oil (protons source phase) was injected through inlets 3, flowing in parallel layers with mineral oil. Cross-linked alginate droplets left the device through the outlet (4). A) Chip design 1: the main channel was designed in a meander-like shape to increase the path length of the microfluidic device. B) Chip design 2: the main channel was replaced by a straight line, avoiding changes in direction and therefore, allowing a consistent flow of alginate beads. Channels dimensions: inlets 1, 2 and 3 were 500 μ m x 400 μ m; main channel was 800 μ m x 700 μ m.

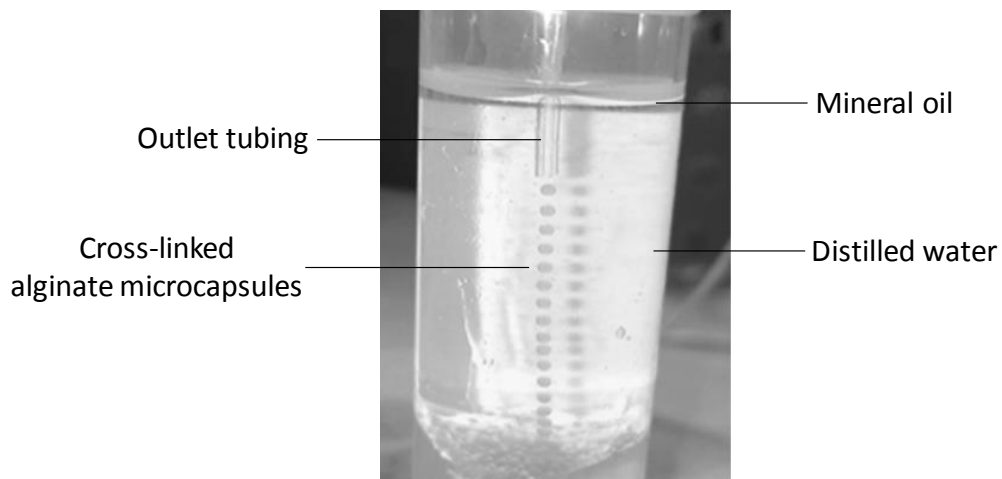


Figure 2.6. *Collection of alginate microcapsules.* Alginate droplets underwent on chip cross-linking by coordination of Ca^{2+} with the guluronic blocks of alginate chains. Beads were collected in distilled water.

2.4.2 Optimization of the reagents concentration

Three different alginate concentrations were tested: 1% (w/v) (low concentrated), 2% (w/v) (medium concentrated) and 4 % (w/v) (high concentrated). Low concentrated alginate gave rise to microspheres with low mechanical stability. Alginate droplets were easily deformed by mechanical pressure, thereby providing microcapsules with poor consistence. High concentrated alginate solution had a high viscosity, which hindered its manipulation and injection through microchannels due to the high hydrodynamic pressure generated by alginate flowing inside the channels. Medium concentrated alginate viscosity permitted an easy manipulation and allowed for the production of microcapsules with good mechanical stability. Hence, 2% (w/v) alginate was selected as the suitable concentration for further experiments. Once the concentration of alginate was established at 2% (w/v), the appropriate concentration of CaCO_3 was investigated (**Figure 2.7**). Based on the reports of others (Workman *et al.* 2007), the concentration of CaCO_3 was generally utilised as 5 mg/ml. In order to investigate the effect of a modification of CaCO_3 concentration on the production of alginate microcapsules, 2% (w/v) alginate solution with 2,5 mg/ml, 5 mg/ml, and 7,5 mg/ml suspended CaCO_3 were tested. 2,5 mg/ml solutions brought about partially gelled alginate microbeads, with random shapes and sizes. On the other hand, 7,5 mg/ml solutions produced stable alginate microspheres with rounded shapes and even diameters. However, small deposits of CaCO_3 were observed within the beads, suggesting that some CaCO_3 was not dissociated. Microcapsules produced with 5 mg/ml CaCO_3 demonstrated spherical shapes of high

consistency, as seen by a defined membrane and no CaCO_3 deposits. Therefore, a concentration of 5 mg/ml CaCO_3 was established for further experiments.

Based on the reports of others groups (Workman *et al.* 2007) 0.3% (v/v) acetic acid has been used for gelation of 2% (w/v) alginate hydrogels. In order to minimize the potential harmful effect on cells in further applications (**Chapter 3**), lower concentrations of acetic acid were tested, namely 0.1% (v/v) and 0.2% (v/v). However, none of these concentrations achieved gelation of alginate microcapsules. Hence, for all the subsequent experiments carried out, the following concentrations were used: 2% (w/v) alginate solution in distilled water containing 5 mg/ml CaCO_3 and 0.3% (v/v) glacial acetic acid in mineral oil.

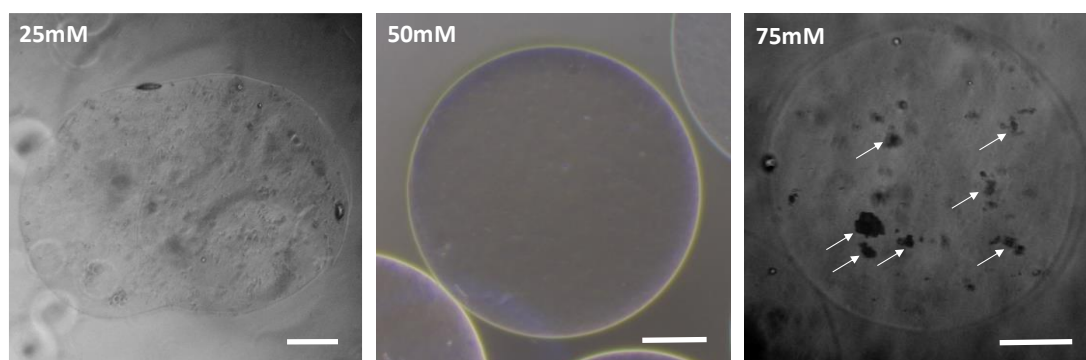


Figure 2.7. Optimization of CaCO_3 concentration. The utilization of alginates with 2,5 mg/ml CaCO_3 gave rise to incomplete gelled beads, as seen by some beads merging with each other. When CaCO_3 was resuspended in an alginate solution at a concentration of 5 mg/ml, microcapsules showed highly spherical shapes. However, when the concentration of CaCO_3 was increased (7,5 mg/ml), some deposits were visible inside the microcapsules. Scale bar = 100 μm .

2.4.3 Optimization of flow rates

One of the main benefits from the use of microfluidics for the production of micrometre-sized droplets is that the diameter of such droplets can be easily modified by variations in flow rates. Depending on the flow rate ratios, emulsification happens through different modes. Dripping mode occurs when the continuous phase and disperse phase flow rate ratio is high, and therefore, the shear force generated by the continuous phase is dominant over the hydrostatic pressure in the dispersed phase (Utada *et al.* 2007). In this case, the droplet “pinch off” takes place at the vicinity of the junction. On the contrary, when the dispersed phase flow rate is greater, and therefore the ratio between both flow rates is lower, the inertial forces become dominant over surface tension. As a result, the dispersed fluid forms a jet which breaks into droplets further downstream due to Rayleigh-Plateau instability (Plateau 1849; Rayleigh 1879). In the jetting mode, polydispersity of droplet diameters is greater, with higher coefficients of variance. Since the main purpose of this project is the microencapsulation of stem cells, a high monodispersity is a fundamental requirement to achieve. Hence, the droplet formation approach utilized in this study was flow focusing in dripping mode.

Alginate beads of different sizes were produced by modification of the flow rates. To ensure reproducibility of bead formation, each condition was performed on three different occasions. Ten beads per condition, per day (total number of beads, $n = 30$) were utilised for the measurement of their diameters, using microscopy and calibrated ImageJ software tools. In order to calculate bead

sphericity, the diameter of each bead was measured twice, lengthwise (d_1), and transversely (d_2).

$$\text{Sphericity} = \frac{d_1}{d_2} \quad (\text{Equation 1.4})$$

The coefficient of variation (CV) was calculated as follows:

$$\text{CV \%} = \frac{\text{Standard Deviation (SD)}}{\text{Mean Diameter}} \times 100 \quad (\text{Equation 1.5})$$

Firstly, alginate flow rate (f_d) was increased from 0.1 ml/h up to 2 ml/h, and a constant value of 10 ml/h was established for the continuous phase (combination of the co-flow shielding phase and proton source phase). According to the results in **Figure 2.8A**, the diameter of the beads increased when the alginate flow rate was augmented. In all cases, coefficients of variance were <2.5%, and the sphericity achieved was close to 1,0 (**Figure 2.9 A-E**).

For stem cell encapsulation purposes, small bead diameters are preferred in order to enhance the diffusion of nutrients and oxygen inside the microcapsule (Ogbonna *et al.* 1991). Therefore, with the chip design described in **Figure 2.2B** and the conditions tested above, an alginate flow rate of 0.1 ml/h should be used to produce the smallest beads. However, the frequency of bead formation with this flow rate was too low, requiring long experimentation times to produce a significant amount of alginate beads (e.g. 10 hours to produce 1ml of alginate beads). Hence, in order to produce small beads at a higher frequency, a second set of experiments were carried out. In this case, alginate flow rate was maintained at a constant value of

1 ml/h, and the continuous phase flow rate (f_c) was modified from 5 ml/h up to 30 ml/h. Results in **Figure 2.8B** show that the size of the beads decreased when the continuous phase flow rate was increased. At 30 ml/h, beads with the smallest diameters were produced ($440 \pm 3 \mu\text{m}$) at a greater frequency than in the previous experiment. Photographs of alginate beads at each condition previously described were taken (**Figure 2.9 F-J**). Hence, the flow rates selected for subsequent experiments were 1 ml/h for dispersed phase, and 30 ml/h for continuous phase, in order to produce the smallest beads in the shortest experimentation time.

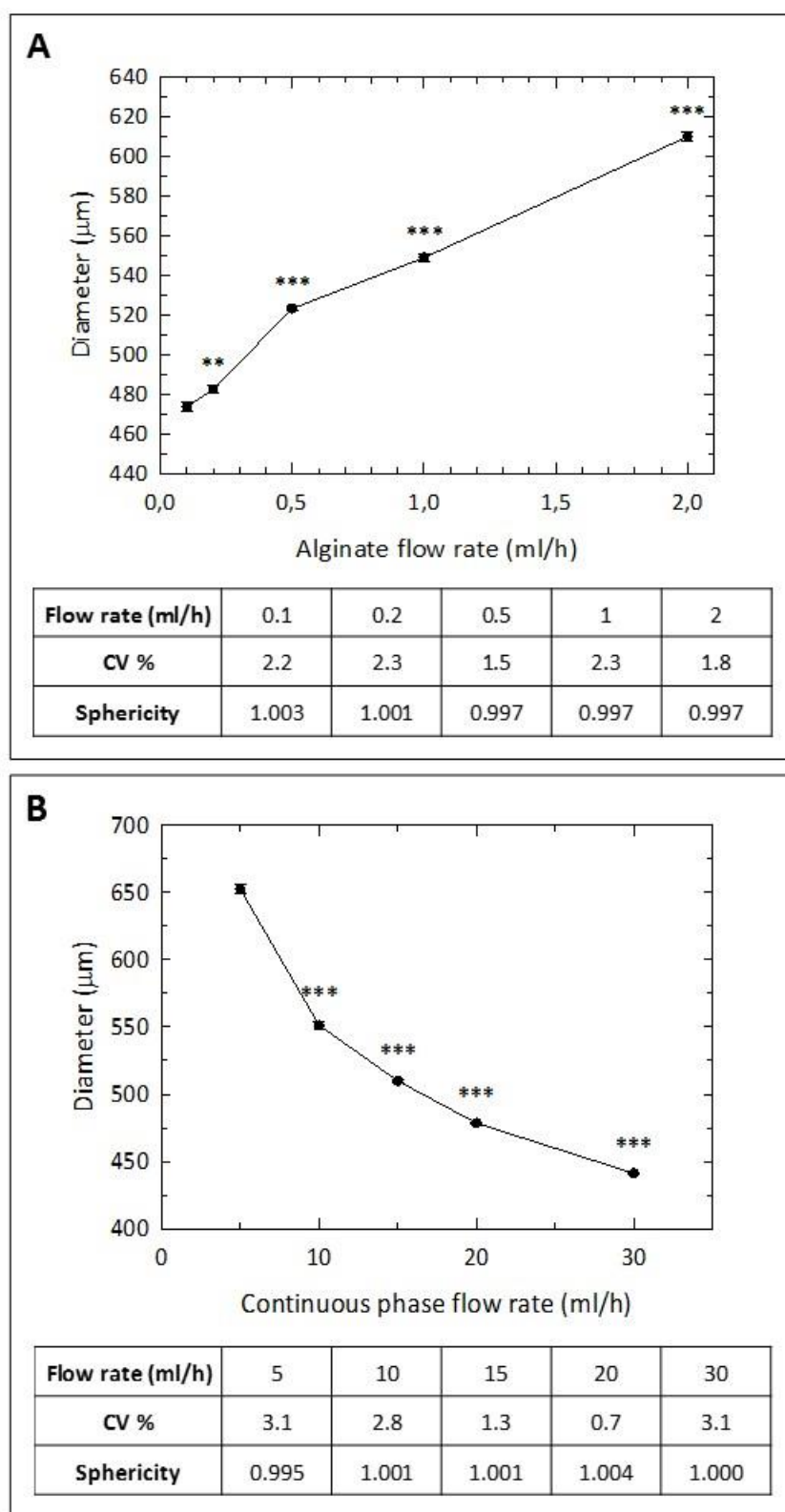


Figure 2.8. Variation of bead diameters with flow rates. A) The size of the beads increased when the alginate flow rate was augmented. B) the size of the beads decreased when the continuous phase flow rate increased. Data shown as mean \pm SEM, are representative of at least three independent experiments made in triplicate. **, $P < 0.01$; ***, $P < 0.001$, Student's t test.

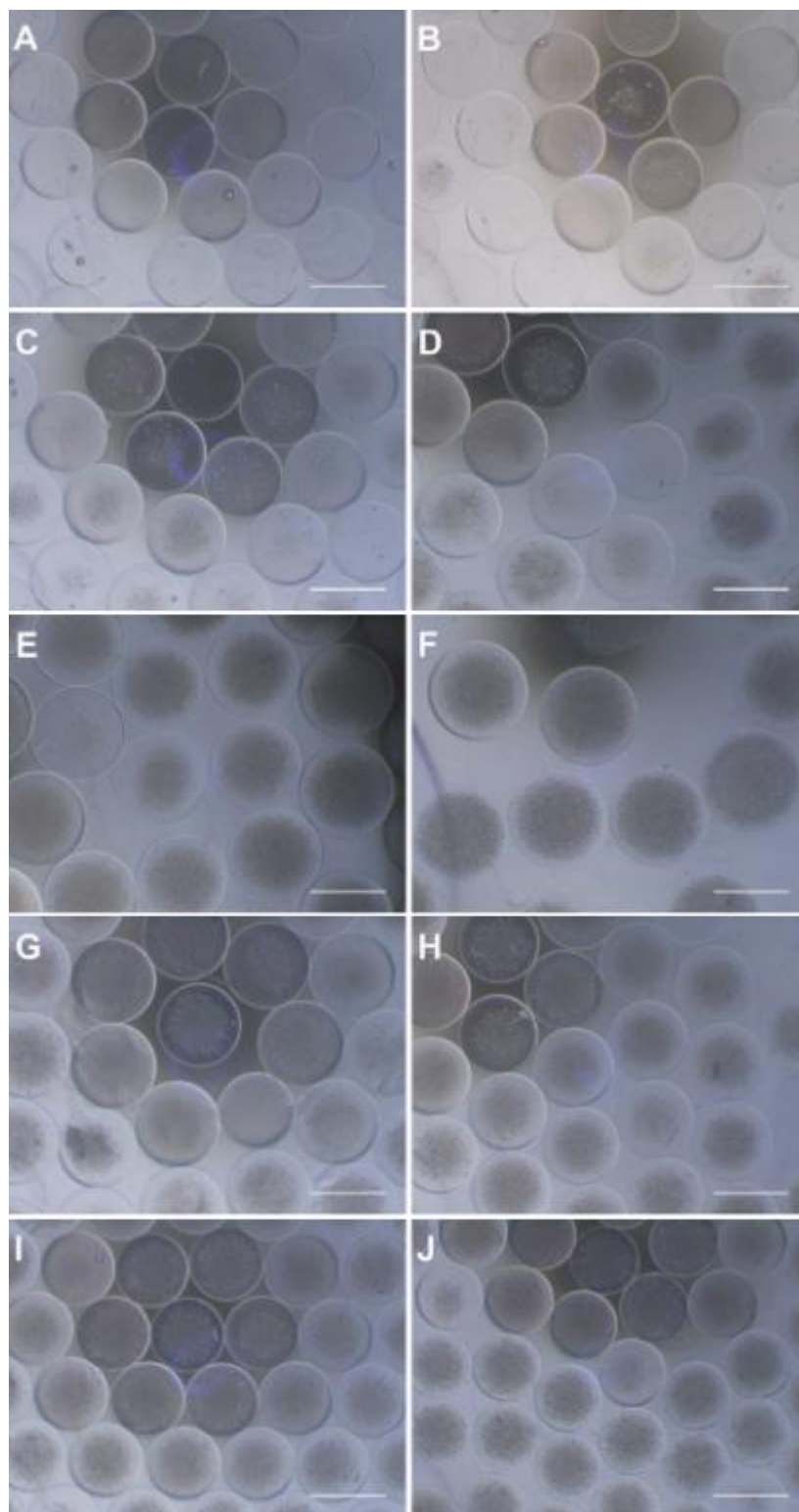


Figure 2.9. *Alginate microcapsules of different sizes were produced by a combination of different flow rates.* In the first experiment, carrier phase flow rate was maintained at 10 ml/h and alginate flow rate was modified as follows: 0.1 ml/h, 0.2 ml/h, 0.5 ml/h, 1 ml/h and 2 ml/h (A, B, C, D and E, respectively). In the second experiment, alginate flow rate was maintained at 1 ml/h and carrier phase flow rate was modified: 5 ml/h, 10 ml/h, 15 ml/h, 20 ml/h and 30 ml/h (F, G, H, I and J, respectively). Scale bar = 500 μ m.

2.5 Discussion

A customized microfluidic PTFE device was fabricated for the production and *on-chip* cross-linking of alginate beads by an internal gelation approach. The diameter of the microspheres was selectively modified by the manipulation of the flow rates.

Since interest in the production of droplets arose, polydispersity has been a major problem in conventional emulsification methods. The use of turbine reactors, colloid mills and homogenizers, imparts high mechanical forces and do not offer sufficient control over the size of the generated droplets (Mollet & Grubenmann 2001). The first attempt of internal gelation was made by Poncelet *et al.* (1992). An alginate solution containing dispersed CaCO_3 was mixed with canola oil in a turbine reactor and emulsified by stirring during 15 minutes. Polymer gelation was achieved by adding acetic acid to the emulsion in a second step. Alginate beads were then filtered through a strainer for their collection and further characterized. The resulting beads demonstrated a size distribution containing several peaks, demonstrating the polydispersity of the generated droplets. The use of microfluidics allows for the production of droplets in a physically gentler manner than the conventional methods mentioned above, thereby offering a high degree of control over their size and shape (Ushikubo *et al.* 2014). Indeed, the coefficient of variance obtained in the results of this chapter highlights a high monodispersity in the production of alginate microcapsules.

Since the dispersed phase used in this project was hydrophilic (alginate aqueous solution) a hydrophobic surface was required for droplet generation in order

to produce high spherical droplets (**Section 1.5.2.1**). Hence, PTFE was chosen as the material for the chip manufacturing. Channel fabrication strategies on this substrate, commonly soft lithography or photolithography, are time-consuming and require several steps (Cuchiara *et al.* 2010). The majority of the microfluidic devices fabricated with PDMS involve inner channels permanently sealed. For example, Shintaku *et al.* (2007) fabricated a PDMS chip for the encapsulation of cells in alginate microcapsules. The method involved the use of an epoxy-based negative photoresist as a mask for PDMS channels manufacturing, requiring 4 hours curing process. The resulting PDMS substrate was then bonded to a previously PDMS coated glass by curing for other 4 hours. In the study presented in this thesis, microchannels were effortlessly fabricated on PTFE discs by a milling process requiring short periods of time, generally less than 30 minutes. The chip was then mounted in a compressed-sealed metallic manifold which allowed the assembly and disassembly of the entire mounting in an effortless and quick manner. The use of a compressed-sealed PTFE device allowed the formation of alginate droplets and their *in situ* gelation in one step, allowing the automatization of the whole process, thereby reducing experimentation times.

An alginate cross-linking approach is crucial to achieve highly monodisperse microcapsules. Using external gelation, unsolidified alginate droplets are collected in a reservoir of divalent cations, acquiring random uncontrolled shapes (Capretto *et al.* 2008). Divalent cations cross-link the surface of the alginate droplet, hindering the diffusion of cations through the core of the droplet. On the contrary, the internal gelation strategy used in this thesis permitted the production of highly monodisperse alginate microbeads (CV < 3%), by adding an insoluble calcium salt, CaCO₃, in the

alginate solution. Droplets were then formed in the microfluidic device and divalent cation release was triggered by the action of acetic acid. This caused cross-linking of the alginate droplets in an evenly and controlled manner, giving rise to microcapsules with a homogeneous matrix structure. The gelling times required for alginate cross-linking using internal gelation are commonly shorter than those needed for external gelation, involving brief experimentation times (a few seconds compared to 15-20 minutes in external gelation). In fact, the drastic reduction of dimensions from macro-scale to micro-scale increases the diffusion rate of the molecules, giving rise to faster kinetics of the processes involved, thereby reducing experimentation times (DeMello 2006).

In this chapter, two different strategies for the *on chip* alginate internal gelation were attempted, using a flow-focusing device. It was hypothesized that the use of a proton source in the continuous phase would provoke alginate emulsification and gelation in one single step. The alginate solution containing disperse CaCO_3 was segmented by an immiscible solution of acetic acid dissolved in mineral oil. The protons in the continuous phase rapidly diffused through the alginate membrane, triggering the release of calcium ions, thereby cross-linking the polymer chains. Continuous droplet formation and solidification was observed over a short period of time, but undesired and prompt solidification of alginate took place at the junction after several minutes, blocking the channel and inhibiting a continuous alginate emulsification. Based on the work reported by Workman *et al.* (2007), the microfluidic device was modified to include a new inlet in the continuous phase, acting as a “shielding” flow, thereby preventing alginate gelation immediately after bead formation. Due to the laminar flow regime, protons diffused through the

shielding phase, inducing the slow release of calcium ions from CaCO_3 , then leading to the alginate cross-linking in a controlled and uniform manner along the path length of the channel. Alginate cross-linking *on chip* has been attempted through different methods. For example, Zhang *et al.* (2006) used a Y-shaped microfluidic planar device for the production of alginate droplets. Alginate emulsification was produced by the shear force imposed by a parallel stream formed by undecanol. Polymer gelation was achieved by the solubilisation of CaCl_2 into the undecanol phase. However, the extrapolation of this strategy for the encapsulation of stem cells would compromise their viability due to the effect of undecanol. In a different approach, Kalyanaraman *et al.* (2009) incorporated an independent channel to introduce the cross-linking agent, CaCl_2 . This was mixed with the alginate solution *on chip* prior to emulsification. However, the droplets produced were different in shape as a consequence of the prompt gelation triggered by the quick dissociation of CaCl_2 . In the method developed in this thesis, beads were highly monodispersed.

Upon optimization of emulsification and cross-linking method, two different chip designs were tested. As a first approach, a meander-like network was designed in order to increase the path-length of the microfluidic device. However, an inconsistent droplet flow was observed due to the adhesion of alginate on the corner walls as a consequence of changes in direction. The unsteady velocity of the droplets could be explained by the changes in flow direction through the meanders. This alginate film led to further undesired interactions between the channel walls and passing droplets, occasionally causing their fragmentation. This led to smaller droplets, which flowed at higher velocity than bigger droplets, giving rise to inter-droplet collisions. As gelation was delayed by the shielding flow, alginate beads were

not completely solidified in the channel and collisions provoked the droplets to merge. Merging beads brought about larger droplets, leading to the production of alginate microcapsules with different shapes and sizes, and the blockage of the outlet due to the formation of large beads. This was resolved by modification of the design of the main channel. The meander-like channel was substituted by a straight line channel, thereby avoiding directional changes, and hence, minimizing alginate adherence on channel walls.

The concentration of the dispersed phase was another parameter optimized in this chapter. Alginate solution viscosity plays a key role in the mechanism of droplet formation. As explained in **Section 1.5.2.2**, droplet generation mode depends upon the balance between the forces taking place, including surface tension, viscosity, hydrodynamic pressure and inertial forces. Dispersed phases with high viscosities give rise to high Capillary numbers (Ca). As a consequence, the shear force required for the generation of the droplet is higher, due to the resistance of the dispersed phase to deformations (Nie *et al.* 2008). On the other hand, low viscosities produce droplets with poor mechanical properties, thereby hindering their further application for cell encapsulation purposes. Thus, three different concentrations of alginate were tested, 1%, 2% and 4% (w/v). Indeed, 1% alginates gave rise to inconsistent microcapsules with low mechanical stability. In contrast, 4% alginates produced highly spherical and stable beads but its manipulation due to its high viscosity was difficult, requiring higher continuous phase flow rates in order to produce alginate emulsification. Finally, 2% alginates provided highly monodispersed beads with good mechanical properties and its manipulation and emulsification was simpler than that of 4% alginate. The suitable concentration of CaCO₃ was also

investigated. High concentration (7,5 mg/ml) produced deposits of CaCO₃ in the produced droplets, which could have a harmful effect for further cell encapsulation experiments. Low concentration (2,5 mg/ml) did not provide enough calcium ions to achieve an even and complete alginate cross-linking, as observed by the formation of inconsistent and merged beads. A medium concentration of CaCO₃ (5 mg/ml) allowed for an adequate alginate cross-linking with no deposits observed within the droplets. Hence, 2% (w/v) alginate solution and 5 mg/ml CaCO₃ were selected for further experiments.

Finally, the influence of flow rates on the size and sphericity of droplets was investigated. Dispersed and continuous flow rates were independently modified and the diameter of the beads produced at each condition were measured. When alginate flow rate was increased from 0.1 ml/h up to 2 ml/h an increase in the diameter of the beads was observed. On the contrary, when continuous phase flow rate was increased from 5 ml/h up to 30 ml/h, a decrease in the size was noticed. Changes in diameter of the beads were not linear-dependent on flow rates. This can be explained by the fact that droplet size cannot be entirely attributed to the influence of flow velocities, but also to channel geometries, fluid viscosities and surface tension (Baroud *et al.* 2010). This behaviour has been observed in other studies analysing droplet size in flow focusing devices (Ward *et al.* 2005; Lapierre *et al.* 2011).

In summary, the production of alginate microdroplets has been achieved by numerous groups, using a wide range of different techniques. However, since the main purpose of the research reported here was the encapsulation of stem cells for

healthcare therapies, only cell-friendly reagents and techniques were investigated. The microfluidic device developed in this chapter provides a simple platform for the selective production of alginate droplets of defined diameters depending on the flow rates of dispersed and continuous phases.

Chapter 3. Optimization of Stem Cell Encapsulation in ECM-based Microcapsules

3.1 Introduction

Cell transplantation is a promising technique in regenerative medicine and wound healing. However, the viability of transplanted cells is often compromised due to the harsh environment within damaged tissues and potential immune rejection after grafting (Orive *et al.* 2015). The result is that the majority of the transplanted cells die and their therapeutic effect is then hindered. To overcome these issues, the administration of immunosuppressants is widely utilised alongside transplantation therapies. However, the use of these drugs should be limited due to their negative side effects, such as immunodeficiency, hypertension and liver/kidney problems (Halloran 2004).

Cell encapsulation techniques have been applied in clinical trials to overcome the problems mentioned above for the treatment of several illnesses including type I diabetes (Calafiore *et al.* 2006) and Huntington's disease (Bachoud-Lévi *et al.* 2000). Encapsulation of cells in a protective environment helps increase the number of viable cells after transplantation, protecting against the negative effects of immune cells and antibodies, and avoiding the need of immunosuppressives (Krishnan *et al.* 2013). Furthermore, whereas the control of cell fate within an organism is often difficult to achieve/control, the immobilization of cells in a confined environment permits a better control of cell-based parameters, such as proliferation, migration and differentiation (Barthes *et al.* 2014).

It has been well reported that cells can be immobilized within polymers of differing formats, e.g. macroscopic hydrogels (Michalopoulos *et al.* 2012) or fibres

(Xu *et al.* 2017). However, the microcapsule approach has received much recent attention due to the high surface area to volume ratio, which enhances mass transfer through the polymer membrane (Liu *et al.* 2014). The polymers used for cell encapsulation need to be biocompatible and biodegradable. This is of key importance in order to avoid immunoreactivity and toxic effects within the organism. Alginate is one of the biopolymers most frequently used for encapsulation due to its relatively mild gelling conditions which are compatible with cell viability (Sun & Tan 2013). At the same time, alginate cross-linking can be easily reversed in a cell-friendly manner, allowing for the controlled release of the encapsulated cells. Importantly, alginate hydrogels provide a porous structure which allows the bidirectional diffusion of nutrients and oxygen inside the capsule and the output of therapeutic agents and waste products emanating from cell metabolism (Andersen *et al.* 2015).

In order to maintain a healthy population of cells within the microcapsules, such 3D structures require an appropriate size, so that nutrients/gases can diffuse through the polymer membrane and reach every cell at the centre of the capsule. Many efforts have been made over the last few decades to obtain micrometre-sized beads fit for such a purpose. It has been subsequently demonstrated that microfluidics is one of the most suitable and reproducible techniques to produce monodisperse cell-laden polymer microcapsules in a sealed environment, thereby avoiding any potential contamination (Pennathur *et al.* 2008; Velasco *et al.* 2012). Polymer microcapsules produced by microfluidic devices have smaller diameter and a narrower distribution size compared to the conventional methods, such as droplet extrusion and emulsification (Dulieu *et al.* 1999; Chan. *et al.* 2002). These methods typically produce polydisperse droplets with diameters > 500 μm , hindering nutrient

diffusion to the centre of the microspheres (Koch *et al.* 2003). The difficult standardization of cell number per microcapsule, as well as the inability to produce large-scale volumes of cell-containing microspheres with conventional methods, have delayed the clinical application of encapsulated cells. In response to this, microfluidics offers a powerful method to rapidly produce large-scale volumes of monodisperse polymer microdroplets with diameters of up to a few hundred micrometres (Tan & Takeuchi 2007; Capretto *et al.* 2008; Workman *et al.* 2008; Martinez *et al.* 2012). Smaller diameters enhance the diffusion of oxygen and nutrients, improving cell viability over extended periods of time (Drury & Mooney 2003; Sugiura *et al.* 2005) and facilitates bead injection for cell transplantation therapies (Yu *et al.* 2010).

3.2 Aims & Objectives

The aims of this chapter are:

- To optimize the parameters for the encapsulation of murine NSCs and DPSCs within ECM-based microcapsules.
- To study the viability and proliferation of the encapsulated cells.
- To study the ability of cells to retain their multipotency after long-term maintenance within the microcapsules.

3.3 Materials & Methods

3.3.1 Cell culture

To maintain sterility, all tissue culture procedures were performed in a Microflow Peroxide Class II advanced biological safety cabinet (Bioquell, UK).

3.3.1.1 Dental pulp stem cell culture

Murine GFP DPSCs were isolated by others in the group of Prof. Ketan Patel, within the School of Biological Sciences (University of Reading). Cells were cultured in α -modification Minimum Essential Medium containing 2 mM glutamine, ribonucleosides and deoxyribonucleosides (Life Technologies, UK). The medium was supplemented with 1% (v/v) penicillin/streptomycin, 20% (v/v) heat-inactivated foetal bovine serum (FBS) (Life Technologies, UK) and 100 μ M l-ascorbic acid 2-phosphate (Sigma-Aldrich, UK). Medium was changed every 2-3 days until cells reached 80-90% confluence.

3.3.1.2 Passaging DPSC Cultures

Upon reaching confluence, culture medium was removed by aspiration and the cells washed with phosphate buffered saline (PBS) (Sigma-Aldrich, UK). Cells were dissociated by adding 0.25% trypsin-EDTA (Sigma-Aldrich, UK) and returning them to the incubator for 3 - 5 minutes until they became rounded and detached.

Culture medium was then added to neutralise the trypsin. The resultant solution of medium plus cells was transferred to 15ml falcon tubes and centrifuged at 400x *g* for 5 minutes. After discarding the supernatant, pellets were resuspended in medium and cell counts performed using a haemocytometer with trypan blue to assess cell viability (**Section 3.3.2.1**). Cells were reseeded on new culture plastics at a density of 4000 viable cells/cm² for continuous culture, or as per experimental requirements.

3.3.1.3 Cryopreservation and re-establishment of DPSCs

DPSCs were cryopreserved at regular intervals during culture. Following passaging, a minimum of 1x10⁶ cells were resuspended at 1x10⁶ cells/ml in heat-inactivated FBS + 20% (w/v) dimethyl sulphoxide (DMSO) (Fisher Scientific, UK) and transferred to 2ml cryovials (Greiner Bio-one, Germany). Cryovials were slowly cooled to -80°C in a propan-2-ol filled *Mr Frosty* (Nalgene, USA). After being stored for 24 hours at -80°C, cryopreserved cells were transferred to liquid nitrogen storage.

As required, DPSCs were re-established from frozen stock by thawing in a 37°C water bath. Thawed cell suspensions were transferred to 15ml conical tubes containing culture medium and centrifuged at 400x *g* for 5 minutes. Following centrifugation, traces of DMSO were removed by discarding the supernatant and resuspending the cell pellets in culture medium and then a further 5-minute centrifugation. Cell counts with trypan blue (**Section 3.3.2.1**) were undertaken and cells reseeded in culture plastics at a density of 4000 cells/cm².

3.3.1.4 Embryonic neural stem cell culture

GFP NSCs isolated from the cortex of E14.5 C57Bl/6 mice by others in the group of Prof. Ketan Patel, within the School of Biological Sciences (University of Reading) were maintained in Dulbecco's Modified Eagle Medium (DMEM)/Ham's F12 (1:1) containing 2.5 mM of L-glutamine and 15mM HEPES buffer (Life Technologies, UK). This was supplemented with 1% (v/v) penicillin/streptomycin, 2% (v/v) B27 supplement (Life Technologies), 10 µg/mL insulin-transferrin-sodium selenite supplement (ITSS) (Roche Life Science, UK), 20 ng/ml bFGF and 20 ng/ml EGF (both Peprtech).

3.3.1.5 Subculturing NSC cultures

NSCs were cultured as floating neurospheres at 37°C with 5% CO₂ and half medium changes performed every 2 days. As neurospheres expanded and increased in size, the centre of the spheres began to turn dark as cells became deprived of nutrients. Before reaching this stage, spheres were subcultured. The media and floating spheres were aspirated and centrifuged at 100x *g* for 5 minutes. 1ml of accutase was used to dissociate the pellet and left to incubate in the water bath at 37°C for 5 minutes, dissociating spheres to a single cell suspension. The action of accutase was then stopped by the addition of PBS. Following a further centrifugation at 100x *g* for 5 minutes, the supernatant was discarded and the cells resuspended in medium. Cells were passed through a 40µm cell strainer (Falcon™) to remove any clumps of cells. Cell counts were performed and the cells resuspended at a density

of 100,000 cells/ml for continuous culture, or, seeded on 50 µg/ml poly-D-lysine (PDL) and 20 µg/ml laminin coated plates for experiments.

3.3.2 Viability and proliferation assays

3.3.2.1 Trypan Blue Exclusion Assay

Trypan blue is a dye that selectively stains non-viable tissues/cells blue. Live cells with intact membranes do not allow the absorption of this stain. However, trypan blue penetrates the compromised membrane of dead cells.

To determine the percentage of viable cells, an aliquot of cell suspension was mixed with an appropriate volume of trypan blue. The mix was then placed in the haemocytometer chamber and cell counting was performed under phase contrast microscopy. The percentage of viable cells was calculated according to the following equation:

$$\text{Percentage of cells viability} = \frac{\text{Number of unstained cells counted}}{\text{Total number of cells counted}} \times 100 \quad (\text{Equation 3. 1})$$

Cell viability was assessed using the trypan blue exclusion assay prior to encapsulation and on days 1, 3, 7, 10, 14 and 21 after encapsulation. The method was slightly modified to be applied on encapsulated cells. 200µl of bead suspension were taken and beads left to settle at the bottom of the tube. Culture medium was removed carefully so as not to remove any of the beads. Beads were dissolved and cells released as described in **Section 3.3.4**. Cells were centrifuged (100x *g* for NSCs and 400x *g* for DPSCs), supernatant removed, and the pellet resuspended in 10µl of culture medium. Since NSCs grew in aggregates within the microcapsules, cells were accutase treated prior to suspension in culture medium in order to obtain a single

cell suspension. 10µl of trypan blue were added, mixed and the cell suspension was placed in a haemocytometer for cell counting.

3.3.2.2 MTT Assay

MTT assay was used to study cell viability/proliferation based on the cell's metabolic activity. MTT (3-(4,5-dimethylthiazol-2-yl)-2,5-diphenyltetrazolium bromide) is reduced to its precipitated formazan product by the action of NAD(P)H-dependent cellular oxidoreductase enzymes. As MTT reduction depends on NAD(P)H-dependent oxidoreductase enzymes, this reaction is related to the cellular metabolic activity due to NAD(P)H flux. Since rapidly dividing cells exhibit high metabolic activity, therefore giving high rates of MTT reduction, this analytical method is suitable to study relative cell proliferation.

MTT (Sigma-Aldrich, UK) aliquots were prepared fresh by dissolving the powder in PBS at a concentration of 5 mg/ml, and were then filter sterilized. Bead suspension was mixed to give a dispersed, homogenous distribution. Cells or beads containing cells were seeded in 96-well plates in 200µL of medium. 20µL of MTT solution was added to each well, including controls, and incubated for 4 hours at 37°C/5% CO₂. Culture medium was then removed and 150µL of DMSO was added to each well to dissolve any formed formazan crystals. Plates were incubated for an additional 30 minutes to allow the precipitate to dissolve completely. Absorbance was subsequently measured at a wavelength of 540nm (FLUOstar Omega microplate reader, BMG Labtech).

In order to test the potential absorbance due to alginate or alginate-collagen microcapsules, empty microcapsules were plated on surfaces in 96-well plates. MTT

reagent was added, incubated and then absorbance measured at 540nm. Measurement values were, in both cases, close to the medium only control. Therefore, a control including empty microcapsules was not required, and only blanks containing culture medium were performed.

3.3.2.3 Live/Dead[®] Viability/Cytotoxicity Assay

The cell-impermeant viability indicator ethidium homodimer-1 (EthD-1) is a high-affinity nucleic acid stain that is weakly fluorescent until bound to DNA. When used with GFP cells (488nm excitation max and 509nm emission max), it allows the simultaneous determination of live and dead cells. Co-expression of green and red fluorescence permits identification of dead/dying cells. Dead or damaged-membrane cells are permeable to EthD-1, which undergoes an increase of fluorescence upon binding to nucleic acids, and producing red fluorescence in dead cells (528nm excitation max and 617nm emission max).

Encapsulated cells were rinsed with PBS three times and then stained with a PBS solution containing EthD-1 at a final concentration of 2 μ M. Cells were incubated for 30 minutes at room temperature and then the dye solution was removed and cells washed three times with PBS before imaging. Laser scanning confocal microscope imaging of encapsulated cells was performed using a Leica SP5 Confocal Microscope and LAS AF imaging software. An argon 488nm laser was used for excitation of GFP and emission light between 505 and 530nm was detected. A HeNe 543nm laser was used for excitation of EthD-1 and emission light over 650nm detected (**Figure 3.1**).

Images of encapsulated cells were acquired from confocal Z scans over a depth of 400 μ m.

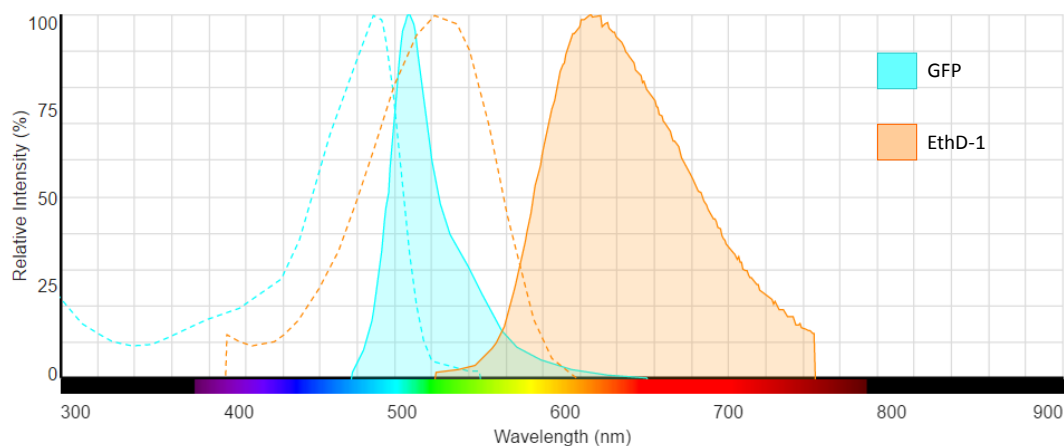


Figure 3.1. Absorption and fluorescence emission spectra of GFP and EthD-1. Blue lines show absorption and fluorescence emission spectra of GFP (488 nm/509 nm). Orange lines show absorption and fluorescence emission spectra of EthD-1 bound to DNA (528nm/617 nm).

3.3.2.4 CellTrace™ Far Red staining for proliferation analysis by Flow Cytometry

A CellTrace™ Far Red Cell Proliferation Kit was used for labelling cells to track proliferation by flow cytometry. The kit contains a cell-permeant, non-fluorescent ester of an amine-reactive fluorescent molecule, which enters cells by diffusion through the plasma membrane. Upon entry into the cell, the non-fluorescent molecule is converted to a fluorescent derivative by cellular esterases. The active succinimidyl ester covalently binds to amine groups in proteins, resulting in long-term dye retention within the cell. Through subsequent cell divisions, daughter cells

receive approximately half of the fluorescent label of their parent cells, allowing for the analysis of the fluorescence intensities of labelled cells. Analysis of the level of fluorescence in the cell populations by flow cytometry permits the determination of the number of generations through which a cell has progressed since the label was applied.

Cells were stained with CellTrace™ Far Red Cell Proliferation Kit according to manufacturer's instructions (Life Technologies, UK). Briefly, cells were dissociated with 0.25% trypsin-EDTA. Culture medium was then added to neutralise the trypsin and cells were centrifuged at 400x *g* for 5 minutes. After discarding the supernatant, pellets were resuspended in PBS at a concentration of 1×10^6 cells/ml. A stock solution of staining reagent was prepared by dissolving CellTrace™ Far Red in DMSO at a final concentration of 1mM. The appropriate volume of CellTrace stock solution was added to cell suspension to give a concentration of $1 \mu\text{M}$. Cells were incubated for 20 minutes at 37 °C protected from light. Five times the original staining volume of culture medium containing at least 20% FBS was added to the cells and incubated for 5 minutes in order to remove any free dye remaining in the solution. Cells were then centrifuged and resuspended in fresh pre-warmed complete culture medium. Cells were then seeded on flasks or encapsulated for further analysis.

Cell samples were analysed using a FACSCanto flow cytometer (BD Biosciences). Output data from the flow cytometer was analysed using FACS Diva Version 6.1.3 software, which presents data as dot plots and histograms, and permits calculation of the mean fluorescent intensity of the cells. To analyse the stained cells, 10,000 events were captured for each sample. Two different lasers were used for

excitation: an argon 488nm laser and a HeNe 633nm laser. Green fluorescence emission for GFP expressing cells (530/30 nm bandpass filter) and red fluorescence emission for CellTrace™ Far Red (660/20 nm long pass filter) were measured. The data was then analysed with FlowJo Version 10.2 software.

3.3.2.5 Inhibition of cell proliferation with Mitomycin C

Mitomycin C is an alkylating agent that inhibits DNA synthesis by covalently reacting with DNA, forming crosslinks between complementary strands of DNA. This interaction prevents separation of complementary DNA strands, inhibiting DNA replication and therefore, cell proliferation.

DPSCs were treated with mitomycin C according to manufacturer's instructions. Briefly, mitomycin C (Fisher Scientific, UK) was reconstituted at 0.5 mg/mL in water. The appropriate volume of mitomycin C solution was added to flasks containing 80-90% confluent DPSCs and culture medium to achieve a 10 µg/ml final concentration. Cells were then incubated for 3 hours at 37°C in humidified incubator with 5% CO₂. Culture medium containing mitomycin C was removed and cells were washed twice with PBS. Cells were then trypsinized and seeded in flasks (**Section 3.3.1.2**).

3.3.3 Encapsulation of stem cells

3.3.3.1 Preparation of encapsulation matrix solutions

3.3.3.1.1 Alginate matrix

Nanocrystalline precipitated CaCO_3 was dispersed in PBS at a final concentration of 5 mg/ml. Medium Viscosity sodium alginate was added to the CaCO_3 suspension at a final concentration of 2% (w/v). The blend was stirred for 2 hours at 50°C and then autoclaved for sterilization.

3.3.3.1.2 Alginate-collagen matrix

Alginate scaffold was modified with type I collagen in **Section 3.4.3**. Hence, an alginate solution of 4% (w/v) in PBS containing 100mM nanocrystalline precipitated CaCO_3 was prepared as mentioned above. Ice cold rat tail type I collagen (5 mg/ml; First Link, UK) was neutralized with 0.25M NaOH and mixed with the 4% (w/v) alginate solution, giving rise final concentrations of 2 mg/mL collagen and 2% (w/v) alginate.

3.3.3.2 Production of cell-laden microspheres

Each component of the microfluidic device (**Figure 2.1**) along with PTFE tubing and nitrile o-rings were sterilized by autoclaving prior to any encapsulation experiment being carried out. The entire assembly was then assembled within a Microflow Peroxide Class II advanced biological safety cabinet (Bioquell, UK) to

maintain sterility. Syringes were loaded with mineral oil and pumped through HPLC fluid connectors and microfluidic chip, in order to lubricate the walls and avoid alginate adhesion and blockages.

Cells were trypsinized (DPSCs) or accutase treated (NSCs) and resuspended in culture medium for cell counting (**Section 3.3.2.1**). The appropriate number of cells was taken and centrifuged at 400x *g* (DPSCs) or 100x *g* (NSCs) for 5 minutes. After the supernatant was removed, the cells were resuspended in the encapsulating matrix solution. Cell suspension, mineral oil, and 0.3% (v/v) acetic acid in mineral oil were introduced in the chip through HPLC tubes (**Section 2.3.4**). Their flow rates were established at 1 ml/h, 15 ml/h and 15 ml/h, respectively, and controlled by syringe pumps. Polymer microcapsules containing cells were collected in pre-warmed culture medium. Residual mineral oil was removed and microcapsules were then washed with PBS before replacement with fresh culture medium. Encapsulated cells were maintained in the incubator under standard conditions (37°C, 5% CO₂) until further experiments were undertaken.

3.3.4 Cell release from microspheres

Encapsulated cells were released from microcapsules following a 5 min incubation with 55mM sodium citrate (Sigma Aldrich, UK) at 37°C. Cells were then centrifuged (100x *g* for NSCs and 400x *g* for DPSCs), supernatant removed and resuspended in culture medium. For alginate-collagen encapsulated cells, an additional incubation step with 1% (w/v) type I collagenase (Sigma Aldrich, UK) was

performed for 5 minutes at 37°C, following incubation with sodium citrate. Cells were then centrifuged, supernatant removed and resuspended in culture medium.

3.3.5 Estimation of number of cells per bead

Specific number of beads were taken for each concentration. Cells were released from microcapsules as previously mentioned and resuspended in specific volumes of culture medium. Cells were counted and the result (total number of cells in the specific volume) was divided by the number of beads taken.

3.3.6 Neuronal differentiation

NSCs isolated from the cortex of E14 C57Bl/6 mice, and DPSCs isolated from 21-28 day old C57/Bl6 mice, by colleagues in Prof. Bing Song's laboratory (School of Dentistry, Cardiff University) were used in **Section 3.4.5**. A nestin expressing clonogenic population of DPSCs previously expanded by colleagues in Song's lab was selected to carry out the experiments in this section. Since DPSCs represents a highly heterogeneous population of cells (**Section 1.2.2.1**), a specific clone with neuronal differentiation potential was selected to carry out the neuronal differentiation experiments, in order to increase the yield of differentiated cells.

3.3.6.1 NSCs neuronal differentiation

Culture plates were coated with 50 µg/ml PDL (Sigma-Aldrich, UK) and incubated overnight at 37°C. This was removed the day after and the surfaces rinsed with PBS. Laminin (Sigma-Aldrich, UK), diluted to 20 µg/ml in PBS, was then used to coat the culture plates at 37°C for 30 minutes. Laminin solution was removed and washed with PBS. The surfaces were then ready for seeding with cells.

Encapsulated NSCs were released from beads 21 days after encapsulation and seeded at a density of 10,000 cells/cm² on poly-d-lysine/laminin-coated plates in DMEM/F12 (1:1) containing L-glutamine and HEPES buffer, 1% (v/v) penicillin/streptomycin, 2% (v/v) B27 supplement, 20 ng/ml bFGF, 20 ng/ml EGF and 10 µg/mL ITSS. When cells reached 80-90% confluence, growth factors were gradually removed by half media changes every other day for up to 10 days with growth factors-free culture medium.

3.3.6.2 DPSCs neuronal differentiation

Culture plates were coated with 10 µg/ml PLL (Sigma-Aldrich, UK) for 5 minutes at 37°C. This was removed and rinsed with PBS. Laminin (Sigma-Aldrich, UK), diluted to 20 µg/ml in PBS, was then used to coat the culture plates at 37 °C. Laminin solution was removed the day after and washed with PBS. The surfaces were then ready for seeding with cells.

Encapsulated DPSCs were released from beads 21 days after encapsulation and seeded at a density of 10,000 cells/cm² on PLL/laminin-coated plates in

DMEM/F12 (1:1) containing L-glutamine and HEPES buffer, 1% (v/v) penicillin/streptomycin, 2% (v/v) B27 supplement, 20 ng/ml bFGF, 20 ng/ml EGF and 10 µg/mL ITSS. After 5 days in culture, cells were washed with PBS and medium replaced with Neurobasal medium supplemented with 1% (v/v) penicillin/streptomycin, 2 mM L-glutamine, 1 x NEAA (Sigma-Aldrich, UK), 10 ng/ml nerve growth factor (NGF), 10 ng/ml BDNF and 10 ng/ml NT-3 (all Peprotech).

3.3.7 Immunocytochemistry staining

After the differentiation protocol and following removal of medium, cells were washed with PBS for 3 minutes before being fixed with 4% (w/v) paraformaldehyde (PFA) for 30 minutes at room temperature. Three further washes with PBS were performed and the cells were then permeabilized with 0.1% (v/v in PBS) Triton X-100 for 30 minutes at room temperature. After three washes, 5% (w/v) bovine serum albumin fraction V (BSA; Fisher Scientific, UK) in PBS was applied for one hour in order to block non-specific binding groups. This was removed and replaced with antibodies against Nestin, Sox2, Oct4, β -III tubulin and Map2 (**Table 1**) and the isotype control (**Table 2**) diluted in 5% (w/v) BSA at a concentration of 5 µg/ml and incubated overnight in a dark humid chamber at 4°C. The following day, three PBS washes were performed. Slides were then incubated with complementary fluorophore-conjugated secondary antibodies (**Table 3**) diluted in 5% (w/v) BSA at a concentration of 4 µg/ml in the dark at room temperature for 1 hour. Three further washes with PBS were performed before the cells were mounted onto glass cover slips using mounting medium supplemented with DAPI stain (VectorLabs, UK). bSlides were

stored at 4°C in the dark to prevent bleaching, until required for imaging (**Section 3.3.8.2**).

3.3.8 Cellular Imaging

3.3.8.1 Phase contrast imaging

Phase contrast images of microspheres and cells in culture were captured using an Eclipse TS100 inverted phase contrast light microscope (Nikon, Japan) equipped with a digital camera (Canon, Japan).

3.3.8.2 Fluorescent imaging

GFP expressing cells and fixed and fluorescent antibody-stained cells were viewed and images acquired using an ultra violet (UV) microscope (Olympus AX70 with a Digital Eclipse DXM1200 digital camera attachment, Tokyo, Japan). The images were captured using the Automatic Camera Tamer (ACT-1) control software (Nikon Digital, Tokyo, Japan).

3.3.8.3 Confocal laser scanning microscopy

A Leica SP5 Confocal laser scanning microscope and LAS AF imaging software were used for all confocal microscopy experiments (Leica Microsystems, Germany). An argon 488nm laser was used for excitation of GFP and emission light between 505

and 530nm was detected. A HeNe 543nm laser was used for excitation of EtDh-1 and emission light over 650nm detected.

3.3.8.4 Image processing

Acquired images were processed and overlapping images merged using freely available ImageJ version 1.47i software.

3.3.9 Statistics

Data are represented as mean \pm SEM, unless otherwise indicated. Statistical significance was determined by Student's t test. $P < 0.05$ was considered statistically significant.

3.4 Results

3.4.1 Study of the cytotoxicity of the reagents used on stem cells

The production of alginate microcapsules with a diameter of $440 \pm 3 \mu\text{m}$ was achieved utilising a customized PTFE microfluidic device developed in **Chapter 2**. Since the main purpose of this project was the encapsulation and maintenance of stem cells within alginate micro beads, a study of the potential toxicity on cells of the reagents used was undertaken.

The technique developed in the previous chapter was based on an internal gelation method for the continuous and reproducible production of alginate microspheres. The alginate stream was “broken-off” by the shear force generated by the immiscible phase mineral oil. The mineral oil used for alginate emulsification in this project was classified as suitable for cell culture, and, therefore, it was assumed that it would not have any toxic effect on cells. However, as an internal gelation approach was used, a source of protons was required to trigger the release of calcium ions to cross-link alginate chains. To this end, acetic acid was dissolved in mineral oil at a final concentration of 0.3% (v/v) and hence the effects of an acidic environment and its potential detrimental effect on cells was investigated.

In the microfluidic system developed in this project, alginate droplets were collected in pre-warmed culture medium, alongside the continuous phase (mineral oil plus acetic acid). Since mineral oil has a lower density than culture medium, it was easily removed with a pipette. However, the acetic acid present in the mineral oil diffused through the interphase between both liquids, which was indicated by a

pH/colour change of the culture medium. Therefore, the effect on cells of the addition of acetic acid into the culture medium was also investigated.

Three similar samples of each cell type suspension were centrifuged and supernatant discarded. Sample 1 was resuspended in mineral oil, sample 2 was resuspended in 0.3% (v/v) acetic acid in mineral oil, and sample 3 was resuspended in 0.3% (v/v) acetic acid in culture medium. Cell suspension in culture medium was used as a control. Since mineral oil is immiscible with aqueous solutions, 10 μ l of culture medium were added to samples 1 and 2 and the mixture was pipetted up and down in order to force the diffusion of the cells into the aqueous phase (culture medium). 10 μ l of each sample were taken and viability was estimated using trypan blue exclusion assay (**Section 3.3.2.1**).

The duration between the beginning of the droplet formation and its collection in culture medium was approximately 30 seconds. To ensure this was not detrimental, the viability of the samples 1 and 2 were determined one minute after resuspension. As demonstrated in **Figure 3.2**, cell viability decreased slightly when either DPSCs or NSCs were resuspended in mineral oil or in 0.3 % (v/v) acetic acid in mineral oil, suggesting a minimal effect on cell viability but not whole scale cell death on exposure to the microfluidic reagents ($P < 0.05$).

Viability of sample 3 was estimated 1, 10 and 20 minutes after resuspension. These time points were chosen as the experimentation times for cell encapsulation were fixed at 1 hour, with the collection medium changed every 10-20 minutes. It was clear that the addition of 0.3% (v/v) of acetic acid into the culture medium had

no toxic effect on cells over the test period, since no significant difference was observed in cell viability throughout the period tested (**Figure 3.3**; $P > 0.05$).

Alginate has been demonstrated to be one of the biocompatible polymers most used for cell encapsulation (Lee & Mooney 2012). However, it was hypothesised that the suspension of crystalline CaCO_3 nanoparticles may have a harmful effect on any cells present within the micro-beads. It is well established that variations in cytosolic Ca^{2+} concentration can affect cellular functions, from the secretion to hormones to the regulation of cell death (Pinton *et al.* 2008). Hence, the study of cell survival within alginate- CaCO_3 matrix solution was also required. The viability of the cells resuspended in the encapsulation matrix (2% (w/v) alginate solution plus 5 mg/ml precipitated CaCO_3) was studied over a period of 5 hours prior to any encapsulation procedure being carried out. As demonstrated in **Figure 3.4** the viability of the cells over the time course of the experiment was not significantly different compared to control ($P > 0.05$).

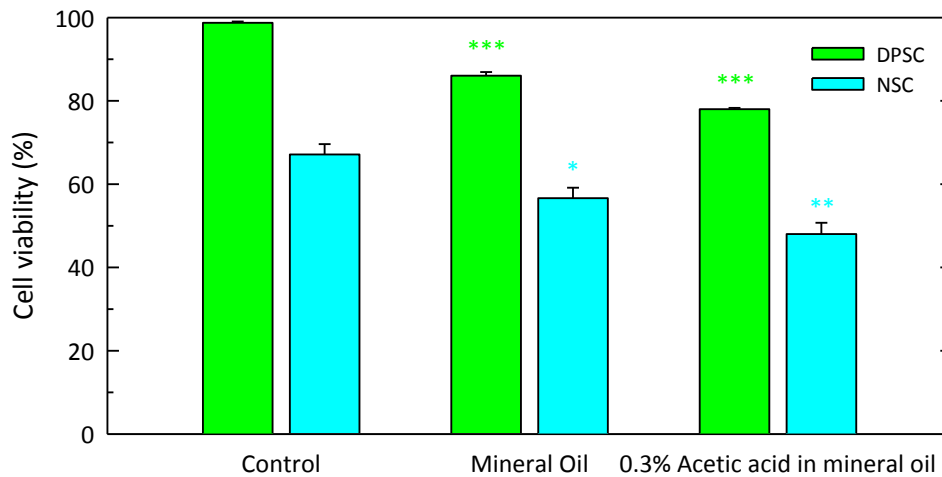


Figure 3.2. Viability of DPSCs (green) and NSCs (blue) resuspended in mineral oil or in 0.3 % (v/v) acetic acid in mineral oil. Cell viability was estimated one minute after resuspension. Data are shown as mean \pm SEM, and are representative of at least three independent experiments made in triplicate. *, $P < 0.05$; **, $P < 0.01$; ***, $P < 0.001$, Student's t test.

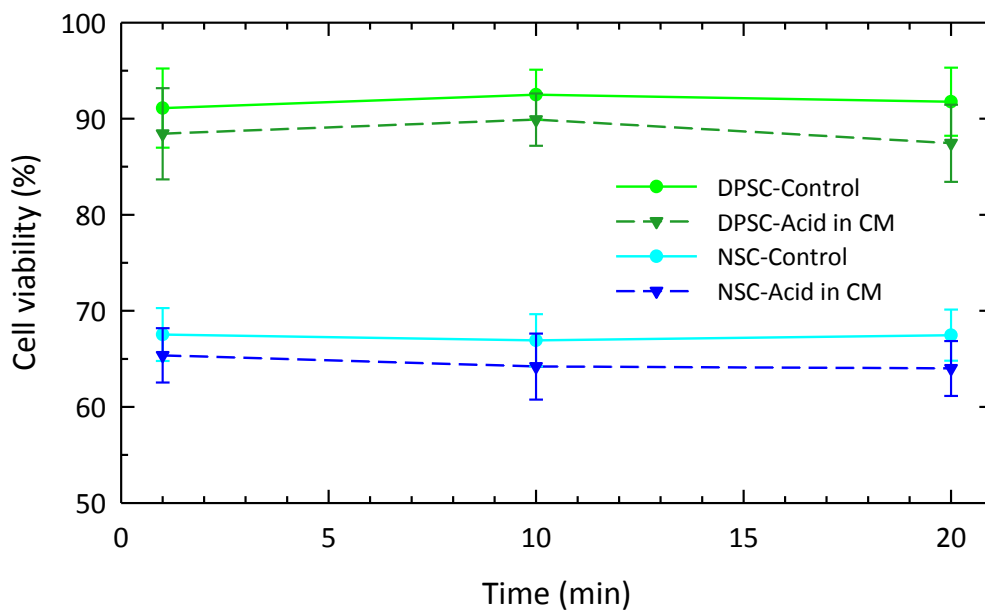


Figure 3.3. Viability of DPSCs (green) and NSCs (blue) resuspended in 0.3% (v/v) acetic acid in culture medium (Acid in CM). Cell viability was determined 1, 10 and 20 minutes after resuspension. Data are shown as mean \pm SEM, and are representative of at least three independent experiments made in triplicate.

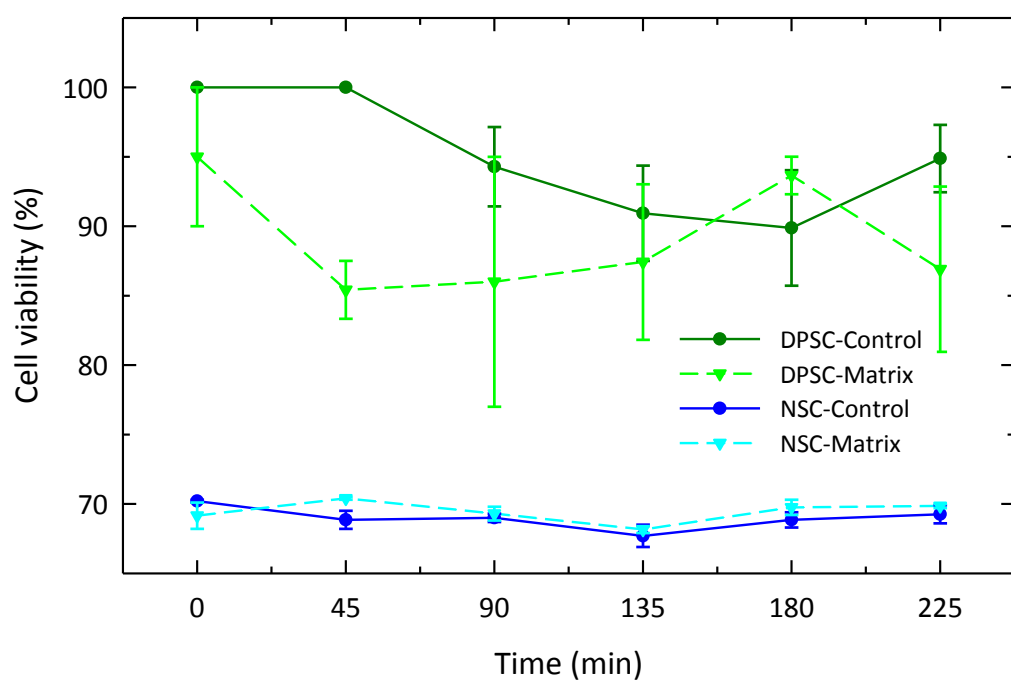


Figure 3.4. Viability of DPSCs (green) and NSCs (blue) resuspended in 2% (w/v) alginate solution containing 5 mg/ml CaCO₃. Cell viability was investigated over a period of 5 hours at intervals of 45 minutes. Data are shown as mean \pm SEM, and are representative of at least three independent experiments made in triplicate.

3.4.2 Optimization of microcapsule initial cell seeding density

Since the ultimate goal of this thesis was the transplantation of encapsulated cells within an animal model of SCI, a study of the microcapsule seeding density was required. It was ultimately hypothesized that a high population of viable cells would have a greater therapeutic effect. Furthermore, it has been reported that cell density plays a crucial role in the cells' functionality, i.e. their proliferation and differentiation (Issa *et al.* 2011). Hence, an investigation of the appropriate initial cell seeding density was undertaken of whether such stem cells within a confined environment would maintain optimal survival.

Preliminary encapsulation experiments with both cell types demonstrated different behaviours (**Figure 3.5**). Whereas NSCs exhibited proliferation within the microcapsules in form of neurospheres, this was not observed with DPSCs. Therefore, it was hypothesized that high NSCs seeding densities would lead to the formation of large cell aggregates in a short period of time, potentially provoking apoptosis in the centre of the neurospheres since the cells could become deprived of nutrients. Hence, two different cell concentrations were tested, namely 1×10^5 cells/ml and 1×10^6 cells/ml. In the case of DPSCs, since no signs of cell proliferation were observed, greater cell seeding densities were investigated: 1×10^6 cells/ml, 2×10^6 cells/ml, 5×10^6 cells/ml, and 1×10^7 cells/ml. Both cell types and all the concentrations mentioned above were encapsulated under the same conditions (**Section 3.3.3.2**).

In **Figure 3.6**, images A, C, E, G, I, K correspond to laser scanning confocal microscope images of the encapsulated cells. The green dots, representing GFP cells, were randomly distributed within the alginate microcapsules. At low concentrations

(1×10^5 cells/ml – 2×10^6 cells/ml) the majority of the space within the capsules was unoccupied, whereas at high concentrations (5×10^6 cells/ml – 1×10^7 cells/ml) cells filled most of the cavities in the microspheres. Images B, D, F, H, J, L are bright field images.

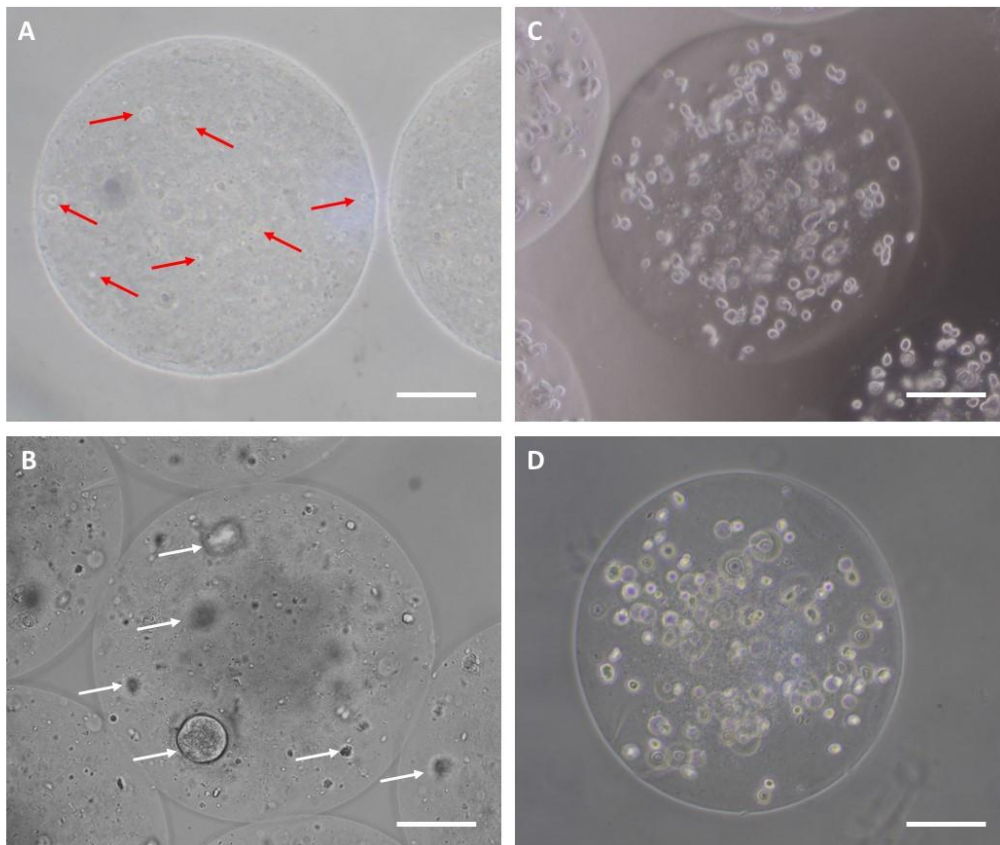


Figure 3.5. Encapsulated NSCs and DPSCs within alginate microcapsules. A-B) Encapsulated NSCs 0 and 5 days after encapsulation, respectively. Single NSCs were visible on day 0 (red arrows), whereas some cell aggregates (white arrows) were observed 5 days after encapsulation. C-D) Encapsulated DPSCs 0 and 5 days after encapsulation, respectively. No cell number increase nor aggregates were observed within microcapsules, suggesting that cells did not proliferate within the beads. Scale bar = 100 μ m.

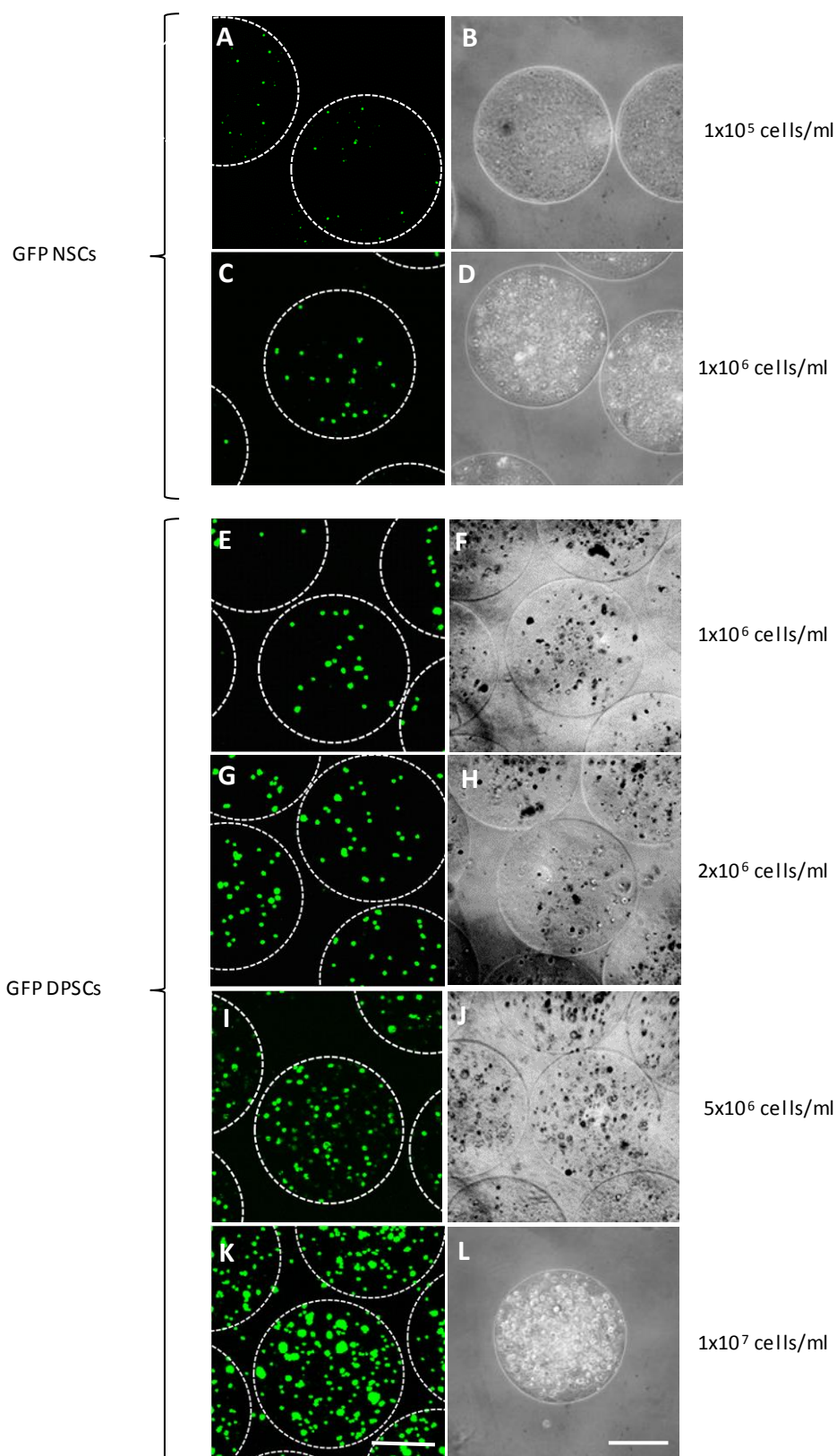


Figure 3.6. Encapsulated cells in alginate microcapsules. Images were taken 1 day after encapsulation. Laser scanning confocal images of encapsulated cells were performed using a Leica SP5 Confocal Microscope. Images of encapsulated cells were acquired from a confocal Z scan over a depth of $400\mu\text{m}$. Optical images were taken with an Eclipse TS100 inverted phase contrast light microscope (Nikon, Japan). Scale bar = $200\mu\text{m}$.

In terms of cell transplantation, an accurate estimation of the number of transplanted cells is important in respect of eventual clinical application. Therefore, both theoretical and experimental estimation of number of cells per bead were carried out for each cell type and condition investigated. In general, (**Table 3.1**) there was good correlation between the different estimated numbers of cells within each bead ($P > 0.05$).

| NSCs | | | |
|--------------------------------------|--------------------------------------|--------------------------------------|------|
| Initial seeding density (cells / ml) | Cells/bead (theoretical calculation) | Cells/bead (experimental estimation) | SD |
| 1,00E+05 | 5 | 3 | 3,4 |
| 1,00E+06 | 45 | 38 | 8,6 |
| DPSCs | | | |
| Initial seeding density (cells/ml) | Cells/bead (theoretical calculation) | Cells/bead (experimental estimation) | SD |
| 1,00E+06 | 45 | 43 | 11,2 |
| 2,00E+06 | 89 | 86 | 13,8 |
| 5,00E+06 | 223 | 230 | 30,5 |
| 1,00E+07 | 446 | 416 | 42,1 |

Table 3.1. Theoretical calculation and experimental estimation of the number of cells per bead. For concentrations greater than 1×10^6 cells/ml there was good correlation between the different estimated numbers of cells within each bead. Value = mean \pm SD (n=9).

3.4.2.1 Study of cell survival within alginate microcapsules using the Trypan Blue Exclusion Assay

The viability of encapsulated cells at each concentration and each cell type was studied over a period of 21 days after encapsulation. Before each measurement, cells were released from the capsules (**Section 3.3.4**) and then viability estimated by Trypan Blue exclusion assay (**Section 3.3.2.1**).

Results in **Figure 3.7 A** demonstrated that NSCs viability remained consistent at a low seeding density (1×10^5 cells/ml) over the period tested, with little sign of cell proliferation. On the contrary, an increase in viability was observed when the microcapsules were laden with a concentration of 1×10^6 cells/ml ($P < 0.001$).

For the DPSCs (**Figure 3.7 B**), cell viability remained high and consistent over the first three days for all the conditions investigated. Seven days after encapsulation, the number of viable cells reduced to around 70 – 80 %, followed by a progressive decrease up to 21 days, regardless the initial cell concentration ($P < 0.001$). No significant differences were observed between concentrations at the same time point ($P > 0.05$).

As mentioned above, a high concentration of cells per microcapsule could have a greater therapeutic effect when transplanted into the site of injury. However, this concentration should permit the optimal survival of the cells within the confined microenvironment. According to the results obtained above, the seeding densities investigated demonstrated little effect on cell survival. Therefore, the highest densities, 1×10^6 cells/ml for NSCs and 1×10^7 cells/ml for DPSCs, were used in subsequent experiments, unless otherwise stated.

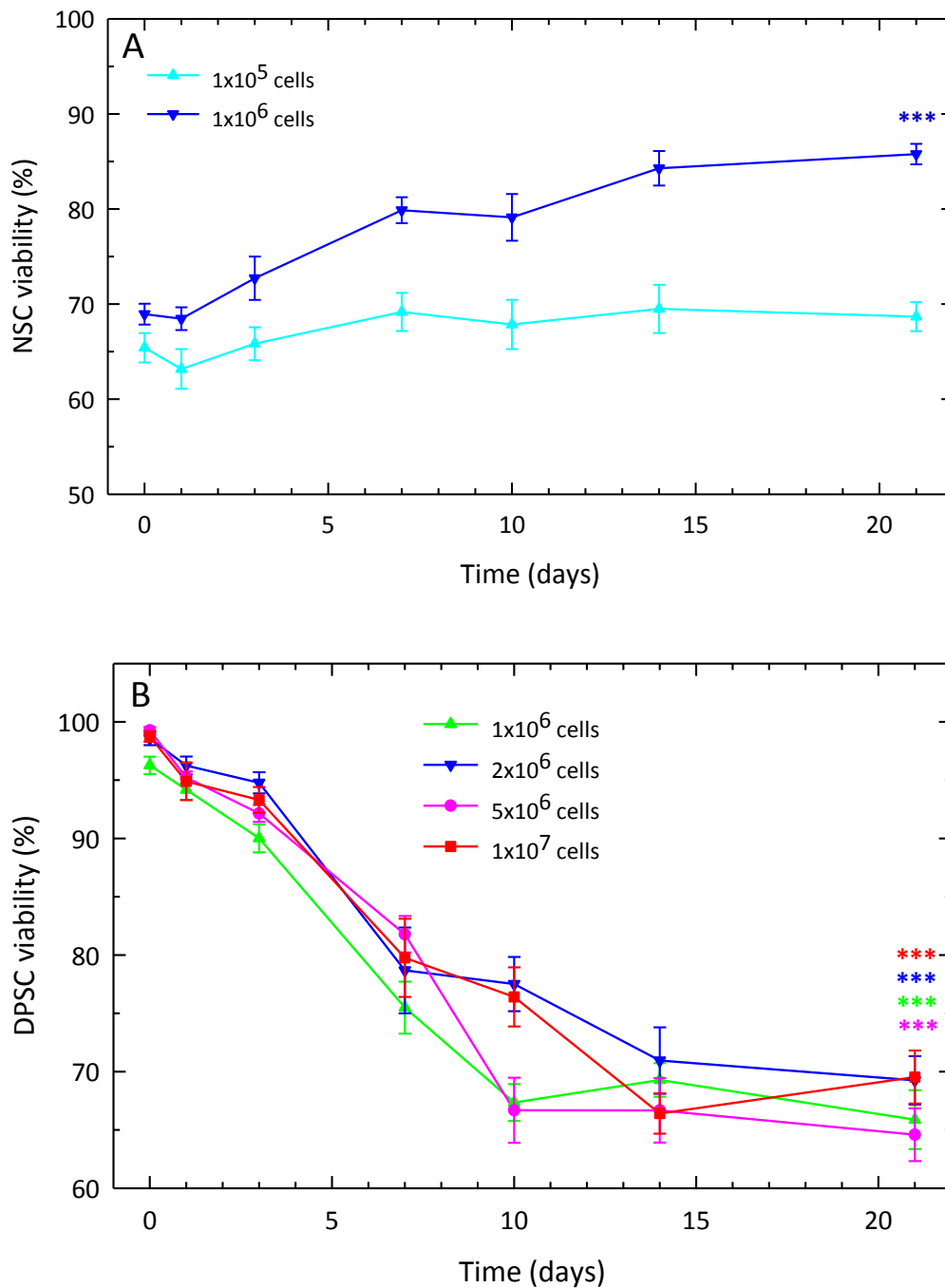


Figure 3.7. Graph showing the influence of initial cell density on cells viability. Pre-encapsulation viability was represented as time point 0. A) Viability of NSCs encapsulated at two different seeding densities within alginate microcapsules. NSCs encapsulated at 1×10^6 cells/ml demonstrated proliferation over the period tested. However, no cell growth was observed when cells were encapsulated at a density of 1×10^5 cells/ml. B) Viability of DPSCs encapsulated at four different seeding densities within alginate microcapsules. For all the concentrations investigated, the viability of encapsulated DPSCs decreased to $\sim 70\%$. Data are shown as mean \pm SEM, and are representative of at least three independent experiments made in triplicate. ***, $P < 0.001$, Student's t test versus first point.

3.4.2.2 Live/Dead® Viability Assay and confocal imaging of encapsulated cells

Encapsulated NSCs and DPSCs were stained 1 and 21 days after encapsulation with EthD-1 stain as described in **Section 3.3.2.3**. Confocal images of the cells were taken using a Leica SP5 Confocal Microscope from confocal Z scan over a depth of 400µm.

As observed in **Figure 3.8**, the behaviour of the two cell types within alginate microcapsules was different. NSCs grew within the microspheres in the form of aggregates, with these aggregates increasing in size (and hence cell density) over the 21 days period. This behaviour was similar to that found when culturing NSCs in the form of neurospheres. However, little sign of proliferation was observed for DPSCs, whose viability was slightly compromised over the period tested, as demonstrated by an increased in the number of dead cells (red) 3 weeks after encapsulation. According to the rounded shape of the cells, neither NSCs nor DPSCs appeared to adhere to the alginate scaffold within the beads.

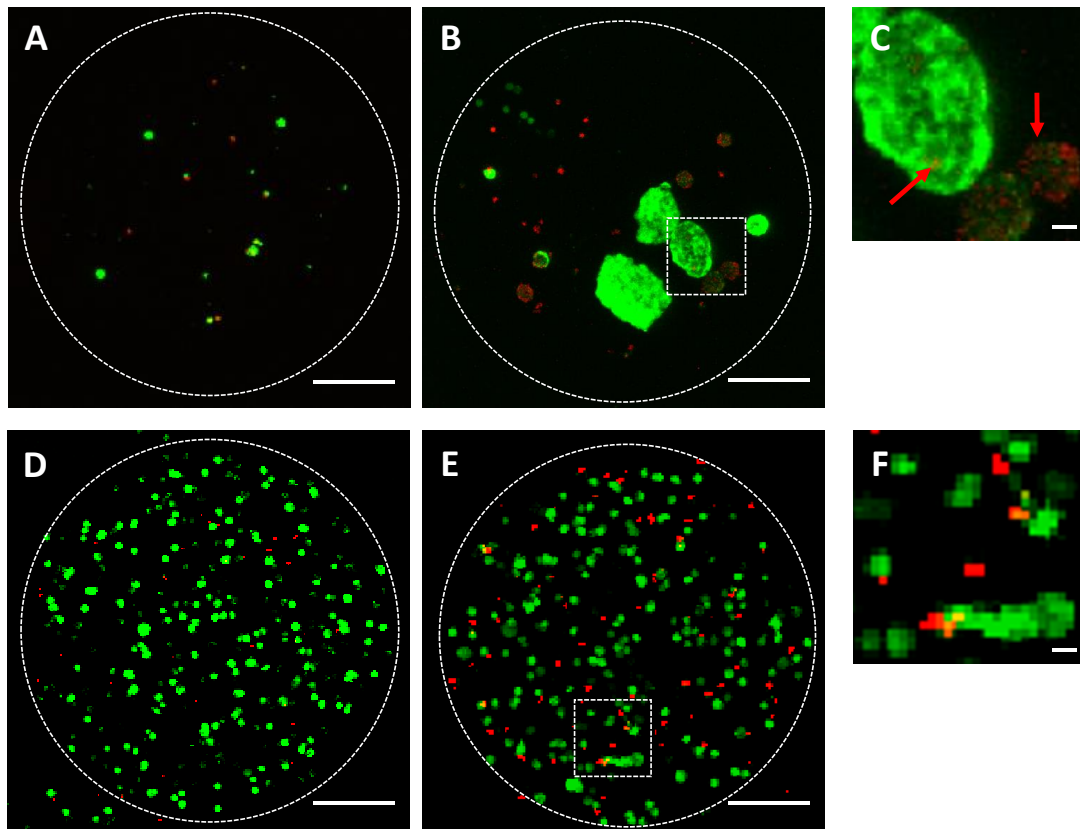


Figure 3.8. Confocal images of encapsulated stem cells within alginate microspheres stained with EthD-1. Green fluorescence was emitted from GFP cells, whereas red fluorescence was emitted from EthD-1 binding the nuclei of dead cells. Encapsulated NSCs 1 and 21 days after encapsulation (A-B, respectively) - NSCs grew in aggregates within the microspheres. Encapsulated DPSCs 1 day and 21 days after encapsulation (D-E, respectively) - little proliferation was observed for DPSCs, with the viability of the cells decreasing over the period tested. Scale bar (A, B, D and E) = 100 μ m. Scale bar (C and F) = 10 μ m.

3.4.2.3 Cell proliferation studies within alginate microcapsules

In order to further investigate cell proliferation within the microspheres, MTT assay were performed for each cell type 1, 3, 7 and 10 days after encapsulation.

MTT solution was added to encapsulated cells and blanks as described in **Section 3.3.2.2**. Formazan was dissolved with DMSO and absorbance measured at 540nm. Results in **Figure 3.9** revealed that NSC proliferated significantly within the microcapsules between days 1 and 10 ($P < 0.001$). However, readings obtained from encapsulated DPSCs demonstrated a slight decreased in overall cell numbers over the time course ($P < 0.01$).

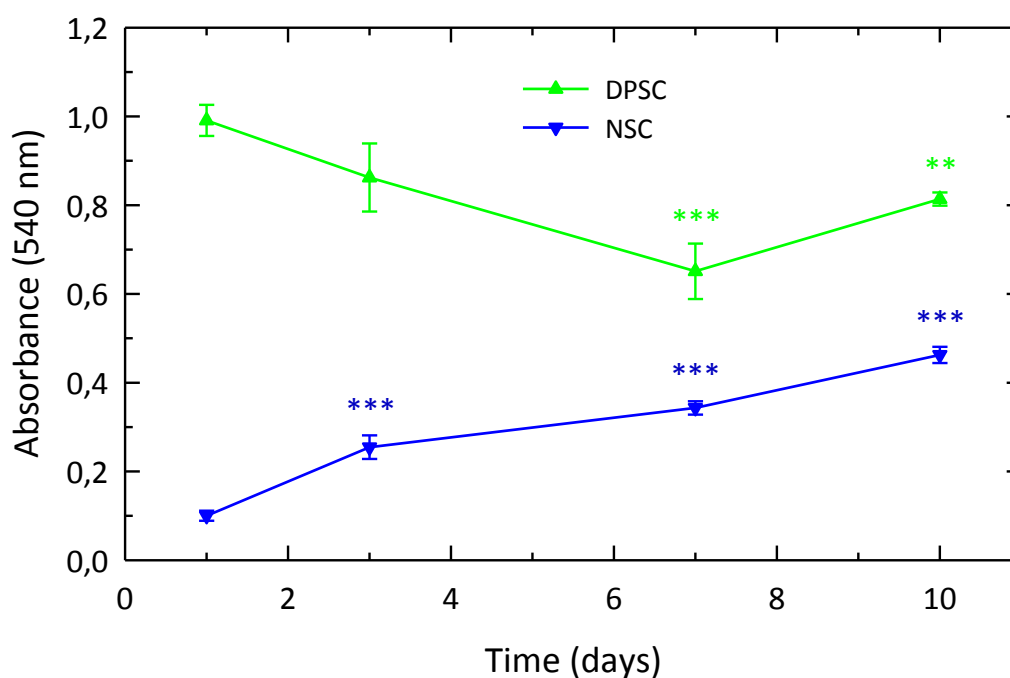


Figure 3.9. Graph of MTT assay on days 1, 3, 7 and 10 after encapsulation. Mean \pm SEM, and are representative of at least three independent experiments made in triplicate. **, $P < 0.01$; ***, $P < 0.001$, Student's t test versus first time point.

Images of the cells after formazan formation were taken at each time point for each cell type (**Figure 3.10**). It was observed that formazan formation increased in encapsulated NSCs. Furthermore, NSCs grew forming a branched network over the alginate microcapsules. However, for the DPSCs, it was noted that some cells actually escaped from the capsules around day 3, adhered onto the tissue culture plastic surface and proliferated. Therefore, the use of the MTT assay to measure relative cell number was deemed to be compromised and not truly reflective of cell number within the beads.

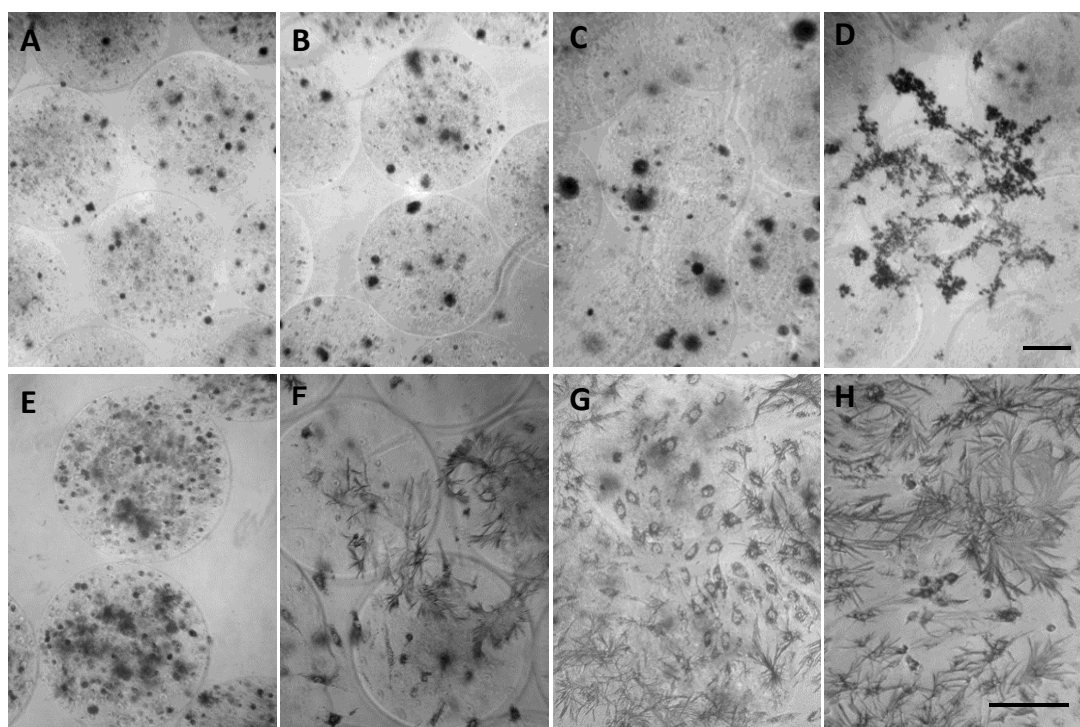


Figure 3.10. *Bright field images of encapsulated cells after formazan formation in MTT assay. (A-D) Encapsulated NSCs 1, 3, 7 and 10 days after encapsulation, respectively. The number of NSC increased over the period tested, as it could be observed by an increase in the precipitate formed. (E-H) Encapsulated DPSCs 1, 3, 7 and 10 days after encapsulation, respectively. Images show cells escaping from microcapsules and proliferating 3 days after encapsulation. Scale bar = 200 μ m.*

3.4.3 Modification of the encapsulation matrix

The main purposes of cell encapsulation process are the protection of the cells from the immune response after grafting and the control of cell fate within the organism. The encapsulation matrix should, at the same time, allow for the controlled migration/egress of the encapsulated cells at the appropriate time in order to integrate within the host organ, replacing lost/damaged tissue, and ultimately lead to recovery of normal tissue function. Therefore, the composition of the scaffold needs to 'entrap' the cells but also allow their controlled migration in due course.

Since cell escape from the alginate microcapsules was observed for DPSCs 3 days after encapsulation, a modification of the encapsulation material was then required in order to delay any such migration. Type I collagen was selected to modify the alginate scaffold, since it is the main component of the extracellular matrix and promotes cell attachment and cell proliferation (Kleinman *et al.* 1981). It was postulated that this collagen would retain the cells within the capsules by providing cell adhesion sites.

Both NSCs and DPSCs were encapsulated in alginate-collagen microcapsules as described in **Section 3.3.3.2**. Viability and proliferation of the cells within the new scaffold was investigated and compared with the results obtained in the previous section, where only alginate was utilised as the encapsulation matrix.

3.4.3.1 Cell viability and proliferation: comparison between alginate and alginate-collagen microcapsules

3.4.3.1.1 Trypan Blue exclusion assay

The viability of the encapsulated cells within alginate-collagen microcapsules was studied by Trypan Blue exclusion assay 1, 3, 7, 10, 14 and 21 days after encapsulation. Alginate-collagen beads were dissolved and cells released as described in **Section 3.3.4**. Cells were then counted and viability estimated (**Section 3.3.2.1**).

Figure 3.11 demonstrates that the addition of type I collagen had little effect on cell viability compared to alginate alone ($P > 0.05$). As for NSCs encapsulated in alginate beads, their viability within the alginate-collagen microcapsules significantly increased up to 21 days ($P < 0.001$). Similarly, the behaviour of DPSCs within alginate-collagen beads did not demonstrate any significant alteration when compared with alginate-encapsulated DPSCs ($P > 0.05$). However, in both scaffolds, the number of viable DPSCs slightly decreased over the period tested ($P < 0.001$).

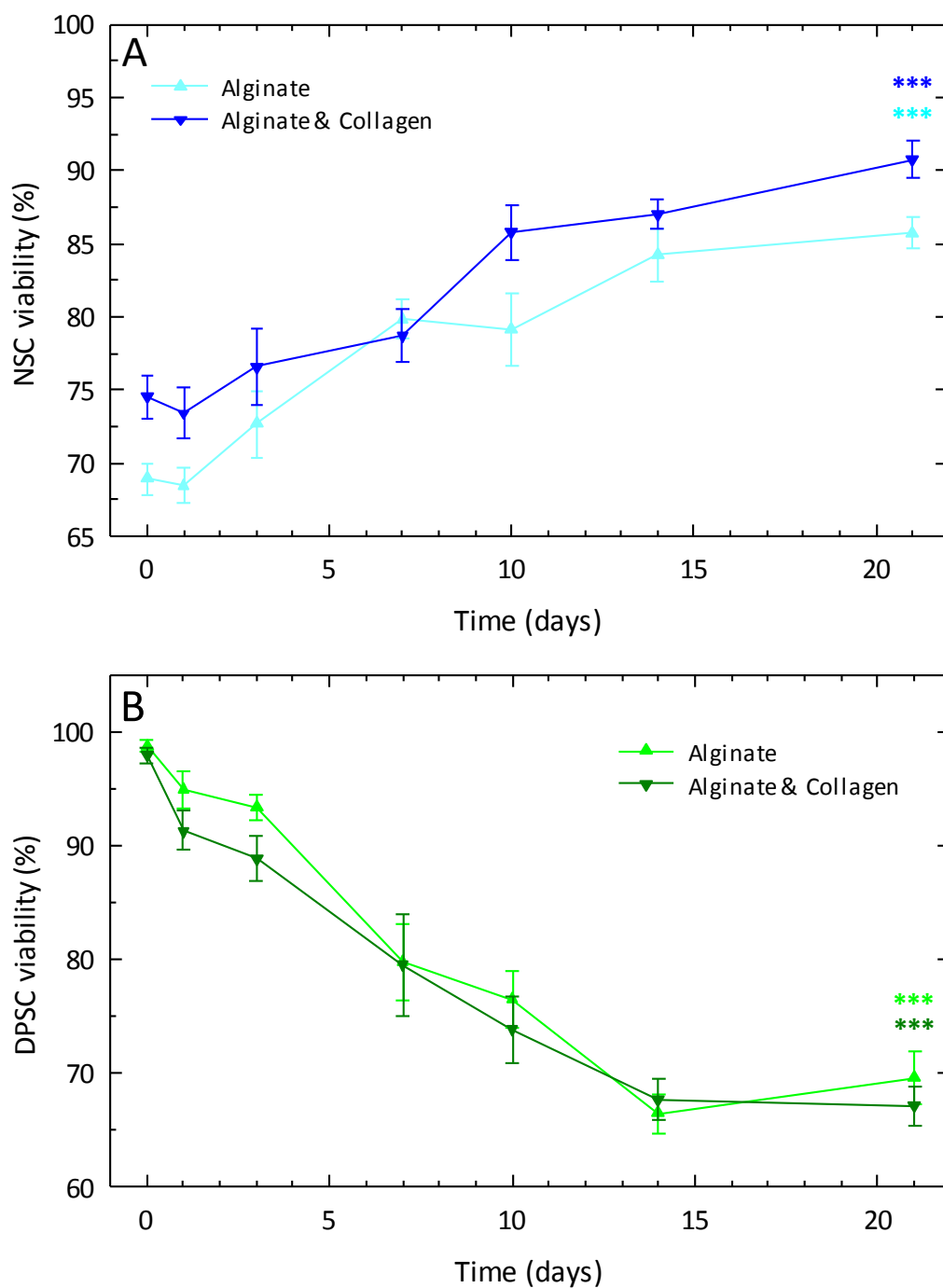


Figure 3.11. Graph showing the influence of the encapsulation matrix on cell viability. Pre-encapsulation viability was represented as time point 0. Data are shown as mean \pm SEM, and are representative of at least three independent experiments made in triplicate. ***, $P < 0.001$, Student's t test versus first point.

3.4.3.1.2 Live/Dead[®] Viability Assay and confocal imaging

Samples from both cell types at day 1 and 21 after encapsulation were stained with EthD-1 dye as described in **Section 3.3.2.3**. As observed in **Figure 3.12**, NSCs maintained in alginate-collagen exhibited a similar behaviour to that in alginate microcapsules alone, with cells growing in aggregates within the microspheres. As in alginate alone, DPSCs within alginate-collagen microcapsules did not demonstrate any sign of cell adhesion and the viability decreased over the period tested, as evidenced by an increase in the number of non-viable cells (red).

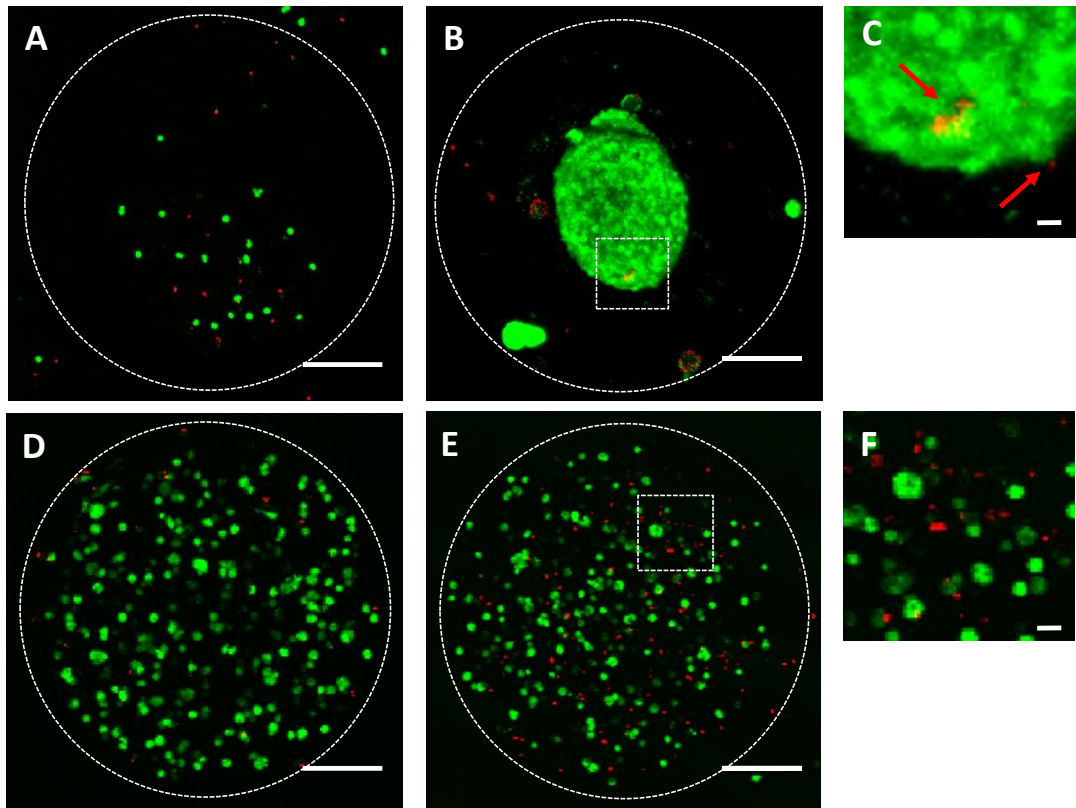


Figure 3.12. Confocal images of encapsulated stem cells within alginate-collagen microspheres stained with EthD-1. Green fluorescence is emitted from GFP cells, whereas red fluorescence is emitted from EthD-1 binding the nuclei of dead cells. Encapsulated NSCs 1 day and 21 days after encapsulation (A-B, respectively). Encapsulated DPSCs 1 day and 21 days after encapsulation (D-E, respectively). Scale bar (A, B, D and E) = 100μm. Scale bar (C and F) = 10μm.

3.4.3.1.3 MTT proliferation assay

MTT assay was also performed on encapsulated cells within alginate-collagen microspheres. For the same cell type, results at the same time point could not be compared, since the quantity of sample seeded for each condition was different (alginate or alginate-collagen microcapsules). Therefore, an analysis of the trend was undertaken. Results in **Figure 3.13** show that over the time course, NSCs proliferated in alginate-collagen in a similar manner to how they did in alginate microcapsules ($P < 0.001$). On the other hand, DPSCs in alginate-collagen demonstrated an overall decrease in absorbance 10 days after encapsulation ($P < 0.01$). This trend was similar to that observed in DPSCs within alginate beads.

In order to investigate whether cell egress was delayed with the modified encapsulation scaffold, pictures of cells after MTT formation were taken at each time point, and compared with those taken of alginate microcapsules (**Figure 3.14**). NSCs grew in aggregates within the microcapsules, regardless of the encapsulation matrix. The formation of cell networks on microcapsules was observed on day 10 in both scaffolds. In the case of DPSCs, a different behaviour was observed when compared with cells encapsulated in alginate beads. Cells escaped from alginate microcapsules approximately 3 days after encapsulation. This migration was not noticed until day 10 in alginate-collagen microspheres. Therefore, the modification of the encapsulation matrix allowed for a delay in cell egress.

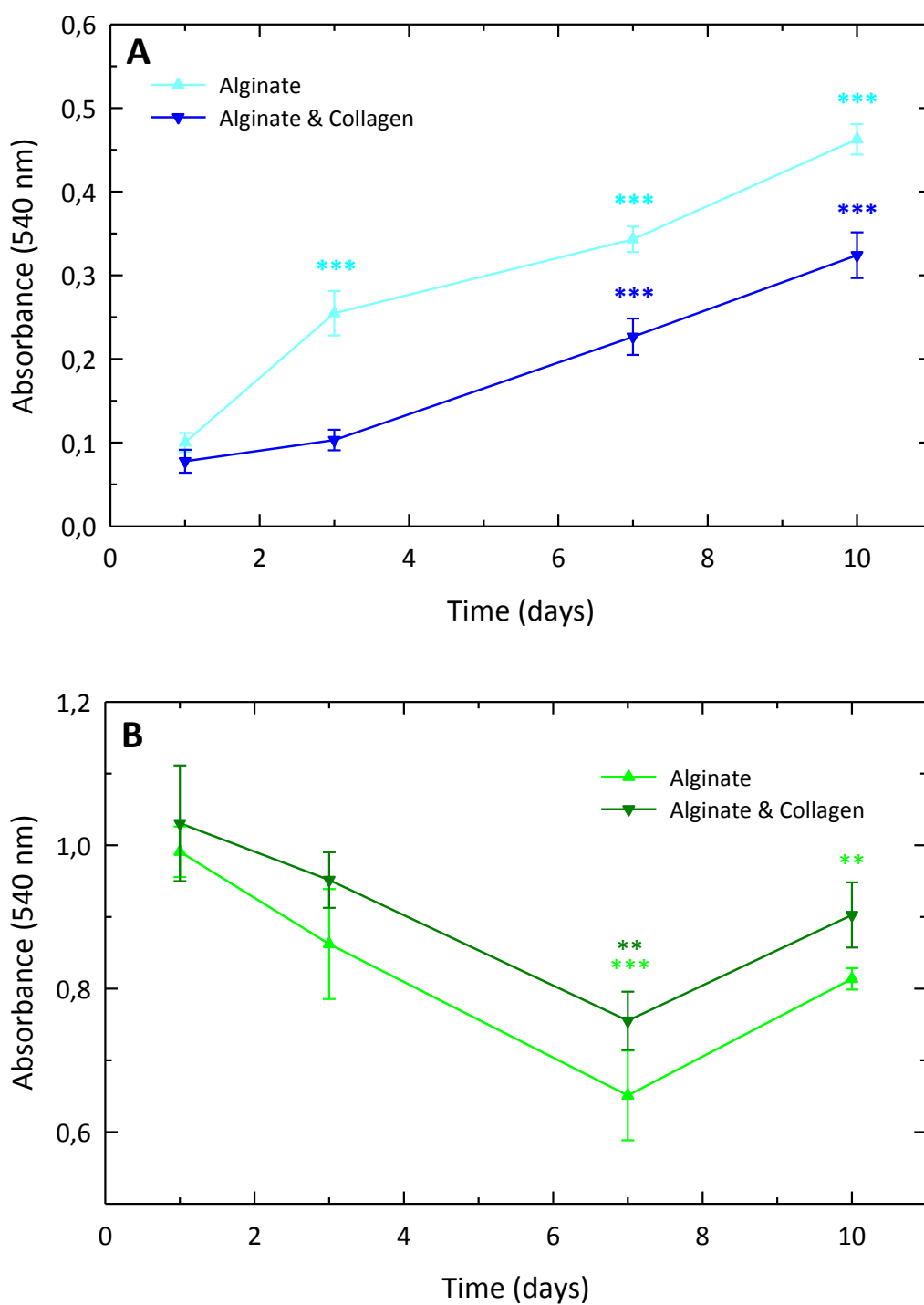


Figure 3.13. Graph of MTT assay on days 1, 3, 7 and 10 after encapsulation within alginate and alginate-collagen microcapsules. A) MTT values of NSCs. B) MTT values of DPSCs. Data are shown as mean \pm SEM, and are representative of at least three independent experiments made in triplicate. **, $P < 0.01$; ***, $P < 0.001$, Student's t test.

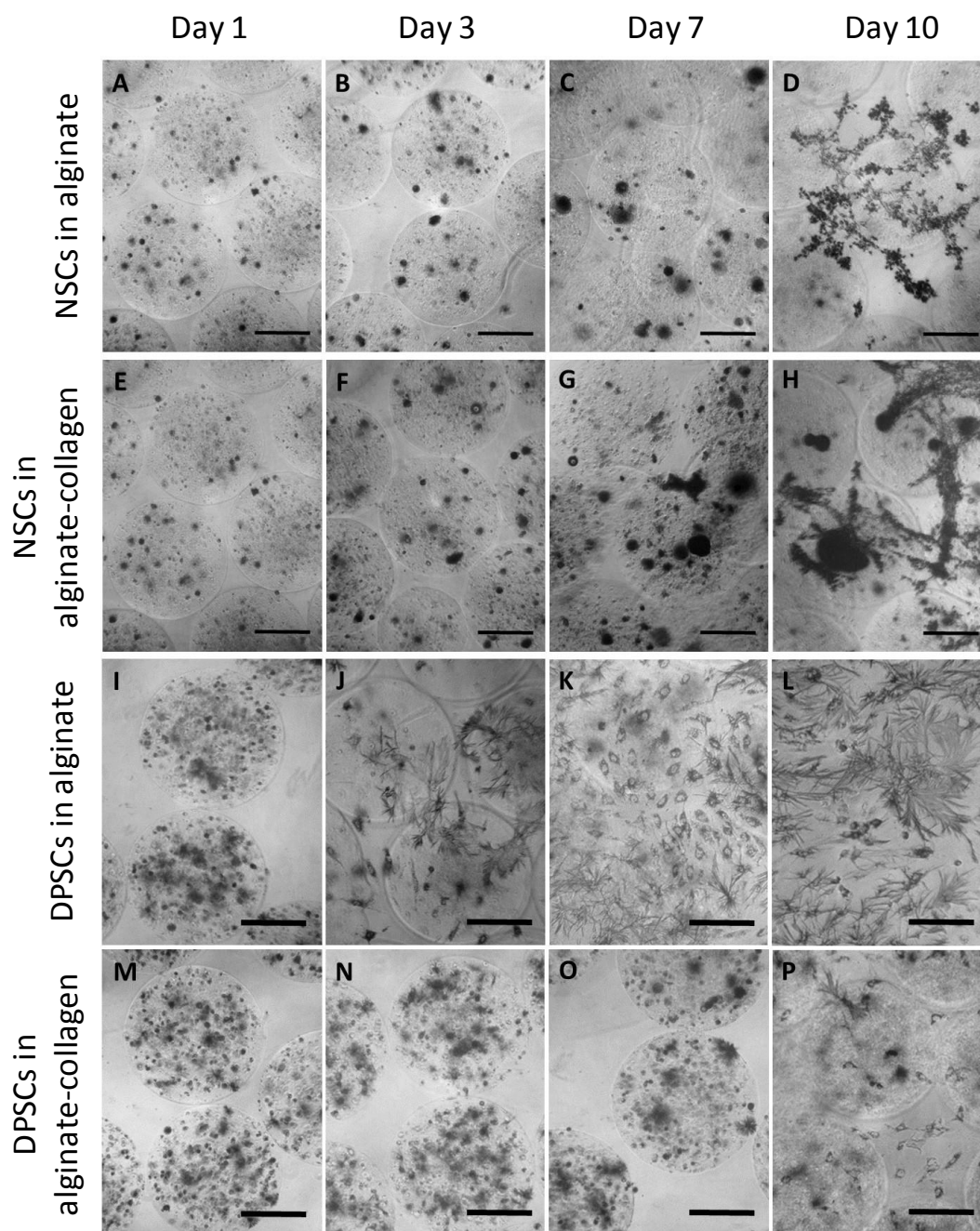


Figure 3.14. *Bright field images of encapsulated cells after formazan formation. (A-H)* Encapsulated NSCs within alginate or alginate-collagen microcapsules after formazan formation 1, 3, 7 and 10 days after encapsulation. (I-P) Encapsulated DPSCs within alginate or alginate-collagen microcapsules after formazan formation 1, 3, 7 and 10 days after encapsulation. Images show that DPSCs migration outside the microcapsules is delayed within the alginate-collagen scaffold. Scale bar = 200 μ m.

3.4.4 Study of cell turnover within alginate-collagen microcapsules using CellTrace™ staining and flow cytometry

Based on the results provided by the Trypan Blue exclusion assay, Live/Dead® staining and MTT assay, it was demonstrated that NSCs proliferated within the microcapsules. However, since no increase in the total number of cells was observed, nor an increase in absorbance after formazan formation by DPSCs, the proliferative behaviour of these cells remained unknown. Whilst the MTT assay is a useful assay to give an overall idea of relative cell number within the microcapsules, it does not inform on actual cell turnover – i.e. are cells dying and being replaced by new cells, or, is the cell number actually relatively static? To investigate this, DPSCs were stained with CellTrace™ Far Red Cell Proliferation Kit and analysed with flow cytometry as described in **Section 3.3.2.4**. Prior to labelling, one group of cells was treated with mitomycin C to inhibit cell proliferation (**Section 3.3.2.5**) and then stained with the CellTrace™ kit (+MC; negative control). A second group of cells was not treated with mitomycin C but labelled with the CellTrace™ kit (-MC; positive control). The third group of cells was stained and encapsulated within alginate-collagen microcapsules (sample). Both controls and encapsulated cells were cultured at standard conditions for up to 7 days. Samples were taken at 1, 3, 5 and 7 days after labelling and cells were analysed by flow cytometry (**Figure 3.15**). Encapsulated cells were released from microcapsules prior to analysis. Untreated monolayer cultures of cells (-MC; positive control) demonstrated clear cellular proliferation as evidenced by a shift and fall off of the fluorescent signal as the cells divided over a period of 7 days, and hence ‘shared’ their fluorescent marker. Treated monolayer

cultures of cells (+MC; negative control) failed to divide, as demonstrated by a consistent fluorescent signal. Pre-stained, encapsulated cells were released from the microcapsules (sample) after set periods of time in culture and analysed. No drop or shift in the fluorescence peak indicated that the DPSCs did not proliferate within the microcapsules.

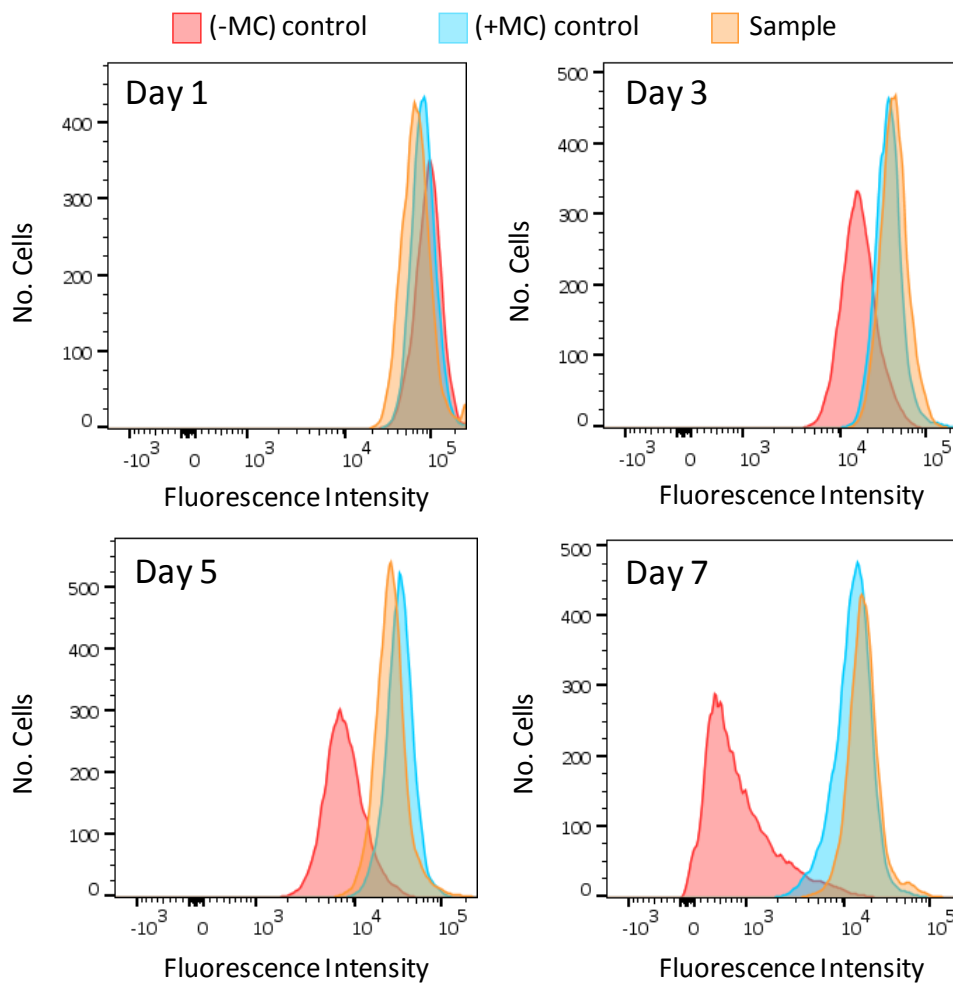


Figure 3.15. Study of DPSCs proliferation within alginate-collagen microcapsules. Both controls and samples were stained with CellTrace™ Far Red Cell Proliferation Kit and analysed by flow cytometry over a period of 7 days. Mitomycin C treated cells (+MC) failed to divide, since no decrease in fluorescent signal was observed. No mitomycin C treated cells (-MC) demonstrated cellular proliferation as evidenced by a shift and fall off of the fluorescent signal over a period of 7 days. No drop or shift in the fluorescence peak of encapsulated cells indicated that the DPSCs did not proliferate within the microcapsules.

3.4.5 Cell functionality studies upon release from alginate-collagen microspheres

The appropriate encapsulation technology should not affect cell functionality. The results described above indicated that cells were successfully encapsulated within alginate-collagen microspheres, showing high viability over extended periods of time. However, further investigation of cellular function was required in order to study the potential of encapsulated cells for cell replacement therapy. Stem cells are characterized by high proliferation rates *in vitro*, but also the expression of pluripotency markers such as Nanog, Oct-4, Sox2 & SSEA4 (Zhao *et al.* 2012). Hence, growth rates and expression of stem cells and neuronal markers by NSCs and DPSCs were investigated before and after neuronal differentiation, upon release from alginate-collagen microcapsules.

3.4.5.1 Cell proliferation potential

NSCs and DPSCs were released from microcapsules 21 days after encapsulation and seeded on 96-well plates at a density of 1,000 cells/well along with appropriate controls (no encapsulated NSCs and DPSCs). Surfaces were pre-coated with 50 µg/ml of PDL and 20 µg/ml of laminin before NSCs seeding to allow cells to grow in monolayer.

MTT proliferation assay was carried out on days 1, 3, 5 and 7 after seeding as described in **Section 3.3.2.2**. Results in **Figure 3.16** demonstrate that released cells

preserved high growth rates (day 7 significantly different to day 1; $P < 0.001$), similar to those observed for the control cultures (never encapsulated).

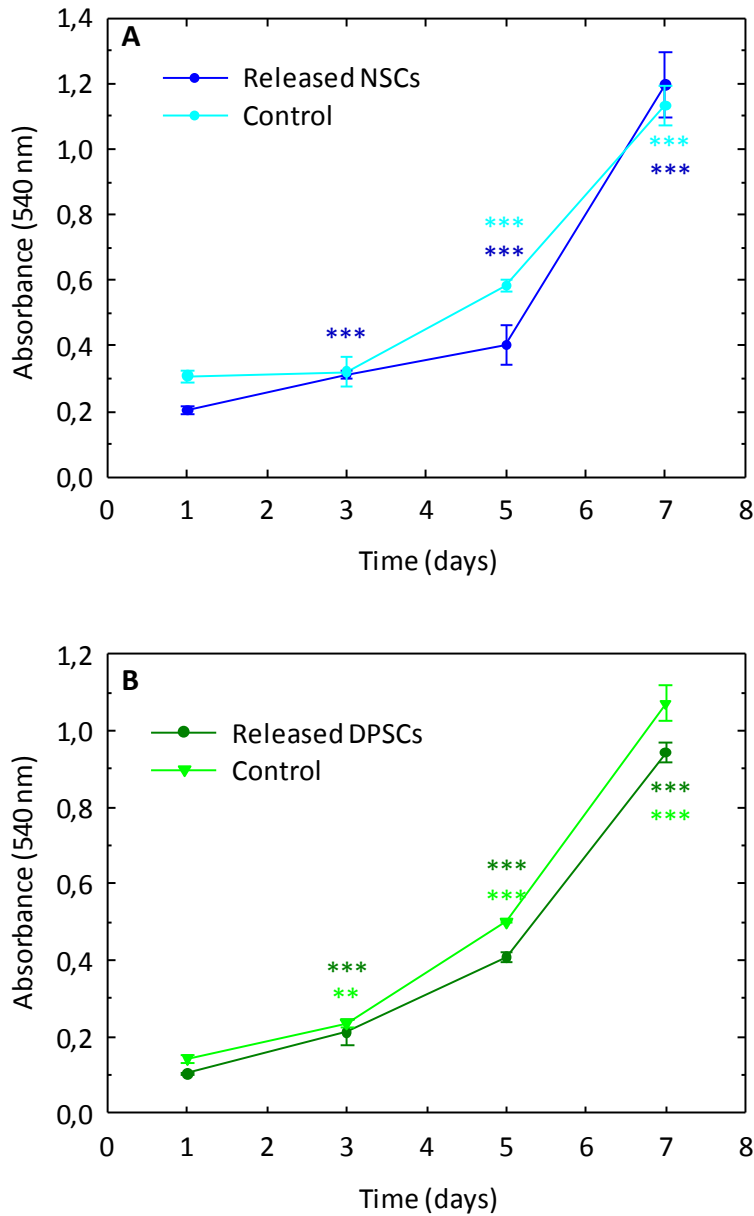


Figure 3.16. NSCs and DPSCs proliferation upon release from alginate-collagen microcapsules. NSCs and DPSCs were released from microcapsules 21 days after encapsulation and seeded on 96-well plates. MTT proliferation assay was carried out on days 1, 3, 5 and 7 and absorbance measured at 540nm. Both cell types showed similar growth rates to the non-encapsulated controls, suggesting that proliferation of cells was not compromised upon release from alginate-collagen microcapsules. Data are shown as mean \pm SEM, and are representative of at least three independent experiments made in triplicate. **, $P < 0.01$; ***, $P < 0.001$, Student's t test.

3.4.5.2 Stemness and neuronal differentiation potential

Neuronal differentiation of DPSCs based on NSCs culture protocols has been previously reported in our group (Young *et al.* 2016). In this study, the aim was to demonstrate that encapsulation of NSCs and DPSCs did not affect their capacity for differentiation into neuronal-like cells *in vitro* after release from microcapsules.

Nestin is one of the markers used to identify cells with potential for neuronal differentiation (Messam *et al.* 1999). Hence, expression of this protein along with the stem cell pluripotency markers Sox2, Oct4, and the neuronal markers β -III tubulin and Map2 (associated with more mature phenotypes), were investigated.

Both NSCs and DPSCs were released from microcapsules 21 days after encapsulation and seeded on pre-coated plates at a density of 10,000 cells/cm² in NSC growth medium (**Section 3.3.6**). Undifferentiated NSCs in growth medium demonstrated bipolar morphology (**Figure 3.17A**). When NSCs reached over 80% confluence, growth factors were gradually removed from medium and half-medium changes were performed every other day for up to 15 days. An increased in cell death was observed as growth factors were gradually removed. After 15 days in culture with growth factor-free medium, surviving cells developed more projections and created connections with adjacent cells (**Figure 3.17B**).

Undifferentiated DPSCs were typically bi-/tri-polar, showing fibroblast-like shapes (**Figure 3.17C**). DPSCs were cultured in NSC growth medium for 5 days to stimulate neuralisation and then medium was changed for neurotrophin containing medium to promote neurogenic maturation. This was replaced every 3 - 4 days for a 10 further days. Cells cultured in NSCs growth medium adopted neuronal-like

phenotypes. Maturation in neurotrophin containing medium led to cells developing rounded bodies with multiple long processes sprouting out and forming neuronal-like connections (**Figure 3.17D**).

Both NSCs and DPSCs were fixed after the differentiation protocol and stained with antibodies against Nestin, Sox2, Oct4, β -III tubulin and Map2, along with the isotype control (**APPENDIX II APPENDIX II**). **Figure 3.18** shows that NSCs stained positively for all markers tested in both undifferentiated and differentiated states, suggesting that full neuronal differentiation had not taken place (as they retained some pluripotency markers). However, significant changes in cell morphology were observed as the cells developed long axons after the differentiation protocol. DPSCs demonstrated production of Nestin before and after differentiation (**Figure 3.19**). Cells stained positively for Sox2 and Oct4 before differentiation, demonstrating retained stem cell properties upon release from the microcapsules, but this was lost after differentiation. DPSCs expressed the mature neuronal markers β -III tubulin and Map2 after 15 days in neurotrophin-containing medium and demonstrated a neuronal-like morphology.

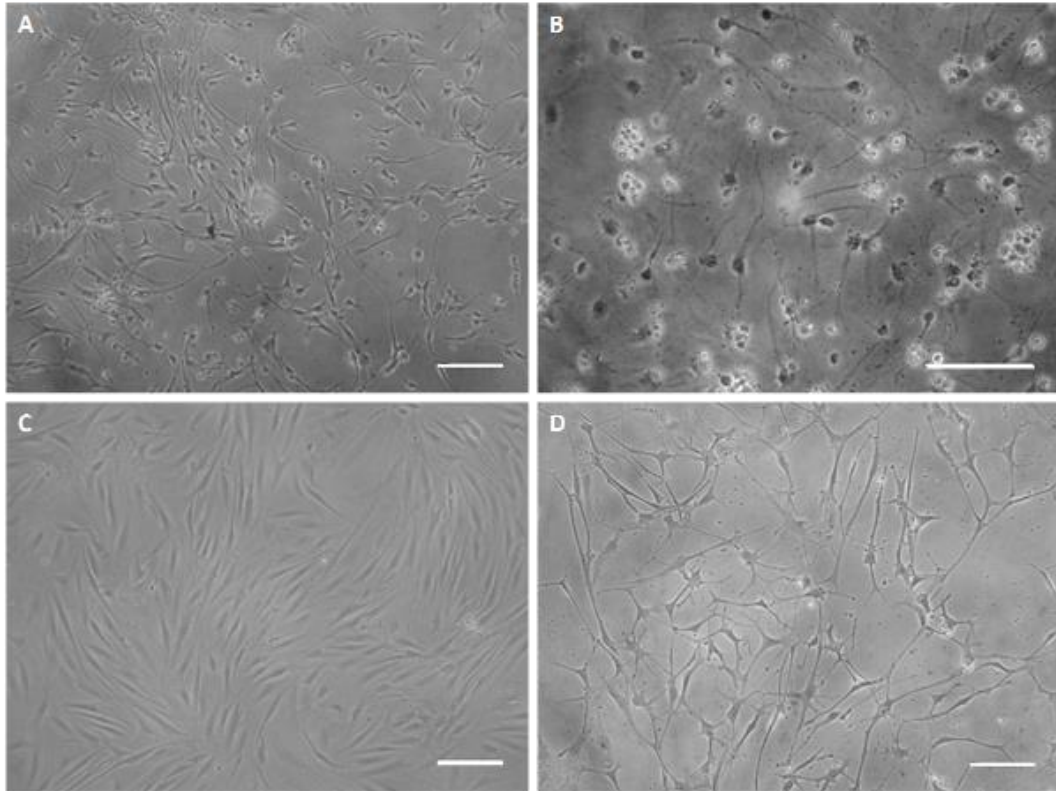


Figure 3.17. *Morphology changes during neuronal differentiation of NSCs and DPSCs.* A) Undifferentiated NSCs in growth medium showing bipolar morphology with rounded bodies. B) Differentiated NSCs developed cell projections emerging from cell body, creating connections with adjacent cells. C) DPSCs in DPSCs medium, before differentiation. Cells were typically bi-/tri-polar and fibroblast-like. D) After the differentiation protocol, DPSCs cell bodies adopted rounded morphology with multiple long processes sprouting out forming neuronal-like connections. Scale bars = 100 μm .

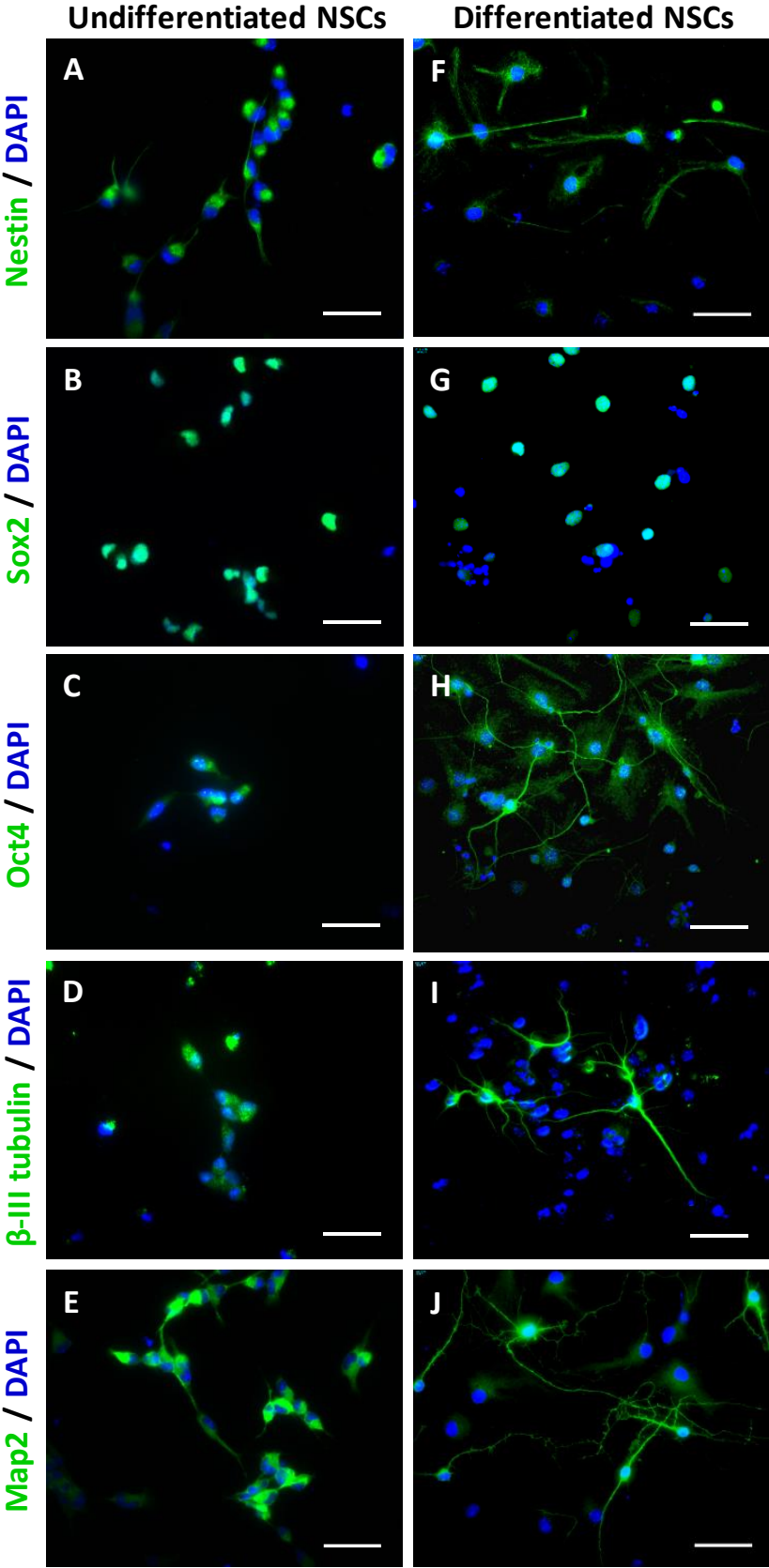


Figure 3.18. Immunocytochemical staining of NSCs before and after neuronal differentiation. NSCs were stained with antibodies against Nestin, Sox2, Oct4, β-III tubulin and Map2 before (A – E) and after differentiation (F – J). Scale bar = 50µm.

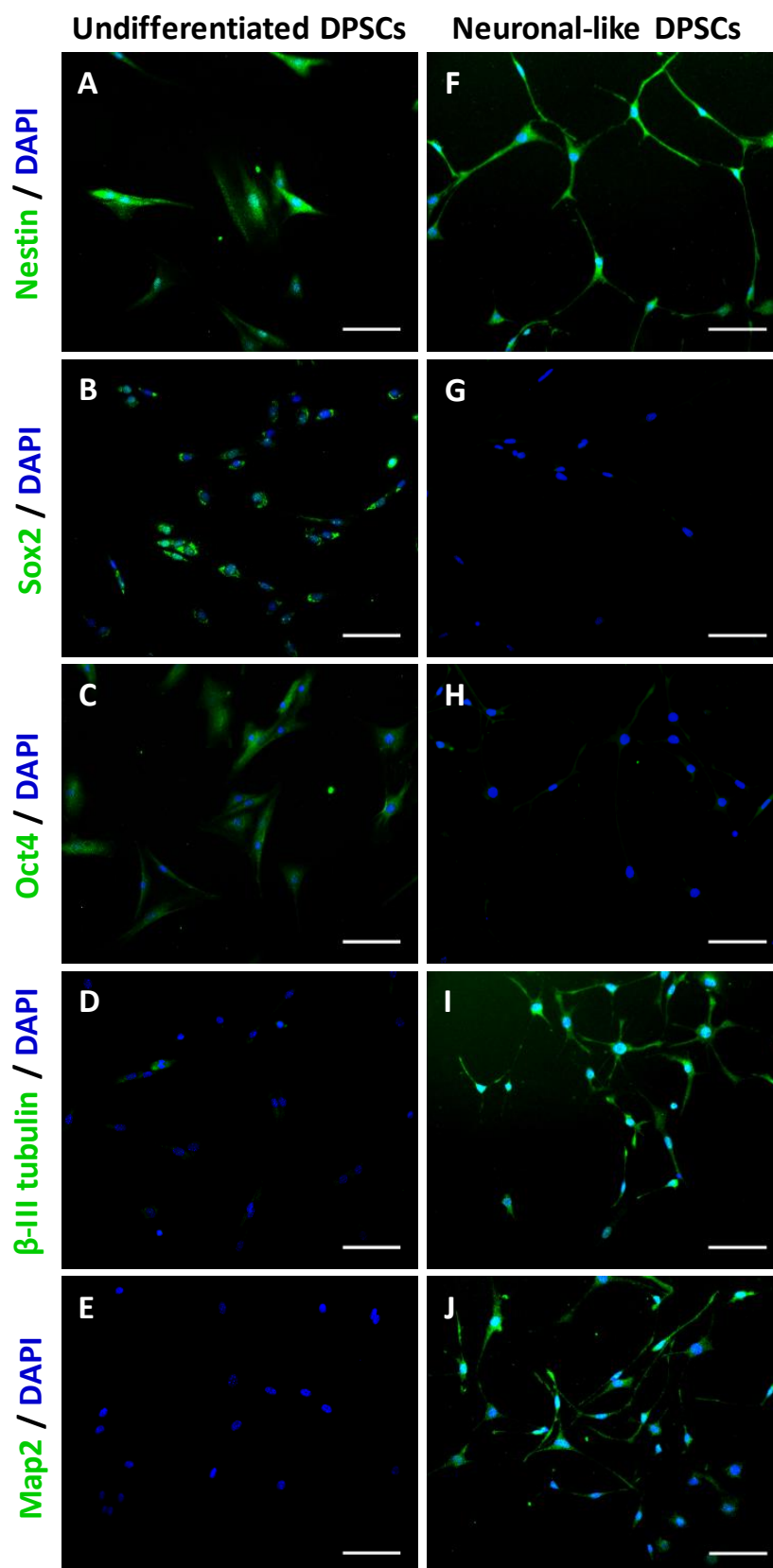


Figure 3.19. Immunocytochemical staining of DPSCs before and after neuronal differentiation. NSCs were stained with antibodies against Nestin, Sox2, Oct4, β -III tubulin and Map2 before (A – E) and after differentiation (F – J). Scale bar = 100 μ m.

3.5 Discussion

This chapter was concerned with the optimization of the parameters for the encapsulation of two types of stem cells, NSCs and DPSCs. The behaviour within microcapsules of the two cell types was compared and their stem cell and neuronal differentiation properties were investigated upon release from hydrogel beads.

3.5.1 Cytotoxicity of reagents used on stem cells

The preliminary study of the potential toxic effect of microfluidic reagents on cell viability was required in order to assess the biocompatibility of the method developed in **Chapter 2**. Whereas some authors have developed successful microfluidic techniques for droplet generation, some of these methods might not be suitable for the immobilization of living systems due to the use of organic solvents (Nie *et al.* 2008; Liu *et al.* 2013). Choi *et al.* (2007) used hexadecane as continuous phase for the microfluidic production of alginate microcapsules containing GFP yeast cells. Although cell fluorescence could be observed after encapsulation, this is not an appropriate indicator of cell survival, since GFP can be observed after cell death. Hence, the use of organic solvents was avoided in the method developed in this thesis in order to prevent detrimental effects on cell viability.

The cellular cytotoxicity of the reagents used for encapsulation was tested. DPSC viability was mildly decreased when resuspended in mineral oil. The mineral oil used was that utilized to prevent dehydration in embryonic cell culture and therefore, it was expected to be cell compatible. It is possible that the slight decrease

in viability was actually due to the mechanical stress that the cells were subjected to when they were forced to diffuse from the organic phase to the aqueous phase as part of the cell counting methodology (i.e. it could damage cell membranes). When cells were resuspended in the reactive phase (0.3% (v/v) acetic acid in mineral oil), the decrease in viability was slightly higher. In this case, not only the mechanical stress but also the alteration in pH, could have been factors in this decline in viability. It should be noted, however, that during the encapsulation procedure cells were also resuspended in alginate solution, and hence a direct/sole contact with either the mineral oil or acetic acid was highly unlikely. Thus, the detrimental effect that these reagents were demonstrated to have on the cells when they were directly resuspended was a 'worst case' scenario. The potential deleterious effect of acidification of culture medium was also investigated. Results demonstrated that cell survival was unaffected when cells were resuspended in a solution of 0.3% (v/v) acetic acid in culture medium. This result is not surprising, as culture medium contains buffers to regulate low changes in pH. Finally, biocompatibility of the encapsulation matrix was demonstrated when cells were resuspended in a 2% (w/v) alginate solution containing 5 mg/ml resuspended CaCO_3 . Although alginate biocompatibility was not an issue, potentially the precipitated CaCO_3 could have a detrimental effect on cell survival. This hypothesis was unfounded when it was observed that the viability of the cells resuspended in the polymer solution was practically unaffected over an extended period of 5 hours.

3.5.2 Viability and proliferation of encapsulated cells

Several methods have been used for cell encapsulation. For example, Aijaz *et al.* 2015 produced encapsulated insulin-producing RIN-m cells by vortexing a cell pre-polymer suspension with mineral oil, although the size of the capsules obtained was highly polydisperse. Other authors have used interfacial polymerization for the encapsulation of mammalian cells (Cruise *et al.* 1999). Polymer capsules produced by this technique present high strength and mechanical stability, allowing the formation of microcapsules ranging from 1 – 30 μm to several mm in diameter (Salaön 2013). However, the method involves several complex steps in which the slow kinetics of the reactions involved is a limiting step. Also, the use of organic solvents constitutes a major problem in terms of potential cell viability (Khademhosseini *et al.* 2005). As an attempt to increase cell survival avoiding the use of organic solvents, complex coacervation arose as an alternative method for encapsulation (Baracat *et al.* 2012). Nonetheless, the polydispersity of the capsules produced is a major problem when using this method (Knezevic *et al.* 2002). Among the numerous methods that have been applied for cell encapsulation, droplet extrusion generation is the most widely used (Duvivier-Kali *et al.* 2001; Murua *et al.* 2007; Wikström *et al.* 2008; Bhujbal *et al.* 2014). Cells are resuspended in the polymer solution and the suspension is extruded through a needle. The resulting droplets are collected in a stirred CaCl_2 solution where they are maintained in agitation for about 10 min for complete ionic gelation.

In this chapter, it was demonstrated that microfluidics represents a highly suitable technique for the continuous and consistent production of cell-laden

microcapsules in a sealed environment, avoiding any cross-contamination. The formation of highly monodisperse droplets allowed for an accurate theoretical estimation of the number of cells per bead, as demonstrated by comparison of these results with the corresponding experimental calculations. This is of a great utility in cell transplantation techniques where the monodispersity of droplets allows an accurate determination of the number of transplanted cells and hence clinical delivery dose (Tan & Takeuchi 2007). However, these estimations were only accurate for seeding densities above 1×10^6 cells/ml. Lower cell concentrations gave rise to microcapsules containing variable numbers of cells or even, empty capsules.

Unlike all the conventional methods mentioned above, the microfluidic method developed in this thesis permitted the production of stem cell microcapsules that were gelled *in situ* in a matter of seconds. This is of a great importance in terms of cell viability, since it permitted the quick transfer of the encapsulated cells to culture medium, minimizing the risk of cell viability loss due to unfavourable conditions, such as contact with gelling baths, polymerizing solvents, etc. Indeed, estimation of the number of viable cells after encapsulation showed that the microfluidic method was compatible with cell survival, since no significant decrease in cell viability was observed for the two cell types studied, regardless the initial seeding density.

Further investigations into the effect on cell viability of initial seeding density was carried out over a period of 3 weeks. In order to establish the highest viable initial cell seeding density, different concentrations of cells were encapsulated in alginate beads. Potentially, a high concentration of cells could be detrimental to

overall cell survival, as a greater number of cells within the capsules could hinder diffusion of nutrients and oxygen throughout the microsphere. Preliminary studies demonstrated that NSCs grew within microcapsules, whereas no increase in total cell number was observed for DPSCs. It was then hypothesized that high NSCs seeding densities would give rise to an overgrowth of cells within the capsules, provoking apoptosis of cells in the centre of the aggregates. Hence, only the seeding densities 1×10^5 cells/ml and 1×10^6 cells/ml were investigated for NSCs. In the case of DPSCs, higher cell concentrations were studied, using 1×10^6 cells/ml, 2×10^6 cells/ml, 5×10^6 cells/ml and 1×10^7 . Differences were found in the two seeding densities in NSCs. Although low seeding density showed a consistent high viability over the period tested, high density led to proliferation of cells within the capsules, increasing both the total number of cells and the number of viable cells. This increase in cell viability was then confirmed by MTT assay, where the absorbance of the encapsulated cells increased over a period of 10 days. Also, laser scanning confocal microscopy showed an increase in the size of NSCs aggregates, supporting the previous observations. The size of the cell aggregates after three weeks in culture was still appropriate to permit the diffusion of oxygen and nutrients, since no dead cells were observed in the centre of the aggregates when samples were stained with EthD-1 and analysed by confocal microscopy. Neurosphere growth in standard culture conditions occurs at a higher rate than that observed in encapsulated NSCs. Hence, it was assumed that encapsulation did not prevent proliferation of NSCs, but it provoked a delay in cell growth. This observation was similar to that found by Wilson *et al.* 2014. The proliferation rate of non-encapsulated and encapsulated embryonic stem cells were compared and results revealed that unencapsulated cells had the highest net growth

rate. Other investigations on the influence of alginate matrix on the proliferation of encapsulated NSCs demonstrated that the growth rate of NSCs decreased with an increase in the hydrogel stiffness (Banerjee *et al.* 2009). Thus, proliferation of cells could be directly related to the mechanical resistance of the surrounding environment.

The initial seeding densities investigated for the DPSCs did not show any significant difference in cell viability at similar time points. Unlike NSCs, DPSCs did not exhibit any sign of cell proliferation, and actually, a decrease in the number of viable cells was observed. However, cell viability at the different seeding concentrations tested was still encouragingly high (more than 60% of viable cells) up to 21 days after encapsulation. Interestingly, both bright field and confocal microscopy images of encapsulated cells showed little evidence of adhered cells as they remained rounded within the alginate microspheres. Other studies on DPSCs immobilized within alginate hydrogels reported similar results (Umemura *et al.* 2011; Kanafi *et al.* 2014). Kanafi *et al.* 2014 highlighted the different morphology of DPSCs depending on the culture conditions. When these cells were cultured in standard 2D culture they acquired fibroblast-like shapes, whereas when the cells were encapsulated within alginate microspheres they adopted rounded morphologies. The same behaviour has been observed in olfactory ensheathing cells, Schwann cells and BMSCs cultured on alginate hydrogels, where the cells acquired atypical spherical shapes and their metabolic activities were inhibited (Novikova *et al.* 2006). However, despite the prolonged period of time that these cells remained rounded within the hydrogels, they were still viable.

MTT studies of encapsulated DPSCs revealed that cell egress was occurring as early as 3 days after encapsulation. The escaped cells attached on tissue culture plates surfaces and proliferated. Hence, whilst the MTT assay in this situation was not a suitable assay (as cells both inside and outside the beads were being measured) it did reveal that cells could escape from the beads over the time course of the investigation.

Early cell egress is a non-desirable event in transplantation therapies, since one purpose of cell encapsulation is their protection and isolation from the immune system to prevent cell death (Lee & Bae 2000; Emerich & Winn 2001; Hao *et al.* 2005). To overcome this, it was hypothesized that type I collagen would prevent cell escape by promoting cell attachment and at the same time that would improve cell viability, as has been reported by others (Hunt & Grover 2010). Unlike collagen, alginate does not interact with mammalian cells, and therefore, does not promote cell adhesion (Rowley *et al.* 1999). Hence, the alginate matrix was modified with type I collagen. As a result, migration of DPSCs from the beads was delayed with no cells observed to escape until day 10 after encapsulation. However, little cell attachment was again observed. Viability and proliferation were again studied for the two cell types in the new encapsulation matrix. Importantly, no differences were observed compared to the results found with alginate alone, with the maintenance of NSCs and DPSCs high viabilities over the 3 weeks period and NSCs proliferating within the alginate-collagen microcapsules.

An alternative method was designed in order to elucidate the proliferation behaviour of DPSCs within microcapsules. This consisted on cell labelling prior to

encapsulation with a stain whose fluorescence intensity decreases as the cells transit through the cell cycle and divide. This clearly demonstrated that the DPSCs did not proliferate within alginate nor alginate-collagen microcapsules. This finding is opposed to that reported by Kanafi *et al.* (2014), where an increase in cell absorbance was observed over a period of 10 days in respect of DPSCs encapsulated within alginate beads. This can be explained by the fact that, in the method developed by Kanafi *et al.* (2014), the MTT reagent was directly added on plates where encapsulated cells were cultured. Some of these cells might have escaped, having attached on the surface of the plates and proliferated. Hence, the MTT absorbance measured was the overall value of encapsulated and escaped cells. However, the CellTrace method developed in this thesis overcame the issue related with cell escape, and demonstrated that DPSCs did not proliferate within alginate-collagen microcapsules. Studies on human MSCs have also reported that cell proliferation was impeded when cells were encapsulated in both alginate and alginate-GRGDY hydrogels, although a retained viability of > 80% was observed 15 days after encapsulation (Markusen *et al.* 2006). These authors postulated that growth inhibition might be due to hindered nutrient access in the alginate hydrogel. However, the random distribution (some in central area and some in more peripheral areas) of dead cells (red) for both cell types observed in this thesis (**Figure 3.8** and **Figure 3.12**) suggests that microsphere nutrients and oxygen diffusion inside the microcapsules was not an issue. The accumulation of dead cells in the centre of the capsules would be a sign of nutrient deprivation due to an ineffective diffusion through the entire sphere. Since this effect was not observed, it can therefore be concluded that the size of the microcapsules was such that it enabled bidirectional diffusion of

nutrients inside the capsules and the efflux of waste products from cell metabolism outside the beads.

Furthermore, the composition of alginate hydrogel could also influence cell behaviour. It has been reported that an increase in molecular weight and concentration of high guluronic acid alginates prolongs the hindrance of glucose metabolism, insulin secretion and cell growth of murine insulinoma β TC3 cells encapsulated in alginate/PLL/alginate (APA) beads (Stabler *et al.* 2001). It is documented in the literature that alginates with a high guluronic acid content form a more compact network due to the coordination of Ca^{2+} ions and contiguous guluronic acid residues from different alginate chains, strengthening the resultant network (Grant *et al.* 1973; Sikorski *et al.* 2007). Thus, the stronger the network the more difficult it is to displace it. Consequently, cell growth might be inhibited within stiffer hydrogels (Stabler *et al.* 2001).

As part of preliminary studies, cells were encapsulated in low viscosity alginate (high content in mannuronic acid residues). These microcapsules exhibited low mechanical stability, as an inconsistent spherical shape was observed. Also, the efficacy of encapsulation was poor since a great number of cells were observed outside the capsules after the encapsulation experiment. Hence, low viscosity alginates were not considered in this thesis.

3.5.3 Cell functionality upon release from microcapsules

One of the initial purposes of this chapter was to test the neuronal differentiation potential of stem cells maintained for prolonged periods of time within microcapsules. The majority of the methods developed for *in vitro* neuronal differentiation require pre-coating of surface plates with substrates that promotes cell attachment, such as poly-lysine, laminin, ornithine, etc. (Reynolds & Weiss 1992; Wang *et al.* 2006). However, little cell attachment was observed for both NSCs and DPSCs in alginate and alginate-collagen microcapsules. Since cell attachment is one pre-requisite for neuronal differentiation, these scaffolds offer a synthetic microenvironment which is able to prevent spontaneous differentiation. Hence, these matrices are good candidates in order to protect the cells from the adverse environment after injury and preventing their auto-differentiation before the acute phase following SCI has ceased.

It should be noted that an objective of this thesis was to use ECM hydrogels as vehicles to protect transplanted cells from an adverse environment after injury and to direct cell location at the site of implantation. Therefore, ECM hydrogels should degrade as the cellular system replaces the 'artificial' matrix after transplantation. To this end, it was observed that cells were able to migrate out from the capsules and proliferate on plates 10 days after encapsulation. Therefore, the studies moved towards the investigation of the cellular functionality upon release from microcapsules 21 days after encapsulation.

It was observed that proliferation of cells within the microcapsules was slowed down in NSCs and inhibited in DPSCs. However, when cells were released from beads

and seeded on plates, they showed growth rates similar to those exhibited by non-encapsulated cells. As mentioned in the previous section, NSCs proliferation might be hindered within microcapsules due to the mechanical stiffness of the hydrogels. On the other hand, DPSCs proliferation only occurred after the release from capsules and seeding on plates. I hypothesized that alginate-collagen microcapsules provide an artificial stem cell niche, where DPSCs reside in a quiescent state. This is like DPSCs residing within the dental pulp of living organisms, usually remaining quiescent when they are within the dental pulps, but responding quickly after injury (Potdar & Jethmalani 2015). Although similar behaviour has been observed in DPSCs and MSCs in several publications (Markusen *et al.* 2006; Novikova *et al.* 2006; Umemura *et al.* 2011; Kanafi *et al.* 2014) none of these studies report on the mechanisms underlying cell survival despite their lack of attachment and proliferation. However, research on how to extend lifespan in yeast gives a hint of the potential mechanisms involved in the behaviour of adherent stem cells encapsulated in low adherence hydrogels. Nagarajan *et al.* 2014 showed that encapsulated yeast cells within calcium alginate beads and fed *ad libitum* ceased to divide but they maintained >95% viability over the course of 17 days. Analysis of gene expression of immobilized yeast cells demonstrated decreasing transcription of genes that regulate the cell cycle. A similar mechanism might take place in non-attached DPSCs within alginate-collagen microcapsules, where cells go into cell cycle arrest but continue to be metabolically active. Since cell aging is related to how many times a cell divides, controlled inhibition of cell division would allow for the temporal extension of stem cell lifespan.

It has been observed in this chapter that the behaviour of NSCs and DPSCs was altered under encapsulation conditions. However, upon release from the capsules,

cells retained stem cell properties, as demonstrated by high growth rates and the expression of both stem cell and neuronal markers. When cells were liberated from hydrogels and seeded on coated plates, both NSCs and DPSCs developed neuronal-like morphologies after application of a neuronal differentiation protocol previously developed in our group (Young *et al.* 2016).

Analysis of protein production showed that NSCs expressed the neuronal markers Nestin, β -III tubulin and Map2 and the stem cell markers Sox2 and Oct4 before and after differentiation. Nestin is a marker commonly used to identify early stage neural cells (Dahlstrand *et al.* 1995; Messam *et al.* 1999). Nestin expression is downregulated when CNS stem/progenitor cells differentiate into neurons or glial cells (Frederiksen & McKay 1988; Dahlstrand *et al.* 1995). After NSCs differentiate, nestin expression is typically replaced by the expression of neuronal or glial specific markers, such as NF-I and GFAP (Hendrickson *et al.* 2011). Expression of nestin after the differentiation protocol suggests that neuronal differentiation was not complete. This presumption was supported by the production of the stem cell marker proteins Sox2 and Oct4 after 15 days in differentiation medium. NSCs also expressed the early stage neuronal markers β -III tubulin and Map2 at both undifferentiated and differentiated state. Co-expression of Nestin and β -III tubulin has been suggested to be involved in the formation of cell processes during the differentiation of NSCs (Liu *et al.* 2013). Although no variations in proteins production was reported by NSCs, it was observed that cells developed long axons and neurites emerging from cell body, creating connections with adjacent cells and adopting neuronal morphology.

Expression of nestin by DPSCs was also observed both before and after differentiation. However, their behaviour differed from that shown by NSCs in that DPSCs produced the stem cell markers Sox2 and Oct4 in the undifferentiated state but not after the differentiation protocol. On the other hand, early stage neuronal markers β -III tubulin and Map2 were only visible in the differentiated state. DPSCs exhibited a change in their phenotype towards a neuronal-like morphology. Cells were typically bi-/tri-polar and fibroblast-like before differentiation. After the differentiation protocol, DPSC cell bodies adopted a rounded morphology with multiple long processes sprouting out forming neuronal-like connections. Although several protocols for DPSCs neuronal differentiation have been developed (Karaöz *et al.* 2011; Ellis *et al.* 2014; Gervois *et al.* 2015), this is the first time that it has been demonstrated that DPSCs maintain their stem cell and neuronal properties after encapsulation within alginate-collagen microcapsules.

The results presented in this chapter demonstrate that the microfluidic technique developed in this thesis allowed for the encapsulation of different types of stem cells. Encapsulation of NSCs and DPSCs within alginate and alginate-collagen microcapsules permitted their culture in 3D scaffolds for up to 21 days. Viability and proliferation assays demonstrated that the cells were viable for this 3-week period. However, proliferation of NSCs was delayed and inhibited in the case of DPSCs. This effect might permit the use of such scaffolds to 'extend' the cell lifespan by positioning them within an appropriate niche which supports cell quiescence. When stem cells were released from the microcapsules, both NSCs and DPSCs clearly

retained stem cell and neuronal-like differentiation properties, as demonstrated by high proliferation rates and the expression of stem cell pluripotency markers and neuronal markers.

Chapter 4. Transplantation of
Encapsulated Stem Cells
into an Organotypic Model
of Spinal Cord Injury

4.1 Introduction

One of the limitations of *in vitro* experiments is that they fail to replicate the precise cellular conditions of an organism (Staton *et al.* 2009). Because of this, *in vitro* studies often lead to results that do not fully correspond to the events occurring within a living organism. For example, intact functional organs or tissues *in vivo* exhibit complex interactions with many different cell types. These mechanisms are difficult to replicate in most *in vitro* cell culture models (Whitehead *et al.* 2012). Therefore, when extrapolation of *in vitro* data to the *in vivo* situation is required, the model must try to reflect the complexity of the studied system. Thus, *ex vivo* systems offer a valuable tool before progressing onto *in vivo* investigations. *Ex vivo* experiments include procedures with living tissues or organs isolated from an organism and cultivated outside that organism in an artificial environment under highly controlled conditions. As such, an *ex vivo* model system in which the full complexity of the host-associated environment can be eliminated, provides an ideal experimental arena in which the underlying cellular and molecular mechanisms between the host and grafted cells can be studied.

Spinal cord explant culture systems preserve partial histological architecture of a surgically removed piece of organ, allowing the study of *in vivo* processes under controlled *ex vivo* conditions (Sypecka *et al.* 2015). Different SCI *ex vivo* models have been established for the study of several aspects of neuroscience investigations. Okada *et al.* (2014) developed a laser-induced SCI model to assess the mechanisms of axonal degeneration in real time. The similarity of the model with clinically relevant contusion/compression-induced axonal pathologies permitted the

differentiation between the primary insult that directly injures axons and secondary injury mechanisms. *Ex vivo* models have also been utilised to study repair strategies after SCI. These include peripheral nerve graft implants into cultured spinal cords (Zhang *et al.* 2010) and cell transplantation (Kim *et al.* 2009; Park *et al.* 2010).

The promising results obtained with *ex vivo* models have encouraged researchers to apply these findings into *in vivo* systems. Indeed, the potential of both NSCs and DPSCs for neuronal repair after SCI have been reported (Ogawa *et al.* 2002; Sakai *et al.* 2012). Most of the times, neuron survival and regrowth after injury is mediated by neurotrophins and growth factors released by the grafted cells rather than by direct cell incorporation/replacement (Corti *et al.* 2010; Rossi *et al.* 2010; De Almeida *et al.* 2011). Current therapies that apply cell replacement to promote neuronal survival and/or growth have had modest success in allowing injured neurons to regrow through the area of the lesion (Pfeifer *et al.* 2004; Parr *et al.* 2007). This is because of the lack of three-dimensional organization in cellular transplantation, resulting in random directions of axonal growth in the lesion site and poor bridging beyond the injury (Pires & Pêgo 2015). Hence, strategies for successful regeneration will require an engineering approach that guide regenerating axons in the proper direction to create a bridge across the injured area (Geller & Fawcett 2002). In fact, when BMSCs were seeded in alginate-based scaffolds with an anisotropic capillary structure, enhanced axonal growth oriented parallel to the hydrogel channel walls was demonstrated (Günther *et al.* 2015). Hence, in this investigation, an *ex vivo* model of SCI and transplantation was utilised to investigate the potential of the grafting of stem cells encapsulated within alginate-collagen microbeads.

4.2 Aims & Objectives

The objectives of this chapter were to:

- Develop a method for the transplantation of encapsulated stem cells into an *ex vivo* model of SCI.
- Study of the behaviour of the transplanted stem cells within the tissue, including cell survival and neuronal differentiation.

4.3 Materials & Methods

4.3.1 Animals

21-28 day old C57/Bl6 mice were used for tissue harvest and obtained from Charles River Laboratories, UK, and maintained at the Joint Biological Services Unit (JBIOS) at Cardiff University, Cardiff, Wales. Mice were sacrificed by CO₂ asphyxiation in accordance with Schedule 1 of the Animals (Scientific Procedures) Act 1986.

4.3.2 Dissection and preparation of murine spinal cord explants

Spinal cord slice cultures were prepared as previously described (Meng *et al.* 2012). Briefly, 21-28 day old C57BL/6 mice were sacrificed by CO₂ asphyxiation and complete spinal cords were dissected on ice. Meninges were carefully removed, so as not to damage the cord, under a dissecting microscope. Cords were then washed twice in PBS supplemented with 1% (v/v) penicillin/streptomycin. Cords were cut

with surgical blades on ice into approximately 1cm long sections. These were transferred to the centres of 35mm tissue culture dishes with the dorsal area facing upwards. An injury was induced on the centre of each section by removing part of the tissue with a scalpel.

4.3.3 Transplantation of encapsulated cells

To allow for easy identification of transplanted cells, a mixed population of NSCs and fibronectin-adherent DPSCs were isolated from transgenic mice expressing GFP (**Section 3.3.1**).

Cells in culture were trypsinized (DPSCs) or accutase-digested (NSCs) and encapsulated in alginate-collagen microcapsules as described in **Section 3.3.3.2**. Neuronal-like pre-differentiated DPSCs were cultured in NSC growth medium for 5 days (**Section 3.3.6.2**) and also encapsulated. Microcapsules were then transplanted with forceps into the spinal cord sections so as to fill the gap generated after injury (2.5mm long and 0.5cm wide, approximately). Six microcapsules were transplanted for each experimental condition and sealed in position with 30µl of Matrigel® (BD Biosciences, UK) to avoid the beads becoming released from the tissue. The plates were then transferred to the tissue culture incubator for 1 hour to allow the Matrigel® to polymerise. Pre-warmed DMEM/F-12 medium containing 25mM HEPES buffer supplemented with 1% (v/v) penicillin/streptomycin and 20% heat-inactivated FBS (all Life Technologies, UK) was then added such that the surface of the spinal cord sections was completely covered with culture medium. Samples were then returned to the incubator and culture medium replaced every other day for up to 10 days.

4.3.4 Cryosectioning of spinal cord tissue samples

Spinal cord tissues were removed from culture and fixed overnight at 4°C with 4% PFA either immediately after transplantation (0 days) or 10 days after transplantation. The following day, samples were washed for 3x 20 minutes in PBS and then washed in 30% (w/v) sucrose (Sigma-Aldrich, UK) solution overnight to provide cryoprotection. Spinal cord tissue was then mounted in OCT embedding compound (Thermoscientific, UK). 20µm-thick longitudinal sections were cut using a Leica CM3050 S cryostat (Leica Microsystems, Germany) and mounted onto glass microscope slides (VWR International, UK). Glass slides were stored at -80°C until required for further analysis.

4.3.5 Apoptosis Tunel Assay

Slides were removed from the -80°C freezer and air dried at room temperature for 20 minutes. Spinal cord slices were permeabilized with 1X Proteinase K solution in PBS for 15 minutes. Samples were washed with PBS twice for 5 min and then post-fixed with 4% (v/v) paraformaldehyde for 5 min at 37°C. Slices were immersed in PBS twice for 5 minutes and after rinsing with deionized water samples were ready for staining.

To induce DNA strand breaks (positive control, **APPENDIX III**), tissues were fixed and permeabilized with 1 unit of DNase I diluted into 1X DNase I Reaction Buffer (20mM Tris-HCl, pH 8.4, 2mM MgCl₂, 50mM KCl) for 30 minutes at room temperature (both LifeTechnologies, UK). Positive control and samples were then stained with

Click-iT® Plus TUNEL Assay (Life Technologies, UK) according to the manufacturer's instructions. Briefly, samples were incubated with TdT reaction buffer for 10 minutes at 37°C. Buffer was removed and TdT reaction mixture containing 94% (v/v) TdT reaction buffer, 2% (v/v) EdUTP and 4% (v/v) TdT enzyme was then added to tissues and incubated for 60 minutes at 37°C. The reaction mixture was removed and slides rinsed with deionized water. Slides were then washed with 3% BSA and 0.1% Triton® X-100 in PBS for 5 minutes before rinsing in PBS. The reaction cocktail was prepared by addition of 87% (v/v) reaction buffer, 2% (v/v) copper protectant, 0.2% (v/v) Alexa Fluor® picolyl azide and 10% (v/v) reaction buffer additive. The mixture was then added to samples and incubated for 30 minutes at 37°C, protected from light. The reaction cocktail was removed and slices washed with 3% BSA before washing in PBS for 5 minutes. Samples were mounted onto glass cover slips using mounting media supplemented with DAPI stain (VectorLabs, UK). Fluorescent images were then acquired of the stained spinal cord tissues. (**Section 3.3.8.2**).

4.3.6 Immunohistochemical staining of spinal slice cultures

Slices were removed from the -80°C freezer and air dried at room temperature for 20 minutes. A ring was created around each slice using a hydrophobic pap pen (Sigma-Aldrich, UK) in order to minimise antibody wastage. Samples were permeabilized with 0.1% (v/v in PBS) Triton X-100 for one hour at room temperature. After three washes with PBS, 5% (w/v) BSA (Fisher Scientific, UK) in PBS was applied for one hour in order to block non-specific binding. This was removed, washed with PBS and replaced with primary antibodies against Nestin, Map2 and GFAP (**Table 1**)

diluted in 5% (w/v) BSA along with the isotype control (**Table 2**) and incubated overnight in a dark humid chamber at 4°C. The following day, three PBS washes were performed before incubation with complementary fluorophore-conjugated secondary antibody diluted in 5% (w/v) BSA (**Table 3**), in the dark at room temperature for 2 hours. Three further washes with PBS were performed before the samples were mounted onto glass cover slips using mounting medium supplemented with DAPI stain (VectorLabs, UK). Slides were stored at 4°C in the dark, to prevent bleaching, until required for imaging (**Section 3.3.8.2**).

4.4 Results

4.4.1 Development of a method for the transplantation of encapsulated stem cells into an organotypic model of spinal cord injury

Most of the methods developed for transplantation of microcapsules use needles to inject the encapsulated cells into the injury site (Sah & Chien 1996; Toso *et al.* 2003; Zhao *et al.* 2016). However, the size of the beads produced in this thesis was too large to use needle injection. The narrow internal diameters of the needles provoked their blockage and injection was impeded. The reduction of microcapsules diameter would have involved the re-optimization of the encapsulation parameters. Hence, a method for implantation of the microcapsules with diameters $\sim 400\mu\text{m}$ was developed in this section.

The transplantation technique should be reproducible in order to compare the behaviour of the transplanted cells. Also, the technique must permit a precise control of graft implantation, which directly affects cell arrangement within the tissue. Whilst conventional cell grafting can promote growth of injured axons, they rarely extend across the lesion site due to the lack of a proper guidance. Hence, a precise control of cell orientation is of a key importance in SCI in order to assess linear axonal regeneration through the injury site (Günther *et al.* 2015).

Following CO₂ asphyxiation, spinal cords from mice were dissected as described in **Section 4.3.2**. After the injury was induced, encapsulated cells were

transplanted following the steps in **Section 4.3.3**. Different strategies were considered in order to induce the injury. Due to the anatomy of the cord (**Figure 4.1A**) the injury could not be too deep since beads would escape underneath the tissue. The first approach involved the removal of the tissue on the dorsal part of the cord in a “V” shape (**Figure 4.1B**). Then beads were implanted to fill the gap completely. However, the number of beads that could be implanted was limited and their arrangement difficult to control. Therefore, a different approach was considered in order to maximize the number of transplanted beads per tissue section. This consisted of the removal of part of the tissue on the surface of the cord in order to induce the injury lengthwise. This method allowed for the visualization of all the beads transplanted in the same section, increasing the number of visible cells (**Figure 4.1**).

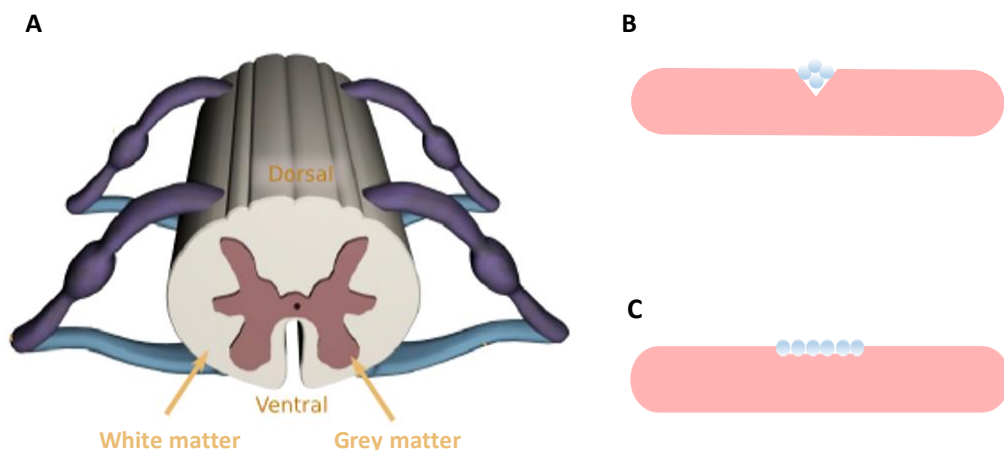


Figure 4.1. Approaches for injury induction into an *ex vivo* model of SCI. A) Schematic representation of the anatomy of the spinal cord. B) Injury induction in a “V” shape. C) Injury induction lengthwise.

The main challenge to overcome was to fix the position of the microcapsules within the injury during the investigation period otherwise they would float free within the culture medium. Therefore, a cell friendly “glue” was utilised to seal the capsules at the injury site. Matrigel® is a biocompatible matrix rich in ECM proteins that mimics *in vivo* environments. When added on the top of the beads and cultured for 1 hour at 37°C, it became solid, thereby entrapping the beads (**Figure 4.2**). In this way, it was possible to improve cell engraftment by sealing the microcapsules at the transplantation site, avoiding the loss of beads during the culture period and preventing any potential spread of the injury. After Matrigel® solidification, explants were fixed, dehydrated and cryosectioned in 20µm thick slices (**Section 4.3.4**). Tissues were then imaged with a fluorescence microscope as described in **Section 3.3.8.2**. **Figure 4.3** shows a longitudinal section of spinal cord tissue after transplantation (day 0). Alginate-collagen capsules containing GFP DPSCs can be observed in the middle of the cord, demonstrating the efficacy of Matrigel® to retain the capsules at the site of implantation.

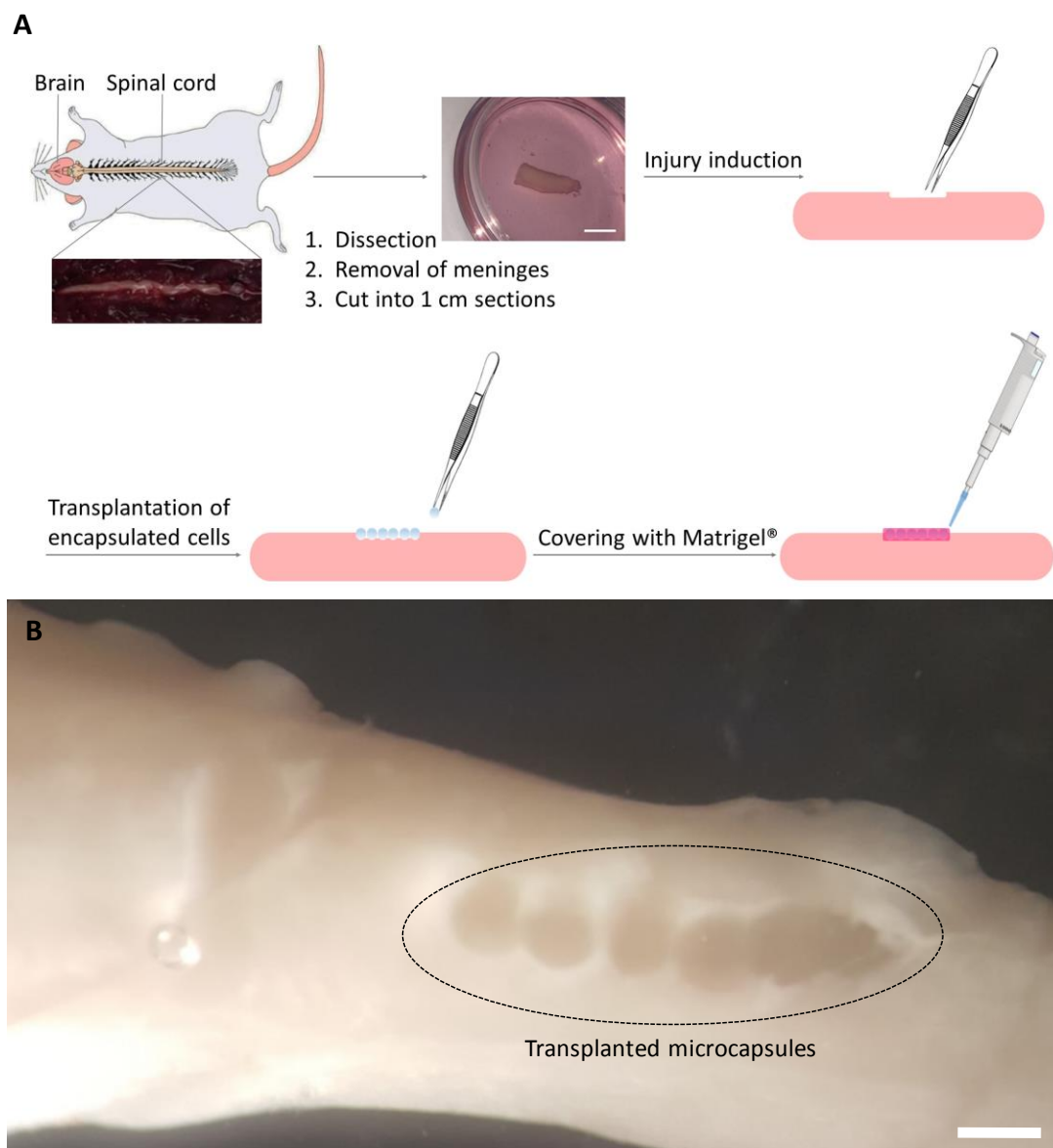


Figure 4.2. *SCI induction and transplantation of encapsulated cells.* A) Murine spinal cord was dissected after CO₂ asphyxiation. Meninges were then removed and an injury was induced on the dorsal part of the cord. Encapsulated cells were transplanted at the site of injury and sealed with Matrigel®. Scale bar = 500mm. B) Picture of spinal cord after transplantation of encapsulated cells. Scale bar = 500µm.

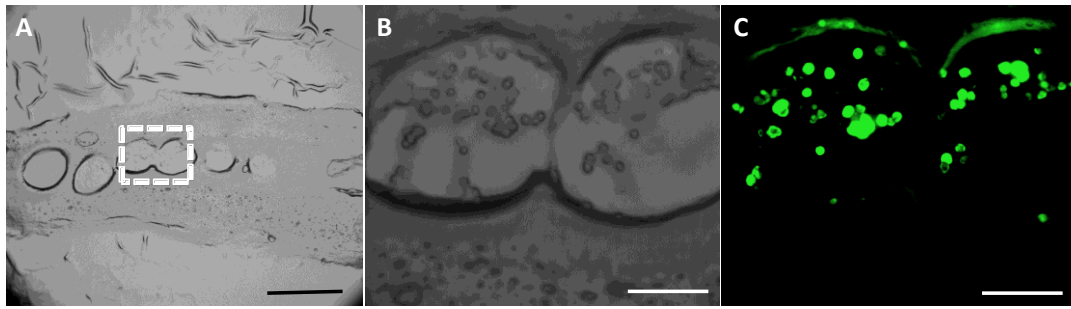


Figure 4.3. *Spinal cord longitudinal section after transplantation of encapsulated cells.* A) 20µm thick frozen section of spinal cord. Scale bar = 1mm. B-C) Detailed images (bright field and fluorescence, respectively) showing encapsulated GFP DPSCs within the spinal cord. Scale bars = 200µm.

In order to highlight the benefits of this cell encapsulation technique for transplantation purposes, a comparison between implantation of unencapsulated and encapsulated cells was carried out. The same number of cells corresponding to the transplantation of 6 beads loaded with cells (~ 2700 cells) were pipetted at the site of injury resuspended in 2µl of culture medium. Matrigel® was then added on the top to seal the injury and to retain the cells at the site of implantation. Tissues were fixed, dehydrated and sliced into 20µm slices (**Section 4.3.4**).

Figure 4.4 demonstrates that cells could be observed after both methods of delivery immediately after transplantation. However, the longer-term localization of the cells differed dependent on the implantation method utilised. After 10 days, no GFP-positive cells were found at the injury site when cells were implanted as cell suspension (non-encapsulated). On the other hand, GFP positive encapsulated cells were observed within the capsules at the injury site 10 days after transplantation.

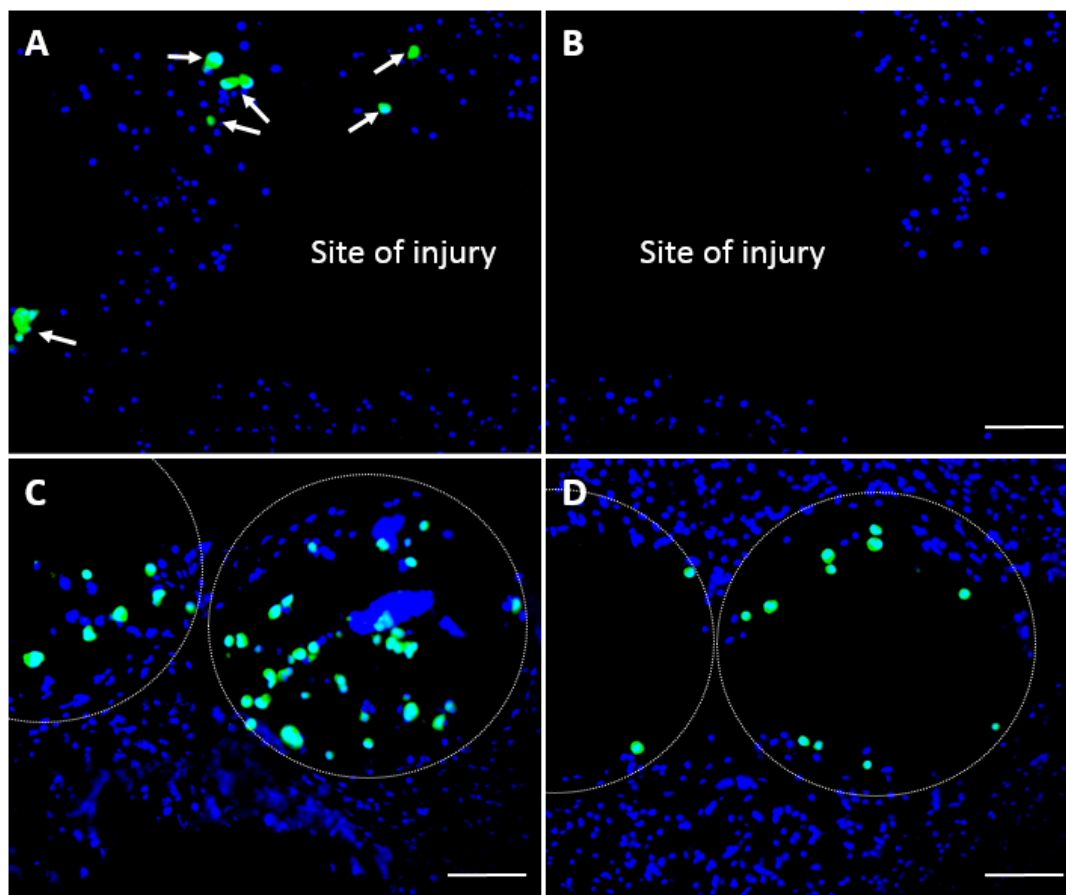


Figure 4.4. Behaviour comparison of non-encapsulated and encapsulated cells transplanted in spinal cord slice cultures. Coexpression of DAPI and GFP. (A) Few unencapsulated cells could be observed within the tissue directly after implantation (white arrows). (B) Ten days post-injection, the injury site remained devoid of any non-encapsulated cells. (C) Encapsulated cells were transplanted and visible at the injury site. (D) Encapsulated cells were still visible 10 days after transplantation. Scale bar = 100 μ m.

Differentiation of transplanted cells *in situ* is heavily influenced by the surrounding tissue/environment (Kshitiz *et al.* 2012; Gattazzo *et al.* 2014; Griffin *et al.* 2015). In this chapter, the behaviour of different cells types was investigated in order to study the influence of the host tissue on the fate of the transplanted cells. The three different conditions investigated were the following: (1) undifferentiated DPSCs, (2) DPSCs pre-differentiated into neuronal-like cells following the protocol described in **Section 3.3.6.2** and (3) undifferentiated NSCs (**Figure 4.5**).

Cells for the three conditions were encapsulated in alginate-collagen microcapsules at an initial density of 1×10^7 cells/ml. Whilst the optimized concentration for encapsulation of NSCs was established at 1×10^6 cells/ml (**Section 3.4.2**), preliminary experiments demonstrated that very few cells were visible after cryosectioning. Hence, it was decided to increase the concentration of initial seeding density for NSCs from 1×10^6 cells/ml to 1×10^7 cells/ml for this set of experiments. The viability and the neuronal differentiation potential of the encapsulated cells were the investigated 1 and 10 days after transplantation into the *ex vivo* SCI model.

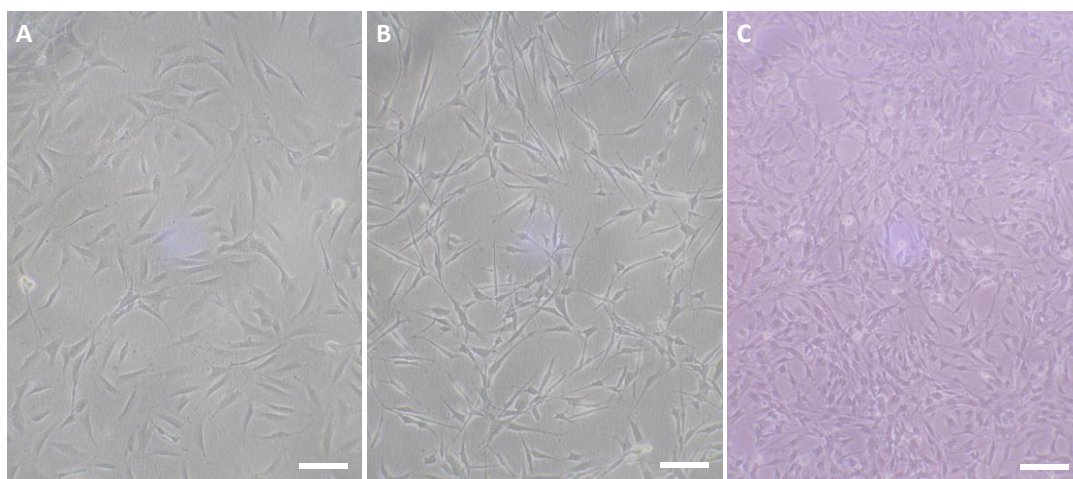


Figure 4.5. Bright field images of cells at three different conditions before encapsulation and transplantation. A) Condition 1: undifferentiated DPSCs. B) Condition 2: pre-differentiated DPSCs into neuronal-like cells. C) Condition 3: undifferentiated NSCs. Scale bar = 100 μ m.

4.4.2 Analysis of cell survival after transplantation

The survival of cells within the alginate-collagen microcapsules was described in the previous chapter. Both DPSCs and NSCs demonstrated high viabilities after 3 weeks in culture within tissue flasks (>65% and >85%, respectively). In order to progress towards further applications in the repair of SCI, the suitability of the encapsulated cells should be investigated within an *ex vivo* model of SCI.

The three different types of encapsulated cells were implanted into spinal cord tissues and cell viability was studied immediately and 10 days after transplantation. Cells were fixed, dehydrated and cryosectioned before staining with Apoptosis TUNEL Assay (**Section 4.3.5**). For the three cell types studied, microcapsules were easy to visualize immediately after transplantation, but no complete capsules were observed after the culture period.

As observed in **Figure 4.6**, cells of all three types were viable at the time of implantation, since no co-expression of **DAPI/GFP/AF 594** was observed. Ten days after transplantation, a number of apoptotic nuclei were observed for cell types 1 and 2, as observed by co-expression of **DAPI/AF 594**. However, some encapsulated cells were still viable for the three cell types. Furthermore, NSCs (cell type 3) proliferated within the tissue and started to form aggregates. No signs of cell proliferation were observed for either DPSCs population. This behaviour was similar to that observed in standard culture of encapsulated cells, where NSCs grew in the form of aggregates but DPSCs did not proliferate (**Section 3.4.3.1.2**)

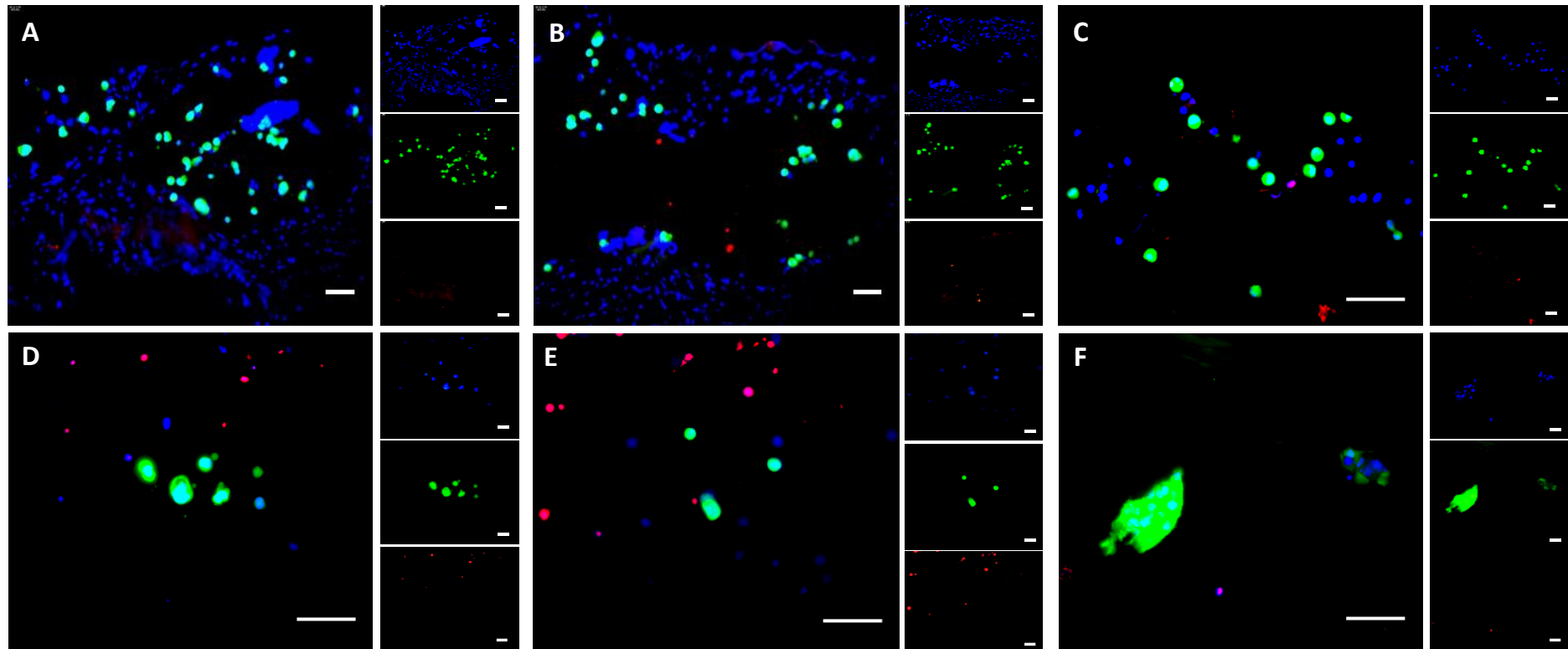


Figure 4.6. *Apoptosis TUNEL Assay of encapsulated cells transplanted into an ex vivo model of SCI.* Co-expression of **DAPI**-stained nuclei, **GFP** cells and **apoptotic nuclei**. Encapsulated cells from the three conditions were transplanted and viability was studied using Apoptosis TUNEL Assay 0 (A-C) and 10 (D-F) days after transplantation. Condition 1: undifferentiated DPSCs (A, D); Condition 2: pre-differentiated DPSCs into neuronal-like cells (B, E); Condition 3: undifferentiated NSCs (C, F). Scale bars = 50 μ m

4.4.3 Study of the neuronal marker levels within encapsulated stem cells transplanted into *ex vivo* spinal cord cultures

All three cell types were encapsulated within alginate-collagen microcapsules, implanted into *ex vivo* spinal cord slices and cultured for 0 or 10 days. Tissue sections were then fixed, dehydrated and stained with antibodies against nestin, map2 and GFAP as described in **Section 4.3.6**, along with the appropriate isotype control (**APPENDIX IV**). An intense endogenous staining of GFAP was observed in the spinal cord cultures, regardless of the cell type or the time point. However, no endogenous staining for nestin and map2 was observed (**APPENDIX V**).

Undifferentiated DPSCs (cell type 1) expressed the neuronal marker nestin before and after culture within the section of spinal cord (**Figure 4.7**). On the other hand, none of the neuronal markers associated with more mature neuronal phenotypes, map2 and GFAP, were observed immediately after transplantation. However, cells did stain positive for these neuronal markers after 10 days in culture.

Unlike undifferentiated DPSCs, neuralised DPSCs (cell type 2) showed staining for both nestin and GFAP before culture, whilst the cells did not stain positive for map2 (**Figure 4.8**). Ten days after culture, nestin and GFAP staining was evident as was positive staining for map2.

Unlike undifferentiated and neuralised DPSCs, undifferentiated NSCs (cell type 3) did not show GFAP expression before or after culture. However, cells stained positively for nestin and map2 at both time points (**Figure 4.9**).

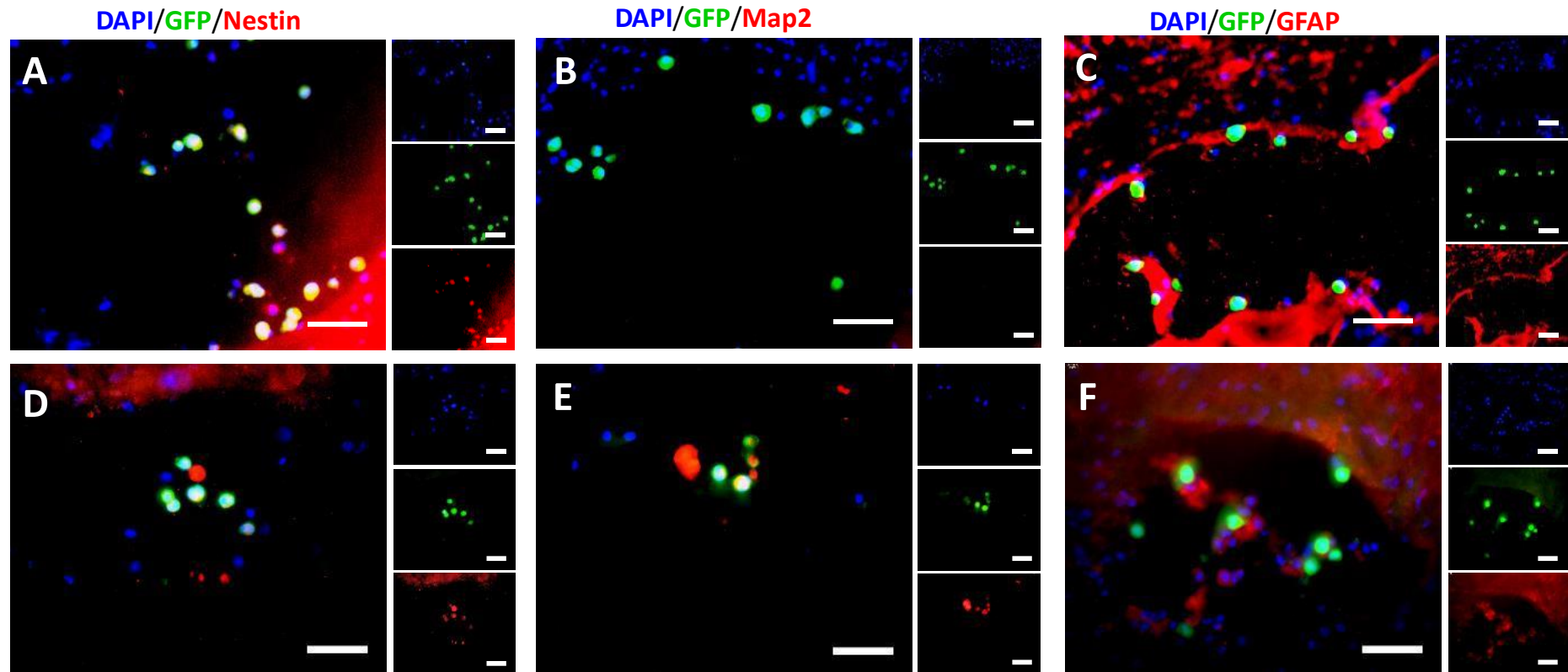


Figure 4.7. Expression of neuronal markers by undifferentiated DPSCs (cell type 1). Alginate-collagen microcapsules loaded with undifferentiated DPSCs were implanted in spinal cord slices and cultured for up to 10 days. Explants were stained with antibodies against nestin, map2 and GFAP before (A - C) and after culture (D - F). Transplanted cells (green) expressed the neuronal marker nestin before and after culture (D - F). On the other hand, none of the neuronal markers associated with more mature phenotypes, map2 and GFAP were observed after transplantation. However, cells stained positive for these proteins after 10 days in culture. Scale bars = 100 μ m.

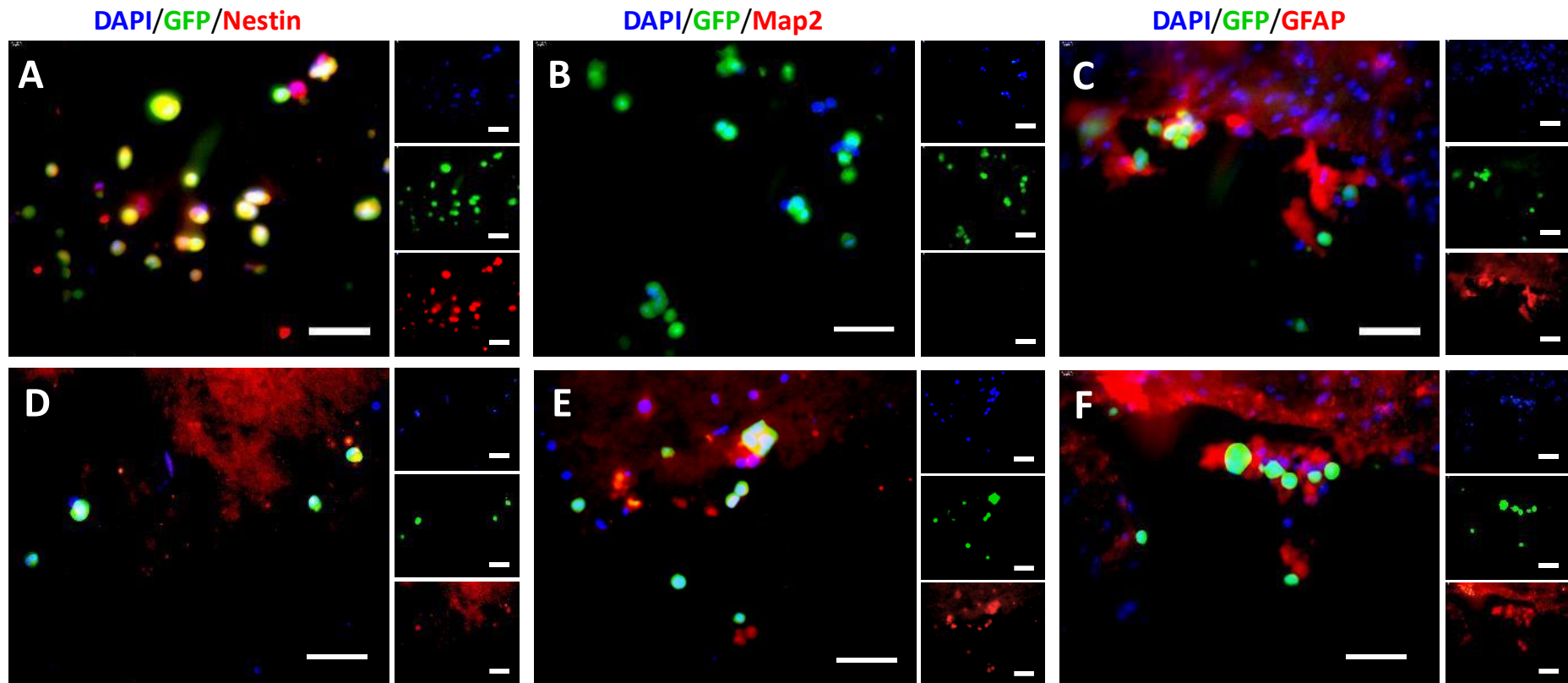


Figure 4.8. Expression of neuronal markers by neuralised DPSCs (cell type 2). Alginate-collagen microcapsules loaded with neuralised DPSCs were implanted in spinal cord slices and cultured for up to 10 days. Explants were stained with antibodies against nestin, map2 and GFAP before (A - C) and after culture (D - F). Neuralised DPSCs (green) showed expression of both nestin and GFAP before culture, while cells did not stain positive for map2. Ten days after culture, cells were positive for all three markers. Scale bar = 100 μ m.

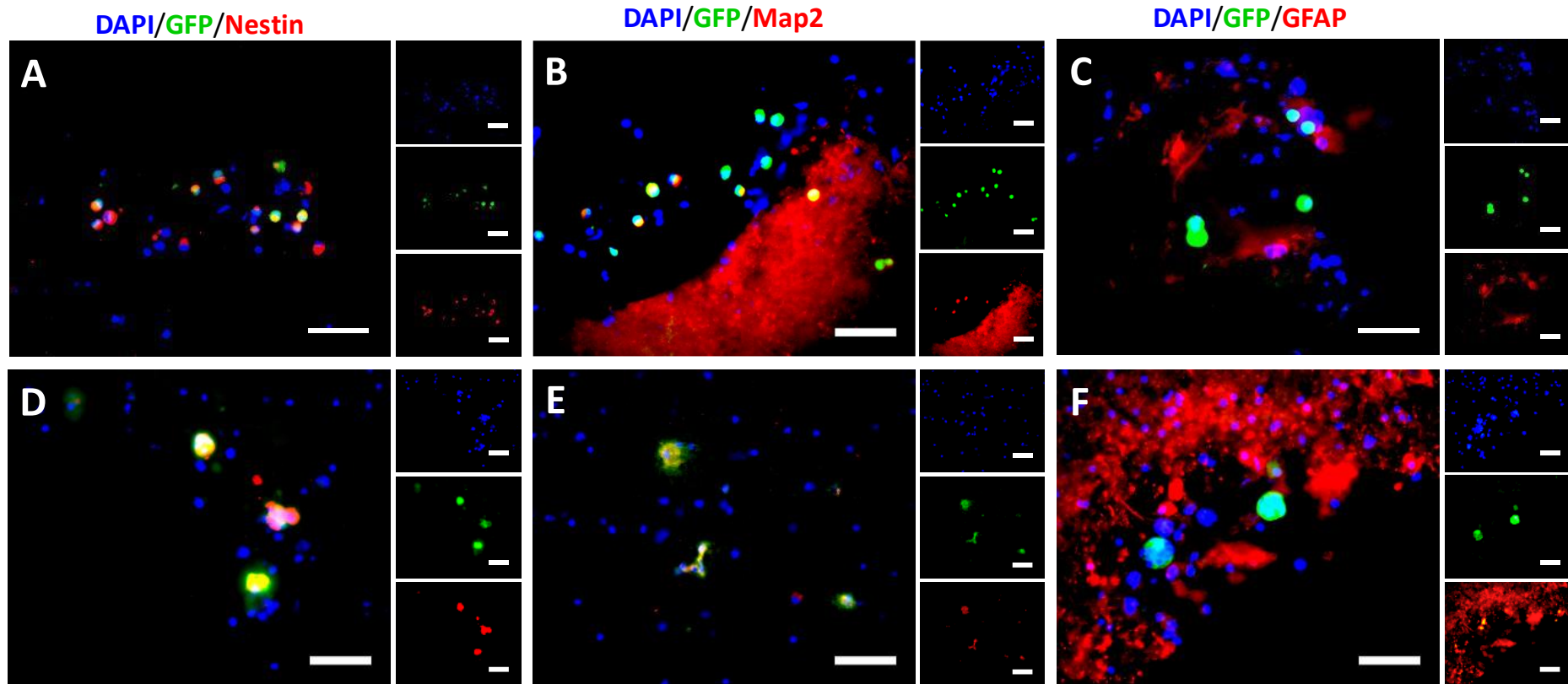


Figure 4.9. Expression of neuronal markers by undifferentiated NSCs (cell type 3). Alginate-collagen microcapsules loaded with undifferentiated NSCs were implanted in spinal cord slices and cultured for up to 10 days. Explants were stained with antibodies against nestin, map2 and GFAP before (A - C) and after culture (D - F). Undifferentiated NSCs (green) did not show GFAP expression before or after culture. However, cells stained positively for nestin and map2 at both time points. Scale bar = 100 μ m.

4.5 Discussion

NSCs and DPSCs encapsulated in alginate-collagen microcapsules exhibited high viabilities after three weeks in culture and retained stem cell and neuronal differentiation potential upon release from microcapsules (**Section 3.4.5**). As an attempt to apply this technique in a clinically relevant model, the behaviour of the encapsulated cells was studied in an *ex vivo* model of SCI developed in this thesis. Organotypic models permit a tight control of the artificial environment, which allows for the reliable comparison of the different conditions studied.

The lack of ECM at the lesion site, that directs and organizes the wound healing cells, is one of the mechanisms that interferes with regenerative processes after SCI (Gaudet & Popovich 2014). Thus, the use of biomaterials to replace ECM and support axonal growth has gained great attention over the last years as a promising strategy for neural tissue engineering. In this thesis, it was demonstrated that encapsulation of cells and further transplantation helps retain the grafted cells at the wound site. Comparison between transplantation of non-encapsulated and encapsulated cells demonstrated that microcapsules aided retention of transplanted cells at the site of injury 10 days after implantation. However, no cells were found after this period of time when cells were implanted as a free cell suspension. This demonstrates the added benefits of using scaffolds as mean of transplantation in cellular therapies. These materials not only help to retain grafted cells at the injury site but also allow manipulation of the direction of cell transplantation in a three-dimensional manner, facilitating the integration of implanted cells within the host tissue (Yoshii *et al.* 2003; Tsai *et al.* 2006; Günther *et al.* 2015; Sugai *et al.* 2015; Fan *et al.* 2017).

After cell transplantation, one of the main challenges is the loss of cellular material due to inflammatory responses (Wilson *and* Chaikof 2009). Thus, immobilization of cells within polymer hydrogels has been useful to protect the enclosed cells from the host's immune response (Zhong *et al.* 2010; Ye *et al.* 2011; Jun *et al.* 2013). The survival of the encapsulated cells after transplantation in the *ex vivo* model of SCI was studied after 10 days in culture. Encapsulated cells of three cell types survived throughout the culture period, as evidenced by limited apoptosis staining. *Ex vivo* slice cultures are avascular and as such, reduced apoptosis as a result of a lack of inflammatory response was expected. Co-culture of organotypic spinal cord slices along with a controlled concentration of pro-inflammatory molecules, such as IL-1 β , IL-6, and TNF- α (Zhang & An 2007), would provide a more accurate *ex vivo* model to study grafted cell survival under the harsh conditions found in SCI. For instance, the co-culture method has been adapted for the study of insulin-secreting cell survival whereby the cells have been encapsulated within anti-inflammatory peptide functionalized hydrogels and then cultured in the presence of diffusible pro-inflammatory cytokines (Su *et al.* 2010).

Although encapsulated cells survived within the spinal cord cultures, neither undifferentiated, nor neuralised DPSCs showed signs of proliferation, since no increased cellular density at the site of grafting could be observed. This behaviour was similar to that observed *in vitro*, where cells did not proliferate but maintained a high percentage of viable cells after 3 weeks in culture. On the other hand, NSCs showed some signs of cell proliferation, as indicated by the observation of small cell aggregates after the culture period. In relation to this it has been demonstrated that immobilized neural progenitor cells within microfibers showed high proliferation

rates after transplantation into an *in vivo* mouse model of SCI (Sugai *et al.* 2015). On the other hand, it has been reported that DPSCs do not proliferate after implantation into the mouse hippocampus but they stimulate proliferation of endogenous neural cells (Huang *et al.* 2008).

Spinal cord slices were analysed in order to elucidate whether transplanted cells migrated out from the capsules and integrated within the host tissue. Since cell escaping from alginate-collagen was observed after 10 days *in vitro* culture (**Section 3.4.3.1.3**), migration of cells within the tissue was expected. However, no cells were found outside the site of implantation in any of the sections analysed. On the contrary, when DPSCs were transplanted in the spinal cord of traumatic injured rats, transplanted cells were observed in the spinal cord tissue reaching a distance of ~1 mm from the lesion epicentre 42 days post-injury (Nicola *et al.* 2016). Hence, cell migration through the host tissue might be a time-dependent factor. It must be borne in mind that the culture periods in the *ex vivo* experiments carried out in this thesis were established at 10 days. Cells might need longer culture times to migrate within this *ex vivo* system. Also, the microcapsules composition might play a key role in cell migration. The coating of culture plastics with laminin, a major constituent of CNS extracellular matrix, and poly-L-ornithine (PLO) increases the migratory capacity *in vitro* of DPSCs and NSCs, respectively (Howard *et al.* 2010; Ge *et al.* 2016). Hence, the modification of microcapsule composition with these proteins could promote cell migration within the spinal cord cultures.

Whilst it was easy to visualize the microcapsules immediately after transplantation, no complete capsules were observed after the culture period. Also,

it was clear that the number of transplanted cells decreased after 10 days in culture. The first hypothesis would consider the possibility of alginate-collagen microcapsule degradation during the culture period. Microcapsules showed good mechanical properties in that no changes in morphology nor signs of bead degradation were observed after three weeks in culture *in vitro* (**Chapter 3**). However, spinal cord tissues might release sodium cations that promote alginate degradation by monovalent ions interchange. Shahriari *et al.* (2016) demonstrated that calcium cross-linked alginate hydrogels did not maintain adequate mechanical integrity *in vivo* 14 days after transplantation in rat spinal cord. Hence, the development of new approaches to decrease the degradation rate of alginate should be pursued to make it a viable scaffold material for nerve regeneration. Also, collagen is a biodegradable material due to the existence of MMPs within the organism, which are responsible for collagen degradation (Harrington 1996). Hence, the consistence of alginate-collagen microcapsules might have been compromised due to the existence of such enzymes within the host tissue. After SCI, activated microglia release proteolytic and oxidative enzymes, which might affect the stability of the polymer microcapsules (Fleming *et al.*, 2006). Thus, collagen cross-linking should be considered to improve the mechanical stability of the microcapsules to guarantee the protection of the encapsulated cells against the inflammatory response. Another possibility might be that microcapsules integrated within the spinal cord tissue, thereby reducing the damaged area. In order to elucidate the fate of alginate-collagen microcapsules within the spinal cord cultures, microcapsule labelling and further visualization under fluorescent microscope would be necessary. Alginate can be fluorescently labelled by covalent binding of the amino groups of fluorescent

molecules to the carboxylic groups of the alginate. A method for alginate labelling using fluoresceinamine has been described (Strand *et al.* 2003). However, the excitation and emission wavelengths are similar to those to visualize GFP-labelled cells, which would hinder the detection of transplanted cells. The last hypothesis considers the loss of microcapsules during the culture period, which also would explain the decrease in cell number. Matrigel® would retain the capsules for a short period of time, but after several days and medium changes, some capsules might have been lost. Culture medium was examined under the microscope in search of floating beads after every medium change but no microcapsules were discovered. Hence, the actual fate of alginate-collagen microcapsules within the spinal cord tissues after the culture period remains to be determined.

The expression of neuronal markers by transplanted cells was also investigated. It is well known that the fate of *in vivo* differentiation of stem cells depends on the niche into which they have been transplanted. When NSCs are transplanted into a neurogenic region e.g. dentate gyrus, or subventricular zone, they will differentiate into neurons (Fricker *et al.* 1999; Shihabuddin *et al.* 2000). However, transplantation into non-neurogenic regions, such as spinal cord, induce neural cells to differentiate towards glial lineage (Cao *et al.* 2001). This demonstrates the importance of environmental cues in directing the differentiation of transplanted cells. Cell differentiation towards undesirable lineages might hinder tissue regeneration. Hence, pre-differentiation of stem cells prior to transplantation is a commonly adopted method used to induce a lineage restriction in CNS regeneration studies (Abeyasinghe *et al.* 2015; Fortin *et al.* 2016). In this thesis, the neuronal marker expression of encapsulated cells transplanted of three different types was compared:

undifferentiated DPSCs, neuralised DPSCs and undifferentiated NSCs. At the time of implantation, undifferentiated and neuralised DPSCs showed distinct marker profiles. Whereas undifferentiated DPSCs only expressed nestin, neuralised cells expressed both nestin and GFAP. None of the cells showed positive staining for Map2. However, after 10 days in culture, both cellular conditions stained positive for the three neuronal markers nestin, map2 and GFAP. Expression of map2 and GFAP by undifferentiated cells and expression of map2 by neuralised cells after the culture period suggests that the local environment provides signals driving the fate of stem cells. Human umbilical cord blood–derived NSCs (HUCB-NSCs) co-cultured with different rat brain–specific primary cultures differentiated towards different lineages depending on the cellular microenvironment (Markiewicz *et al.* 2011). The presence of astrocytes and oligodendrocytes promoted neuronal differentiation of HUCB-NSCs, whereas postmitotic neurons induced oligodendroglialogenesis of these cells. Hence, transplanted DPSCs could have received signals from the spinal cord culture microenvironment that stimulated their differentiation towards neuronal lineages in the absence of external growth factors in the culture medium. On the other hand, the marker profile of NSCs did not change along the culture period. Cells stained positive for nestin and map2, but not for GFAP, before or after culture. As mentioned before, spinal cord cultures with transplanted NSCs showed the presence of cell aggregates after several days in culture, suggesting cell proliferation. As cells differentiate, their rate of proliferation usually decreases. Since NSCs were still proliferative within the tissue explants, the cells did not just completely commit to the differentiation process. This highlights the different behaviour of different stem

cell types under the same conditions and the need for a cell-dependent methodology in order to direct differentiation.

Nonetheless, the three cell types investigated in this thesis showed poor immunofluorescent labelling for the three markers studied. Because the host tissue presented high endogenous fluorescence, it was difficult to elucidate whether the positive staining was produced by the transplanted cells or by the spinal cord cultures. Analysis of tissue sections by laser scanning confocal microscopy might have provided more evidence about the fluorescence origin. Also, retrieval of transplanted cells from the tissues and further gene analysis expression by polymerase chain reaction would provide unequivocal information about the neuronal behaviour of the grafted cells.

Although the results reported in this thesis represent a promising method for further application in neuronal tissue restoration, there are still several issues to be addressed. First of all, cells must be able to migrate and proliferate at the site of injury to completely bridge the gap and reconnect both sides of the lesion site. Although it has been demonstrated that alginate-collagen microcapsules are useful to retain cells at the site of injury, the number of transplanted cells might represent a limitation in this technique. Due to the three-dimensional structure of alginate-collagen microcapsules, the number of cells that can be implanted in the injury site is lower than that when cells are transplanted by simple cell injection. Since it has been proven that transplanted DPSCs might direct endogenous repair by the release of tropic factors (Huang et al. 2008), the number of cells might influence the degree of therapeutic effect in terms of concentration of released growth factors. Thus, a

greater therapeutic effect would be achieved with a higher release of growth factors that, in turn, would depend on the number of grafted cells.

All in all, neuronal replacement after SCI represents a challenging procedure due to the harsh environment after damage, which is naturally inhibitive of axonal regrowth. But also, the different cell types involved in the correct function of spinal cord makes necessary the implantation of simultaneous therapies to ensure a complete recovery. Cell transplantation has been proven to be ineffective when no control of cell orientation can be achieved. Hence, combination of cellular material with appropriate scaffolds that mimic the ECM in the central nervous system and directs axon regeneration is, so far, the most attractive approach.

Chapter 5. General Discussion

The use of cell encapsulation technology has increased over the past decades due to the great number of fields in which it can be applied (Acarregui *et al.* 2013). Although it was first intended as a method for immunoisolation of cells in transplantation therapies (Freimark *et al.* 2010), the great variety of encapsulation techniques, matrices and cell types that can be combined has contributed to this versatility. Pancreatic islet encapsulation is, by far, the most studied method (Buder *et al.* 2013). The successful immobilization of islet cells encouraged researches to apply this technology in living organisms. Indeed, promising results allowed the establishment of the first clinical trial involving cell encapsulation for the treatment of type I diabetes (Soon-Shiong *et al.* 1994).

Encapsulation of different cell types, specifically stem cells, has permitted the expansion of the applicability of this technique. Stem cells offer a renewable source of cells with the potential to transform into virtually any cell type within the organism. Stem cells have been isolated from both embryonic and adult tissues. It has been demonstrated that ESCs can be expanded and differentiated *in vitro* into any cell type within the three germ layers (ectoderm, mesoderm and endoderm). However, the therapeutic application of human ESCs is still debated due to ethical issues and problems of allogeneic rejection and uncontrolled development of malignancies (Hentze *et al.* 2007). These obstacles have attracted the attention of the researches towards the study of ASCs. Although it was first hypothesized that these cells had a lineage restricted differentiation potential, further studies have demonstrated that, under the appropriate reprogramming mechanisms, ASCs could be manipulated to differentiate towards cell lineages different from their tissue of origin in a process known as transdifferentiation (Filip *et al.* 2004).

ASCs have been typically isolated from bone marrow but this process involves painful and invasive procedures. Hence, different sources of adult stem cells have been investigated, including adipose tissue (Lindroos *et al.* 2011), skin (Nowak & Fuchs 2009) and umbilical cord (Zhang *et al.* 2008) to name a few. In 2000, Gronthos *et al.* isolated, for the first time, a stem cell population from the dental pulp. A similar marker profile to that demonstrated for BMSCs was observed for DPSCs, thereby these cells were classified as MSCs (Kawashima 2012). However, further studies revealed that DPSCs also expressed embryonic stem cell markers, such as Oct4 and Sox2 (Kerkis *et al.* 2007) and even markers associated with more mature phenotypes, including muscle (Patel *et al.* 2009) and neural cells (Karaöz *et al.* 2011). These findings have attracted attention of researches towards the application of DPSCs for the treatment of CNS diseases and injuries.

The main benefit of using DPSCs is their isolation procedure. Cells can be easily isolated from the pulp of teeth extracted in routine orthodontic treatments or from deciduous teeth naturally shed in childhood (Tatullo *et al.* 2015). *In vitro* expansion of these cells could provide a personalized stem cell bank readily available to be used in the cure of diverse conditions. Specifically, the potential of DPSCs to differentiate down to neural lineages has been investigated by our group in Cardiff (Young *et al.* 2016). Since DPSCs represent a highly heterogeneous population of stem cells, their marker expression and differentiation potential varies between clonogenic populations. The work presented by Young *et al.* (2016) provides a potential method for the identification of DPSCs populations with neuronal differentiation potential, based on the levels of nestin expression. Furthermore, several protocols have been developed for DPSCs neuronal differentiation

(Nosrat *et al.* 2004; Hisham *et al.* 2013; Young *et al.* 2016). The success of these protocols along with the ability of these cells to release growth factors and neurotrophins involved in the maintenance and development of the CNS, have contributed to the application of DPSCs to the CNS *in vivo* (Huang *et al.* 2008; Leong *et al.* 2012; Sakai *et al.* 2012).

The cellular and molecular mechanisms involved after SCI create an adverse environment which is extremely challenging with respect to the application of cell replacement therapies. Although significant progress has been achieved over the last years, the application of single therapies does not provide fully recovery after spinal cord damage (Pfeifer *et al.* 2004; Parr *et al.* 2007). Whilst cell transplantation provides trophic support for regenerating axons (Huang *et al.* 2008) the loss of ECM after injury and the lack of a three-dimensional organization of cellular grafts hinders complete recover after damage. Hence, the combination of cellular replacement with appropriate scaffolds that provide support and mimic the ECM conditions, could provide an effective alternative for the regeneration of neuronal tissue after SCI.

In this thesis, a method for the successful encapsulation of DPSCs and NSCs was developed. In order to further apply encapsulated cells in clinical therapies, microcapsules should be highly monodisperse. Microcapsules with narrow size distributions allows for an accurate estimation of the number of cells per bead, permitting the determination of the clinical dose before transplantation (Tan & Takeuchi 2007). Also, in order to bring this technology towards clinical application, large batches of encapsulated cells need to be produced with high reproducibility. Most of the conventional methods for cell encapsulation do not provide reproducible

results, only producing small batches of encapsulated cells with wide polydispersity (Poncelet *et al.* 1992; Mollet & Grubenmann 2001). Comparison of theoretical calculation and experimental estimation of number of cells per bead demonstrated that the microfluidic device developed in this thesis provides a reproducible method to produce polymer microcapsules.

The use of microfluidics for the formation of polymer microcapsules, provides several benefits, including a better control of shape and size of the microcapsules and the use of small volumes of reagents, leading to a reduction in experimentation costs and expenses. Several strategies have been developed for the formation of polymer droplets within microfluidic devices. The simplest consists on the co-flow of two immiscible fluids through concentric capillaries (Cramer *et al.* 2004). Different approaches utilize a T-junction format for the emulsification of the dispersed phase (Sivasamy *et al.* 2011) or droplets has been achieved utilising flow focusing devices (Dreyfus *et al.* 2003; Anna *et al.* 2003). Flow focusing provides the most reproducible method, since the formation of droplets depend on several parameters including flow rates, channels geometry and fluids viscosities (Baroud *et al.* 2010). The manipulation of these parameters allows for a better control of the size of the droplets produced, giving rise to a greater dynamic size range from a given device compared with other strategies.

In order to fabricate a flow focusing microfluidic device, PTFE was selected as the most suitable material. PTFE offers several advantages over other materials used, such as PDMS. Firstly, PTFE's chemical properties means that it is predominantly non-reactive and therefore has stable wetting properties. In contrast, PDMS undergoes

swelling and deformation in the presence of strong organic solvents and uncontrolled adsorption of substances is a major issue (Uchida *et al.* 2003). Secondly, PTFE's high hydrophobicity allows for the formation of alginate droplets with high contact angles, thereby producing highly spherical microcapsules. In the study presented in this thesis, microchannels were easily fabricated on PTFE discs by a milling process requiring short periods of time, generally less than 30 minutes. They were then mounted in a compressed-sealed metallic manifold which allowed the assembly/disassembly of the entire mounting in an effortless and quick manner. Other methods utilized for the fabrication of microfluidic devices generate permanently sealed constructs (hindering their application in cases of blockages) which often involve multiple steps in their assembly and hence are time consuming to use (Shintaku *et al.* 2007).

The flow focusing microfluidic device fabricated in this thesis allowed for the production and on-chip cross-linking of alginate-based microcapsules via internal gelation. The design incorporated a continuous phase formed by a laminar flow of mineral oil (shielding flow) and acetic acid dissolved in mineral oil (protons source phase). The controlled and smooth diffusion of protons through parallel layers within the continuous phase led to the release of calcium ions from CaCO_3 dispersed in the alginate solution. Unlike other methods utilized by other authors (Poncelet *et al.* 1992; Capretto *et al.* 2008), the system applied in this investigation permitted the emulsification and cross-linking of alginate capsules in one single step, minimizing experimentation times. This is of a key importance in cell encapsulation, where cell viability might be compromised due to the cells residing in unfavourable conditions for long periods of time. In conventional external gelation approaches, encapsulated

cells are collected in a CaCl_2 bath where they reside for 15-20 min in order to achieve proper gelation rates (Duvivier-Kali *et al.* 2001; Murua *et al.* 2007; Bhujbal *et al.* 2014). In contrast, the method developed in this thesis permitted gelation times < 1 min, as observed by the collection of solidified droplets from the outlet of the microfluidic chip. External gelation of alginate microcapsules has been attempted within microfluidic devices (Choi *et al.* 2007). In this approach, two separate inlets containing alginate phase and CaCl_2 solution were continuously injected into a flow of water-immiscible hexadecane, where they spontaneously separated and broke up into stream droplets. Once the alginate solution was in contact with the Ca^{2+} ions, it immediately transformed into a gel. A similar approach was utilized by Shintaku *et al.* (2007), where the incorporation of an additional channel containing CaCl_2 solution after alginate emulsification permitted the hydrogel cross-linking. However, the alginate microbeads showed random shapes and were highly polydisperse.

Hence, although the experimentation times of external gelation can be reduced using microfluidic devices, poorly controlled gelation kinetics due to the high solubility of CaCl_2 in aqueous solutions remains an issue. Therefore, an internal gelation approach is the method preferred in order to produce highly monodisperse microcapsules. For example, Liu *et al.* (2013) produced highly monodisperse alginate microcapsules via an internal gelation approach within a glass capillary microfluidic device. However, in order to assess a proper emulsification, the use of surfactants was required. The microfluidic device developed in this thesis allowed for the production of highly monodisperse microcapsules without the need of surfactants, minimizing the number of washing steps.

The encapsulation technology presented in this work permitted the immobilization of two different types of stem cells, DPSCs and NSCs. It is noteworthy that the behaviour of these two cell types *in vitro* is different. Whereas DPSCs adhere on plastic surfaces and grow in monolayers, NSCs proliferate in suspension as neurospheres. However, the same encapsulation procedure and encapsulation matrix could be applied for the successful encapsulation of both cell types, highlighting the versatility of the method developed in this investigation. Two different encapsulation matrices were tested. First of all, alginate was selected as the encapsulation scaffold due to its biocompatibility, mild gelling conditions and good mechanical properties (Lee & Mooney 2012). Cell viability and proliferation were studied and results revealed a different behaviour between DPSCs and NSCs. NSCs proliferated within the capsules and their viability increased up to 3 weeks in culture. However, the proliferation rate was delayed when compared with standard culture conditions. On the contrary, no signs of cell proliferation were observed in DPSCs, whose viability decreased to ~ 70% after the same culture period. Cell viability and proliferation were studied with three different methods, including trypan blue exclusion assay, the MTT assay and Live/Dead staining. The trypan blue exclusion assay provided the only quantitative method between those tested. Live/Dead staining and confocal microscopy allowed for the observation of live and dead cells localization and shape within the microcapsules. The random distribution of dead cells (red) suggested that the diameter of the microcapsules was appropriate for the survival of the encapsulated cells, since no dead cells accumulation at the centre of the capsules were observed, which would be the result of inefficient diffusion of oxygen and nutrients through the entire capsule. However, the MTT assay did not

provide conclusive results about the proliferation behaviour of the cells as it was observed that DPSCs escaped from the microcapsules as early as 3 days after encapsulation. Hence, the absorbance measured was not only that from the encapsulated cells but the overall of encapsulated and plastic bound 'escaped' cells.

Therefore, the encapsulation matrix was modified in order to prevent/delay cell egress. Thus, alginate microcapsules were modified by the addition of type I collagen. Collagen is one of the most widely utilised biomaterials due to its inherent compatibility and its ability to induce cell attachment (Parenteau-Bareil *et al.* 2010). This modification delayed cell migration out of the microcapsules until about 10 days post-encapsulation. However, like alginate microcapsules, cells did not attach on this scaffold, as observed by the formation of NSCs aggregates and rounded DPSCs. Similar behaviour in encapsulated adherent cells has been reported (Markusen *et al.* 2006; Novikova *et al.* 2006; Umemura *et al.* 2011; Kanafi *et al.* 2014) but this behaviour has not been fully explained. It was hypothesized in this thesis that alginate-based microcapsules provided the cells with an artificial niche in which cells reside in a metabolic quiescent state.

Cell adhesion within alginate-collagen scaffolds has been demonstrated by other groups. Sang *et al.* (2011) demonstrated that cells attached and proliferated within alginate-collagen fibrils. They observed that the degree of cell proliferation was directly related with the concentration of collagen in the scaffolds. Hence, in order to promote cell attachment, an increased concentration of collagen in the microcapsules would have been helpful. However, due to its low mechanical stability (Shoulders & Raines 2010), microcapsules with high concentrations of collagen would

result in beads with poor mechanical properties. In order to fabricate alginate-collagen hydrogels that promote cell attachment without the loss of mechanical stiffness, one approach would involve the formation of collagen-core microcapsules with an alginate shell. Perez *et al.* (2014) utilized this technique to immobilize MSCs. Cells were able to attach and proliferate within this scaffold, and underwent osteogenic differentiation under the appropriate stimuli, providing a promising tool in bone tissue regeneration. Also, alginate has been modified with RGD sequences (Alsberg *et al.* 2001) or fibronectin (Mosaheb *et al.* 2003) to promote cell adherence, thereby improving cell viability and proliferation. Viability of DPSCs immobilized within low adherence biomaterials could also be increased by the modification of the culture conditions. DPSCs culture in NSC growth medium transforms these cells into neurospheres-like aggregates that grow in suspension culture (Gervois *et al.* 2015). Thus, under these conditions, cell attachment is not a requisite to maintain high viability.

The lack of cell adhesion on the alginate-collagen microcapsules produced in this thesis permitted the prevention of spontaneous differentiation of cells. However, upon release from microcapsules, NSCs and DPSCs exhibited retained stem cell and neuronal differentiation properties, as demonstrated by high proliferation rates and production of neuronal markers. Cell phenotypes evolved from an undifferentiated state, where NSCs were bipolar and DPSCs were typically bi-/tripolar and fibroblast-like shaped, to a more mature phenotype. NSCs developed neurites sprouting out from cell bodies and long axons. DPSCs developed several processes from cell bodies, forming neuronal-like connexions. Differentiation of stem cells into neuronal cells within hydrogel microcapsules have been achieved by

different groups. Pan *et al.* (2009) showed that hydrogel composition plays a key role in directing cell differentiation. Whereas hyaluronic acid (HA) combined with PLL hydrogels support cell viability, attachment and proliferation, modification of HA with Nogo receptor antibody (NgR-Ab) induced the differentiation of NSCs into neurons and glial cells. In a different study, ESCs were differentiated towards neuronal lineages within alginate-based microcapsules. The addition of fibronectin to the scaffold induced cell attachment and further addition of HA allowed ESCs neuronal differentiation under differentiation culture medium (Bozza *et al.* 2014). The alginate-collagen microcapsules produced in this thesis provided the cells with a favourable environment for cell survival, working as an artificial stem cell “niche” capable of maintaining the cells in a quiescent state. Analysis of gene expression of cells under encapsulation conditions would provide a better understanding of the metabolic state of the encapsulated cells. Nagarajan *et al.* (2014) demonstrated that immobilized yeast cells within alginate beads exhibited a stable pattern of gene expression that differed markedly from growing cells, highly expressing genes in glycolysis, cell wall remodelling, and stress resistance, but decreasing transcription of genes that regulate the cell cycle. Hence, investigation of the gene expression profile of encapsulated cells would provide a defined correlation of cell behaviour depending on the physico-chemical properties of the encapsulating biomaterial.

In the last stage of the investigation carried out in this thesis, the potential of alginate-collagen microcapsules as cell transplantation systems was investigated in an *ex vivo* model of SCI. The microcapsules were implanted into the dissected tissues after partial injury on the dorsal part of the cord. The effectiveness of hydrogel microcapsules as a method to control integration of transplanted cells was

demonstrated. Whereas cells transplanted as a free cell suspension were easily lost within the tissue and did not integrate within the large injury cavity, encapsulated cells stayed at the site of injury over the culture period. Indeed, the difficult control of cell disposition and fate within an organism is a major challenge in cell transplantation therapies (Gaudet & Popovich 2014). Due to the lack of ECM production after SCI, transplanted cells lack a three-dimensional structure with which to interact, which hinders their integration within the host. The combination of hydrogel scaffolds to guide axon regeneration has been successfully applied by several groups (Yoshii *et al.* 2003; Tsai *et al.* 2006; Günther *et al.* 2015; Fan *et al.* 2017).. However, some of these scaffolds are typically macroscopic and their implantation involves surgical procedures. Polymer microcapsules provide a less invasive method for cellular replacement assisted by an artificial ECM. Nonetheless, the diameter of the microcapsules developed in this thesis (~400 μm), was too large to permit cell implantation by simple injection. Hence, in order to further apply this technology in *in vivo* SCI models, the size of the microcapsules should be reduced. This might be easily achieved by reduction of dimensions in the microfluidic device, along with an increase in the continuous and dispersed flow rates ratio. Also, the formation of injectable microfibers rather than microcapsules would allow for a better control of cell guidance parallel to axonal growth.

The alginate-collagen microcapsules developed in this thesis allowed for the retention of the encapsulated cells at the site of injury. The viability of encapsulated NSCs and DPSCs was studied after transplantation. Results demonstrated that the cells remained viable within the tissues, which was most probably assisted by the lack of blood vessels and immune response in the *ex vivo* slices. DPSCs survival after

implantation in the CNS in *in vivo* models has already been demonstrated (Huang *et al.* 2008; Leong *et al.* 2012; Sakai *et al.* 2012). In fact, DPSCs have been demonstrated to possess immunomodulatory properties that could help decrease the risk of cell death in cases of allo- or xenotransplantation (Zhao *et al.* 2012). The neuronal marker expression of the encapsulated cells after transplantation was also studied in this thesis. It was hypothesized that the pre-differentiation of DPSCs into neuronal-like cells prior to encapsulation and further implantation could restrict the differentiation lineage, thereby avoiding the differentiation towards glial cells. However, this was demonstrated to be limited since the expression of GFAP was observed by this group of cells. However, map2 and nestin was also expressed by both undifferentiated and pre-differentiated DPSCs. In contrast, NSCs stained positive for nestin and map2 but no expression of GFAP was observed.

An emerging idea to control cell differentiation is based on the effect on cells of biomaterial behaviour. As cells acquire information from their environment, (e.g. the materials that surround them) the biomaterials in which cells are encapsulated can give messages to stem cells in the form of by-products upon degradation, swelling, compression, etc. (Place *et al.* 2009). Khetan *et al.* (2013) demonstrated that the fate of human MSCs is guided by degradation-mediated cellular-traction. Whereas HA hydrogels that permit cell-mediated degradation favoured osteogenesis, the switch towards a hydrogel with restricted degradation caused adipogenesis. Hence, the physico-chemical properties of hydrogels can be easily adjusted to guide differentiation. Also, the incorporation of growth factors within the scaffolds that are released upon biomaterial degradation is an attractive approach for the control of cell behaviour. In this sense, the co-encapsulation of

growth factors promoting neuronal differentiation along with stem cells might provide an area of investigation to further develop the work presented in this thesis. Because SCI results in the damage of different cell types, one single therapy would not provide completely functional recovery. Hence, implantation of different stem cell types encapsulated along with appropriate “sets” of growth factors that promote differentiation down to different neuronal cell types, would provide a complete recovery after SCI. It has been demonstrated that DPSCs release growth factors and neurotrophins that promotes endogenous axonal regeneration (Sakai *et al.* 2012). However, regenerating axons require remyelination to allow the transmission of electrical signals along the spinal cord. Co-encapsulation of oligodendrocyte precursors along with specific growth factors that promotes their maturation would provide remyelination of the regenerating axons (Watkins *et al.* 2008). Also, the replacement of non-activated astrocytes at the injury site would allow for the reestablishment of the homeostasis, providing trophic support to the repaired cells. Altogether, these wound healing mechanisms would allow for a complete functional recovery.

In summary, the investigations presented in this project demonstrate the development of a microfluidic technique for the successful encapsulation of two different cell types (examples of adherent and non-adherent cells). The method developed is compatible with cell survival and the maintenance of stem cell properties upon encapsulation and subsequent release from the ECM-based microcapsules. Although neuronal differentiation of DPSCs have been extensively reported in 2D culture (Nosrat *et al.* 2004; Hisham *et al.* 2013; Young *et al.* 2016), to our knowledge, any protocol for the neuronal differentiation of DPSCs within

hydrogel microcapsules have been yet described. Hence, DPSC's ability for neuronal differentiation linked to the successful development of a cell encapsulation technique represent an opportunity for further studies beyond the findings of this thesis.

REFERENCES

- Abeyasinghe, H.C.S., Bokhari, L., Quigley, A., Choolani, M., Chan, J., Dusting, G.J., Crook, J.M., Kobayashi, N.R. and Roulston, C.L. 2015. "Pre-Differentiation of Human Neural Stem Cells into GABAergic Neurons prior to Transplant Results in Greater Repopulation of the Damaged Brain and Accelerates Functional Recovery after Transient Ischemic Stroke." *Stem Cell Research and Therapy*, 6 (1), 186.
- Acarregui, A., Orive, G., Pedraz, J.L. and Hernández R.M. 2013. Immobilization of Enzymes and Cells: Third Edition, Methods in Molecular Biology. Vol. 1051. Springer Science+Business Media New York.
- Acarregui, A., Herrán, E., Igartua, M., Blanco, F.J., Pedraz, J.L., Orive, G. and Hernandez, R.M. 2014. "Multifunctional Hydrogel-Based Scaffold for Improving the Functionality of Encapsulated Therapeutic Cells and Reducing Inflammatory Response." *Acta Biomaterialia* 10 (10): 4206–16.
- Adachi, K., Suemori, H., Yasuda, S.Y., Nakatsuji, N. and Kawase, E.. 2010. "Role of SOX2 in Maintaining Pluripotency of Human Embryonic Stem Cells." *Genes to Cells*, 15 (5): 455–70.
- Addad, S., Exposito, J.Y., Faye, C., Ricard-Blum S., Lethias C. 2011. "Isolation, Characterization and Biological Evaluation of Jellyfish Collagen for Use in Biomedical Applications." *Marine Drugs*, 9, 967–83.
- Aijaz, A., Faulknorn R., Berthiaumem F. and Olabisi, R.M. 2015. "Hydrogel Microencapsulated Insulin-Secreting Cells Increase Keratinocyte Migration, Epidermal Thickness, Collagen Fiber Density, and Wound Closure in a Diabetic Mouse Model of Wound Healing." *Tissue Eng Part A*, 21 (21, 22): 2723–32.
- Al-Shamkhani, A. and Duncan, R. 1995. "Radioiodination of Alginate via Covalently-Bound Tyrosinamide Allows Monitoring of Its Fate In Vivo." *Journal of Bioactive and Compatible Polymers* 10 (1): 4–13.
- Al-Munajjed, A.A., Gleeson, J.P. and O'Brien, F.J. 2008. "Development of a Collagen Calcium-Phosphate Scaffold as a Novel Bone Graft Substitute." *Studies in Health Technology and Informatics*, 133: 11-20.
- Aloisi, F. 2001. "Immune Function of Microglia." *GLIA* 36 (2): 165-79.
- Alsberg, E., Anderson, K.W., Albeiruti, A., Franceschi, R.T., Mooney, D.J. 2001. "Cell-Interactive Alginate Hydrogels for Bone Tissue Engineering." *Journal of Dental Research*, 80 (11): 2025–29.
- Andersen, T., Melvik, J.E., Gåserød, O., Alsberg, E., Christensen, B.E. 2012. "Ionically Gelled Alginate Foams: Physical Properties Controlled by Operational and Macromolecular Parameters." *Biomacromolecules* 13 (11): 3703–10.
- Andersen, T., Auk-Emblem, P. and Dornish, M. 2015. "3D Cell Culture in Alginate Hydrogels." *Microarrays*, 4 (2): 133–61.
- Anderson, D.J., Gage, F.H. and Weissman, I.L. 2001. "Can Stem Cells Cross Lineage Boundaries?" *Nature Medicine*, 7 (4): 393–95.
- Anderson, M.A., Burda, J.E., Ren, Y., Ao, Y., O'Shea, T.M., Kawaguchi, R., Coppola, G., Khakh, B.S., Deming, T.J., Sofroniew, M.V. 2016. "Astrocyte Scar Formation Aids

- Central Nervous System Axon Regeneration." *Nature*, 532, 195–200.
- Anna, S.L., Bontoux, N. and Stone, H.A. 2003. "Formation of Dispersions Using 'flow Focusing' in Microchannels." *Applied Physics Letters*, 82, 364.
- Anna, S.L., and Mayer, H.C. 2006. "Microscale Tipstreaming in a Microfluidic Flow Focusing Device." *Physics of Fluids* 18 (12).
- Arthur, A., Rychkov, G., Shi, S., Koblar, S.A., Gronthos, S. 2008. "Adult Human Dental Pulp Stem Cells Differentiate toward Functionally Active Neurons under Appropriate Environmental Cues." *Stem Cells*, 26 (7): 1787–95.
- Asghari, F., Samiei, M., Adibkia, K., Akbarzadeh, A., Davaran, S. 2017. "Biodegradable and biocompatible polymers for tissue engineering application: a review." *Artificial Cells, Nanomedicine and Biotechnology*, 45 (2): 185-192.
- Azari, H., Sharififar, S., Rahman, M., Ansari, S. and Reynolds, B.A. 2011. "Establishing Embryonic Mouse Neural Stem Cell Culture Using the Neurosphere Assay." *Journal of Visualized Experiments*, 47.
- Babavalian, H., Latifi, A.M., Shokrgozar, M.A., Bonakdar, S., Mohammadi, S., Moghaddam, M.M. 2015. "Analysis of Healing Effect of Alginate Sulfate Hydrogel Dressing Containing Antimicrobial Peptide on Wound Infection Caused by Methicillin-Resistant Staphylococcus Aureus." *Jundishapur Journal of Microbiology*, 8 (9): 0–6.
- Bachoud-Lévi, A.C., Déglon, N., Nguyen, J.P., Bloch, J., Bourdet, C., Winkel, L., Rémy, P., Goddard, M., Lefaucheur, J.P., Brugières, P., Baudic, S., Cesaro, P., Peschanski, M., Aebischer, P. 2000. "Neuroprotective Gene Therapy for Huntington's Disease Using a Polymer Encapsulated BHK Cell Line Engineered to Secrete Human CNTF." *Human Gene Therapy* 11 (12): 1723–29.
- Bai, X.P., Zheng, H.X., Fang, R., Wang, T.R., Hou, X.L., Li, Y., Chen, X.B., Tian, W.M. 2011. "Fabrication of Engineered Heart Tissue Grafts from Alginate/collagen Barium Composite Microbeads." *Biomedical Materials (Bristol, England)* 6 (4): 45002.
- Banerjee, A., Arha, M., Choudhary, S., Ashton, R.S., Bhatia, S.R., Schaffer, D.V., Kane, R.S. 2009. "The Influence of Hydrogel Modulus on the Proliferation and Differentiation of Encapsulated Neural Stem Cells." *Biomaterials*, 30 (27): 4695–4699.
- Baracat, M.M., Nakagawa, A.M., Casagrande, R., Georgetti, S.R., Verri, W.A. Jr, de Freitas, O. 2012. "Preparation and Characterization of Microcapsules Based on Biodegradable Polymers: Pectin/Casein Complex for Controlled Drug Release Systems." *AAPS PharmSciTech* 13 (2): 364–372.
- Baroud, C. N., Gallaire, F. and Dangla, R. 2010. "Dynamics of Microfluidic Droplets." *Lab on a Chip* 10 (16): 2032.
- Barthes, J., Özçelik, H., Hindié, M., Ndreu-Halili, A., Hasan, A. and Vrana, N.E. 2014. "Cell Microenvironment Engineering and Monitoring for Tissue Engineering and Regenerative Medicine : The Recent Advances." *BioMed Research International*, 2014.

- Beebe, D.J., Mensing, G.A. and Walker, G.M. 2002. "Physics and Applications of Microfluidics in Biology." *Annual Review of Biomedical Engineering* 4(1): 261–86.
- Bhatia, S.N. and Ingber, D.E. 2014. "Microfluidic Organs-on-Chips." *Nature Biotechnology*, 32: 760–772.
- Bhujbal, S.V., Paredes-Juarez, G.A., Niclou, S.P., de Vos P. 2014. "Factors Influencing the Mechanical Stability of Alginate Beads Applicable for Immunoisolation of Mammalian Cells." *Journal of the Mechanical Behavior of Biomedical Materials*, 37: 196–208.
- Bisceglie, V. 1933. "Über Die Antineoplastische Immunität; Heterologe Einpflanzung von Tumoren in Hühner-Embryonen." *Zeitschrift Für Krebsforschung*, 40: 122–140.
- Bloomfield, S.E., Miyata, T., Dunn, M.W., Bueser, N., Stenzel, K.H., Rubin, A.L. 1978. "Soluble Gentamicin Ophthalmic Inserts as a Drug Delivery System." *Archives of Ophthalmology*, 96(5):885-7.
- Boontheekul, T., Kong, H.J., Mooney, D.J. 2005. "Controlling Alginate Gel Degradation Utilizing Partial Oxidation and Bimodal Molecular Weight Distribution." *Biomaterials*, 26 (15): 2455–65.
- Boyer, L.A., Lee, T.I., Cole, M.F., Johnstone, S.E., Levine, S.S., Zucker, J.P., Guenther, M.G., Kumar, R.M., Murray, H.L., Jenner, R.G., Gifford, D.K., Melton, D.A., Jaenisch, R., Young, R.A. 2005. "Core Transcriptional Regulatory Circuitry in Human Embryonic Stem Cells." *Cell* 122 (6): 947–56.
- Bozza, A., Coates, E.E., Incitti, T., Ferlin, K.M., Messina, A., Menna, E., Bozzi, Y., Fisher, J.P., Casarosa, S. 2014. "Neural Differentiation of Pluripotent Cells in 3D Alginate-Based Cultures." *Biomaterials*, 35(6):4636-45.
- Bradl, M., and Lassmann H.. 2010. "Oligodendrocytes: Biology and Pathology." *Acta Neuropathologica*, 119 (1): 37–53.
- Branco da Cunha C., Klumpers, D.D., Li, W.A., Koshy, S.T., Weaver, J.C., Chaudhuri, O., Granja, P.L., Mooney, D.J. 2014. "Influence of the Stiffness of Three-Dimensional Alginate/collagen-I Interpenetrating Networks on Fibroblast Biology." *Biomaterials*, 35 (32): 8927–36.
- Brody, J.P., Yager, P. Goldstein, R.E. and Austin. R.H. 1996. "Biotechnology at Low Reynolds Numbers." *Biophysical Journal*, 71(6): 3430–3441.
- Bruchet, M., and Melman, A. 2015. "Fabrication of Patterned Calcium Cross-Linked Alginate Hydrogel Films and Coatings through Reductive Cation Exchange." *Carbohydrate Polymers*, 131:57-64.
- Buchet, D., and Baron-Van Evercooren, A. 2009. "In Search of Human Oligodendroglia for Myelin Repair." *Neuroscience Letters*, 456(3):112-9.
- Buder, B., Alexander, M., Krishnan, R., Chapman, D.W. and Lakey, J.R.T. 2013. "Encapsulated Islet Transplantation: Strategies and Clinical Trials." *Immune Network* 13 (6): 235–239.
- Bugarski, B., Li, Q., Goosen, M.F.A., Poncelet, D., Neufeld, R.J., and G. Vunjak. 1994.

- “Electrostatic Droplet Generation: Mechanism of Polymer Droplet Formation.” *AIChE Journal* 40 (6): 1026–31.
- Burdick, J.A., Mauck, R.L., and Gerecht, S. 2016. “To Serve and Protect: Hydrogels to Improve Stem Cell-Based Therapies.” *Cell Stem Cell* 18 (1): 13–15.
- Caceres, A., Banker, G.A., and Binder, L. 1986. “Immunocytochemical Localization of Tubulin and Microtubule-Associated Protein 2 during the Development of Hippocampal Neurons in Culture.” *Journal of Neuroscience* 6 (3): 714–22.
- Calafiore, R., Basta, G., Luca, G., Lemmi, A., Montanucci, M.P., Calabrese, G., Racanicchi, L., Mancuso, F., and P. Brunetti. 2006. “Microencapsulated Pancreatic Islet Allografts Into Nonimmunosuppressed Patients With Type 1 Diabetes: First Two Cases.” *Diabetes Care* 29 (1): 137–38.
- Cao, Q.L., Zhang, Y.P., Howard, R.M., Walters, W.M., Tsoulfas, P., Whittemore, S.R. 2001. “Pluripotent Stem Cells Engrafted into the Normal or Lesioned Adult Rat Spinal Cord Are Restricted to a Glial Lineage.” *Experimental Neurology* 167(1):48-58.
- Capretto, L., Mazzitelli, S., Balestra, C., Tosi, A., and Nastruzzi, C. 2008. “Effect of the Gelation Process on the Production of Alginate Microbeads by Microfluidic Chip Technology.” *Lab on a Chip* 8 (4): 617–21.
- Cen, L., Liu, W., Cui, L., Zhang, W., Cao, Y. 2008. “Collagen Tissue Engineering: Development of Novel Biomaterials and Applications.” *Pediatric Research* 63 (5): 492–96.
- Chambers, I., Colby, D., Robertson, M., Nichols, J., Lee, S., Tweedie, S., Smith, A. 2003. “Functional Expression Cloning of Nanog, a Pluripotency Sustaining Factor in Embryonic Stem Cells.” *Cell* 113(5):643-55.
- Chan, L.W., Lee, H.Y., Heng, P.W.S. 2002. “Production of Alginate Microspheres by Internal Gelation Using an Emulsification Method.” *International Journal of Pharmaceutics* 242 (1–2): 259–62.
- Chan, W.P., Kung, F.C., Kuo, Y.L., Yang, M.C., Lai, W.F. 2015. “Alginate/poly(γ -Glutamic Acid) Base Biocompatible Gel for Bone Tissue Engineering.” *BioMed Research International* 2015.
- Chan, B.P., Hui, T.Y., Wong, M.Y., Yip, K.H., and Chan, G.C. 2010. “Mesenchymal Stem Cell-Encapsulated Collagen Microspheres for Bone Tissue Engineering.” *Tissue Engineering Part C: Methods* 16 (2): 225–35.
- Chao, H., Zhang, Q., Ma, R., Xie, L., Qiu, T., Wang, L., Mitchelson, K., Wang, J., Huang, G., Qiao, J., Cheng, J. 2010. “Integration of Single Oocyte Trapping, in Vitro Fertilization and Embryo Culture in a Microwell-Structured Microfluidic Device.” *Lab on a Chip* 10 (21): 2848–54.
- Chen, Y.W., Kuo, C.W., Chueh, D.Y., and Chen, P. 2015. “Surface Modified Alginate Microcapsules for 3D Cell Culture.” *Surface Science* 648: 47–52.
- Chen, Y., Tang, Y., Vogel, L., and DeVivo, M. 2013. “Causes of Spinal Cord Injury.” *Topics in Spinal Cord Injury Rehabilitation* 19 (1): 1–8.
- Cheung, D.T., Perelman, N., Ko, E.C., and Nimni, M.E. 1985. “Mechanism of

- Crosslinking of Proteins by Glutaraldehyde III. Reaction with Collagen in Tissues." *Connective Tissue Repair* 13 (2): 109–15.
- Cho, J.K., Jin, Y.G., Rha, S.J., Kim, S.J., Hwang, J.H. 2014. "Biochemical Characteristics of Four Marine Fish Skins in Korea." *Food Chemistry* 159: 200–207.
- Choi, C.H., Jung, J.H., Rhee, Y.W., Kim, D.P., Shim, S.E., Lee, C.S. 2007. "Generation of Monodisperse Alginate Microbeads and in Situ Encapsulation of Cell in Microfluidic Device." *Biomedical Microdevices* 9 (6): 855–62.
- Choi S, Shin JH, Cheong Y, Jin KH, Park HK. 2013. "Structural and Biomechanical Effects of Photooxidative Collagen Cross-Linking with Photosensitizer Riboflavin and 370 Nm UVA Light on Human Corneoscleral Tissues." *Microscopy and Microanalysis* 19 (5): 1334–40.
- Comalada, M., Yeramian, A., Modolell, M., Lloberas, J., and Celada, A. 2012. *Arginine and Macrophage Activation. Methods in Molecular Biology*. Vol. 844. Springer Science+Business Media, LLC.
- Corti, S., Nizzardo, M., Nardini, M., Donadoni, C., Salani, S., Ronchi, D., Simone, C., Falcone, M., Papadimitriou, D., Locatelli, F., Mezzina, N., Gianni, F., Bresolin, N., Comi, G.P. 2010. "Embryonic Stem Cell-Derived Neural Stem Cells Improve Spinal Muscular Atrophy Phenotype in Mice." *Brain* 133 (2): 465-81.
- Coutinho, D.F., Sant, S.V., Shin, H., Oliveira, J.T., Gomes, M.E., Neves, N.M., Khademhosseini, A., and R.L. Reis. 2010. "Modified Gellan Gum Hydrogels with Tunable Physical and Mechanical Properties." *Biomaterials* 31(29):7494-502.
- Coyne, T.M., Marcus, A.J., Woodbury, D., and Black, I.B. 2006. "Marrow Stromal Cells Transplanted to the Adult Brain Are Rejected by an Inflammatory Response and Transfer Donor Labels to Host Neurons and Glia." *Stem Cells* 24 (11): 2483–92.
- Cramer, C., Fischer, P., and Windhab, E.J. 2004. "Drop Formation in a Co-Flowing Ambient Fluid." *Chemical Engineering Science* 59 (15): 3045–3058.
- Cregg, J.M., DePaul, M.A., Filous, A.R., Lang, B.T., Tran, A. and Silver, J. 2014. "Functional Regeneration beyond the Glial Scar." *Experimental Neurology* 253: 197–207.
- Cruise, G.M., Hegre, O.D., Lamberti, F.V., Hager, S.R., Hill, R., Scharp, D.S., Hubbell, J.A. 1999. "In Vitro and in Vivo Performance of Porcine Islets Encapsulated in Interfacially Photopolymerized Poly(ethylene Glycol) Diacrylate Membranes." *Cell Transplantation* 8 (3): 293–306.
- Cuchiara, M.P., Allen, A.C.B., Chen, T.M., Miller, J.S., and West, J.L. 2010. "Multilayer Microfluidic PEGDA Hydrogels." *Biomaterials* 31 (21): 5491–97.
- Dahlstrand, J., Lardelli, M., and Lendahl, U. 1995. "Nestin mRNA Expression Correlates with the Central Nervous System Progenitor Cell State in Many, but Not All, Regions of Developing Central Nervous System." *Developmental Brain Research* 84 (1): 109–29.
- Danysh, B.P., Patel, T.P., Czymmek, K.J., Edwards, D.A., Wang, L., Pande, J., and Duncan, M.K. 2010. "Characterizing Molecular Diffusion in the Lens Capsule." *Matrix Biology* 29 (3): 228-36.

- Darr, H., Mayshar, Y., and Benvenisty, N. 2006. "Overexpression of NANOG in Human ES Cells Enables Feeder-Free Growth While Inducing Primitive Ectoderm Features." *Development* 133 (6): 1193-201.
- Davidenko, N., Bax, D.V., Schuster, C.F., Farndale, R.W., Hamaia, S.W., Best, S.M., Cameron, R.E. 2016. "Optimisation of UV Irradiation as a Binding Site Conserving Method for Crosslinking Collagen-Based Scaffolds." *Journal of Materials Science: Materials in Medicine* 27 (1): 1–17.
- De Almeida, F.M., Marques, S.A., Ramalho, B.D.S., Rodrigues, R.F., Cadilhe, D.V., Furtado, D., Kerkis, I., Pereira, L.V., Rehen, S.K. and Martinezm A.M.B. 2011. "Human Dental Pulp Cells: A New Source of Cell Therapy in a Mouse Model of Compressive Spinal Cord Injury." *Journal of Neurotrauma* 28 (9): 1939-49.
- De Matteis, R., Zingaretti, M.C., Murano, I., Vitali, A., Frontini, A., Giannulis, I., Barbatelli, G., Marcucci, F., Bordicchia, M., Sarzani, R., Raviola, E., Cinti, S. 2009. "In Vivo Physiological Transdifferentiation of Adult Adipose Cells." *Stem Cells* 27 (11): :2761-8.
- De menech, M., Garstecki, P., Jousse, F., and Stone, H.A. 2008. "Transition from Squeezing to Dripping in a Microfluidic T-Shaped Junction." *Journal of Fluid Mechanics* 595: 141-161.
- De Vos, P., Andersson, A., Tam, S.K., Faas, M.M., and Hallé, J.P. 2006. "Advances and Barriers in Mammalian Cell Encapsulation for Treatment of Diabetes." *Immunology, Endocrine and Metabolic Agents in Medicinal Chemistry* 6: 139-153.
- DeMello, A.J. 2006. "Control and Detection of Chemical Reactions in Microfluidic Systems." *Nature* 442: 394-402.
- Di, S., Liu, X., Liu, D., Gong, T., Lu, L., and Zhou, S. 2016. "A Multifunctional Porous Scaffold with Capacities of Minimally Invasive Implantation, Self-Fitting and Drug Delivery." *Materials Today Chemistry* 1–2. 52–62.
- Discher, D.E., Mooney, D.J.m and Zandstra, P.W. 2009. "Growth Factors, Matrices, and Forces Combine and Control Stem Cells." *Science* 324 (5935): 1673–77.
- Donnelly, D.J., and Popovich, P.G. 2008. "Inflammation and Its Role in Neuroprotection, Axonal Regeneration and Functional Recovery after Spinal Cord Injury." *Experimental Neurology* 209 (2): 378–88.
- Draget, K. I., Skjåk-Bræk. G., and Smidsrød, O. 1997. "Alginate Based New Materials." *International Journal of Biological Macromolecules* 21 (1–2): 47–55.
- Dreyfus, R., Tabeling, P., and Willaime, H. 2003. "Ordered and Disordered Patterns in Two-Phase Flows in Microchannels." *Physical Review Letters* 90 (14).
- Drury, J.L., and Mooney, D.J. 2003. "Hydrogels for Tissue Engineering: Scaffold Design Variables and Applications." *Biomaterials* 24 (24): 4337–51.
- Dulieu, C., Poncelet, D., and Neufeld, R.J. 1999. "Encapsulation and Immobilization Techniques." In *Cell Encapsulation Technology and Therapeutics*, Boston, MA: Birkh{ä}user Boston.
- Dusseault, J., Tam, S.K., Ménard, M., Polizu, S., Jourdan, G., Yahia, L., and Hallé, J.P.

2006. "Evaluation of Alginate Purification Methods: Effect on Polyphenol, Endotoxin, and Protein Contamination." *J Biomed Mater Res A* 76A (2): 243–251.
- Duvivier-Kali, V.F., Omer, A., Parentm R.J., O'Neil, J.J., Weir, G.C. 2001. "Complete Protection of Islets Against Allojection and Autoimmunity by a Simple Barium-Alginate Membrane." *Diabetes* 50 (8): 1698-705.
- Eaves, C.J. 2015. "Hematopoietic Stem Cells: Concepts, Definitions, and the New Reality." *Blood* 125 (17): 2605–14.
- Eggers, J. 1993. "Universal Pinching of 3D Axisymmetric Free-Surface Flow." *Physical Review Letters* 71 (21): 3458-3460.
- Ellis, K.M., O'Carroll, D.C., Lewis, M.D., Rychkov, G.Y., Koblar, S.A. 2014. "Neurogenic Potential of Dental Pulp Stem Cells Isolated from Murine Incisors." *Stem Cell Research & Therapy* 5 (1). *Stem Cell Research & Therapy* 5(1):30.
- Emerich, D.F., and Thanos, C.G. 2006. "Intracompartmental Delivery of CNTF as Therapy for Huntingtons Disease and Retinitis Pigmentosa." *Current Gene Therapy* 6(1):147-59.
- Emerich, D.F., and Winn, S.R. 2001. "Immunoisolation Cell Therapy for CNS Diseases." *Critical Reviews in Therapeutic Drug Carrier Systems* 18 (3).
- Emerich, D.F., Aebischer, P., and Kordower, J.H. 1998. "Encapsulated PC12 Cell Transplants for Treatment of Parkinson's Disease." US, US5853385 A, 1994.
- Evans, M.J., and Kaufman, M.H. 1981. "Establishment in Culture of Pluripotential Cells from Mouse Embryos." *Nature* 292 (5819): 154–56.
- Fan, C., Li, X., Xiao, Z., Zhao, Y., Liang, H., Wang, B., Han, S. Lia, X., Xua, B., Wang, N., Liub, S., Xue, W., and Dai, J.. 2017. "A Modified Collagen Scaffold Facilitates Endogenous Neurogenesis for Acute Spinal Cord Injury Repair." *Acta Biomaterialia*
- Fields, G.B. 2013. "Interstitial Collagen Catabolism." *Journal of Biological Chemistry* 288 (13): 8785–93.
- Filip, S., English, D., and Mokry, J. 2004. "Issues in Stem Cell Plasticity." *Journal of Cellular and Molecular Medicine* 8 (4): 572–77.
- Fleming, J.C., Norenberg, M.D., Ramsay, D.A., Dekaban, G.A., Marcillo, A.E., Saenz, A.D., Pasquale-Styles, M., Dietrich, W.D., and Weaver L.C. 2006. "The Cellular Inflammatory Response in Human Spinal Cords after Injury." *Brain* 129 (12): 3249-69.
- Fortin, J.M., Azari, H., Zheng, T., Darioosh, R.P., Schmoll, M.E., Vedam-Mai, V., Deleyrolle, L.P., and Reynolds, B.A. 2016. "Transplantation of Defined Populations of Differentiated Human Neural Stem Cell Progeny." *Scientific Reports* 6.
- Fragonas, E., Valente, M., Pozzi-Mucelli, M., Toffanin, R., Rizzo, R., Silvestri, F., Vittur, F. 2000. "Articular Cartilage Repair in Rabbits by Using Suspensions of Allogenic Chondrocytes in Alginate." *Biomaterials* 21 (8): 795–801.
- Frederiksen, K., and McKay, R.D. 1988. "Proliferation and Differentiation of Rat

- Neuroepithelial Precursor Cells in Vivo." *Journal of Neurosciences* 8: 1144–51.
- Freimark, D., Pino-Grace, P.P., Pohl, S., Weber, C., Wallrapp, C., Geigle, P., Pörtner, R., and Czermak, P. 2010. "Use of Encapsulated Stem Cells to Overcome the Bottleneck of Cell Availability for Cell Therapy Approaches." *Transfusion Medicine and Hemotherapy* 37 (2): 66–73.
- Fricker, R.A., Carpenter, M.K., Winkler, C., Greco, C., Gates, M.A., and Björklund, A. 1999. "Site-Specific Migration and Neuronal Differentiation of Human Neural Progenitor Cells after Transplantation in the Adult Rat Brain." *Journal of Neuroscience* 19 (14): 5990-6005.
- Friend, J., and Yeo, L. 2010. "Fabrication of Microfluidic Devices Using Polydimethylsiloxane." *Biomicrofluidics* 4 (2).
- Gao, Q., Guo, M., Jiang, X., Hu, X., Wang, Y., and Fan, Y. 2014. "A Cocktail Method for Promoting Cardiomyocyte Differentiation from Bone Marrow-Derived Mesenchymal Stem Cells." *Stem Cells International* 2014.
- Garstecki, P., Fuerstman, M.J., Stone, H.A., and Whitesides, G.M. 2006. "Formation of Droplets and Bubbles in a Microfluidic T-Junction - Scaling and Mechanism of Break-Up." *Lab on a Chip - Miniaturisation for Chemistry and Biology* 6: 437-446.
- Gattazzo, F., Urciuolo, A. and Bonaldo, P. 2014. "Extracellular Matrix: A Dynamic Microenvironment for Stem Cell Niche." *Biochimica et Biophysica Acta - General Subjects* 1840 (8). Elsevier B.V.: 2506–19.
- Gaudet, Andrew D., and Phillip G. Popovich. 2014. "Extracellular Matrix Regulation of Inflammation in the Healthy and Injured Spinal Cord." *Experimental Neurology* 258: 24–34.
- Ge, H., Yu, A., Chen, J., Yuan, J., Yin, Y., Duanmu, W., Tan, L., Yang Y., Lan, C., Chen, W., Feng, H., and Hub, R. 2016. "Poly-L-Ornithine Enhances Migration of Neural Stem/progenitor Cells via Promoting α -Actinin 4 Binding to Actin Filaments." *Scientific Reports* 6.
- Gehrmann, J., Matsumoto, Y., Kreutzberg, G.W. 1995. "Microglia: Intrinsic Immune Effector Cell of the Brain." *Brain Research Reviews* 20 (3): 269–87.
- Geller, H.M., and Fawcett, J.W. 2002. "Building a Bridge: Engineering Spinal Cord Repair." *Experimental Neurology* 174(2):125-36.
- Gervois, P., Struys, T., Hilkens, P., Bronckaers, A., Ratajczak, J., Politis, C., Brône, B., Lambrichts, I., Martens, W. 2015. "Neurogenic Maturation of Human Dental Pulp Stem Cells Following Neurosphere Generation Induces Morphological and Electrophysiological Characteristics of Functional Neurons." *Stem Cells and Development* 24 (3): 296–311.
- Ghasemi-Mobarakeh, L., Prabhakaran, M.P., Tian, L., Shamirzaei-Jeshvaghani, E., Deghani, L. and Ramakrishna, S. 2015. "Structural Properties of Scaffolds: Crucial Parameters towards Stem Cells Differentiation." *World Journal of Stem Cells* 7 (4): 728 –744.
- Glowacki, J., and Mizuno, S. 2008. "Collagen Scaffolds for Tissue Engineering." *Biopolymers* 89 (5): 338–44.

- Gough, J.E., Scotchford, C.A. and Downes, S. 2002. "Cytotoxicity of Glutaraldehyde Crosslinked Collagen/poly(vinyl Alcohol) Films Is by the Mechanism of Apoptosis." *Journal of Biomedical Materials Research* 61 (1): 121–30.
- Grant, G.T., Morris, E.R., Rees, D.A., Smith, P.J.C., and Thom, D. 1973. "Biological Interactions between Polysaccharides and Divalent Cations: The Egg-Box Model." *FEBS Letters* 32 (1): 195–98.
- Graziano, A., d'Aquino, R., Laino, G., Proto, A., Giuliano, M.T., Pirozzi, G., De Rosa, A., Di Napoli, D., Papaccio, G. 2008. "Human CD34⁺ Stem Cells Produce Bone Nodules in Vivo." *Cell Proliferation* 41(1):1-11.
- Griffin, M.F., Butler, P.E., Seifalian, A.M., and Kalaskar, D.M. 2015. "Control of Stem Cell Fate by Engineering Their Micro and Nanoenvironment." *World Journal of Stem Cells* 7 (1): 37–50.
- Gronthos, S., Brahim, J. Li, W., Fisher, L.W., Cherman, N., Boyde, A., Denbesten, P., Robey, P.G., and Shi, S. 2002. "Stem Cell Properties of Human Dental Pulp Stem Cells." *Journal of Dental Research* 81 (8): 531–35.
- Gronthos, S., Mankani, M., Brahim, J., Robey, P.G. and Shi, S. 2000. "Postnatal Human Dental Pulp Stem Cells (DPSCs) in Vitro and in Vivo." *Proceedings of the National Academy of Sciences of the United States of America* 97 (25): 13625–30.
- Guarino, V., Caputo, T., Altobelli, R., and Ambrosio, L. 2015. "Degradation Properties and Metabolic Activity of Alginate and Chitosan Polyelectrolytes for Drug Delivery and Tissue Engineering Applications." *AIMS Materials Science* 2 (4): 497–502.
- Guber, A.E., Hecke, M., Herrmann, D., Muslija, A., Saile, V., Eichhorn, L., Gietzelt, T., Hoffmann, W., Hauser, P.C., Tanyanyiwad, J., Gerlache, A., Gottschliche, N., Knebele, G. 2004. "Microfluidic Lab-on-a-Chip Systems Based on Polymers - Fabrication and Application." *Chemical Engineering Journal* 101 (1–3): 447–53.
- Guillot, P., and Colin, A. 2005. "Stability of Parallel Flows in a Microchannel after a T Junction." *Physical Review E - Statistical, Nonlinear, and Soft Matter Physics* 72 (6).
- Günther, M.I., Weidner, N., Müller, R., and Blesch, A. 2015. "Cell-Seeded Alginate Hydrogel Scaffolds Promote Directed Linear Axonal Regeneration in the Injured Rat Spinal Cord." *Acta Biomaterialia* 27: 140–50.
- Guo, C., Kong, W. 2002. "Application of Rat Tail Collagen in Patch Clamp Experiment with Vestibular Hair Cells." *Zhonghua Er Bi Yan Hou Ke Za Zhi* 37 (4): 307–9.
- Guo, W., Patzlaff, N.E., Jobe, E.M., and Zhao, X. 2012. "Isolation of Multipotent Neural Stem or Progenitor Cells from Both the Dentate Gyrus and Subventricular Zone of a Single Adult Mouse." *Nature Protocols* 7 (11): 2005–2012.
- Hains, B.C., Klein, J.P., Saab, C.Y., Craner, M.J., Black, J.A. and Waxman, S.G. 2003. "Upregulation of Sodium Channel Nav1.3 and Functional Involvement in Neuronal Hyperexcitability Associated with Central Neuropathic Pain after Spinal Cord Injury." *Journal of Neuroscience* 23 (26): 8881-92.
- Halloran, P.F. 2004. "Immunosuppressive Drugs for Kidney Transplantation." *The*

- New England Journal of Medicine* 351: 2715–29.
- Hao, S., Su, L., Guo, X., Moyana, T., and Xiang, J. 2005. "A Novel Approach to Tumor Suppression Using Microencapsulated Engineered J558/TNF- α Cells." *Experimental Oncology* 27 (1): 56-60.
- Harrington, .D.J. 1996. "Bacterial Collagenases and Collagen-Degrading Enzymes and Their Potential Role in Human Disease." *Infection and Immunity* 64 (6): 1885–91.
- Haugh, M.G., Jaasma, M.J., O'Brien, F.J. 2009. "The Effect of Dehydrothermal Treatment on the Mechanical and Structural Properties of Collagen-GAG Scaffolds." *Journal of Biomedical Materials Research - Part A* 89 (2): 363–69.
- Hendrickson, M.L., Rao, A.J., Demerdash, O.N.A., and Kalil, R.E. 2011. "Expression of Nestin by Neural Cells in the Adult Rat and Human Brain." *PLoS ONE* 6 (4): e18535.
- Hentze, H., Graichen, R., and Colman. A., 2007. "Cell Therapy and the Safety of Embryonic Stem Cell-Derived Grafts." *Trends in Biotechnology* 25 (1): 24–32.
- Hirst, E., Rees, D.A. 1965. "The Structure of Alginic Acid. Part V. Isolation and Unambiguous Characterization of Some Hydrolysis Products of the Methylated Polysaccharide." *Journal of the Chemical Society*, 1182–87.
- Hoesli, C.A., Raghuram, K., Kiang, R.L., Mocinecová, D., Hu, X., Johnson, J.D., Lacík, I., Kieffer, T.J., Piret, J.M. 2011. "Pancreatic Cell Immobilization in Alginate Beads Produced by Emulsion and Internal Gelation." *Biotechnology and Bioengineering* 108 (2): 424–34.
- Howard, C., Murray, P.E., Namerow, K.N. 2010. "Dental Pulp Stem Cell Migration." *Journal of Endodontics* 36(12):1963-6
- Huang, L.L.H., Sung, H.W., Tsai, C.C., Huang, D.M. 1998. "Biocompatibility Study of a Biological Tissue Fixed with a Naturally Occurring Crosslinking Reagent." *Journal of Biomedical Materials Research* 42 (4): 568–76.
- Huang, A.H.C., Snyder, B.R., Cheng, P.H., and Chan, A.W.S. 2008. "Putative Dental Pulp-Derived Stem/stromal Cells Promote Proliferation and Differentiation of Endogenous Neural Cells in the Hippocampus of Mice." *Stem Cells* 26 (10): 2654–2663.
- Huang, S., Xu, L., Sun, Y., Wu, T., Wang, K., Li, G. 2015. "An Improved Protocol for Isolation and Culture of Mesenchymal Stem Cells from Mouse Bone Marrow." *Journal of Orthopaedic Translation* 3 (1): 26–33.
- Hulsebosch, C.E. 2002. "Recent Advances in Pathophysiology and Treatment of Spinal Cord Injury." *American Journal of Physiology - Advances in Physiology Education* 26 (1–4): 238-55.
- Hunt, N.C., and Grover, L.M. 2010. "Cell Encapsulation Using Biopolymer Gels for Regenerative Medicine." *Biotechnology Letters* 32 (6): 733–42.
- Ismagilov, R.F., Stroock, A.D., Kenis, P.J.A., Whitesides, G., and Stonem H.A. 2000. "Experimental and Theoretical Scaling Laws for Transverse Diffusive Broadening in Two-Phase Laminar Flows in Microchannels." *Applied Physics Letters* 76 (17):

2376-2378.

- Issa, R.I., Engebretson, B., Rustom, L., McFetridge, P.S., and Sikavitsas, V.I. 2011. "The Effect of Cell Seeding Density on the Cellular and Mechanical Properties of a Mechanostimulated Tissue-Engineered Tendon." *Tissue Engineering. Part A* 17 (11–12): 1479–87.
- Jang, M., Yang, S., and Kim, P. 2016. "Microdroplet-based cell culture models and their application." *Biochip Journal* 10 (4): 310-317.
- Janmey, P.A., and Miller, R.T. 2011. "Mechanisms of Mechanical Signaling in Development and Disease." *Journal of Cell Science* 124 (1): 9-18.
- Jeffrey, G.M., Guilak, F., Nuttall, M.E., Sathishkumar, S., Vidal, M., and Bunnell, B.A. 2008. "In Vitro Differentiation Potential of Mesenchymal Stem Cells." *Transfusion Medicine and Hemotherapy* 35 (3): 228–38.
- Jiang, K., Lu, A.X., Dimitrakopoulos, P., DeVoe, D.L., and Raghavan, S.R. 2015. "Microfluidic Generation of Uniform Water Droplets Using Gas as the Continuous Phase." *Journal of Colloid and Interface Science* 448: 275–279.
- Jontell, M., Okiji, T., Dahlgren, U., and Bergenholtz, G. 1998. "Immune Defense Mechanisms of the Dental Pulp." *Critical Reviews in Oral Biology and Medicine* 9(2): 179-200.
- Joosten, E.A., Veldhuis, W.B., Hamers, F.P. 2004. "Collagen Containing Neonatal Astrocytes Stimulates Regrowth of Injured Fibers and Promotes Modest Locomotor Recovery after Spinal Cord Injury." *Journal of Neuroscience Research* 77 (1): 127-42.
- Ju, Y.M., Yu, B., West, L., Moussy, Y., Moussy, F. 2010. "A Novel Porous Collagen Scaffold around an Implantable Biosensor for Improving Biocompatibility. II. Long-Term in Vitro/in Vivo Sensitivity Characteristics of Sensors with NDGA- Or GA-Crosslinked Collagen Scaffolds." *Source of the Document Journal of Biomedical Materials Research - Part A* 92 (2): 650–58.
- Jun, Y., Kim, M.J., Hwang, Y.H., Jeon, E.A., Kang, A.R., Lee, S.H., Lee, D.Y. 2013. "Microfluidics-Generated Pancreatic Islet Microfibers for Enhanced Immunoprotection." *Biomaterials* 34 (33): 8122–30.
- Juste, S., Lessard, M., Henley, N., Ménard, M., Hallé, J.P. 2005. "Effect of Poly-L-Lysine Coating on Macrophage Activation by Alginate-Based Microcapsules: Assessment Using a New in Vitro Method." *Journal of Biomedical Materials Research - Part A* 72(4):389-98.
- Kalyanaraman, Meena, Scott T. Retterer, Timothy E. McKnight, M. Nance Ericson, Steve L. Allman, James G. Elkins, Anthony V. Palumbo, Martin Keller, and Mitchel J. Doktycz. 2009. "Controlled Microfluidic Production of Alginate Beads for in Situ Encapsulation of Microbes." *2009 1st Annual ORNL Biomedical Science and Engineering Conference, BSEC 2009*, 1–4.
- Kamaly, N., Yameen, B., Wu, J., and Farokhzad, O.C. 2016. "Degradable Controlled-Release Polymers and Polymeric Nanoparticles." *Chemical Reviews* 116 (4): 2602–2663.

- Kanafi, M.M., Ramesh, A., Gupta, P.K., and Bhonde, R.R. 2014. "Dental Pulp Stem Cells Immobilized in Alginate Microspheres for Applications in Bone Tissue Engineering." *International Endodontic Journal* 47 (7): 687–97.
- Kanafi, M., Majumdar, D., Bhonde, R., Gupta, P., Datta, I. 2014. "Midbrain Cues Dictate Differentiation of Human Dental Pulp Stem Cells towards Functional Dopaminergic Neurons." *Journal of Cellular Physiology* 229 (10): 1369–77.
- Karaöz, E., Demircan, P.C., Sağlam, O., Aksoy, A., Kaymaz, F., Duruksu, G. 2011. "Human Dental Pulp Stem Cells Demonstrate Better Neural and Epithelial Stem Cell Properties than Bone Marrow-Derived Mesenchymal Stem Cells." *Histochemistry and Cell Biology* 136 (4): 455–73.
- Karaöz, E., Doğan, B.N., Aksoy, A., Gacar, G., Akyüz, S., Ayhan, S., Genç, Z.S., Yürüker, S., Duruksu, G., Demircan, P.C., Sariboyaci, A.E. 2010. "Isolation and in Vitro Characterisation of Dental Pulp Stem Cells from Natal Teeth." *Histochemistry and Cell Biology* 133 (1): 95–112.
- Karaöz, E., Demircan, P.C., Sağlam, O., Aksoy, A., Kaymaz, F., Duruksu, G. 2011. "Human Dental Pulp Stem Cells Demonstrate Better Neural and Epithelial Stem Cell Properties than Bone Marrow-Derived Mesenchymal Stem Cells." *Histochemistry and Cell Biology* 136 (4): 455–73.
- Karsy, M., and Hawryluk, G. 2017. "Pharmacologic Management of Acute Spinal Cord Injury." *Neurosurgery Clinics of North America* 28 (1): 49–62.
- Kawano, H., Kimura-Kuroda, J., Komuta, Y., Yoshioka, N., Li, H.P., Kawamura, K., Li, Y., and Raisman, G. 2012. "Role of the Lesion Scar in the Response to Damage and Repair of the Central Nervous System." *Cell and Tissue Research* 349 (1): 169–80.
- Kawashima, N. 2012. "Characterisation of Dental Pulp Stem Cells: A New Horizon for Tissue Regeneration?" *Archives of Oral Biology* 57 (11). Elsevier Ltd: 1439–58.
- Keller, G. 2005. "Embryonic Stem Cell Differentiation: Emergence of a New Era in Biology and Medicine." *Genes and Development* 19 (10): 1129–55.
- Kerkis, I., Kerkis, A., Dozortsev, D., Stukart-Parsons, G.C., Gomes Massironi, S.M., Pereira, L.V., Caplan, A.I., Cerruti, H.F. 2007. "Isolation and Characterization of a Population of Immature Dental Pulp Stem Cells Expressing OCT-4 and Other Embryonic Stem Cell Markers." *Cells Tissues Organs* 184 (3–4): 105–16.
- Khademhosseini, A., May, M.H., and Sefton, M.V. 2005. "Conformal Coating of Mammalian Cells Immobilized onto Magnetically Driven Beads." *Tissue Engineering* 11 (11–12): 1797–1806.
- Khetan, S., Guvendiren, M., Legant, W.R., Cohen, D.M., Chen, C.S., and Burdick, J.A. 2013. "Degradation-Mediated Cellular Traction Directs Stem Cell Fate in Covalently Crosslinked Three-Dimensional Hydrogels." *Nat Mater* 12 (5). Nature Publishing Group: 458–65.
- Kim, H.W., Lim, J., Rhie, J.W., and Kim, D.S. 2017. "Investigation of Effective Shear Stress on Endothelial Differentiation of Human Adipose-Derived Stem Cells with Microfluidic Screening Device." *Microelectronic Engineering* 174. Elsevier B.V.:

24–27.

- Kim, H.M., Hwang, D.H., Lee, J.E., Kim, S.U., Kim, B.G. 2009. "Ex Vivo VEGF Delivery by Neural Stem Cells Enhances Proliferation of Glial Progenitors, Angiogenesis, and Tissue Sparing after Spinal Cord Injury." *PLoS ONE* 4 (3): e4987.
- Kimelberg, H.K., and Nedergaard, M. 2010. "Functions of Astrocytes and Their Potential As Therapeutic Targets." *Neurotherapeutics* 7 (4): 338–53.
- Király, M., Porcsalmy, B., Pataki, A., Kádár, K., Jelitai, M., Molnár, B., Hermann, P., Gera, I., Grimm, W.-D., Ganss, B., Zsembery, A., Varga, G. 2009. "Simultaneous PKC and cAMP Activation Induces Differentiation of Human Dental Pulp Stem Cells into Functionally Active Neurons." *Neurochemistry International* 55 (5): 323–32.
- Kleinman, H.K., Klebe, R.J., and Martin, G.R. 1981. "Role of Collagenous Matrices in the Adhesion and Growth of Cells." *Journal of Cell Biology* 88 (3): 473–85.
- Knezevic, Z., Bobic, S., Milutinovic, A., Obradovic, B., Mojovic, L., and Bugarski, B. 2002. "Alginate-Immobilized Lipase by Electrostatic Extrusion for the Purpose of Palm Oil Hydrolysis in Lecithin/isooctane System." *Process Biochemistry* 38 (3): 313–18.
- Koch, S., Schwinger, C., Kressler, J., Heinzen, C., and Rainov, N.G. 2003. "Alginate Encapsulation of Genetically Engineered Mammalian Cells: Comparison of Production Devices, Methods and Microcapsule Characteristics." *Journal of Microencapsulation* 20: 303–316.
- Komada, Y., Yamane, T., Kadota, D., Isono, K., Takakura, N., Hayashi, S., Yamazaki, H. 2012. "Origins and Properties of Dental, Thymic, and Bone Marrow Mesenchymal Cells and Their Stem Cells." *PLoS ONE* 7 (11): e46436.
- Kong, H.J., Kaigler, D., & Mooney, D.J. 2004. "Controlling Rigidity and Degradation of Alginate Hydrogel Via Molecular Weight Distribution." *Biomacromolecules* 5: 1720–27.
- Krishnan, R., Alexander, M., Robles, L., Foster 3rd, and Lakey, J.R.T. 2013. "Islet and Stem Cell Encapsulation for Clinical Transplantation." *The Review of Diabetic Studies* 11 (1): 84–101.
- Kshitiz, Park, J., Kim, P., Helen, W., Engler, A.J., Levchenko, A., and Kima, D.H. 2012. "Control of Stem Cell Fate and Function by Engineering Physical Microenvironments." *Integrative Biology* 4 (9): 1008–18.
- Kuo, C.K., and Ma, P.X. 2001. "Ionically Crosslinked Alginate Hydrogels as Scaffolds for Tissue Engineering: Part 1. Structure, Gelation Rate and Mechanical Properties." *Biomaterials* 22 (6): 511–21.
- Kuribayashi-Shigetomi, K., Tsuda, Y., Nakamura, H., and Takeuchi, S. 2010. "High Resolution Patterning of Cells with a Phosphorylcholine-Based Polymer in a Microfluidic Channel Using a Parylene DRY Film Mask." *14th International Conference on Miniaturized Systems for Chemistry and Life Sciences 2010, MicroTAS 2010*. Vol. 3.
- Kurup, S., and Bhonde, R.R. 2002. "Analysis and Optimization of Nutritional Set-up for

- Murine Pancreatic Acinar Cells." *Journal of the Pancreas* 3 (1): 8-15.
- Lapierre, F., Wu, N., and Zhu, Y. 2011. "Influence of Flow Rate on the Droplet Generation Process in a Microfluidic Chip." *SPIE 8204, Smart Nano-Micro Materials and Devices*
- Lazovic, G., Colic, M., Grubor, M., and Jovanovic, M. 2005. "The Application of Collagen Sheet in Open Wound Healing." *Annals of Burns and Fire Disasters* 18 (3): 151–56.
- Lee, K.Y., Bouhadir, K.H., and Mooney, D.J. 2004. "Controlled Degradation of Hydrogels Using Multi-Functional Cross-Linking Molecules." *Biomaterials* 25 (13): 2461–66.
- Lee, K.Y., and Mooney, D.J. 2001. "Hydrogels for Tissue Engineering." *Chemical Reviews* 101 (7): 1869–79.
- Lee, K.Y., and Mooney, D.J. 2012. "Alginate: Properties and Biomedical Applications." *Progress in Polymer Science* 37 (1): 106–26.
- Lee, M.K., and Bae, Y.H. 2000. "Cell Transplantation for Endocrine Disorders." *Advanced Drug Delivery Reviews* 42 (1–2): 103-20.
- Lee, M., Lo, A.C., Cheung, P.T., Wong, D., Chan, B.P. 2009. "Drug Carrier Systems Based on Collagen-Alginate Composite Structures for Improving the Performance of GDNF-Secreting HEK293 Cells." *Biomaterials* 30 (6). 1214–21.
- Lee, M.K., and Cleveland, D.W. 1996. "Neuronal Intermediate Filaments." *Annual Review of Neuroscience*. 19:187-217.
- Leong, W.K., Henshall, T.L., Arthur, A., Kremer, K.L., Lewis, M.D., Helps, S.C., Field, J. Hamilton-Bruce, M.A., Warming, S., Manavis, J., Vink, R., Gronthos, S., Koblar, S.A. 2012. "Human Adult Dental Pulp Stem Cells Enhance Poststroke Functional Recovery through Non-Neural Replacement Mechanisms." *Stem Cells Translational Medicine* 1 (3): 177-87.
- Li L., Chen X., Wang W.E., Zeng C. 2016. "How to Improve the Survival of Transplanted Mesenchymal Stem Cell in Ischemic Heart?." *Stem Cells Int*. 2016: 9682757.
- Li, L., Davidovich, A.E., Schloss, J.M., Chippada, U., Schloss, R.R., Langrana, N.A., and Yarmush, M.L. 2011. "Neural Lineage Differentiation of Embryonic Stem Cells within Alginate Microbeads." *Biomaterials* 32 (20): 4489–97.
- Li, J., Ren, N., Qiu, J., Jiang, H., Zhao, H., Wang, G., Boughton, R.I., Wang, Y., Liu, H. 2013. "Carbodiimide Crosslinked Collagen from Porcine Dermal Matrix for High-Strength Tissue Engineering Scaffold." *International Journal of Biological Macromolecules* 61: 69–74.
- Liang, H.C., Chang, W.H., Lin, K.J., Sung, H.W. 2003. "Genipin-Crosslinked Gelatin Microspheres as a Drug Carrier for Intramuscular Administration: In Vitro and in Vivo Studies." *J Biomed Mater Res A* 65: 271–282.
- Lignos, I.G., Wootton, R.C.R., DeMello, A.J., Stone, B.M. 2012. "Segmented Flow Microfluidics BT - Encyclopedia of Biophysics." Berlin, Heidelberg: Springer Berlin Heidelberg.

- Lindroos, B., Suuronen, R., Miettinen, S. 2011. "The Potential of Adipose Stem Cells in Regenerative Medicine." *Stem Cell Reviews and Reports* 7 (2): 269–291.
- Liu, K., Ding, H.J., Liu, J., Chen, Y., and Zhao, X.Z. 2006. "Shape-Controlled Production of Biodegradable Calcium Alginate Gel Microparticles Using a Novel Microfluidic Device." *Langmuir* 22 (22): 9453–9457.
- Liu, H., S. Gronthos, and S. Shi. 2006. "Dental Pulp Stem Cells." *Methods in Enzymology*. 419: 99–113.
- Liu, L., Wu, F., Ju, W.J., Xie, R., Wang, W., Niu, C.H., and Chu, L.Y. 2013. "Preparation of Monodisperse Calcium Alginate Microcapsules via Internal Gelation in Microfluidic-Generated Double Emulsions." *Journal of Colloid and Interface Science* 404: 85–90.
- Liu, C., Zhong, Y., Apostolou, A., and Fang, S. 2013. "Neural differentiation of human embryonic stem cells as an in vitro tool for the study of the expression patterns of the neuronal cytoskeleton during neurogenesis." *Biochemical and Biophysical Research Communications* 439(1): 154-159.
- Lizier, N.F., Kerkis, A., Gomes, C.M., Hebling, J., Oliveira, C.F., Caplan, A.I., and Kerkis, I. 2012. "Scaling-up of Dental Pulp Stem Cells Isolated from Multiple Niches." *PLoS ONE* 7 (6): e39885.
- Lodish, H., Berk, A., Zipursky, S.L., Matsudaira, P., Baltimore, D., and Darnell, J. 2000. "Collagen: The Fibrous Proteins of the Matrix." *Molecular Cell Biology*. New York, W. H. Freeman.
- Løvschall, H., Tummers, M., Thesleff, I., Füchtbauer, E.M., and Poulsen, K. 2005. "Activation of the Notch Signaling Pathway in Response to Pulp Capping of Rat Molars." *European Journal of Oral Sciences* 113 (4): 312-7.
- Ma, L., Gao, C., Mao, Z., Zhou, J., and Shen, J. 2004. "Biodegradability and Cell-Mediated Contraction of Porous Collagen Scaffolds: The Effect of Lysine as a Novel Crosslinking Bridge." *Journal of Biomedical Materials Research - Part A* 71 (2): 334–42.
- MacLennan, J.D., Mand, I.I., Howes, E.L. 1953. "Bacterial Digestion of Collagen." *Journal of Clinical Investigation* 32: 1317–1322.
- Maeda, K., Onoe, H., Takinoue, M., and Takeuchi, S. 2012. "Controlled Synthesis of 3D Multi-Compartmental Particles with Centrifuge-Based Microdroplet Formation from a Multi-Barrelled Capillary." *Advanced Materials* 24 (10): 1340–46.
- Maguire, T., Davidovich, A.E., Wallenstein, E.J., Novik, E., Sharma, N., Pedersen, H., Androulakis, I.P., Schloss, R., Yarmush, M. 2007. "Control of Hepatic Differentiation Via Cellular Aggregation in an Alginate Microenvironment." *Biotechnology and Bioengineering* 98 (3): 631-44.
- Marco Tatullo, Massimo Marrelli, Kevin M. Shakesheff and Lisa J. White. 2015. "Dental Pulp Stem Cells: Function, Isolation and Applications in Regenerative Medicine." *Journal of Tissue Engineering and Regenerative Medicine* 9: 1205–1216.

- Markiewicz, I., Sypecka, J., Domanska-Janik, K., Wyszomirski, T., and Lukomska, B. 2011. "Cellular Environment Directs Differentiation of Human Umbilical Cord Blood-Derived Neural Stem Cells in Vitro." *Journal of Histochemistry and Cytochemistry* 59 (3): 289–301.
- Marks, M.G., Doillon, C., Silver, F.H. 1991. "Effects of Fibroblasts and Basic Fibroblast Growth Factor on Facilitation of Dermal Wound Healing by Type I Collagen Matrices." *Journal of Biomedical Materials Research* 25 (5): 683-96.
- Markusen, J.F., Mason, C., Hull, D.A., Town, M.A., Tabor, A.B., Clements, M., Boshoff, C.H., Dunnill, P. 2006a. "Behavior of Adult Human Mesenchymal Stem Cells Entrapped in Alginate-GRGDY Beads." *Tissue Engineering* 12 (4): 821-30.
- Markusen, J.F., Mason, C., Hull, D.A., Town, M.A., Tabor, A.B., Clements, M., Boshoff, C.H., and Dunnill, P. 2006b. "Behavior of Adult Human Mesenchymal Stem Cells Entrapped in Alginate-GRGDY Beads." *Tissue Engineering* 12 (4): 821–30.
- Martín-Banderas, L., Flores-Mosquera, M., Riesco-Chueca, P., Rodríguez-Gil, A., Cebolla, A., Chávez, S., Gañán-Calvo, A.M. 2005. "Flow Focusing: A Versatile Technology to Produce Size-Controlled and Specific-Morphology Microparticles." *Small* 1 (7): 688–92.
- Martin, G.R. 1981. "Isolation of a Pluripotent Cell Line from Early Mouse Embryos Cultured in Medium Conditioned by Teratocarcinoma Stem Cells." *Proceedings of the National Academy of Sciences of the United States of America* 78 (12 II): 7634–38.
- Martinez, C.J., Kim, J.W., Ye, C., Ortiz, I., Rowat, A.C., Marquez, M., Weitz, D. 2012. "A Microfluidic Approach to Encapsulate Living Cells in Uniform Alginate Hydrogel Microparticles." *Macromolecular Bioscience* 12 (7): 946–51.
- McKeon, R.J., Schreiber, R.C., Rudge, J.S., and Silver, S. 1991. "Reduction of Neurite Outgrowth in a Model of Glial Scarring Following Cns Injury Is Correlated With the Expression of Inhibitory Molecules on Reactive Astrocytes." *Journal of Neuroscience* 11 (11): 3398–3411.
- McTigue, D.M. 2008. "Potential Therapeutic Targets for PPAR γ after Spinal Cord Injury." *PPAR Research* 2008:517162.
- Meghezi, S., Seifu, D.G., Bono, N., Unsworth, L., Mequanint, K., Mantovani, D. 2015. "Engineering 3D Cellularized Collagen Gels for Vascular Tissue Regeneration." *Journal of Visualized Experiments*, 100: e52812.
- Mei, J.C., Wu, A.Y., Wu, P.C., Cheng, N.C., Tsai, W.B., Yu, J. 2014. "Three-Dimensional Extracellular Matrix Scaffolds by Microfluidic Fabrication for Long-Term Spontaneously Contracted Cardiomyocyte Culture." *Tissue Engineering Part A* 20 (21–22): 2931–41.
- Meijs, M.F., Timmers, L., Pearse, D.D., Tresco, P.A., Bates, M.L., Joosten, E.A., Bunge, M.B., Oudega, M. 2004. "Basic Fibroblast Growth Factor Promotes Neuronal Survival but Not Behavioral Recovery in the Transected and Schwann Cell Implanted Rat Thoracic Spinal Cord." *Journal of Neurotrauma* 21 (10):1415-30.
- Ménard, M., Dusseault, J., Langlois, G., Baille, W.E., Tam, S.K., Yahia, L., Zhu, X.X.,

- Hallé, J.P. 2010. "Role of Protein Contaminants in the Immunogenicity of Alginates." *Journal of Biomedical Materials Research - Part B Applied Biomaterials* 93 (2): 333-40.
- Meng, X., W. Li, F. Young, R. Gao, L. Chalmers, M. Zhao, and B. Song. 2012. "Electric Field-Controlled Directed Migration of Neural Progenitor Cells in 2D and 3D Environments." *Journal of Visualized Experiments* 60: 3453.
- Mescher, A.L. 2016. "Junqueira's Basic Histology Text & Atlas". Bloomington, McGraw-Hill Education
- Messam, C.A., Hou, J., and Major, E.O. 1999. "Coexpression of Nestin in Neural and Glial Cells in the Developing Human CNS Defined by a Human-Specific Anti-Nestin Antibody." *Experimental Neurology* 161 (2): 585–96.
- Mi, F.L., Tan, Y.C., Liang, H.F., Sung, H.W. 2002. "In Vivo Biocompatibility and Degradability of a Novel Injectable-Chitosan-Based Implant." *Biomaterials* 23 (1): 181–91.
- Michalczyk, K., and Ziman, M. 2005. "Nestin Structure and Predicted Function in Cellular Cytoskeletal Organisation." *Histology and Histopathology* 20 (2): 665-71.
- Michalopoulos, E., Knight, R.L., Korossis, S., Kearney, J.N., Fisher, J., and Ingham, E. 2012. "Development of Methods for Studying the Differentiation of Human Mesenchymal Stem Cells Under Cyclic Compressive Strain." *Tissue Engineering Part C: Methods* 18 (4): 252–62.
- Miller, A. 1984. "Collagen: The Organic Matrix of Bone." *Philosophical Transactions of the Royal Society B* 304: 455–77.
- Mollet, H., Grubenmann, A., and Payne, H. 2001. *Formulation Technology: Emulsions, Suspensions, Solid Forms*. 1st ed. Strauss Offsetdruck, Wiley-VCH Verlag.
- Moore, B.A., Aznavoorian, S., Engler, J.A., and Windsor, L.J. 2000. "Induction of Collagenase-3 (MMP-13) in Rheumatoid Arthritis Synovial Fibroblasts." *Biochimica et Biophysica Acta - Molecular Basis of Disease* 1502 (2).
- Moore, K.A., and Lemischka, I.R. 2006. "Stem Cells and Their Niches." *Science* 311 (5769): 1880–85.
- Morgan, A.J.L., Hidalgo San Jose, L., Jamieson, W.D., Wymant, J.M., Song, B., Stephens, P., Barrow, D.A., and Castell. O.K. 2016. "Simple and Versatile 3D Printed Microfluidics Using Fused Filament Fabrication." *Plos One* 11 (4): e0152023.
- Morshead, C.M., Reynolds, B.A., Craig, C.G., McBurney, M.W., Staines, W.A., Morassutti, D., Weiss, S., Van der Kooy, D. 1994. "Neural Stem Cells in the Adult Mammalian Forebrain: A Relatively Quiescent Subpopulation of Subependymal Cells." *Neuron* 13 (5): 1071-82.
- Mosahebi, A., Wiberg, M., and Terenghi, G. 2003. "Addition of fibronectin to alginate matrix improves peripheral nerve regeneration in tissue-engineered conduits." *Tissue Engineering* 9: 209–18.
- Muiznieks, L.D., and Keeley, F.W. 2013. "Molecular Assembly and Mechanical

- Properties of the Extracellular Matrix: A Fibrous Protein Perspective.” *Biochimica et Biophysica Acta - Molecular Basis of Disease* 1832 (7): 866–75.
- Murua, A., de Castro, M., Orive, G., Hernández, R.M., and Pedraz, J.L. 2007. “In Vitro Characterization and in Vivo Functionality of Erythropoietin-Secreting Cells Immobilized in Alginate-Poly-L-Lysine-Alginate Microcapsules.” *Biomacromolecules* 8 (11): 3302–7.
- Nagarajan, S., Kruckeberg, A.L., Schmidt, K.H., Kroll, E., Hamilton, M., McInnerney, K., Summers, R., Taylor, T., and Rosenzweig, F. 2014. “Uncoupling Reproduction from Metabolism Extends Chronological Lifespan in Yeast.” *Proceedings of the National Academy of Sciences of the United States of America* 111 (15): E1538–47.
- Nam, J., and Yeo, W.S. 2016. “Controlled Drug Release Using Ascorbate-Responsive Quercetin-Conjugated Alginate Hydrogels.” *Applied Biological Chemistry* 59 (4): 579–84.
- Neufeld, R., Frere, Y., Poncelet, D., and Perignon, C. 2014. “Microencapsulation by Interfacial Polymerisation : Membrane Formation and Structure” 2048: 1–15..
- Neufeld, T., Ludwig, B., Barkai, U., Weir, G.C., Colton, C.K., Evron, Y., Balyura, M., Yavriyants, K., Zimmermann, B., Azarov, D., Maimon, S., Shabtay, N., Rozenshtein, T., Lorber, D., Steffen, A., Willenz, U., Bloch, K., Vardi, P., Taube, R., de Vos, P., Lewis, E.C., Bornstein, S.R., Rotem, A. 2013. “The Efficacy of an Immunoisolating Membrane System for Islet Xenotransplantation in Minipigs.” *PLoS ONE* 8 (8): e70150.
- Nichols, J., and Smith, A. 2012. “Pluripotency in the Embryo and in Culture.” *Cold Spring Harbor Perspectives in Biology* 4: 1–15.
- Nicola, F.C., Rodrigues, L.P., Crestani, T., Quintiliano, K., Sanches, E.F., Willborn, S., Aristimunha, D., Boisserand, L., Pranke, P., and Netto, C.A. 2016. “Human Dental Pulp Stem Cells Transplantation Combined with Treadmill Training in Rats after Traumatic Spinal Cord Injury.” *Brazilian Journal of Medical and Biological Research* 49 (9): 1–11.
- Nie, Z., Seo, M., Xu, S., Lewis, P.C., Mok, M., Kumacheva, E., Whitesides, G.M., Garstecki, P., and Stone, H.A. 2008. “Emulsification in a Microfluidic Flow-Focusing Device: Effect of the Viscosities of the Liquids.” *Microfluidics and Nanofluidics* 5 (5): 585–94.
- Nillesen, S.T., Geutjes, P.J., Wismans, R., Schalkwijk, J., Daamen, W.F., Van Kuppevelt, T.H. 2007. “Increased Angiogenesis and Blood Vessel Maturation in Acellular Collagen-Heparin Scaffolds Containing Both FGF2 and VEGF.” *Biomaterials* 28 (6): 1123–31.
- Nisisako, T., Okushima, S., and Torii, T. 2005. “Controlled Formulation of Monodisperse Double Emulsions in a Multiple-Phase Microfluidic System.” *Soft Matter*: 23–27.
- Nisisako, T., Torii, T., Takahashi, T., and Takizawa, Y. 2006. “Synthesis of Monodisperse Bicolored Janus Particles with Electrical Anisotropy Using a Microfluidic Co-Flow System.” *Advanced Materials* 18 (9): 1152–1156.

- Niwa, H., Miyazaki, J.I., and Smith, A.G. 2000. "Quantitative Expression of Oct-3/4 Defines Differentiation, Dedifferentiation or Self-Renewal of ES Cells." *Nature Genetics* 24 (4): 372–76.
- Nolte, C., Matyash, M., Pivneva, T., Schipke, C.G., Ohlemeyer, C., Hanisch, U.K., Kirchhoff, F., and Kettenmann, H. 2001. "GFAP Promoter-Controlled EGFP-Expressing Transgenic Mice: A Tool to Visualize Astrocytes and Astrogliosis in Living Brain Tissue." *GLIA* 33 (1): 72-86.
- Nosrat, I.V., Smith, C.A., Mullally, P., Olson, L., Nosrat, C.A. 2004. "Dental Pulp Cells Provide Neurotrophic Support for Dopaminergic Neurons and Differentiate into Neurons in Vitro; Implications for Tissue Engineering and Repair in the Nervous System." *European Journal of Neuroscience* 19 (9): 2388–98.
- Novikova, L.N., Mosahebi, A., Wiberg, M., Terenghi, G., Kellerth, J.O., Novikov, L.N. 2006. "Alginate Hydrogel and Matrigel as Potential Cell Carriers for Neurotransplantation." *Journal of Biomedical Materials Research - Part A* 77 (2): 242-52.
- Nowak, J.A., Fuchs, E. 2009. "Isolation and Culture of Epithelial Stem Cells." *Methods in Molecular Biology* 482: 215–32.
- Ntambi, J.M., Young-Cheul, K. 2000. "Adipocyte Differentiation and Gene Expression." *Journal of Nutrition* 130 (12): 3122S-3126S.
- Numpaisal, P., Rothrauff, B.B., Gottardi, R., Chien, C., and Tuan, R.S. 2016. "Rapidly Dissociated Autologous Meniscus Tissue Enhances Meniscus Healing: An in Vitro Study." *Connective Tissue Research*. In Press.
- O'Brien, F.J. 2011. "Biomaterials & Scaffolds for Tissue Engineering." *Materials Today* 14 (3): 88–95.
- O'Rahilly, R., Müller, F., Carpenter, S., and Swenson, R. 2004. "The Spinal Cord and Meninges." *Basic Human Anatomy*, Dartmouth.
- Ogata, K., and Kosaka, T. 2002. "Structural and Quantitative Analysis of Astrocytes in the Mouse Hippocampus." *Neuroscience* 113 (1): 221-33.
- Ogawa, Y., Sawamoto, K., Miyata, T., Miyao, S., Watanabe, M., Nakamura, M., Bregman, B.S., Koike, M., Uchiyama, Y., Toyama, Y., Okano, H. 2002. "Transplantation of in Vitro-Expanded Fetal Neural Progenitor Cells Results in Neurogenesis and Functional Recovery after Spinal Cord Contusion Injury in Adult Rats." *Journal of Neuroscience Research* 69 (6): 925–33.
- Ogbonna, J.C., Matsumura, M., Kataoka, H. 1991. "Effective Oxygenation of Immobilized Cells through Reduction in Bead Diameters: A Review." *Process Biochemistry* 26 (2): 109–21.
- Ogbonna, J.C., Matsumura, M., and Kataoka, H. 1991. "Effective Oxygenation of Immobilized Cells through Reduction in Bead Diameters: A Review." *Process Biochemistry* 26 (2): 109-121.
- Okada, S.L., Stivers, N.S., Stys, P.K., and Stirling, D.P. 2014. "An Ex Vivo Laser-Induced Spinal Cord Injury Model to Assess Mechanisms of Axonal Degeneration in Real-Time." *Journal of Visualized Experiments*, 93: e52173.

- Okano, H., Ogawa, Y., Nakamura, M., Kaneko, S., Iwanami, A., and Toyama, Y. 2003. "Transplantation of Neural Stem Cells into the Spinal Cord after Injury." *Seminars in Cell & Developmental Biology* 14 (3): 191–98.
- Ong, S.E., Zhang, S., Du, H., Fu, Y. 2008. "Fundamental Principles and Applications of Microfluidic Systems." *Frontiers in Bioscience* 1 (13): 2757–73.
- Orive, G., Santos, E., Poncelet, D., Hernández, R.M., Pedraz, J.L., Wahlberg, L.U., De Vos, P., and Emerich, D. 2015. "Cell Encapsulation: Technical and Clinical Advances." *Trends in Pharmacological Sciences* 36 (8): 537–46.
- Otterlei, M., Ostgaard, K., Skjakbraek, G., Smidsrod, O., Soonshiong, P., and Espevik, T. 1991. "Induction of Cytokine Production from Human Monocytes Stimulated with Alginate." *Journal of Immunotherapy* 10 (4): 286–91.
- Pagano, S.F., Impagnatiello, F., Girelli, M., Cova, L., Grioni, E., Onofri, M., Cavallaro, M., Etteri, S., Vitello, F., Giombini, S., Solero, C.L., Parati, E.A. 2000. "Isolation and Characterization of Neural Stem Cells from the Adult Human Olfactory Bulb." *Stem Cells (Dayton, Ohio)* 18 (4): 295–300.
- Pamme, N. 2007. "Continuous Flow Separations in Microfluidic Devices." *Lab on a Chip - Miniaturisation for Chemistry and Biology* 7 (12): 1644–59.
- Pan, L., Ren, Y., Cui, F., Xu, Q. 2009. "Viability and Differentiation of Neural Precursors on Hyaluronic Acid Hydrogel Scaffold." *Journal of Neuroscience Research* 87 (14): 3207–20.
- Pardridge, W.M. 2005. "The Blood-Brain Barrier: Bottleneck in Brain Drug Development." *The Journal of the American Society for Experimental NeuroTherapeutics* 2(1): 3–14.
- Parenteau-Bareil, R., Gauvin, R., and Berthod, F. 2010. "Collagen-Based Biomaterials for Tissue Engineering Applications." *Materials* 3 (3): 1863–87.
- Park, H.W., Cho, J.S., Park, C.K., Jung, S.J., Park, C.H., Lee, S.J., Oh, S.B., Park, Y.S., Chang, M.S. 2012. "Directed Induction of Functional Motor Neuron-like Cells from Genetically Engineered Human Mesenchymal Stem Cells." *PloS One* 7 (4): e35244.
- Park, H.W., Lim, M.J., Jung, H., Lee, S.P., Paik, K.S., Chang, M.S. 2010. "Human Mesenchymal Stem Cell-Derived Schwann Cell-like Cells Exhibit Neurotrophic Effects, via Distinct Growth Factor Production, in a Model of Spinal Cord Injury." *Glia* 58 (9): 1118–32.
- Parr, A.M., Kulbatski, I., Tator, C.H. 2007. "Transplantation of Adult Rat Spinal Cord Stem/progenitor Cells for Spinal Cord Injury." *Journal of Neurotrauma* 24 (5): 835–45.
- Patel, M., Smith, A.J., Sloan, A.J., Smith, G., Cooper, P.R. 2009. "Phenotype and Behaviour of Dental Pulp Cells during Expansion Culture." *Archives of Oral Biology* 54 (10): 898–908.
- Pauling, L., Corey, R.B. 1951. "The Structure of Fibrous Proteins of the Collagen-Gelatin Group." *Proceedings of the National Academy of Sciences* 37 (5): 272–81.

- Pendleton, C., Li, Q., Chesler, D.A., Yuan, K., Guerrero-Cazares, H., Quinones-Hinojosa, A. 2013. "Mesenchymal Stem Cells Derived from Adipose Tissue vs Bone Marrow: In Vitro Comparison of Their Tropism towards Gliomas." *PLoS ONE* 8 (3): e58198.
- Pennathur, S, Meinhart, C.D., and Soh, H.T. 2008. "How to Exploit the Features of Microfluidics Technology." *Lab on a Chip* 8 (1): 20–22.
- Perez, R.A., Kim, M., Kim, T.H., Kim, J.H., Lee, J.H., Park, J.H., Knowles, J.C., Kim, H.W. 2014. "Utilizing Core–Shell Fibrous Collagen-Alginate Hydrogel Cell Delivery System for Bone Tissue Engineering." *Tissue Engineering Part A* 20 (1–2): 103–14.
- Pessina, A., and Gribaldo, L. 2006. "The Key Role of Adult Stem Cells: Therapeutic Perspectives." *Current Medical Research and Opinion* 22 (11): 2287-300..
- Pfeifer, K., Vroemen, M., Blesch, A., and Weidner, N. 2004. "Adult Neural Progenitor Cells Provide a Permissive Guiding Substrate for Corticospinal Axon Growth Following Spinal Cord Injury." *European Journal of Neuroscience* 20 (7): 1695–1704.
- Phanat, K., Soottawat, B., Wonnop, V. 2010. "Isolation and Properties of Acid and Pepsin-Soluble Collagen from the Skin of Blacktip Shark (*Carcharhinus limbatus*)." *European Food Research and Technology* 230: 475–483.
- Pickering, J.G. 2001. "Regulation of Vascular Cell Behavior by Collagen : Form Is Function." *Circulation Research* 88 (5): 458–59.
- Pinton, P., Giorgi, C., Siviero, R., Zecchini, E. and Rizzuto, R. 2008. "Calcium and apoptosis: ER-mitochondria Ca^{2+} transfer in the control of apoptosis." *Oncogene*, 27(50): 6407-6418.
- Pinzon, A., Calancie, B., Oudega, M., and Noga, B.R. 2001. "Conduction of Impulses by Axons Regenerated in a Schwann Cell Graft in the Transected Adult Rat Thoracic Spinal Cord." *Journal of Neuroscience Research* 64 (5): 533-41.
- Pires, L.R., and Pêgo, A.P. 2015. "Bridging the Lesion-Engineering a Permissive Substrate for Nerve Regeneration." *Regenerative Biomaterials* 2 (3): 203–14.
- Place, E.S., Evans, N.D., and Stevens, M.M. 2009. "Complexity in Biomaterials for Tissue Engineering." *Nature Materials* 8, 457-470.
- Plateau, J. 1849. "Statique Experimentale et Theorique Des Liquides Soumis Aux Seules Forces Moleculaires." *Acad. Sci. Brux. Mem* 23 (5).
- Pollack, M.G., Shenderov, A.D., and Fair, R.B. 2002. "Electrowetting-Based Actuation of Droplets for Integrated Microfluidics." *Lab on a Chip - Miniaturisation for Chemistry and Biology* 2 (2): 96-101.
- Poncelet, D., Lencki, R., Beaulieu, C., Halle, J.p., Neufeld, R.J., and Fournier, A. 1992a. "Production of Alginate Beads by Emulsification/internal Gelation. I. Methodology." *Applied Microbiology and Biotechnology* 38 (1): 39–45.
- Ponnaiyan, D., and Jegadeesan, V. 2014. "Comparison of Phenotype and Differentiation Marker Gene Expression Profiles in Human Dental Pulp and Bone

- Marrow Mesenchymal Stem Cells." *European Journal of Dentistry* 8 (3): 307–313..
- Potdar, P.D, and Jethmalani, Y.D. 2015. "Human Dental Pulp Stem Cells: Applications in Future Regenerative Medicine." *World Journal of Stem Cells* 7 (5): 839–51.
- Prasad, D., and Schiff, D. 2005. "Malignant Spinal-Cord Compression." *Lancet Oncology* 6 (1): 15–24.
- Purger, D., Gibson, E.M., and Monje, M. 2016. "Myelin Plasticity in the Central Nervous System." *Neuropharmacology* 110.
- Qutachi, O., Shakesheff, K.M., BATTERY, L.D. 2013. "Delivery of Definable Number of Drug or Growth Factor Loaded Poly(dl-Lactic Acid-Co-Glycolic Acid) Microparticles within Human Embryonic Stem Cell Derived Aggregates." *Journal of Controlled Release* 168 (1): 18–27.
- Rajan, N., Habermehl, J., Coté, M.F., Doillon, C.J., and Mantovani, D. 2006. "Preparation of Ready-to-Use, Storable and Reconstituted Type I Collagen from Rat Tail Tendon for Tissue Engineering Applications." *Nature Protocols* 1 (6): 2753–58.
- Ramachandran, G.N., Kartha, G. 1954. "Structure of Collagen." *Nature* 174: 269–270.
- Rayleigh, Lord. 1879. "On the Capillary Phenomena of Jets." *Proc. R. Soc. Lond.* 29: 71–97.
- Reynolds, B.A. , and Weiss, S. 1992. "Generation of Neurons and Astrocytes from Isolated Cells of the Adult Mammalian Central Nervous System." *Science* 255 (5052): 1707–10.
- Reynolds, O. 1883. "An Experimental Investigation of the Circumstances Which Determine Whether the Motion of Water Shall Be Direct or Sinuous, and of the Law of Resistance in Parallel Channels." *Philosophical Transactions of the Royal Society of London* 174: 935–82.
- Roe, S.C., Milthorpe, B.K., Schindhelm, K. 1990. "Collagen Cross-Linking and Resorption: Effect of Glutaraldehyde Concentration." *Artificial Organs* 14 (6): 443–48.
- Rolls, A., Shechter, R., London, A., Segev, Y., Jacob-Hirsch, J., Amariglio, N., Rechavi, G., and Schwartz, M. 2008. "Two Faces of Chondroitin Sulfate Proteoglycan in Spinal Cord Repair: A Role in Microglia/ Macrophage Activation." *PLoS Medicine* 5 (8): e171.
- Rossi, S.L., Nistor, G., Wyatt, T., Yin, H.Z., Poole, A.J., Weiss, J.H., Gardener, M.J., Dijkstra, S., Fischer, D.F., Keirstead, H.S. 2010. "Histological and Functional Benefit Following Transplantation of Motor Neuron Progenitors to the Injured Rat Spinal Cord." *PLoS ONE* 5 (7): e11852.
- Rouillard, A.D., Berglund, C.M., Lee, J.Y., Polacheck, W.J., Tsui, Y., Bonassar, L. J., and Kirby, B.J. 2011. "Methods for Photocrosslinking Alginate Hydrogel Scaffolds with High Cell Viability." *Tissue Engineering. Part C, Methods* 17 (2): 173–79.
- Rowley, J.A., Madlambayan, G., and Mooney, D.J. 1999. "Alginate Hydrogels as Synthetic Extracellular Matrix Materials." *Biomaterials* 20 (1): 45–53.

- Rowley, J.A., and Mooney, D.J. 2002. "Alginate Type and RGD Density Control Myoblast Phenotype." *Journal of Biomedical Materials Research* 60 (2): 217–23.
- Ruijgrok, J.M., de Wijn, J.R., and Boon, M.E. 1994. "Glutaraldehyde Crosslinking of Collagen: Effects of Time, Temperature, Concentration and Presoaking as Measured by Shrinkage Temperature." *Clinical Materials* 17: 23–27.
- Sah, H., and Chien, Y.W. 1996. "Prolonged Immune Response Evoked by a Single Subcutaneous Injection of Microcapsules Having a Monophasic Antigen Release." *Journal of Pharmacy and Pharmacology* 48 (1): 32–6.
- Sakai, K., Yamamoto, A., Matsubara, K., Nakamura, S., Naruse, M., Yamagata, M., Sakamoto, K., Tauchi, R., Wakao, N., Imagama, S., Hibi, H., Kadomatsu, K., Ishiguro, N., Ueda, M. 2012. "Human Dental Pulp-Derived Stem Cells Promote Locomotor Recovery after Complete Transection of the Rat Spinal Cord by Multiple Neuro-Regenerative Mechanisms." *Journal of Clinical Investigation* 122 (1): 80–90.
- Sakai, S., Mu, C., Kawabata, K., Hashimoto, I., Kawakami, K. 2006. "Biocompatibility of Subsieve-Size Capsules versus Conventional-Size Microcapsules." *Journal of Biomedical Materials Research - Part A* 78 (2): 394–8.
- Sakakibara, S., Nakamura, Y., Yoshida, T., Shibata, S., Koike, M., Takano, H., Ueda, S., Uchiyama, Y., Noda, T., Okano H.. 2002. "RNA-Binding Protein Musashi Family: Roles for CNS Stem Cells and a Subpopulation of Ependymal Cells Revealed by Targeted Disruption and Antisense Ablation." *Proceedings of the National Academy of Sciences of the United States of America* 99 (23): 15194–9.
- Salaön, F. 2013. "Microencapsulation by Interfacial Polymerization." *Encapsulation Nanotechnologies*, Hoboken, NJ, USA: John Willey & Sons. 137–73.
- Sang, L., Luo, D., Xu, S., Wang, X., and Li, X. 2011a. "Fabrication and Evaluation of Biomimetic Scaffolds by Using Collagen-Alginate Fibrillar Gels for Potential Tissue Engineering Applications." *Materials Science and Engineering C* 31 (2): 262–71.
- Santoro, M., Tatara, A.M., Mikos, A.G. 2014. "Gelatin Carriers for Drug and Cell Delivery in Tissue Engineering." *Journal of Controlled Release* 190: 210–8.
- Sato, H., Kitazawa, H., Adachi, I., Horikoshi, I. 1996. "Microdialysis Assessment of Microfibrous Collagen Containing a P-Glycoprotein-Mediated Transport Inhibitor, Cyclosporine A, for Local Delivery of Etoposide." *Pharmaceutical Research* 13(10):1565–9.
- Schmitt, A., Rödel, P., Anamur, C., Seeliger, C., Imhoff, A.B., Herbst, E., Vogt, S., Van Griensven, M., Winter, G., and Engert, J. 2015. "Calcium Alginate Gels as Stem Cell Matrix -Making Paracrine Stem Cell Activity Available for Enhanced Healing after Surgery." *PLoS ONE* 10 (3): 1–18.
- Sedgwick, J.D., Schwender, S., Imrich, H., Dörries, R., Butcher, G.W., ter Meulen. V. 1991. "Isolation and Direct Characterization of Resident Microglial Cells from the Normal and Inflamed Central Nervous System." *Proceedings of the National Academy of Sciences of the United States of America* 88(16):7438–42.

- Shahriari, D., Koffler, J., Lynam, D.A., Tuszynski, M.H., and Sakamoto, J.S. 2016. "Characterizing the Degradation of Alginate Hydrogel for Use in Multilumen Scaffolds for Spinal Cord Repair." *Journal of Biomedical Materials Research - Part A* 104 (3): 611–19.
- Shapiro, L., and Cohen, S. 1997. "Novel Alginate Sponges for Cell Culture and Transplantation." *Biomaterials* 18 (8): 583–90.
- Sheerin, F. 2004. "Spinal Cord Injury: Anatomy and Physiology of the Spinal Cord." In *Emergency Nurse*, 30–36.
- Shi, S., and Gronthos, S. 2003. "Perivascular Niche of Postnatal Mesenchymal Stem Cells in Human Bone Marrow and Dental Pulp." *Journal of Bone and Mineral Research* 18(4):696-704..
- Shihabuddin, L.S., Horner, P.J., Ray, J., and Gage, F.H. 2000. "Adult Spinal Cord Stem Cells Generate Neurons after Transplantation in the Adult Dentate Gyrus." *Journal of Neuroscience* 20 (23): 8727-8735.
- Shintaku, H., Kuwabara, T., Kawano, S., Suzuki, T., Kanno, I., and Kotera, H. 2007. "Micro Cell Encapsulation and Its Hydrogel-Beads Production Using Microfluidic Device." *Microsystem Technologies* 13 (8–10): 951–58.
- Shoulders, M.D., and Raines, R.T. 2010. "Collagen Structure and Stability." *Annu Rev Biochem* 78: 929–58.
- Sia, S.K, and Kricka, L.J. 2008. "Microfluidics and Point-of-Care Testing." *Lab on a Chip* 8 (12). The Royal Society of Chemistry: 1982–83.
- Siddique, R., and Thakor, N. 2013. "Investigation of Nerve Injury through Microfluidic Devices." *Journal of The Royal Society Interface* 11 (90): 20130676.
- Sikorski, P., Mo, F., Skjak-Braek, G., and Stokke, B.T. 2007. "Evidence for Egg-Box-Compatible Interactions in Calcium-Alginate Gels from Fiber X-Ray Diffraction." *Biomacromolecules* 8 (7): 2098–2103.
- Silvipriya, K.S., Kumar, K.K., Bhat, A.R., Kumar, B.D., John, A., and Lakshmanan, P. 2015. "Collagen: Animal Sources and Biomedical Application." *Journal of Applied Pharmaceutical Science* 5 (3): 123–27.
- Sinescu, C., Popa, F., Grigorean, V.T., Onose, G., Sandu, A.M., Popescu, M., Burnei, G., Strambu, V., and Popa, C. 2010. "Molecular Basis of Vascular Events Following Spinal Cord Injury." *Journal of Medicine and Life* 3 (3): 254–61.
- Singh, M.N., Hemant, K.S.Y., Ram, M., and Shivakumar, H.G. 2010. "Microencapsulation: A Promising Technique for Controlled Drug Delivery." *Research in Pharmaceutical Sciences* 5 (2): 65–77.
- Sivasamy, J., Wong, T.N., Nguyen, N.T., and Kao, L.T.H. 2011. "An Investigation on the Mechanism of Droplet Formation in a Microfluidic T-Junction." *Microfluidics and Nanofluidics* 11 (1): 1–10.
- Smidsrød, O. and Skjåk-Braek, G. 1990. "Alginate as immobilization matrix for cells." *Trends in Biotechnology* 8 (3):71-8.

- Smith, A.G., Nichols, J., Robertson, M., Rathjen, P.D 1992. "Differentiation Inhibiting Activity (DIA LIF) and Mouse Development." *Developmental Biology* 151 (2): 339-51.
- Smith, A.J., Cassidy, N., Perry, H., Bègue-Kirn, C., Ruch, J.V., Lesot, H. 1995. "Reactionary Dentinogenesis." *International Journal of Developmental Biology* 39 (1): 273-80.
- Soleimani, M., Nadri, S. 2009. "A Protocol for Isolation and Culture of Mesenchymal Stem Cells from Mouse Bone Marrow." *Nature Protocols* 4 (1): 102–6.
- Song, H., Chen, D.L., Ismagilov, R.F. 2006. "Reactions in Droplets in Microfluidic Channels." *Angewandte Chemie - International Edition* 45 (44): 7336-56.
- Soon-Shiong, P., Heintz, R.E., Merideth, N., Yao, Q.X., Yao, Z., Zheng, T., Murphy, M., Moloney, M.K., Schmehl, M., Harris, M., Mendez, R., Mendez, R., Sandford, P.A. 1994. "Insulin Independence in a Type 1 Diabetic Patient after Encapsulated Islet Transplantation." *The Lancet* 343 (8903): 950–51.
- Soria, J.M., Sancho-Tello, M., Esparza, M.A., Mirabet, V., Bagan, J.V., Monleón, M., Carda, C. 2011. "Biomaterials Coated by Dental Pulp Cells as Substrate for Neural Stem Cell Differentiation." *Journal of Biomedical Materials Research - Part A* 97(1): 85-92.
- Stabler, C., Wilks, K., Sambanis, A., Constantinidis, I. 2001. "The Effects of Alginate Composition on Encapsulated betaTC3 Cells." *Biomaterials* 22 (11): 1301–10.
- Staton, C. A., Reed, M.W.R., and Brown, N.J. 2009. "A Critical Analysis of Current in Vitro and in Vivo Angiogenesis Assays." *International Journal of Experimental Pathology* 90 (3): 195–221.
- Stone, H.A., Stroock, A.D., and Ajdari, A. 2004. "Microfluidics toward a Lab-on-a-Chip." *Engineering Flows in Small Devices: Annual Review of Fluid Mechanics*. 36:1-455.
- Strand, B.L., Mørch, Y.A., Espevik, T., and Skjåk-Bræk, G. 2003. "Visualization of Alginate-Poly-L-Lysine-Alginate Microcapsules by Confocal Laser Scanning Microscopy." *Biotechnology and Bioengineering* 82 (4): 386–94.
- Streets, A.M., and Huang, Y. 2013. "Chip in a Lab: Microfluidics for next Generation Life Science Research." *Biomicrofluidics* 7 (1): 11302.
- Stroock, A.D., and Fischbach, C. 2010. "Microfluidic Culture Models of Tumor Angiogenesis." *Tissue Engineering - Part A* 16 (7): 2143-6.
- Su, J., Hu, B.H., Lowe, W.L. Jr, Kaufman, D.B., Messersmith, P.B. 2010. "Anti-Inflammatory Peptide-Functionalized Hydrogels for Insulin-Secreting Cell Encapsulation." *Biomaterials* 31 (2): 308-14.
- Sugai, K., Nishimura, S., Kato-Negishi, M., Onoe, H., Iwanaga, S., Toyama, Y., Matsumoto, M., Takeuchi, S., Okano, H., and Nakamura, M. 2015. "Neural Stem/progenitor Cell-Laden Microfibers Promote Transplant Survival in a Mouse Transected Spinal Cord Injury Model." *Journal of Neuroscience Research* 93 (12): 1826–38.
- Suggs, W., Van Wart, H., Sharefkin, J.B. 1992. "Enzymatic Harvesting of Adult Human

- Saphenous Vein Endothelial Cells: Use of a Chemically Defined Combination of Two Purified Enzymes to Attain Viable Cell Yields Equal to Those Attained by Crude Bacterial Collagenase Preparations." *Journal of Vascular Surgery* 15 (1): 205-13.
- Sugiura, S., Oda, T., Izumida, Y., Aoyagi, Y., Satake, M., Ochiai, A., Ohkohchi, N., Nakajima, M. 2005. "Size Control of Calcium Alginate Beads Containing Living Cells Using Micro-Nozzle Array." *Biomaterials* 26 (16): 3327–31.
- Suh, R.S., Zhu, X., Phadke, N., Ohl, D.A., Takayama, S., Smith, G.D. 2006. "IVF within Microfluidic Channels Requires Lower Total Numbers and Lower Concentrations of Sperm." *Human Reproduction* 21 (2): 477-83.
- Sullivan, M.T., and Stone, H.A. 2008. "The Role of Feedback in Microfluidic Flow-Focusing Devices." *Philosophical Transactions. Series A, Mathematical, Physical, and Engineering Sciences* 366 (1873): 2131–43.
- Sun, J., and Tan, H. 2013. "Alginate-Based Biomaterials for Regenerative Medicine Applications." *Materials* 6 (4): 1285–1309.
- Sun, S., Ning, X., Zhang, Y., Lu, Y., Nie, Y., Han, S., Liu, L., Du, R., Xia, L., He, L., Fan, D. 2009. "Hypoxia-Inducible Factor-1 α Induces Twist Expression in Tubular Epithelial Cells Subjected to Hypoxia, Leading to Epithelial-to-Mesenchymal Transition." *Kidney International* 75 (12): 1278-87.
- Suri, S., Singh, A., Nguyen, A.H., Bratt-Leal, A.M., McDevitt, T.C., and Lu, H. 2013. "Microfluidic-Based Patterning of Embryonic Stem Cells for in Vitro Development Studies." *Lab on a Chip - Miniaturisation for Chemistry and Biology* 13 (23): 4617–4624.
- Suzuki, Y., Nishimura, Y., Tanihara, M., Suzuki, K., Nakamura, T., Shimizu, Y., Yamawaki, Y., Kakimaru, Y. 1998. "Evaluation of a Novel Alginate Gel Dressing: Cytotoxicity to Fibroblasts in Vitro and Foreign-Body Reaction in Pig Skin in Vivo." *Journal of Biomedical Materials Research* 39 (2): 317-22.
- Sypecka, J., Koniusz, S., Kawalec, M., and Sarnowska, A. 2015. "The Organotypic Longitudinal Spinal Cord Slice Culture for Stem Cell Study." *Stem Cells International* 2015: 471216.
- Szot, G.L., Lee, M.R., Tavakol, M.M., Lang, J., Dekovic, F., Kerlan, R.K., Stock, P.G., and Posselt, A.M. 2009. "Successful Clinical Islet Isolation Using a GMP-Manufactured Collagenase and Neutral Protease." *Transplantation* 88 (6): 753–756.
- Takahashi, K., and Yamanaka, S. 2006. "Induction of Pluripotent Stem Cells from Mouse Embryonic and Adult Fibroblast Cultures by Defined Factors." *Cell* 126 (4): 663–76.
- Tam, S.K., Dusseault, J., Bilodeau, S., Langlois, G., Hallé, J.P., and Yahia, L. 2011. "Factors Influencing Alginate Gel Biocompatibility." *Journal of Biomedical Materials Research - Part A* 98 (1): 40-52.
- Tan, W., and Desai, T.A. 2003. "Microfluidic Patterning of Cells in Extracellular Matrix Biopolymers: Effects of Channel Size, Cell Type, and Matrix Composition on

- Pattern Integrity." *Tissue Engineering* 9 (2): 255-67.
- Tan, W. H., and Takeuchi, S. 2007. "Monodisperse Alginate Hydrogel Microbeads for Cell Encapsulation." *Advanced Materials* 19 (18): 2696–2701.
- Tang Z., Yue, Y. 1995. "Crosslinkage of Collagen by Polyglycidyl Ethers." *American Society for Artificial Internal Organs* 41 (1): 72–78.
- Tasaki, I., and Mizuguchi, K. 1948. "Response of Single Ranvier Nodes to Electrical Stimuli." *Journal of Neurophysiology* 11 (4): 295–303.
- Teh, Shia-Yen, Robert Lin, Lung-Hsin Hung, and Abraham P Lee. 2008. "Droplet Microfluidics." *Lab on a Chip* 8 (2): 198–220.
- Teng, Y.D., Lavik, E.B., Qu, X., Park, K.I., Ourednik, J., Zurakowski, D., Langer, R., and Snyder, E.Y. 2002. "Functional Recovery Following Traumatic Spinal Cord Injury Mediated by a Unique Polymer Scaffold Seeded with Neural Stem Cells." *Proceedings of the National Academy of Sciences of the United States of America* 99 (5): 3024–3029.
- Thomson, M., Liu, S.J., Zou, L.N., Smith, Z., Meissner, A., Ramanathan, S. 2011. "Pluripotency Factors in Embryonic Stem Cells Regulate Differentiation into Germ Layers." *Cell* 145 (6): 875-89.
- Thornton, A.J., Alsberg, E., Hill, E.E., Mooney, D.J. 2004. "Shape Retaining Injectable Hydrogels for Minimally Invasive Bulking." *The Journal of Urology* 172 (2): 763–68.
- Tiwari, G., Tiwari, R., Sriwastawa, B., Bhati, L., Pandey, S., Pandey, P., and Bannerjee, S.K. 2012. "Drug Delivery Systems: An Updated Review." *International Journal of Pharmaceutical Investigation* 2 (1): 2–11.
- Tobias, C.A., Han, S.S., Shumsky, J.S., Kim, D., Tumolo, M., Dhoot, N.O., Wheatley, M.A., Fischer, I., Tessler, A., Murray, M. 2005. "Alginate Encapsulated BDNF-Producing Fibroblast Grafts Permit Recovery of Function after Spinal Cord Injury in the Absence of Immune Suppression." *Journal of Neurotrauma* 22 (1): 138-56.
- Toso, C., Oberholzer, J., Ceausoglu, I., Ris, F., Rochat, B., Rehor, A., Bucher, P., Wandrey, C., Schuldt, U., Belenger, J., Bosco, D., Morel, P., Hunkeler, D. 2003. "Intra-Portal Injection of 400-Mm Microcapsules in a Large-Animal Model." *Transplant International* 16 (6): 405–410.
- Tsai, E.C., Dalton, P.D., Shoichet, M.S., Tator, C.H. 2006. "Matrix Inclusion within Synthetic Hydrogel Guidance Channels Improves Specific Supraspinal and Local Axonal Regeneration after Complete Spinal Cord Transection." *Biomaterials* 27: 519–33.
- Uchida, D, Sugiura, S., Shirasaki Y., Go, J. S., Nakanishi, H., Funatsu, T., and Shoji, S. 2003. "Pdms Microfluidic Devices With Ptfе Passivated Channels." *7th International Conference on Miniaturized Chemical and Biochemical Analysts Systems, Squaw Valley, Callifornia USA*, 429-432.
- Umemura, E. Yamada, Y., Nakamura, S., Ito, K., Hara, K., and Ueda, M. 2011. "Viable Cryopreserving Tissue-Engineered Cell-Biomaterial for Cell Banking Therapy in an Effective Cryoprotectant." *Tissue Engineering. Part C, Methods* 17 (8): 799–

807.

- Ushikubo, F.Y., Birribilli, F.S., Oliveira, D.R.B., and Cunha, R.L. 2014. "Y- and T-Junction Microfluidic Devices: Effect of Fluids and Interface Properties and Operating Conditions." *Microfluidics and Nanofluidics* 17 (4): 711–20.
- Utada, A.S., Fernandez-Nieves, A., Stone, H.A., and Weitz, D.A. 2007. "Dripping to Jetting Transitions in Coflowing Liquid Streams." *Physical Review Letters* 99 (9): 094502.
- Utada, A.S., Lorenceau, E., Link, D.R., Kaplan, P.D., Stone, H.A., and Weitz, D.A. 2005. "Monodisperse Double Emulsions Generated from a Microcapillary Device." *Science* 308 (5721): 537-41
- Utada, A.S., Fernandez-Nieves, A., Stone, H.A., and Weitz, D.A. 2007. "Dripping to Jetting Transitions in Coflowing Liquid Streams." *Physical Review Letters* 99 (9): 1–4.
- Vaithilingam, V., and Tuch, B.E. 2011. "Islet Transplantation and Encapsulation: An Update on Recent Developments." *Review of Diabetic Studies* 8 (1): 51–67.
- Van Belle, T., and Von Herrath, M. 2008. "Immunosuppression in Islet Transplantation." *Journal of Clinical Investigation* 118 (5): 1625-8.
- Van der Helm, M.W., Van der Meer, A.D., Eijkel, J.C.T., Van den Berg, A., and Segerink, L.I. 2016. "Microfluidic Organ-on-Chip Technology for Blood-Brain Barrier Research." *Tissue Barriers* 4 (1): e1142493.
- Velasco, D., Tumarkin, E., and Kumacheva, E. 2012. "Microfluidic Encapsulation of Cells in Polymer Microgels." *Small* 8 (11): 1633–42.
- Vincenti, M.P., and Brinckerhoff, C.E. 2002. "Transcriptional Regulation of Collagenase (MMP-1, MMP-13) Genes in Arthritis: Integration of Complex Signaling Pathways for the Recruitment of Gene-Specific Transcription Factors." *Arthritis Research* 4 (3): 157-64.
- Wagers, A.J., and Weissman, I.L. 2004. "Plasticity of Adult Stem Cells." *Cell* 116 (5): 639-48..
- Wallace K.M., Vandervort, N.W., David, P.J., Deeter, B.D., Melchior, G.J., Brazzle, J.R., Muzyk, K.R., Miranda, F.R., Cheung, T.W., Bain, O.G., Frienden, J.E., Mars, D.A., Hendrickson, W.A. 2010. *Plant treatment compositions and methods for their use*. WO2010101659 A1.
- Walsh, E., Feuerborn, A., and Cook, P.R. 2016. "Formation of Droplet Interface Bilayers in a Teflon Tube." *Scientific Reports* 6:34355.
- Wang, H., and Yang, Y.G. 2012. "Innate Cellular Immunity and Xenotransplantation." *Current Opinion in Organ Transplantation* 17 (2): 162–67.
- Wang, N., Adams, G., Buttery, L., Falcone, F.H., and Stolnik, S. 2009. "Alginate Encapsulation Technology Supports Embryonic Stem Cells Differentiation into Insulin-Producing Cells." *Journal of Biotechnology* 144 (4): 304–12.
- Wang, T., Gu, Q., Zhao, J., Mei, J., Shao, M., Pan, Y., Zhang, J., Wu, H., Zhang, Z., and Liu, F. 2015. "Calcium Alginate Enhances Wound Healing by up-Regulating the

- Ratio of Collagen Types I/III in Diabetic Rats." *International Journal of Clinical and Experimental Pathology* 8 (6): 6636–45.
- Wang, T.T.H., Jing, A.H., Luo, X.Y., Li, M., Kang, Y., Zou, X.L., Chen, H., Dong, J., and Liu, S. 2006. "Neural Stem Cells: Isolation and Differentiation into Cholinergic Neurons." *NeuroReport* 17 (13): 1433–36.
- Liu, W., Hu, S., Liu, G., Pan, F., Wu, H., Jiang, Z., Wang, B., Li, Z., and Cao, X. 2014. "Creation of Hierarchical Structures within Membranes by Incorporating Mesoporous Microcapsules for Enhanced Separation Performance and Stability." *Journal of Materials Chemistry A* 2 (15): 5267–79.
- Wang, R., and Ward, M.M. 2015. "Arthritis of the Spine". *Spinal Imaging and Image Analysis*, 18:31–66. Springer International Publishing Switzerland.
- Ward, T., Faivre, M., Abkarian, M., and Stone, H.A. 2005. "Microfluidic Flow Focusing: Drop Size and Scaling in Pressure versus Flow-Rate-Driven Pumping." *Electrophoresis* 26 (19): 3716–24.
- Watkins, T.A., Emery, B., Mulinyawe, S. and Barres, B.A. 2008. "Distinct Stages of Myelination Regulated by γ -Secretase and Astrocytes in a Rapidly Myelinating CNS Coculture System." *Neuron* 60 (4): 555–69.
- Weigl, B.H., and Yager, P. 1999. "Microfluidic Diffusion-Based Separation and Detection." *Science* 283 (5400): 346–347.
- Wen, J., Xu, N., Li, A., Bourgeois, J., Ofosu, F.A., Hortelano, G. 2007. "Encapsulated Human Primary Myoblasts Deliver Functional hFIX in Hemophilic Mice." *The Journal of Gene Medicine* 9 (11): 1002–10.
- Whitehead, K.A., Matthews, J., Chang, P.H., Niroui, F., Dorkin, J.R., Severgnini, M., Anderson, D.G. 2012. "The in Vitro – in Vivo Translation of Lipid Nanoparticles for Hepatocellular siRNA Delivery" 6 (8): 6922–29.
- Wikström, J., Elomaa, M., Syväjärvi, H., Kuokkanen, J., Yliperttula, M., Honkakoski, P., and Urtti, A. 2008. "Alginate-Based Microencapsulation of Retinal Pigment Epithelial Cell Line for Cell Therapy." *Biomaterials* 29 (7): 869–76.
- Wilhelm, S.M., Eisen, A.Z., Teter, M., Clark, S.D., Kronberger, A., and Goldberg, G. 1986. "Human Fibroblast Collagenase: Glycosylation and Tissue-Specific Levels of Enzyme Synthesis." *Proceedings of the National Academy of Sciences of the United States of America* 83 (11): 3756–60.
- Williams, D.F. 1999. *The Williams Dictionary of Biomaterials*. Liverpool University Press.
- Williams, D.F. 2015. "Regulatory Biocompatibility Requirements for Biomaterials Used in Regenerative Medicine." *Journal of Materials Science: Materials in Medicine* 26:89: 5421–27.
- Wilson, J.L., Najia, M.A., Saeed, R., and Mcdevitt, T.C. 2014a. "Alginate Encapsulation Parameters Influence the Differentiation of Microencapsulated Embryonic Stem Cell Aggregates." *Biotechnology and Bioengineering* 111 (3): 618–31.
- Wilson, J.T., and Chaikof, E.L. 2009. "Challenges and Emerging Technologies in the Immun isolation of Cells and Tissues." *Advanced Drug Delivery Reviews* 60 (2):

124–45.

- Workman, V. L., S. B. Dunnett, P. Kille, and Dan Palmer. 2007. "Microfluidic Chip-Based Synthesis of Alginate Microspheres for Encapsulation of Immortalized Human Cells." *Biomicrofluidics* 1 (1): 014105.
- Workman, V.L., Dunnett, S.B., Kille, P., and Palmer, D.D. 2008. "On-Chip Alginate Microencapsulation of Functional Cells." *Macromolecular Rapid Communications* 29 (2): 165–70.
- Wu, S., Suzuki, Y., Kitada, M., Kitaura, M., Kataoka, K., Takahashi, J., Ide, C., Nishimura, Y. 2001. "Migration, Integration, and Differentiation of Hippocampus-Derived Neurosphere Cells after Transplantation into Injured Rat Spinal Cord." *Neuroscience Letters* 312 (3): 173-6.
- Xu, W., Shen, R., Yan, Y., and Gao, J. 2017. "Preparation and Characterization of Electrospun alginate/PLA Nanofibers as Tissue Engineering Material by Emulsion Eletrospinning." *Journal of the Mechanical Behavior of Biomedical Materials* 65: 428–38.
- Wu, X., Black, L., Santacana-Laffitte, G., Patrick, C.W. Jr. 2007. "Preparation and Assessment of Glutaraldehyde-Crosslinked Collagen–chitosan Hydrogels for Adipose Tissue Engineering." *Journal of Biomedical Materials Research - Part A* 81 (1): 59–65.
- Yanase, M., Sakou, T., and Fukuda, T. 1995. "Role of N-Methyl-D-Aspartate Receptor in Acute Spinal Cord Injury." *Journal of Neurosurgery* 83 (5): 884–88.
- Yang, W.D., Chen, S.J., Mao, T.Q., Chen, F.L., Lei, D.L., Tao, K., Tang, L.H., Xiao, M.G. 2000. "A Study of Injectable Tissue-Engineered Autologous Cartilage." *The Chinese Journal of Dental Research : The Official Journal of the Scientific Section of the Chinese Stomatological Association (CSA)* 3 (4): 10–15.
- Yang, Ji Sheng, Ying Jian Xie, and Wen He. 2011. "Research Progress on Chemical Modification of Alginate: A Review." *Carbohydrate Polymers* 84 (1): 33–39.
- Yang, Y.G., and Sykes, M. 2007. "Xenotransplantation: Current Status and a Perspective on the Future." *Nature Reviews Immunology* 7 (7): 519-31.
- Ye, Z., Zhou, Y., Cai, H., and Tan, W. 2011. "Myocardial Regeneration: Roles of Stem Cells and Hydrogels." *Advanced Drug Delivery Reviews* 63 (8): 688-97.
- Yoshii, S., Oka, M., Shima, M., Akagi, M., Taniguchi, A. 2003. "Bridging a Spinal Cord Defect Using Collagen Filament." *Spine* 28 (20): 2346-51.
- Yoshii, S., Oka, M., Shima, M., Taniguchi, A., Taki, Y., Akagi, M. 2004. "Restoration of Function after Spinal Cord Transection Using a Collagen Bridge." *J Biomed Mater Res A* 70: 569–575.
- Young, F.I., Telezhkin, V., Youde, S.J., Langley, M.S., Stack, M., Kemp, P.J., Waddington, R.J., Sloan, A.J., and Song, B. 2016. "Clonal Heterogeneity in the Neuronal and Glial Differentiation of Dental Pulp Stem / Progenitor Cells". *Stem Cells International* 2016.
- Yu, J., Du, K.T., Fang, Q., Gu, Y., Mihardja, S.S., Sievers, R.E., Wu, J.C., and Lee, R.J. 2010. "The Use of Human Mesenchymal Stem Cells Encapsulated in RGD

- Modified Alginate Microspheres in the Repair of Myocardial Infarction in the Rat." *Biomaterials* 31(27): 7012–7020.
- Zainal Ariffin, S.H., Kermani, S., Zainol Abidin, I.Z., Megat Abdul Wahab, R., Yamamoto, Z., Senafi, S., Zainal Ariffin, Z., Abdul Razak, M. 2013. "Differentiation of Dental Pulp Stem Cells into Neuron-Like Cells in Serum-Free Medium" 2013:250740.
- Zeb, H.A., Khan, I.N., Munir, I., Ramadan, W.S., Ahmad, M.A., Hussein, D., Kamal, M.A., and Al Karim, S. 2016. "Updates on Therapeutics in Clinical Trials for Spinal Cord Injuries: Key Translational Applications of Human Embryonic Stem Cells-Derived Neural Progenitors." *CNS and Neurological Disorders - Drug Targets* 15 (10): 1266-1278.
- Zhang, X., Chen, X., Yang, T., Zhang, N., Dong, L., Ma, S., Liu, X., Zhou, M., Li, B. 2014. "The Effects of Different Crossing-Linking Conditions of Genipin on Type I Collagen Scaffolds: An in Vitro Evaluation." *Cell and Tissue Banking* 15 (4): 531–541.
- Zhang, H., Tumarkin, E., Peerani, R., Nie, Z., Sullan, R.M., Walker, G.C., and Kumacheva, E. 2006. "Microfluidic Production of Biopolymer Microcapsules with Controlled Morphology." *Journal of the American Chemical Society* 128 (37): 12205–10.
- Zhang, J.X., Li, R., Zhao, P., Shi, L., Cheng, Z.H., You, Y.P. and Fu, Z. 2008. "Culture and Identification of Endothelial Progenitor Cells from Cord Blood with CD133 Immunomagnetic Sorting." *Chinese Journal of Cancer Biotherapy* 15 (2): 159-162.
- Zhang, J., O'Carroll, S.J., Wu, A., Nicholson, L.F.B., and Green, C.R. 2010. "A Model for Ex Vivo Spinal Cord Segment Culture-A Tool for Analysis of Injury Repair Strategies." *Journal of Neuroscience Methods* 192 (1): 49–57.
- Zhang, J.M., and An, J. 2007. "Cytokines, Inflammation and Pain." *International Anesthesiology Clinics*. 45 (2): 27–37.
- Zhang, W., and He, X. 2009. "Encapsulation of Living Cells in Small (Approximately 100 Microm) Alginate Microcapsules by Electrostatic Spraying: A Parametric Study." *Journal of Biomechanical Engineering* 131 (7): 74515.
- Zhang, Y., Xu, B., and Chow, M.J. 2011. "Experimental and Modeling Study of Collagen Scaffolds with the Effects of Crosslinking and Fiber Alignment." *International Journal of Biomaterials* 172389.
- Zhao, S., Xu, Z., Wang, H., Reese, B.E., Gushchina, L.V., Jiang, M., Agarwal, P., Xu, J., Zhang, M., Shen, R., Liu, Z., Weisleder, N., He, X. 2016. "Bioengineering of Injectable Encapsulated Aggregates of Pluripotent Stem Cells for Therapy of Myocardial Infarction." *Nature Communications* 7:13306.
- Zhao, W., Ji, X., Zhang, F., Li, L., Ma, L. 2012. "Embryonic Stem Cell Markers." *Molecules (Basel, Switzerland)* 17 (6): 6196–6236.
- Zhao, X., Huebsch, N., Mooney, D.J., and Suo, Z. 2010. "Stress-Relaxation Behavior in Gels with Ionic and Covalent Crosslinks." *Journal of Applied Physics* 107 (6): 063509.

- Zhao, Y., Wang, L., Jin, Y., and Shi, S. 2012. "Fas Ligand Regulates the Immunomodulatory Properties of Dental Pulp Stem Cells." *Journal of Dental Research* 91 (10): 948–54.
- Zhao, Z., Hu, H., and Shi, S. 2005. "The Optimization of the Method of Culturing Neural Stem Cells in Neonatal Rat Brain." *Zhongguo Xiu Fu Chong Jian Wai Ke Za Zhi = Zhongguo Xiufu Chongjian Waike Zazhi = Chinese Journal of Reparative and Reconstructive Surgery* 19 (7): 544-7.
- Zhong, J., Chan, A., Morad, L., Kornblum, H.I., Fan, G., and Carmichael, S.T. 2010. "Hydrogel Matrix to Support Stem Cell Survival after Brain Transplantation in Stroke." *Neurorehabilitation and Neural Repair* 24 (7): 636-44.
- Zhu, J., and Marchant, R.E. 2011. "Design Properties of Hydrogel Tissue-Engineering Scaffolds." *Expert Review of Medical Devices* 8 (5): 607–26.

APPENDIX I : Tables of antibodies

Table 1. Primary antibodies

| Antibody | Manufacturer | Cat. No. | Host Species | Isotype | Concentration (µg/ml) |
|---------------|-------------------|-----------|--------------|------------|-----------------------|
| Nestin | Sigma | N5413 | Rabbit | Polyclonal | 10 |
| Sox2 | Abcam | ab97959 | Rabbit | Polyclonal | 10 |
| Oct4 | Abcam | ab18976 | Rabbit | Polyclonal | 2.5 |
| GFAP | Life Technologies | PA5-16291 | Rabbit | Polyclonal | 2 |
| β-III tubulin | Cell Signalling | 5568S | Rabbit | IgG | 5 |
| Map2 | Cell Signalling | 8707S | Rabbit | IgG | 5 |

Table 2. Isotype control

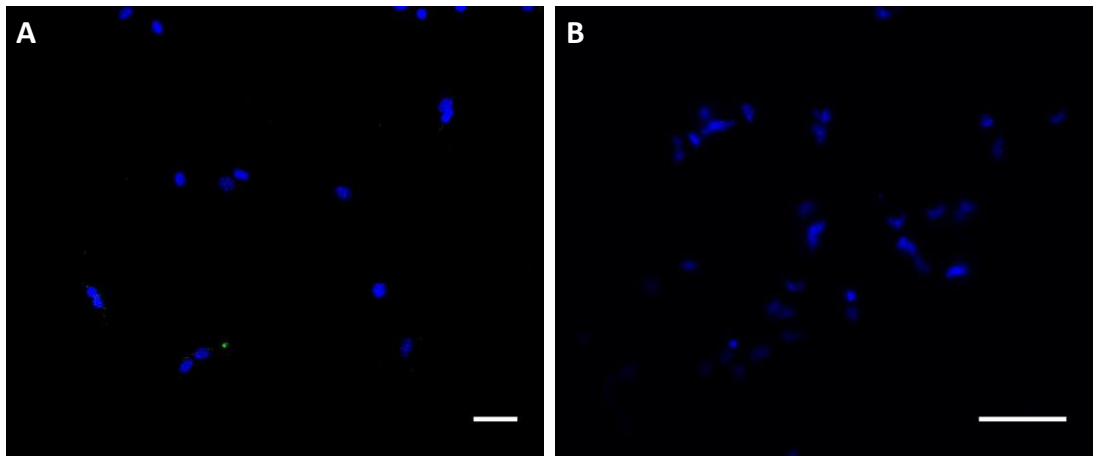
| Antibody | Manufacturer | Cat. No. | Concentration (µg/ml) |
|-------------------|--------------|----------|-----------------------|
| Normal rabbit IgG | Santa Cruz | sc-2027 | 5 |

Table 3. Secondary antibodies

| Antibody | Manufacturer | Cat. No. | Host Species | Fluorophore | Concentration (µg/ml) |
|-----------------------|-------------------|----------|--------------|-----------------|-----------------------|
| Anti-rabbit IgG (H+L) | Life Technologies | A-11008 | Goat | Alexa Fluor 488 | 4 |
| Anti-rabbit IgG (H+L) | Life Technologies | A-11012 | Goat | Alexa Fluor 594 | 4 |

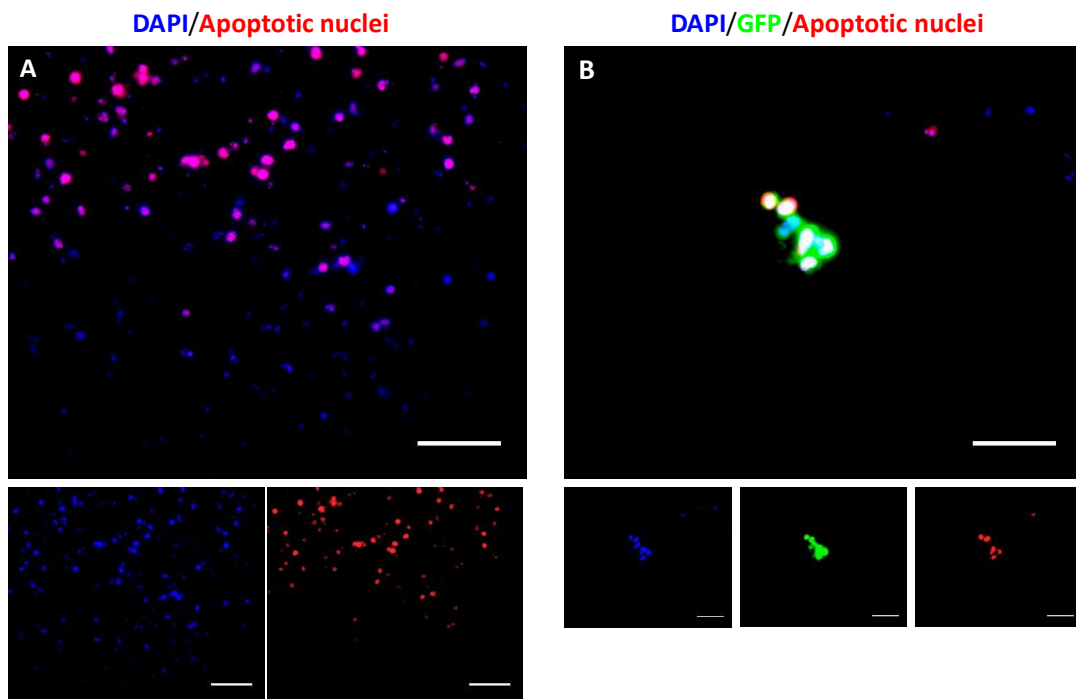
APPENDIX II : ISOTYPE CONTROL IN MONOLAYER CULTURES

DAPI/Isotype control



Merged images for rabbit IgG as an isotype control for β -III tubulin and Map2 in DPSCs (A) and NSC (B) in monolayer culture. Scale bars = 50 μ m.

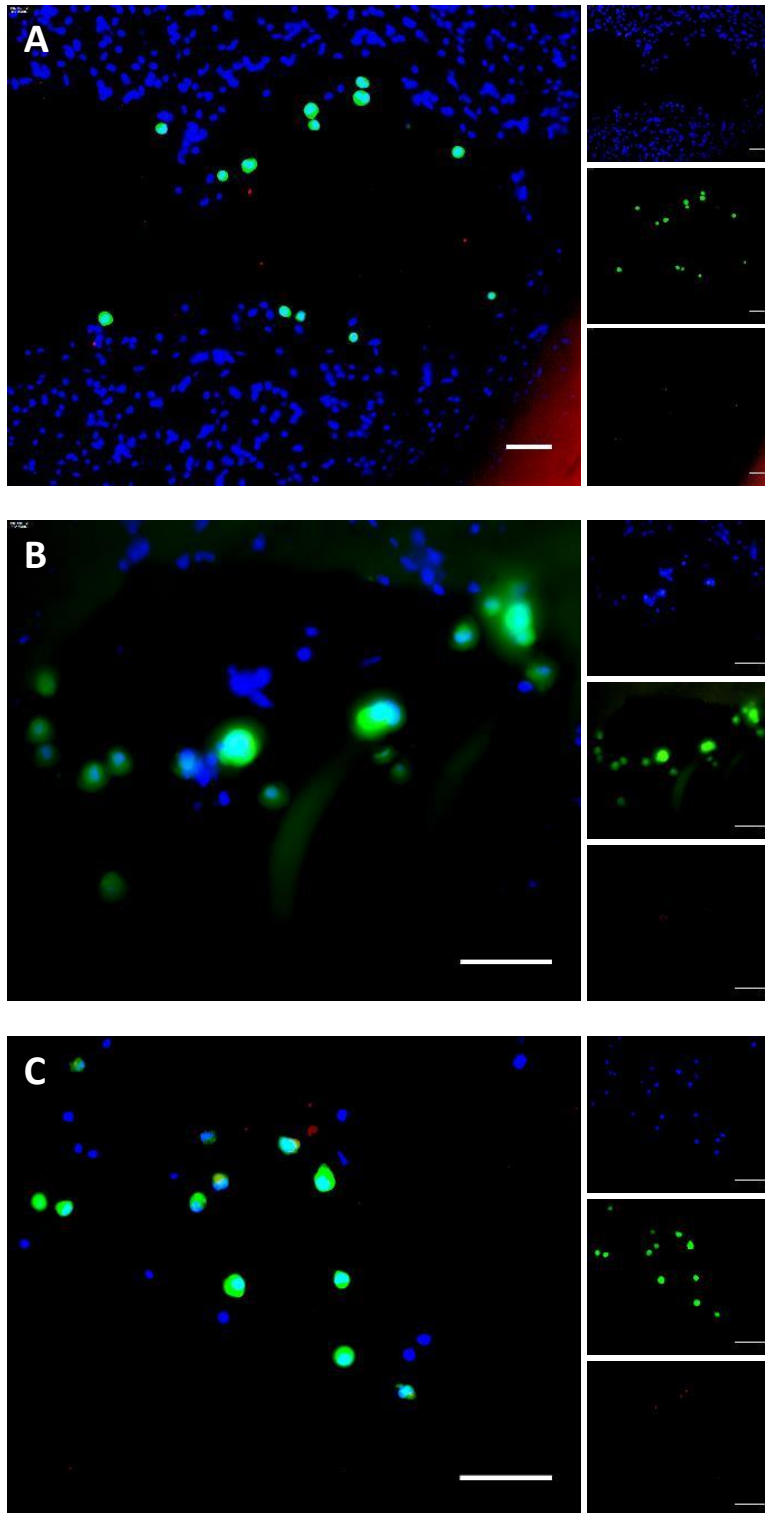
APPENDIX III : APOPTOSIS TUNEL ASSAY POSITIVE CONTROL



Merged images of apoptotic nuclei of spinal cord tissue (A) and encapsulated cells transplanted into the *ex vivo* SCI model (B). Samples were DNase treated prior to staining with Apoptosis TUNEL Assay kit. Scale bar = 50 μ m.

APPENDIX IV : EX VIVO ISOTYPE CONTROL

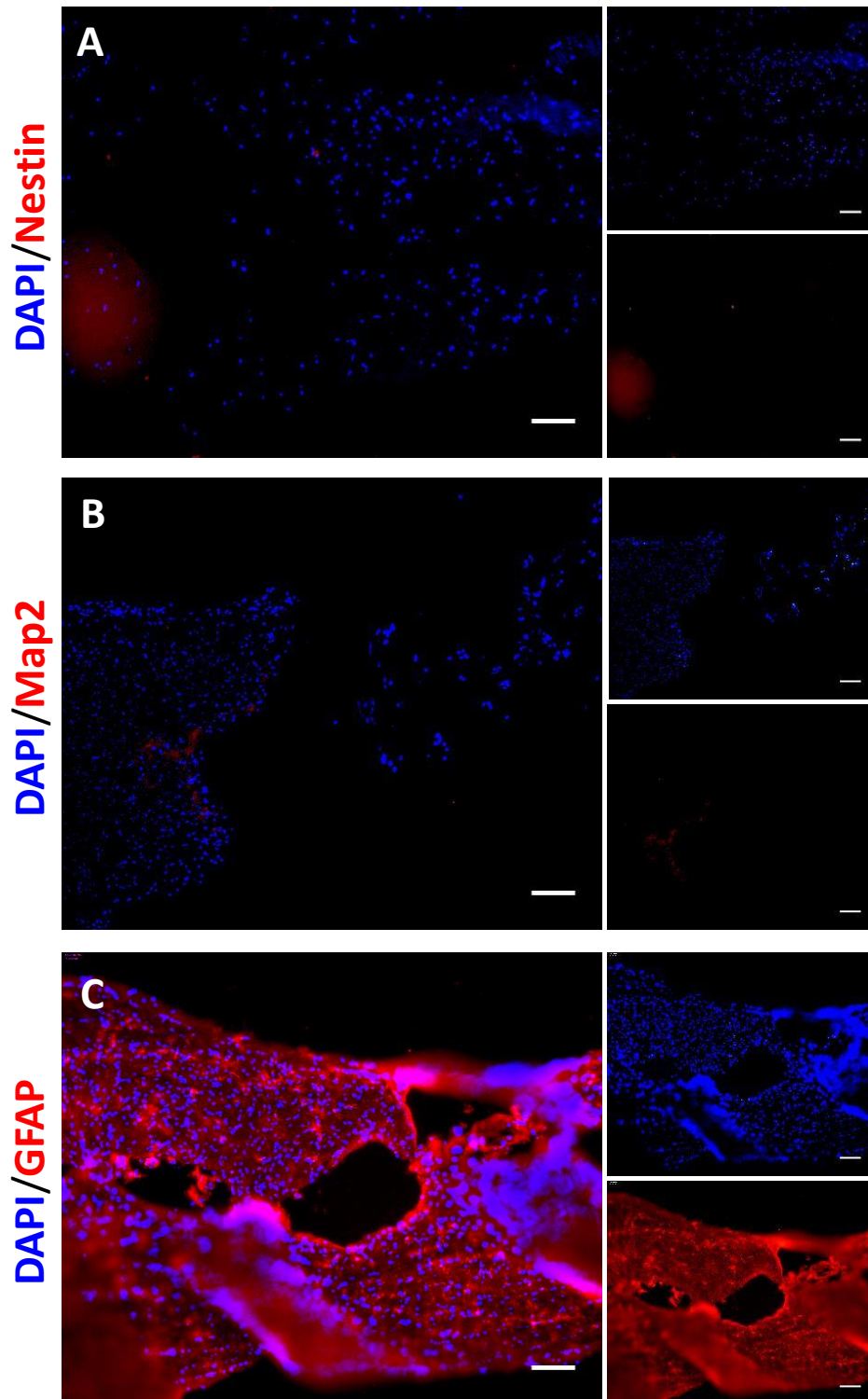
DAPI/GFP/Isotype control



Ex vivo spinal cord slice cultures from the three cell types investigated ((A) Undifferentiated DPSCs, (B) Pre-differentiated DPSCs and (C) Undifferentiated NSCs) were negatively stained

with Rabbit IgG isotype, demonstrating specificity for monoclonal antibodies, Map2 and GFAP. Scale bar = 50 μ m.

APPENDIX V : ENDOGENOUS PRODUCTION OF NEURONAL
MARKERS



Endogenous production of neuronal markers: (A) Nestin, (B) Map2 and (C) GFAP.
Scale bar = 100 μ m.

